Keto Acid Phosphoranes: Structure, Synthesis, and Bromolactonisation.

A Thesis

presented for the Degree

of

Doctor of Philosophy in Chemistry

in the

University of Canterbury

by

John O. Trent

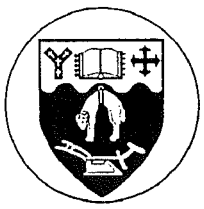

University of Canterbury

Christchurch

New Zealand

1992

List of Publications

A Novel Bromo Lactonisation of Acylated Phosphoranes: A New Route to Bromo Enol Lactones. A. D. Abell, J. O. Trent, *J. Chem Soc., Chem Commun.*, 1989, 409.

Low Temperature Nuclear Magnetic Resonance Study of the Acylation of a Stabilised Ylide: C- vs O- Acylation, A. D. Abell, J. O. Trent, B. I. Wittington, *J. Org. Chem.*, 1989, 54, 2762.

The Design and Preparation of Reactive Amino Acid Analogues -Potential Antiviral Agents, A. D. Abell, J. O. Trent, J. C. Litten, *N.Z. Med. J.*, 1989, 102(879), 592.

Carboxy to Ketone Dimeric and Catemeric Hydrogen Bonding in a Keto Acid Phosphorane: X-Ray Structure of 6-Ethoxycarbonyl-5-oxo-6-(triphenylphosphoranylidine)hexanoic Acid. A. D. Abell, J. O. Trent, W. T. Robinson, *J. Chem Soc., Chem Commun.*, 1991, 362.

Combined X-Ray Crystallographic and Infrared and Raman Spectroscopic Study of Hydrogen Bonding Patterns in Keto Acid Phosphoranes. A. D. Abell, J. O. Trent, K. B. Morris, *J. Chem Soc., Perkins Trans II* , 1991, 1077.

Table of Contents

List of Schemes, Figures, and Tables.

Abstract

This thesis examines the structure, synthesis, and bromolactonisation of keto acid phosphoranes.

Chapter One discusses the structure and the intra- and intermolecular hydrogen bonding preferences of a number of keto acid phosphoranes. The mode of hydrogen bonding was determined by X-ray crystallography, infrared spectroscopy, and Raman spectroscopy. *1-ethoxycarbonyl-5-carboxy-2-oxopentylidenetriphenylphosphorane* **1.8**, is shown to exist as a carboxyl to ketone catemer, and a unique sixteen-membered acid carboxyl to ketone intermolecular dimer, in the solid state.

Chapter Two introduces a new synthesis of halo enol lactones via a modified SCOOPY reaction on a keto acid phosphorane. A mechanistic investigation of this bromolactonisation reaction is reported, in particular, the participation of phosphonium salts and allenes in the mechanism is discussed. The synthesis of keto acid phosphoranes via a Wittig Anhydride Carbonyl Olefination reaction, and the reaction of acid chlorides with a stabilised ylide, is also described. The acid chloride reaction was shown, by low temperature ^{1}H, ^{13}C, and ^{31}P NMR spectroscopy, to proceed via an initial O-acylphosphonium salt that readily rearranges to a C-acylphosphonium salt. The synthesis of the five-membered *E*- and *Z*-succinic bromo enol lactones, and the X-ray crystal structure of *ethyl bromo-(Z-5-oxotetrahydrofuran-2-ylidene)acetate* **2.34**, is reported.

Chapter Three extends the bromolactonisation reaction to the six-membered glutaric bromo enol lactones. The synthesis of *E*- and *Z*-glutaric, 3-methylglutaric, and the 3,3-dimethylglutaric bromo enol lactones are reported.

Chapter Four further extends the bromolactonisation reaction to the five-membered aromatic *E*- and *Z*-phthalic bromo enol lactones. The reaction of phthalic anhydride with the bromo ylide **2.31** forms the *E*- and

Z-phthalic bromo enol lactones **4.25** and **4.26**, in the same stereoisomeric ratio as the bromolactonisation reaction. The X-ray crystal structure of *ethyl bromo-(Z-3-oxo-1,3-dihydroisobenzofuran-1-ylidene)acetate* **4.26** is reported. The reactivity of the keto acid phosphoranes was shown to be increased by 3-methyl aromatic substitution, and decreased by 3-nitro aromatic substitution.

Chapter Five deals with the application of keto acid phosphoranes to the synthesis of amino acid analogues. The bromolactonisation reaction is extended to include amine and aromatic substituents. The synthesis of *E*- and *Z*-3-phenylglutaric bromo enol lactones is reported. The synthesis of bromo enol lactones from asymmetric phenylsuccinic, acetyl protected aspartic, and benzyloxycarbonyl protected aspartic derived keto acid phosphoranes is discussed. A versatile synthesis of β-Cbz-aspartic bromo enol lactones, via protection of the α-carboxylic acid of Cbz-L-aspartic acid, is reported.

Acknowledgements

My most sincere and grateful thanks are extended to my supervisor, Dr. Andrew Abell, for his enthusiasm, knowledge, and guidance throughout this research project.

I would like to thank the other members of the research group, in particular Deborah, who read the final draft of this thesis.

I wish to thank the other academic and technical staff of the Department of Chemistry, especially Dr. Graeme Wright, and Dr. Ward Robinson for their helpful advice.

I would like to thank all my friends who have at some time, one way or another, contributed in the production of this thesis.

Also, I wish to thank the University Grants Committee for financial support in the form of a Scholarship.

My most special thanks to Victoria, for her support, tolerance enthusiasm, encouragement, and for many hours of accurate typing.

Finally, but by no means least, I wish to thank my family, particularly my parents, Hazel and Olaf Trent, for their constant encouragement, support, and understanding.

Introduction

Phosphorus ylides, or phosphoranes, have gained considerable attention as synthetic reagents in the Wittig reaction. The first intentional preparation[0.1] of an alkylidenephosphorane, $Ph_3PCHCO_2CH_2CH_3$, occurred in 1919. $Ph_3PCHCO_2CH_2CH_3$ **0.1**, an ylide discussed in detail in this thesis, was first prepared[0.2] by accident in 1894. It's structure, however, was assigned incorrectly. Ylides referred to hereafter in this thesis will be phosphorus ylide reagents.

An ylide is defined as a molecule in which a carbanion is attached directly to a heteroatom carrying a high degree of positive charge, Figure 0.1. Ylides are useful as a source of stable carbanions, whereas carbanions are seldom isolatible. The heteroatoms of ylides[0.3] include antimony, asernic, nitrogen, and sulphur, as well as phosphorus, Figure 0.1.

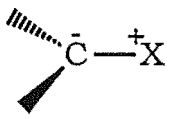

$H_2\bar{C}-\overset{+}{X}$

$H_2\bar{C}-\overset{+}{S}bPh_3$

$H_2\bar{C}-\overset{+}{A}sPh_3$

$H_2\bar{C}-\overset{+}{N}(CH_3)_3$

$H_2\bar{C}-\overset{+}{S}(CH_3)_2$

Figure 0.1

The Wittig reaction, since it's discovery in 1953[0.4], has become one of the most widely used reactions in organic synthesis[0.5, 0.6]. The classical Wittig reaction is the reaction of an ylide with the carbonyl of an aldehyde or ketone to form a carbon-carbon double bond, Scheme 0.1. Advantages of the Wittig reaction include control of the carbon-carbon double bond

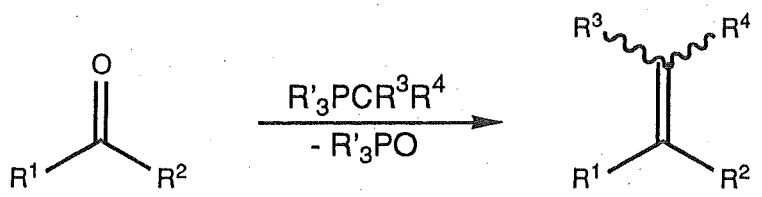

Scheme 0.1

stereochemistry and mild reaction conditions, compatible with sensitive compounds[0.7] such as caretenoids, and methylene steroids, and other natural products. In fact without the Wittig reaction the synthesis of many important compounds would be difficult, if not impossible.

The reactivity of the ylide and the stereochemical outcome of the Wittig reaction depends on the substituents on the carbon and phosphorus[0.8]. The stereochemistry of olefin formation via the Wittig reaction is discussed in Chapter 2. Ylides can be drawn as two canonical forms, **0.2a** and **0.2b**, Figure 0.2.

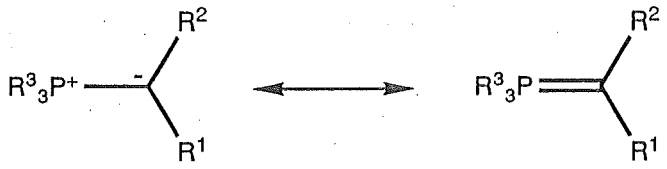

0.2a **0.2b**

Figure 0.2

0.2b contributes more to the resonance stabilisation when R^1 and R^2 are electron withdrawing and the ylide is therefore less reactive. Alternatively, if R^1,R^2 are electron donating then **0.2a** contributes more to the resonance stabilisation and the ylide is more reactive. An electron withdrawing R^3 group (-I effect) gives increased d orbital participation in resonance

stabilisation. The result is to increase the contribution of **0.2b** and hence decrease the reactivity of the ylide. However, if R^3 is electron donating (+I effect), the d orbital participation is decreased, such that **0.2a** contributes more and reactivity of the ylide is increased. A phenyl group is the most common R^3 group, possessing a -I effect. Ylides with both R^3 = Ph and electron donating R^1,R^2 groups are very reactive, and further activation with an R^3 = alkyl group is seldom required[0.8]. A large number of ylides with many different R^1, R^2, and R^3 groups is known[0.9].

Phosphoranes undergo a number of synthetically important reactions[0.10a,b,c], other than the Wittig reaction. For example, acetylenes can be synthesized either by thermolysis of β-ketophosphoranes[0.10a], Scheme 0.2, or by elimination of HI[0.10a], Scheme 0.3.

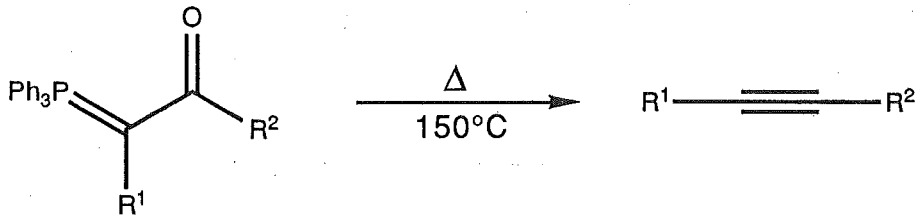

Scheme 0.2

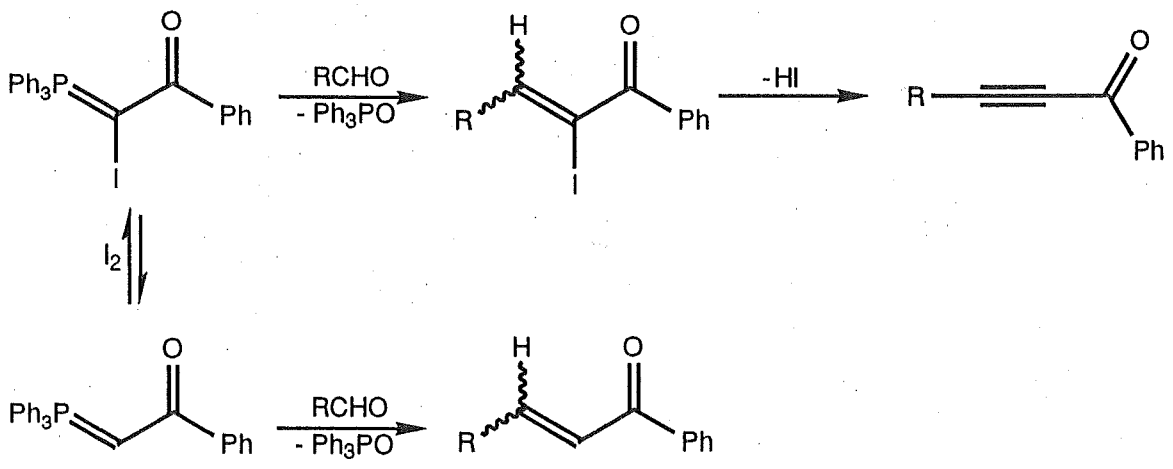

Scheme 0.3

Transylidation[0.10a,b] is also an important reaction of ylides and the product phosphorane and phosphonium salt are both synthetically useful, Scheme 0.4.

Scheme 0.4

The C-acylation of ylides represents an important reaction, Scheme 0.5. The discovery that this reaction proceeds via an initial O-acylphosphonium salt for the ylide $Ph_3PCCH_3CO_2Et$ is discussed in Chapter 2.

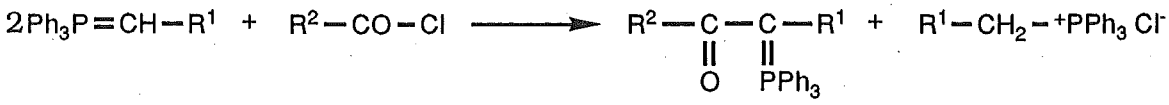

Scheme 0.5

The syntheses of carboxylic acid derivatives via a transylidation alkoxycarbonylation reaction[0.10a] and by a substitution reaction[0.10a] have also been reported, Scheme 0.6A and 0.6B, respectively. These syntheses are useful as the product ylide can form either a saturated ester[0.10b] upon hydrolysis or the α,β-unsaturated ester[0.10b] in the normal Wittig reaction, Scheme 0.6C and 0.6D respectively.

Keto phosphoranes have proved particularly useful in the synthesis of α,β-unsaturated carbonyl compounds[0.10a,b] (Scheme 0.3), allenes[0.10c], and 1,2 diketones[0.10c], Scheme 0.7. The synthesis of allenes using the ylide Ph_3PCXCO_2Et (X=Br,CH_3) is addressed in Chapter 2.

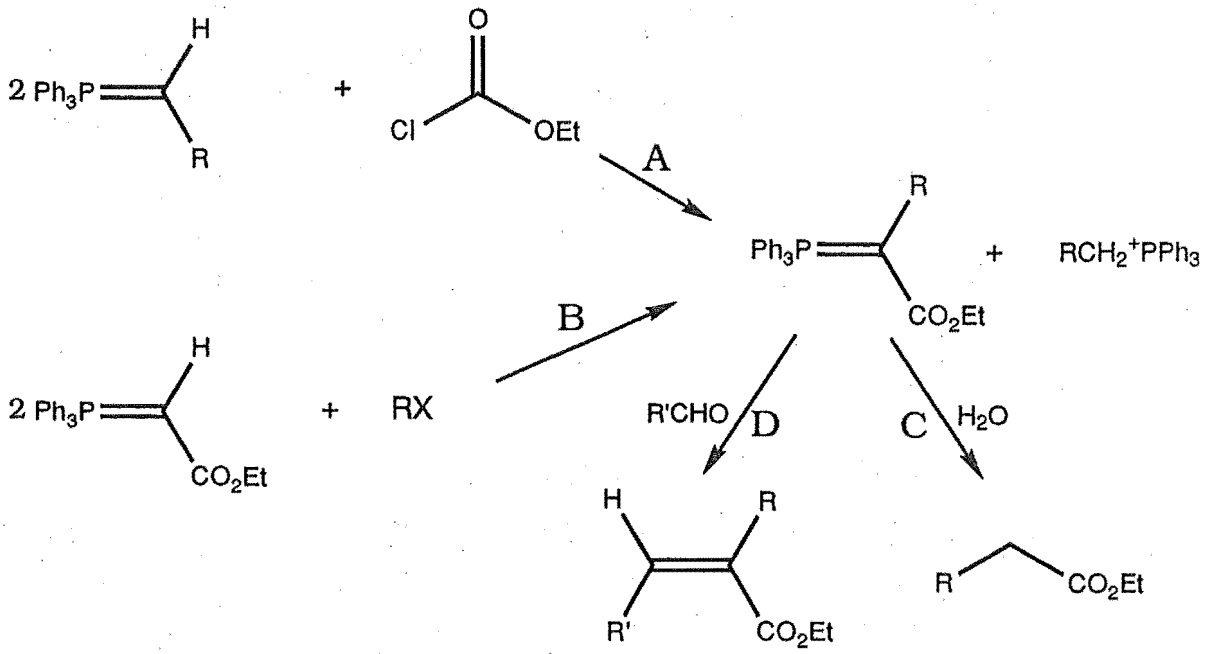

Scheme 0.6

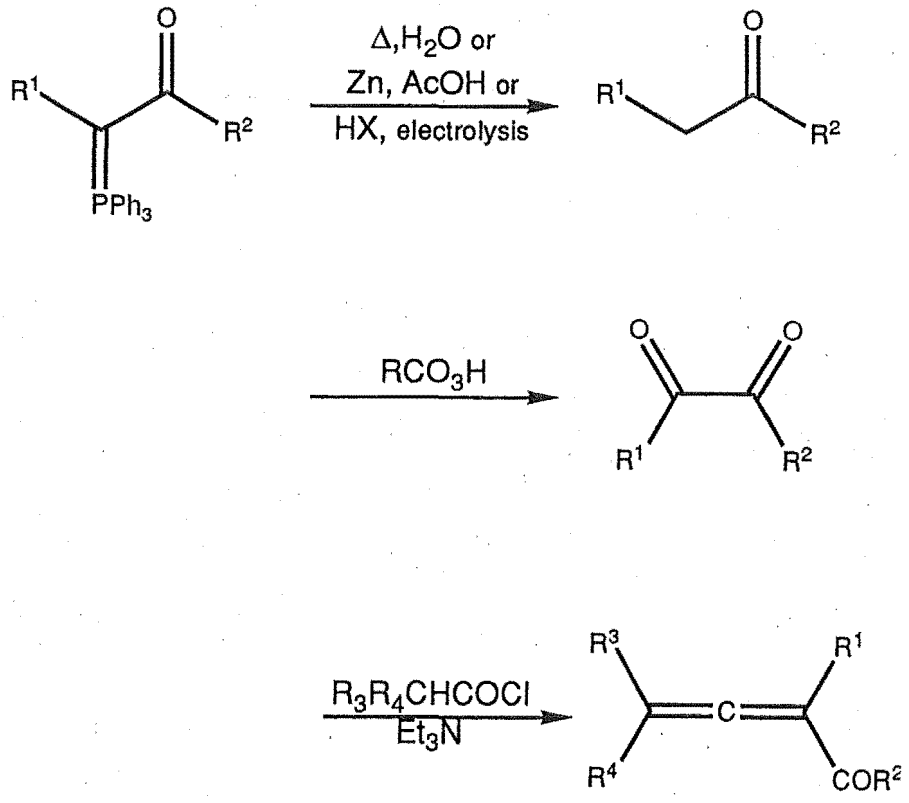

Scheme 0.7

Ylides can react with C=C double bonds in a variety of ways. The simple addition of an ylide to an alkene can give either a new phosphorane or a substituted cyclopropane[0.10c], Scheme 0.8. A Michael addition is also possible for cyano substituted olefins[0.10c], Scheme 0.9.

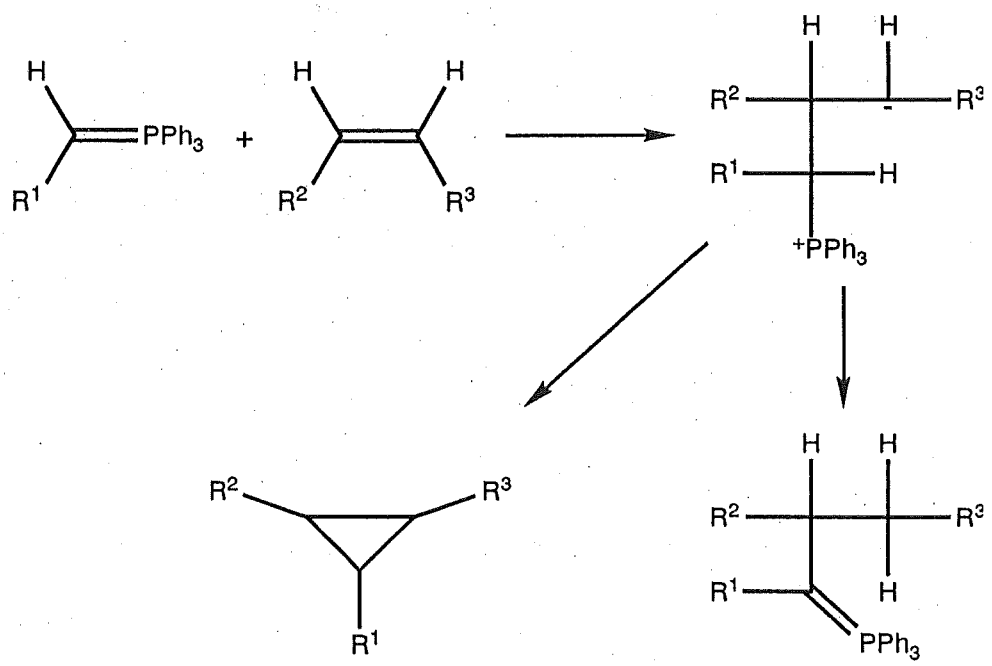

Scheme 0.8

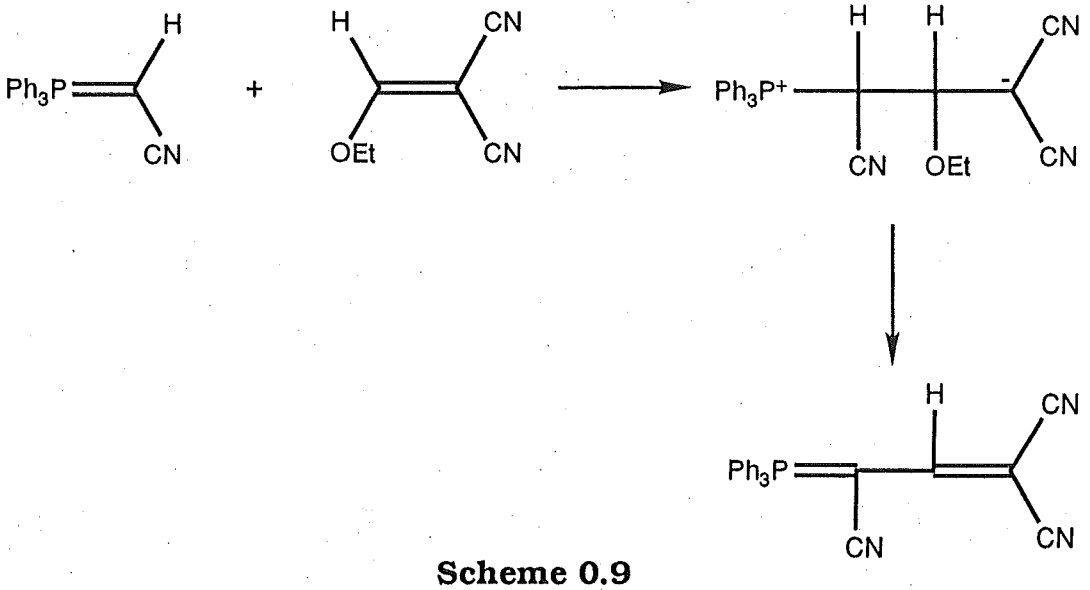

Scheme 0.9

The versatility of the Wittig reaction has meant that it is not limited to the reactions of aldehydes and ketones (see 2.1: Introduction and reference 0.5 for a recent review). For example imines[0.5] react with ylides to give olefins, Scheme 0.10.

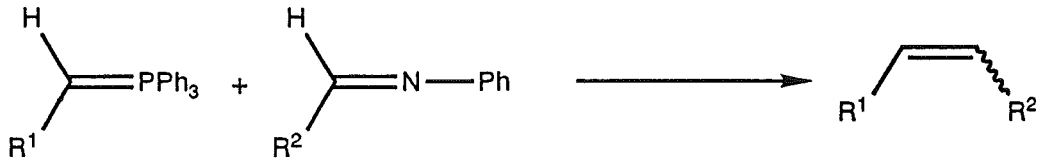

Scheme 0.10

The Wittig reaction of an anhydride and an ylide, the socalled Wittig Anhydride carbonyl olefination reaction[0.11], Scheme 0.11, represents an important extension of the Wittig reaction. The ylide **0.1** is moderately reactive as the electron withdrawing ester enhances the contribution of **0.2b** (Figure 0.2) in the resonance stabilisation, as discussed earlier. An isolatible acylphosphorane intermediate

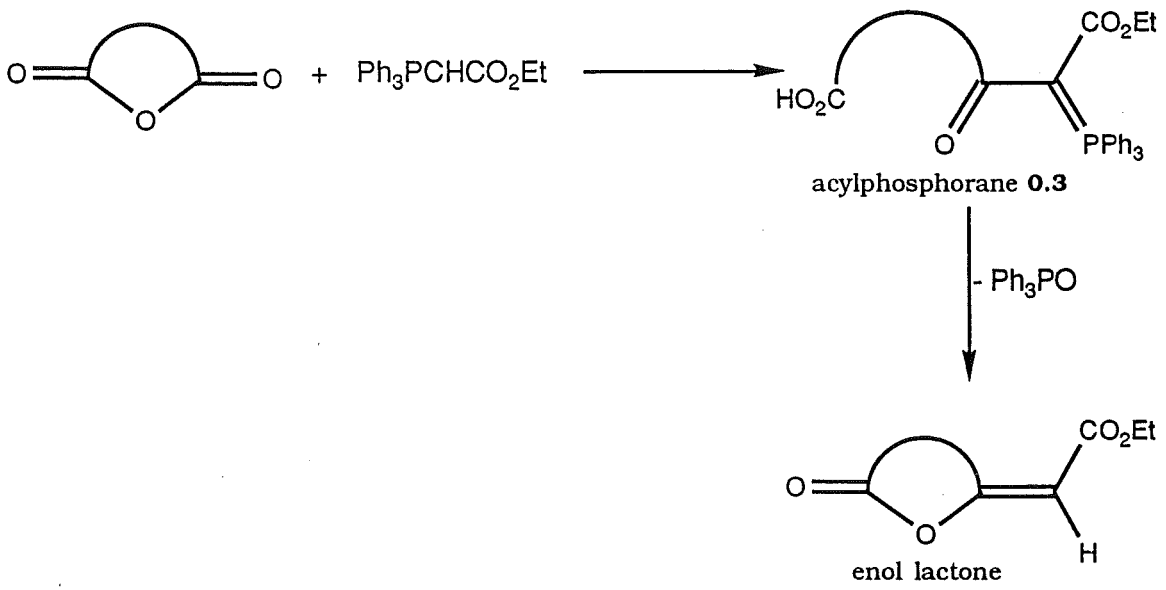

Scheme 0.11

is formed when the ylide **0.1** is C-acylated by the anhydride carbonyl. The acylphosphoranes **0.3** are intermediates to enol lactones and are also of interest for determining the extent of π delocalisation and modes of hydrogen bonding in keto acids. Hydrogen bonding may occur between the acid carboxyl with either the acid carbonyl of another molecule or the ketone carbonyl of the same or a different molecule (see Chapter 1 for a discussion).

Enol lactones are found in many natural products[0.12] and in 1974 Rando[0.13] proposed that halo enol lactones, Figure 0.3, may act as mechanism-based inactivators of serine proteases. This was subsequently confirmed by Katzenellenbogen in 1981[0.14].

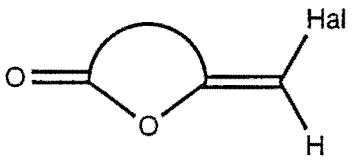

Halo enol lactone

Figure 0.3

Known syntheses[0.15] of halo enol lactones (see Chapters 2, 3, 4, and 5) are generally based on the halolactonisation of acetylenic acids, Scheme 0.12.

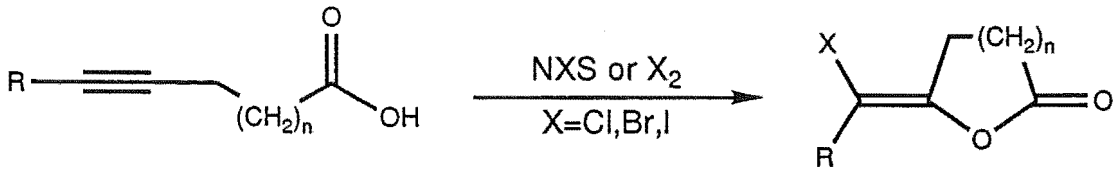

Scheme 0.12

An alternative synthetic route to halo enol lactones based on the Wittig Anhydride carbonyl olefination reaction is discussed in this thesis. The

new bromolactonisation reaction, Scheme 0.13, utilises the acylphosphorane formed as an intermediate in the Wittig Anhydride carbonyl olefination reaction.

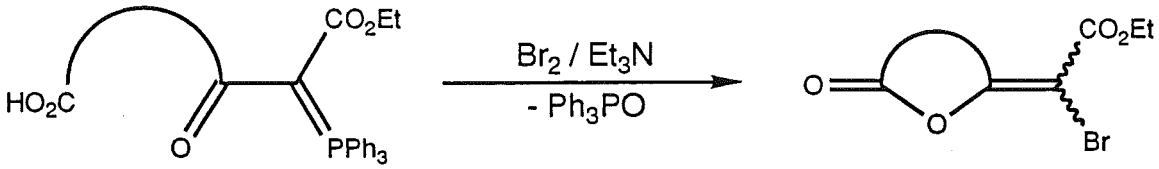

Scheme 0.13

Reported[0.14] structure-activity relationships for the inhibition of proteases by enol lactones are used to extend this reaction (see Chapters 4 and 5). The concepts of enzyme inhibition and in particular mechanism-based inactivation are therefore examined in some detail at this point.

In recent years there has been considerable interest in using enzyme inhibition as a means of designing drugs[0.16] to inhibit natural metabolic pathways under enzymic control. An inhibitor, as the name implies, reversibly inhibits the catalytic function of the enzyme. Inactivation on the other hand implies irreversibility and thus permanent inhibition of the catalytic function of the enzyme. Inhibitors that form strong noncovalent interactions with the enzyme fall into two categories, transition state analogues and the slow reversible inhibitors.

Transition state analogues[0.17] mimic a transition state of the catalytic reaction carried out by the enzyme. Enzymes cause rate enhancements by stabilising[0.18] a transition state of the reaction, so a transition state analogue will bind very tightly to the enzyme and prevent the normal enzyme catalysis. Thus, after binding tightly to the enzyme there is no release mechanism for the analogue. The use of transition state analogues is also of biological interest in the generation of catalytic antibodies[0.19].

Similarly, slow reversible inhibitors[0.17] inhibit the enzymes function by binding to the enzyme or by forming a stable enzyme-substrate complex. In contrast to transition state analogues, slow reversible inhibitors contain a release mechanism. Reversible inhibitors thus slow down the enzymes catalytic function. Enol lactones have recently[0.20] been shown to be reversible inhibitors of chymotrypsin, a serine protease. The S-enantiomer, Figure 0.4, resembles to the natural S-amino acid of the substrate and the enzyme therefore carries out the normal hydrolysis. Although the R-enantiomer, Figure 0.4, does not bind tightly to the enzyme, it does reduce the enzymes activity by having a slow release mechanism.

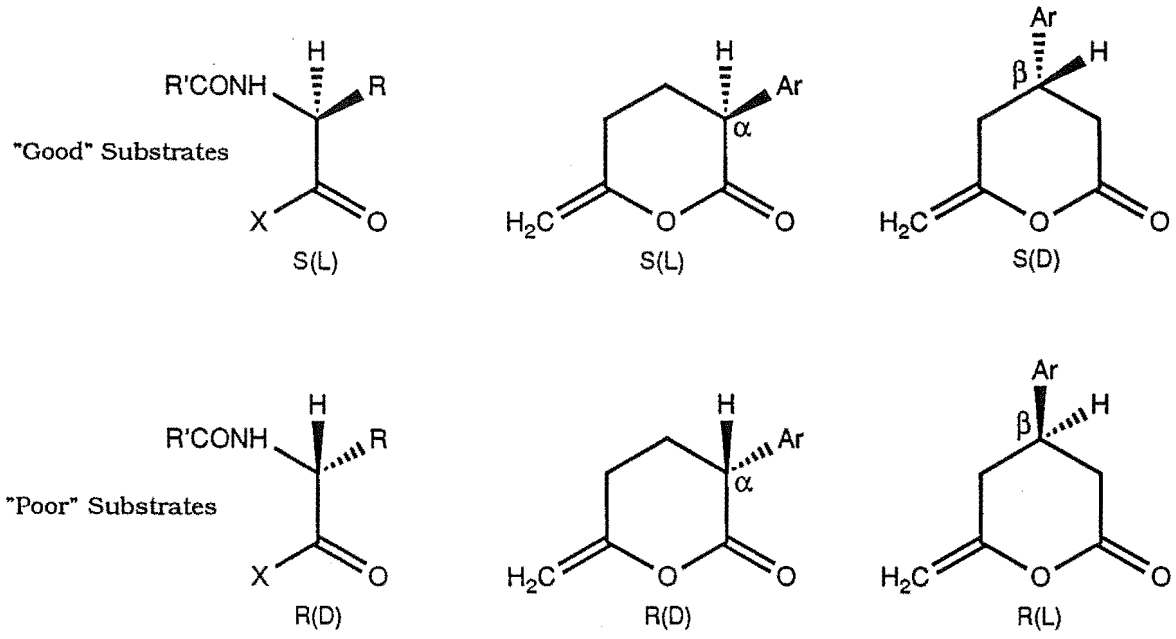

Figure 0.4

Inhibitors that form covalent interactions with the enzyme are generally referred to as inactivators. The two main categories of inactivators are affinity labels[0.21] and mechanism-based inactivators[0.22]. The affinity labels contain a reactive functional group, for example an α-

halo ketone or isocyanate, that reacts with the active site via an S_N2-like alkylation or acylation, respectively. This inactivation irreversibly blocks the active site of the enzyme. However, as affinity labels are reactive species there are many possible side reactions *in vivo* due to non-specificity. Many cancer chemotherapeutic drugs[0.16] are in fact affinity labels and nonspecific interactions cause side effects and toxicity.

Mechanism-based inactivators have attracted considerable interest in recent years[0.22]. Although the concept of mechanism-based inactivation has been long known[0.23], it was not until 1970 that Bloch[0.24] *et al.* described the mechanism of irreversible inhibition of β-hydroxydecanoylthioester dehydratase by 3-decanoylthioesters that interest mounted. Mechanism-based inactivators are essentially unreactive molecules that are recognised as substrates by the enzyme. The key feature is, however, that mechanism-based inactivators have latent reactivity. It is the target enzymes own catalytic machinery that reveals the reactive species in the active site. As the reactive species is only generated in the active site, highly specific inactivation is possible. There are only certain functional groups[0.22] that can be inserted into a molecule so that a reactive species will be revealed by the catalytic function of the enzyme. Some examples are given in Table 0.1.

Mechanism-based inactivators are particularly amenable to the design of specific, low toxicity drugs as, ideally, only one target enzyme is capable of converting the inactivator to it's reactive form. This eliminates the disadvantages of affinity labels discussed above. Further, in contrast to reversible inhibitors that require a high concentration of inhibitor (repeated administration) at the active site, only one mechanism-based inactivator is needed per enzyme molecule.

Mechanism-based inactivators are useful in enzyme mechanistic studies as well as drug design. Firstly, a mechanism-based inactivator with a known mechanism of action can be used to elucidate the catalytic

Table 0.1: Examples of Functional Groups with Latent Reactivity.

Masked species	Reactive species
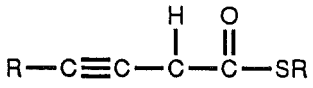	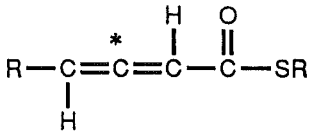
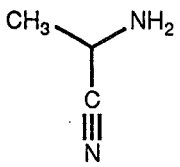	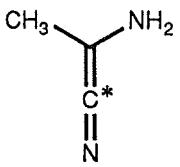
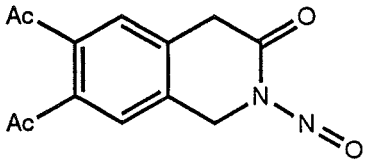	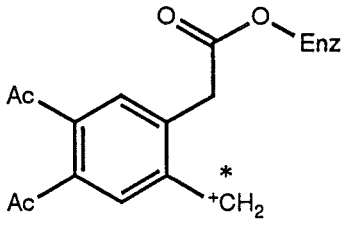
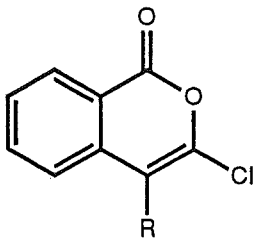	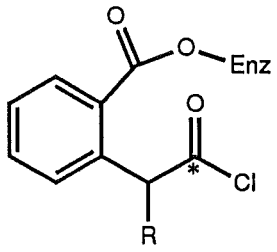
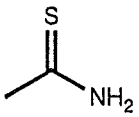	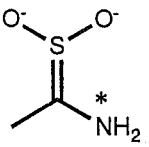
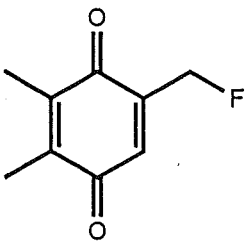	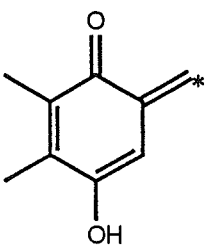

* indicates the position for covalent bond formation to the enzyme

mechanism of an enzyme, or conversely, a specific mechanism-based inactivator may be designed to target and hence test an enzymes catalytic mechanism. Drug design can then use the results of the mechanistic studies. Many enzymes have been targeted for mechanism-based inactivation and some examples are given in Table 0.2. Some therapeutic drugs in use at present are mechanism-based inactivators[0.16], Table 0.3.

Table 0.3: Therapeutic Drugs that are Mechanism-Based Inactivators*[0.16]

Therapeutic goal	Drug Example
Antibiotic	chloramphenicol**
Antifertility	norethindrone
Anesthetics	halothane
	fluoroxene
Sedative	ethclorvynol
Diuretic & antihypersensitive	spironolactone
Pituitary suppressant	danazol
Pigmentation agent	metoxsalen
Hypnotic	novonal

* Determined *ex post facto*
** Natural Compound

Halo enol lactones are inactivators[0.14] of a hydrolytic class of enzymes, known as serine proteases. Several serine proteases[0.16] are responsible for human biological disorders, Table 0.4, and consequently have been the target of a number of different approaches to enzyme inhibition[0.25], Table 0.5.

Table 0.2: Enzymes Already Targeted for Mechanism-Based Inactivation

Enzyme	Therapeutic goal	Drug Example
Monoamine oxidase	antidepressant agent	tranylcypromine phenelzine
	antihypertensive agent	hydralazine pargylyline
	antiparkinsonian agent	deprenyl
β-Lactamase	synergistic with antibiotics	clavulanic acid*
Aromatic amino acid decarboxylase	synergistic with antiparkinson drug	
Thyroid peroxidase	antithyroid agent	methimazole methylthiouracil propylthiouracil
Xanthine oxidase	uricosuric agent	allopurinol
Thymidylate synthetase	anticancer agent	5-fluorouracil
Testosterone 5α-reductase	anticancer agent	
Aromatase	anticancer agent	
Dihydroorotate dehydrogenase	anticancer agent antiparasitic agent	
Ornithine decarboxylase	anticancer- antiprotozoal agent	eflornithine**
Dihydrofolate reductase	anticancer agent antiprotozoal agent antibacterial agent	
D-Amino acid aminotransferase	antibacterial agent	
Arginine decarboxylase	antibacterial agent	
γ–Aminobutyric acid aminotransferase	anticonvulsant agent	γ-vinyl GABA**
Histidine decarboxylase	antihistamine anti-ulcer drug	
Vitamin K epoxide reductase	anticoagulant agent	
Dopamine β-hydroxylase	pheochromocytoma agent antihypertensive agent	
S-Adenosylhomocysteine hydrolase	antiviral agent	
DNA Polymerase I	antiviral agent	
HIV retrovirus	antiviral agent	

* Natural Compound
** Specifically designed as Mechanism-based Inactivators that are in Clinical Trials

Table 0.4: Therapeutic Goals for Serine Proteases[0.16]

anticoagulant agent
antiviral agent
treatment of emphysema
inflammation
arthritis
adult respiratory distress syndrome
pancreatitis
certain degenerative skin disorders
digestive disorders

Chymotrypsin, a common pancreatic enzyme, is perhaps the most studied of the serine proteases. The active site has been well characterised by X-ray crystallography[0.26] and the transition states of the hydrolysis reaction are known[0.26]. Chymotrypsin catalyses the cleavage (hydrolysis) of peptide bonds in polypeptides (proteins) within the mammalian gut[0.27]. The cleavage is specific and occurs on the carboxyl side of amino acids that have an aromatic residue, phenylalanine, tryptophan, and tyrosine, Figure 0.5. The aromatic residue fits into a complimentary hydrophobic pocket in the enzyme.

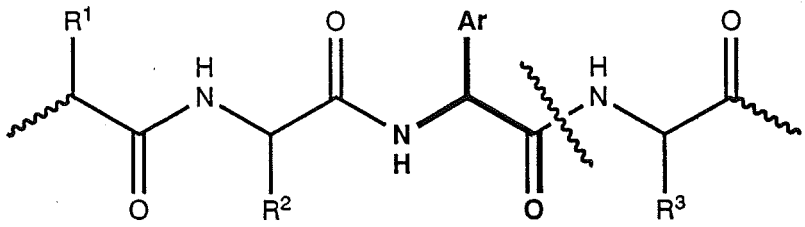

Figure 0.5

Table 0.5: Classes of Serine Protease Inhibitor

Type	Example	References[0.25]
noncovalent		
	fatty acids	Ashe & Zimmerman, 1977
	elasnin & analogs	Omura et al., 1978; Ohno et al., 1978 Groutas et al., 1984; Spencer et al., 1985
carbonyl agents		
	peptidyl aldehydes	Hassall et al., 1985
	peptidyl trifluoromethyl ketones	Gelb et al., 1985
boron analogs	peptidyl boronic acids	Kettner & Shenvi, 1984; Kinder & Katzenellenbogen, 1985
acylating agents		
acyclic	azapeptide carbamates	Gupton et al., 1984; Powers et al., 1984
	peptidyl carbamates & related acylating agents	Tsuji et al., 1984; Groutas et al., 1985a,b
cyclic	lactones	Tobias et al., 1969; Izbicka & Bolen,1981
	saccharins	Zimmerman et al., 1980; Ashe et al., 1981
	chloropyrones	Westkaemper & Abeles, 1983
	isatoic anhydrides, etc.	Moorman & Abeles, 1982; Weidmann & Abeles, 1984
	benzoazinones	Teshima et al., 1982; Hedstrom et al., 1984
	chloroisocoumarins, phthalides, etc.	Harper et al., 1985; Hemmi et al., 1985
heteroatomic	aryl sulfonyl flourides	Yoshimura et al., 1982
	peptidyl phosphonyl fluorides	Lamden & Bartlett, 1983
alkylating agents		
direct	peptidyl chloromethyl ketones	Shaw et al., 1981
masked	2-bromomethyl -benzoxazinone	Alazard et al., 1973
	6-bromomethyl-3, 4-dihydro-coumarins	Béchet et al., 1973
	nitrosoamides	White et al., 1977
	7-amino-4-chloroisocoumarins	Harper & Powers, 1984, 1985
	halo enol lactones	Chakravarty et al.,1982; Daniels et al.,
	ynenol lactones	Tam et al., 1984; Coop et al., 1987

The mechanism of peptide hydrolysis by chymotrypsin is well understood[0.26], Figure 0.6. The driving force for the hydrolysis is the catalytic triad of Asp102, His57, and Ser195. The Asp102 and His57 residues act as an electron sink and source in a charge relay system that promotes the nucleophilicity of the Ser195 OH residue. The Ser195 OH is acylated by the substrate to give the acylenzyme intermediate with release of the N-terminal amino acid, steps 2 and 3 in Figure 0.6[0.27]. The reaction proceeds via the tetrahedral intermediate, stabilised by hydrogen bonding to the NH groups in the oxyanion hole of the peptide backbone. The acylenzyme is finally hydrolysed to yield the C-terminal amino acid, steps 4 and 5 in Figure 0.6.

The primary specificity pocket of the enzyme (the above mentioned hydrophobic pocket) determines if a molecule will be recognised as a substrate by the enzyme. This interaction is crucial to the design of mechanism-based inactivators, and in the case of halo enol lactones[0.14] this substituent must be incorporated into the inactivator to ensure that the molecule is recognised by the enzyme.

The proposed[0.13,0.14] mechanism of inactivation of chymotrypsin by a halo enol lactone is shown in Figure 0.7. The acylation of the Ser195 OH, step 1, reveals the reactive α-halo ketone moiety that is highly electrophilic. A nucleophile in or near the active site may then attack the α-halo ketone and form a covalent bond to the acylenzyme to give the bis adduct, step 2a. Hydrolysis of the Ser195 OH link in the bis adduct leaves the keto acid covalently bound to and inactivating the enzyme, step 3a. His57 is the most likely candidate for the nucleophilic attack such that the charge relay system is broken for further hydrolysis of substrates. Alternatively, hydrolysis of the acylenzyme may occur to give the free α-halo keto acid, step 2b, this may then undergo nucleophilic attack by a nearby nucleophile and inactivate the enzyme, step 3b. If the free α-halo keto acid leaves the active site it is not a true mechanism-based inactivator

Figure 0.6: Mechanism of Peptide Hydrolysis by Chymotrypsin.

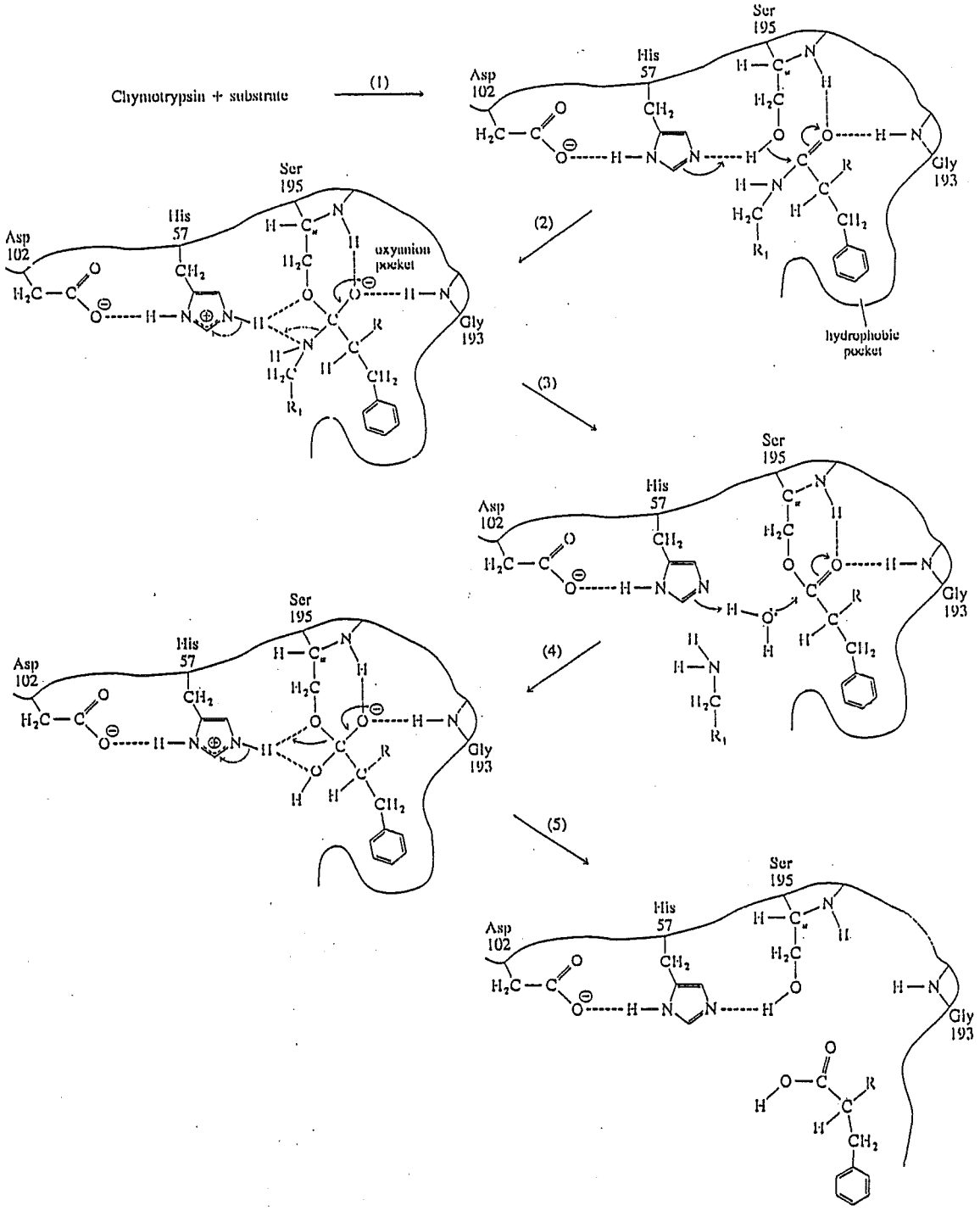

Figure 0.7: Proposed Mechanism for Halo Enol Lactone Inactivation of a Serine Protease

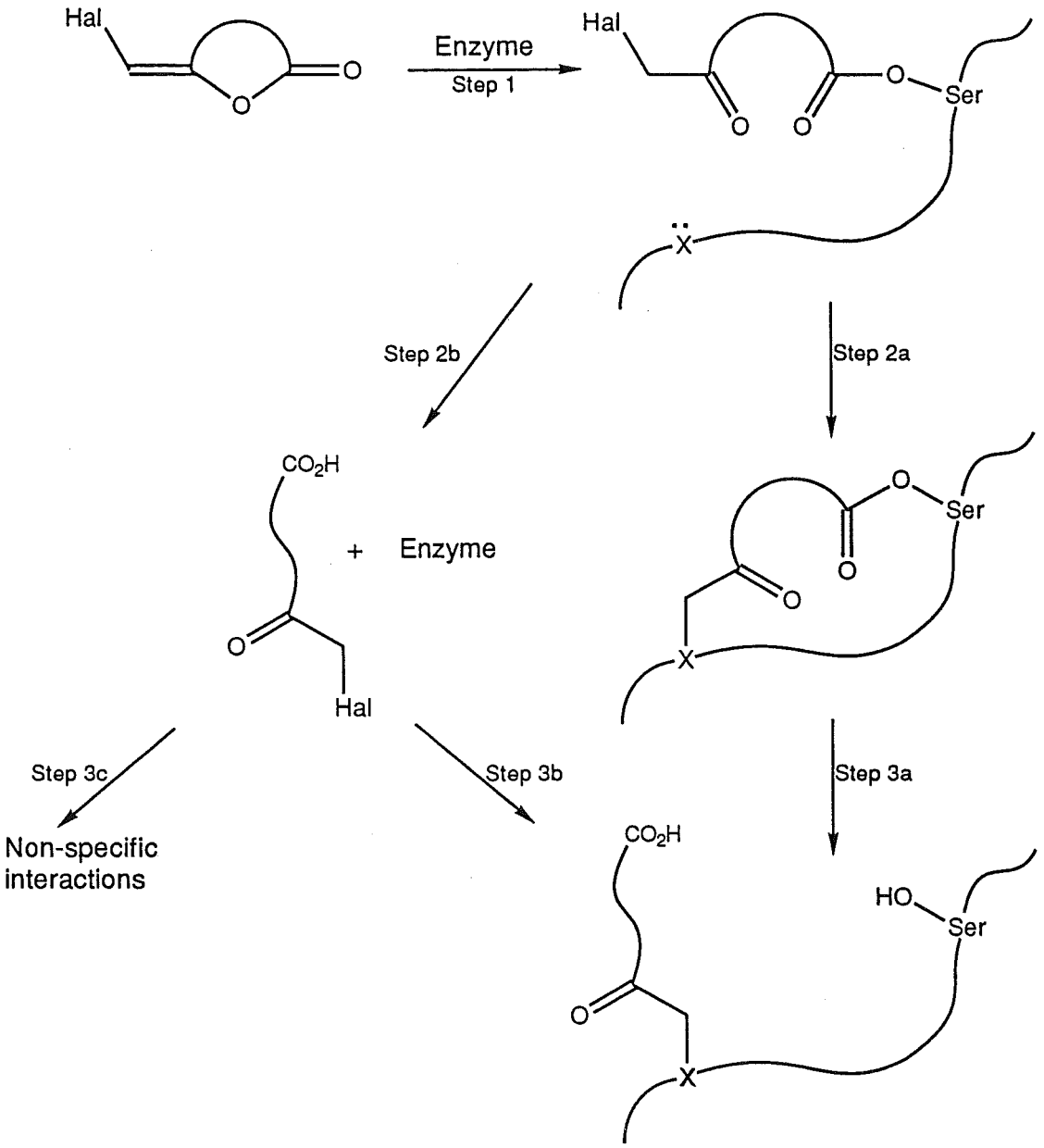

as nonspecific reactions may occur, step 3c. However, if the free α-halo keto acid returns to the active site to give inactivation, then this is termed paracatalytic mechanism-based inactivation.

As described earlier, the primary substituent on a halo enol lactone must be aromatic for recognition by the primary specificity pocket of the enzyme. Therefore, it is important to extend the new bromolactonisation reaction to include the aromatic substituent in the bromo enol lactone, an

aspect discussed in Chapters 4 and 5. Secondary substrate binding sites of the enzyme may also exist for substrate recognition. These provide the opportunity for increasing the binding specificity of a synthetic inactivator. As the substrates of chymotrypsin are proteins (polypeptides), the secondary binding will be due to interactions of the amino acids of the protein with those of the enzyme. Extension of the bromolactonisation reaction by the inclusion of an amine substituent would be advantageous (see Chapter 5). This could mean that peptides could be coupled to the amine substituent in the aim to increase the secondary binding stabilisation.

This research project investigates and develops a new bromolactonisation reaction to include aromatic and amine substituents.

Chapter One

Structure and Spectroscopy of Keto Acid Phosphoranes

1.1: Introduction

Much effort has gone into understanding the preferences of functional group classes for specific hydrogen bonded patterns in crystalline structures[1.1]. Indeed, these preferences have been used to establish empirical 'rules' for predicting hydrogen bonding patterns[1.1]. Hydrogen bonding may occur in any system that has a proton donor group (X-H) and a proton acceptor group (Y) if the s orbital of the participating hydrogen can overlap with the p or π orbital of the acceptor. All good proton acceptors and donors are used in the solid state to give hydrogen bonding. Intramolecular hydrogen bonding to give a six-membered ring is particularly stable and is preferred to intermolecular hydrogen bonding. Intermolecular hydrogen bonding will only occur in preference to intramolecular hydrogen bonding if sterically more favoured. The strength of the hydrogen bond is at a maximum when the proton is colinear with the axis of the lone pair orbitals and in a position to give maximum overlap of the orbitals. The strength of the hydrogen bond is inversely proportional to it's length.

Hydrogen bonding, especially the intramolecular variety, changes many chemical properties of the molecule. For example, hydrogen bonding plays a significant role in determining reaction rates by influencing molecular conformation[1.2]. Hydrogen bonding is also of major

biological importance. For example, the strands of the double helix of DNA are held together by hydrogen bonding between base pairs[1.3].

Techniques, such as Nuclear Magnetic Resonance, Infrared, Raman, Ultra Violet, Ion Cyclotron, Neutron Scattering spectroscopy, and X-ray Diffraction, have been used to study hydrogen bonding[1.4]. Historically, Infrared is the most important spectroscopic method because of the sensitivity of the vibration modes to the presence of hydrogen bonds. The major spectral changes that occur when hydrogen bonds form are an increase in the (X-H) bending frequency, a decrease in the (X-H) stretching frequency and an increase in the band width and intensity of the (X-H) stretching frequency.

Hydrogen bonding to electronegative atoms, for example N, O, F, and Cl, is common. In the case of oxygen, the proton acceptor is usually the oxygen of a carbonyl group (C=O). The carbonyl may be of an aldehyde, ketone, carboxylic acid, or acid derivative origin. Carboxylic acids may also act as a proton donor through the hydroxyl (O-H). The carboxyl to carbonyl hydrogen bond is strongest when the C=O--O angle is 120° and the =O--H-O angle is linear (Figure 1.1), as this gives maximum overlap of the orbitals.

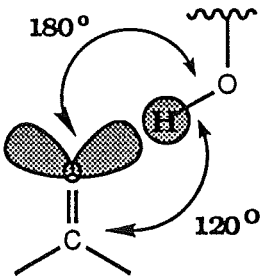

Figure 1.1

Simple crystalline keto carboxylic acids have received little attention with regard to hydrogen bonding patterns but it is known[1.5], from

published X-ray data, that in the crystalline state either intermolecular or far less commonly intramolecular hydrogen bonding can occur[1.5]. Carboxylic acid pairing[1.5], for example **1.1**, is the most common type of hydrogen bonding for keto acids. The less common acid carboxyl to ketone chain[1.5,1.6], for example **1.2** and **1.3**, and carboxyl to ketone intramolecular[1.5,1.6] hydrogen bonding, for example **1.4**, and **1.5**, and **1.6**, have also been reported[1.5,1.6]. In this thesis a previously unknown acid carboxyl to ketone hydrogen bonded dimeric association is reported. The chain-like motif has been described as a catemer (Latin: *catena* chain) and will be referred to as such in this Chapter.

Phosphoranes of the type **1.7-1.11** have received much attention as synthetic intermediates to enol lactones[1.7], acetylenes[1.8] and allenes[1.9] (Schemes 0.2, 0.3, and 0.7). We were interested in the application of phosphoranes to the preparation of biologically important molecules, for example halo enol lactones. The uses of phosphoranes in this way is discussed in greater detail in Chapters 2, 3, 4, and 5. In this Chapter the structure, and in particular, the hydrogen bonding modes adopted by the crystalline keto acid phosphoranes is discussed. This work is of interest for a number of reasons. Firstly, it represents a detailed and systematic study of hydrogen bonding in keto acids. Previous work[1.5] in this area has been of a fragmented nature rather than of a closely related series of compounds. The work was also initiated to help rationalise the ease of cyclisation of the phosphoranes to give enol lactones (see Chapter 2 for discussion). A detailed structural understanding of these phosphoranes was deemed necessary to enhance their utility as enol lactone precursors.

Recent work in Canterbury has resulted in the publication of a number of phosphorane crystal structures without detailed reference to the mode of keto acid hydrogen bonding. The succinic anhydride derived

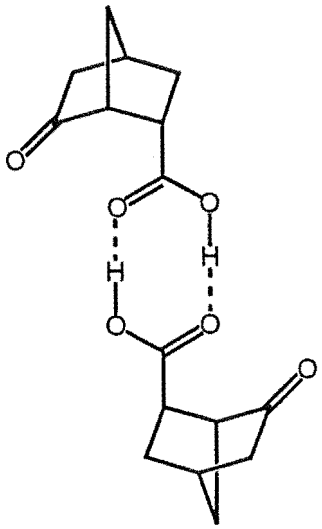

1.1

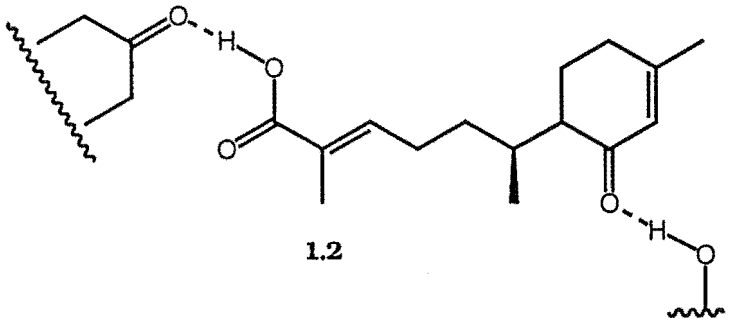

1.2

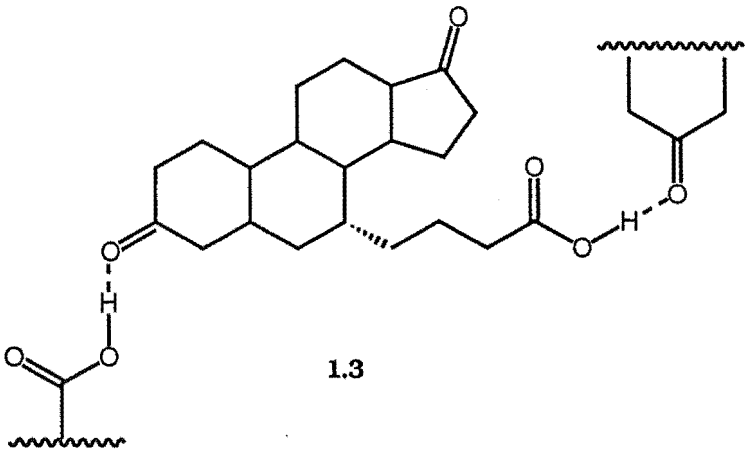

1.3

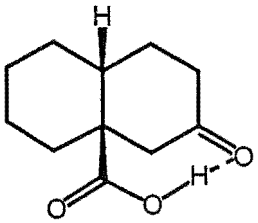

1.4

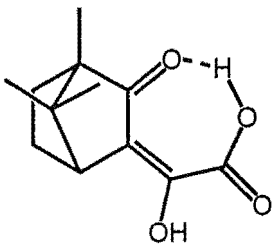

1.5

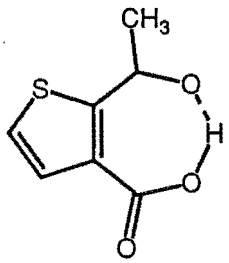

1.6

1.7[1.10] (Scheme 1.1), adipic **1.10**[1.11], diphenic **1.11**, **1.12**[1.6], acetic anhydride **1.13**, **1.14**[1.12], and in this thesis, glutaric **1.8** and dimethylglutaric **1.9** (Scheme 1.2).

This keto acid phosphorane series represents examples of the

Scheme 1.1

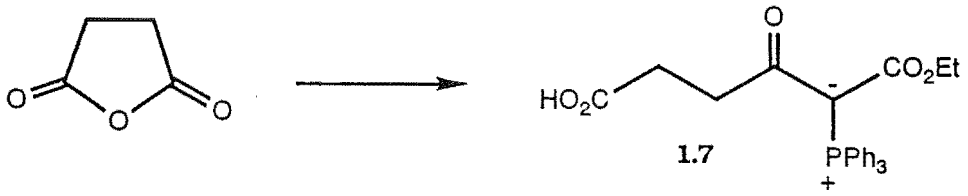

1.7

Scheme 1.2

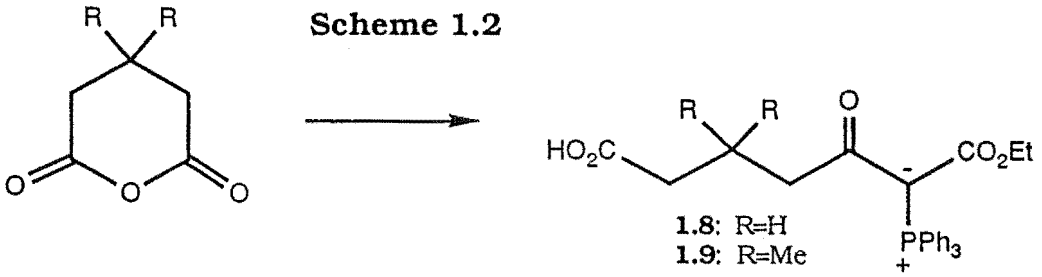

1.8: R=H
1.9: R=Me

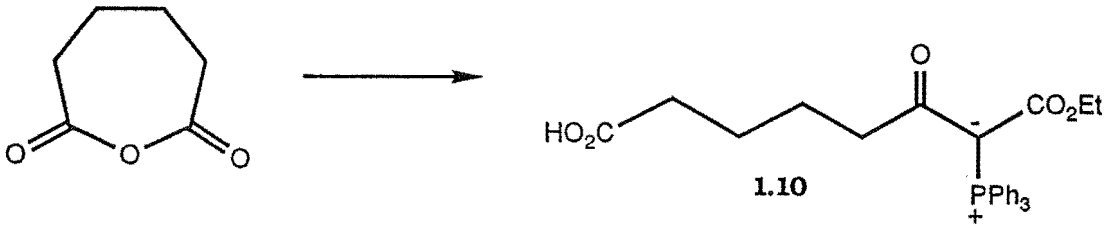

1.10

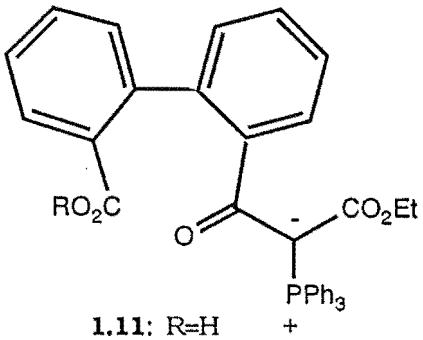

1.11: R=H
1.12: R=Me

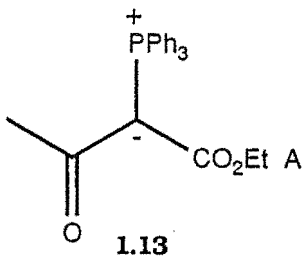

1.13

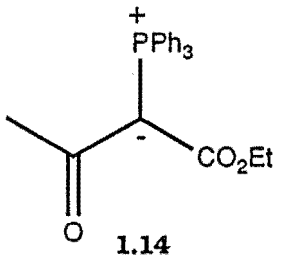

1.14

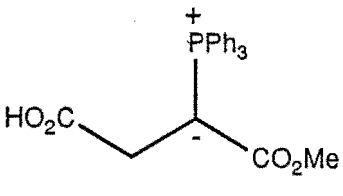

1.15

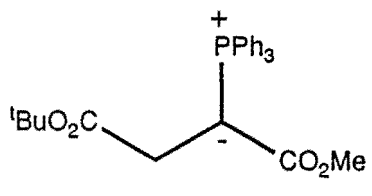

1.16

four above mentioned hydrogen bonded classes, the acid to acid dimer (aad) *e.g.* **1.7**, acid carboxyl to ketone catemer (akc) *e.g.* **1.8**, and **1.10**, acid carboxyl to ketone intramolecular (aki) *e.g.* **1.9**, and **1.11** and in addition a fourth, to our knowledge, unique acid carboxyl to ketone dimer **1.8** (akd).

In contrast to hydrogen bonding in crystalline keto acids, carboxylic acids have been extensively investigated. Keto acids have by definition a carboxylic acid group, and many of the observations reported for carboxylic acids are therefore relevant to understanding the hydrogen bonding adopted by keto acids. X-ray crystal structures represent minimum energy states, and if a sufficient number of similar structures are compared, it is possible to discover trends in the type of bonding.

The carboxyl group exists in two geometrical conformations[1.13], the *antiplaner* form (A1.2) and the more common *synplaner* form (S1.2) (Figure 1.2). The *synplaner* form (S1.2) has been found to be the more

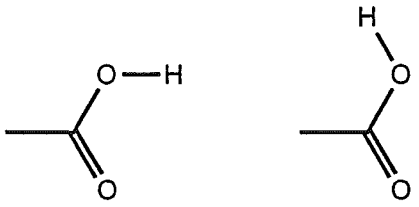

(S1.2) (A1.2)

Figure 1.2

stable conformer, and the *antiplaner* form (A1.2) exists only in compounds with intramolecular hydrogen bonding (discussed later). This generalisation is also apparent for keto acids, for example the carboxyl group conformation is *synplaner* (S1.2) in **1.1**, **1.2**, and **1.3**, and *antiplaner* (A1.2) in **1.4**, **1.5**, and **1.6**. The conformation of the carboxyl group in α,β-saturated carboxylic acids is always *synplaner* (S1.3) with respect to the

beta carbon (C^{β}) and the carbonyl group[1.13], Figure 1.3. This is due to nonbonded interactions between the protons on C^{β} and the hydroxyl and carbonyl oxygen atoms. A preference for the *synplaner* form (S1.3) exists for α,β-unsaturated carboxylic acids, but the *antiplaner* form (A1.3) is also observed. Similar *synplaner/antiplaner* preferences are observed for keto acids. For example the *synplaner* form (S1.3) of the α,β-saturated

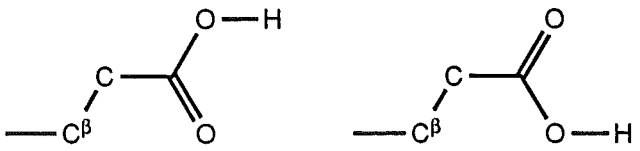

Synplaner ***Antiplaner***

(S1.3) (A1.3)

Figure 1.3

keto acids **1.1** and **1.3**, and the *antiplaner* form (A1.3) of the α,β-unsaturated keto acids **1.2**, **1.5**, and **1.6** are preferred. The carboxyl conformations are often a consequence of the mode of hydrogen bonding adopted between (intermolecular) and within (intramolecular) molecules.

A dimer, which may exhibit disorder in the crystalline state, is the most common type of hydrogen bonding in carboxylic acids. Static disorder[1.13] involves the random inclusion of the two dimer orientations (a) and (b) (Figure 1.4) in the crystalline state. Dynamic disorder[1.13] involves delocalisation of the proton, either centrally situated, or rapidly oscillating, across the =O--H-O bond and if the crystal O-H and =O--H distances are similar, then disorder exists. Disorder, characteristic of acid dimers, is also possible for the keto acid phosphorane **1.7**(aad). Disorder in the keto acid phosphoranes **1.8-1.11**, and **1.13** would require the formation of an eight-membered transition state (Figure 1.5), to enable the ketone to enolise and the carbonyl to be protonated. This represents a

sterically unfavourable conformation as it requires the acid carbonyl to be close in space to the α-protons of the ketone.

(a) (b)

Figure 1.4. Carboxylic Acid Dimer

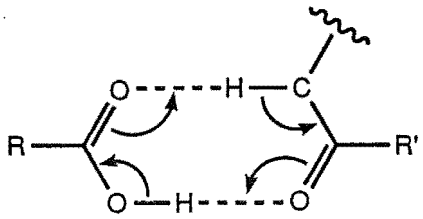

Figure 1.5

Carboxylic acids also exhibit chain-like catemers but this is very rare. However, if another electronegative proton acceptor is introduced into the molecule, such as a keto group, the possible modes of hydrogen bonding increase as mentioned earlier and discussed in detail below.

1.2: X-ray Crystallography and Hydrogen Bonding in Keto Acid Phosphoranes

A perspective drawing for **1.7**(aad), **1.8**(akc), **1.8**(akd), **1.9**(aki), **1.10**(akc), **1.11**(aki), and **1.13** is shown with atom labelling in Figures 1.6, 1.7, 1.8, 1.10, 1.11, 1.13, and 1.14, respectively. The acid carboxyl to ketone catemeric hydrogen bonding for **1.8**(akc) and **1.10**(akc) is shown in Figures 1.9 and 1.12, respectively. Table 1.1 lists selected bond lengths and angles with standard deviations in parentheses for **1.9**(aki), as determined in this thesis, and **1.10**(akc). A complete list of bond lengths and angles is given in the Experimental section for Chapter 1.

The nature of hydrogen bonding in structures of the type **1.7-1.11** is clearly dependent on the carbon chain length between the acid and ketone groups as well as the nature of the substitution. The X-ray crystal structure of the keto acid phosphorane with the longest chain length, HO_2C-$(CH_2)_4$-CO-, of the adipic derived **1.10**(akc) revealed helical catemeric acid carboxyl to ketone hydrogen bonding (Figure 1.12). The ketone O(3) to carboxyl O(5a) separation of 2.59Å is well within hydrogen bonding limits[1.14]. The solvent of crystallisation was ethyl acetate. X-ray crystallography of a crystal grown from ethyl acetate-light petroleum gave identical cell parameters to the above determination and hence it is assumed that catemeric hydrogen bonding is also present in this case.

A crystal structure[1.6] of **1.7**(aad) revealed hydrogen bonding between the two carboxyl groups forming an eight-membered ring dimer with an acid carbonyl O(4) to carboxyl O(5a) separation of 2.64Å (Figure 1.6). It is clear that crystal packing for the keto acid phosphorane with the shortest carbon chain, HO_2C-$(CH_2)_2$-CO-, does not favour helix formation but rather the observed acid to acid pairing.

The intermediate carbon chain length, HO_2C-$(CH_2)_3$-CO-, of the glutaric derived **1.8** surprisingly gave two different modes of hydrogen bonding for independent crystals grown from ethyl acetate. One, the

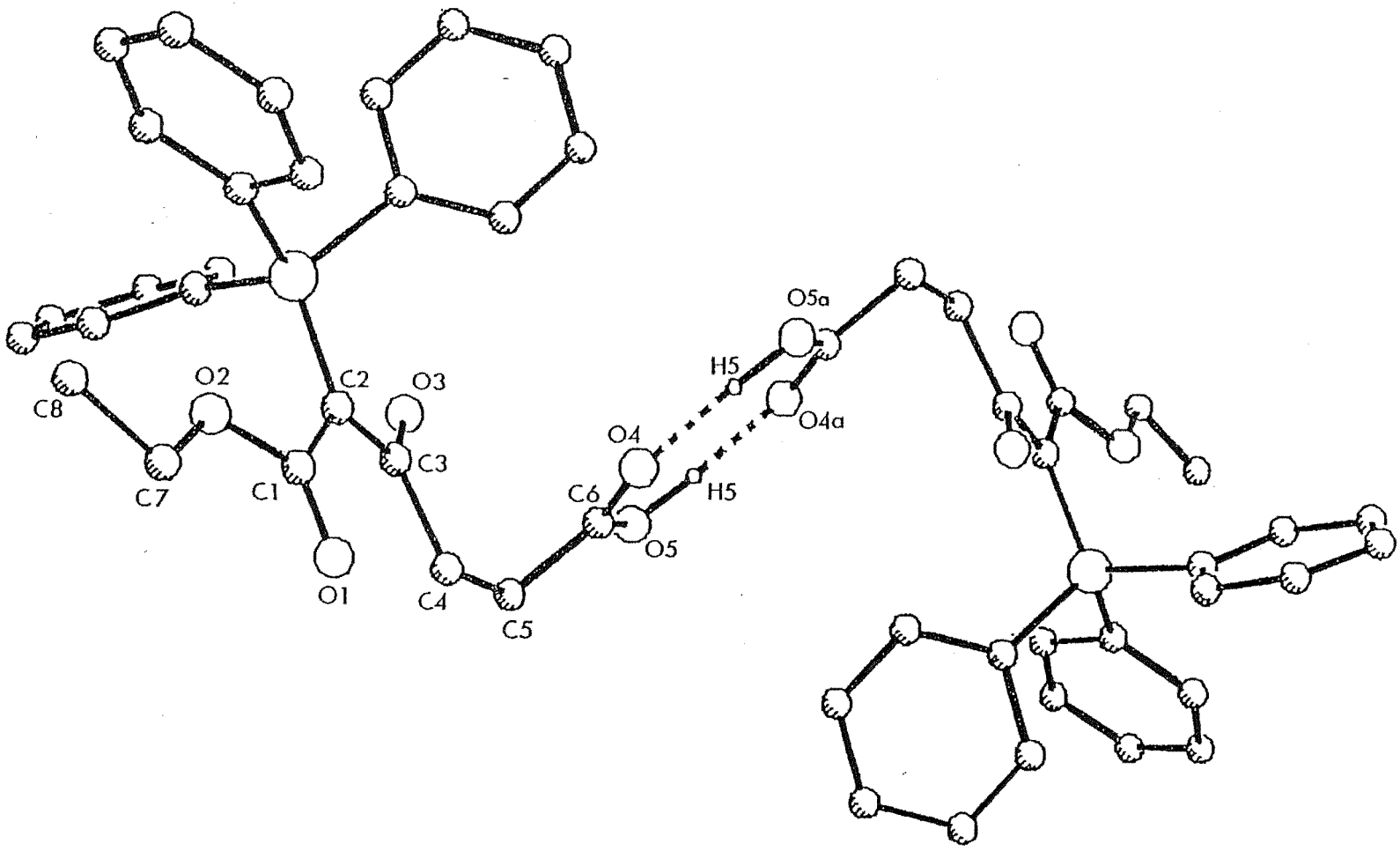

Figure 1.6: Perspective View and Atom Labelling for 1.7(aad) Showing Intermolecular Hydrogen Bonding

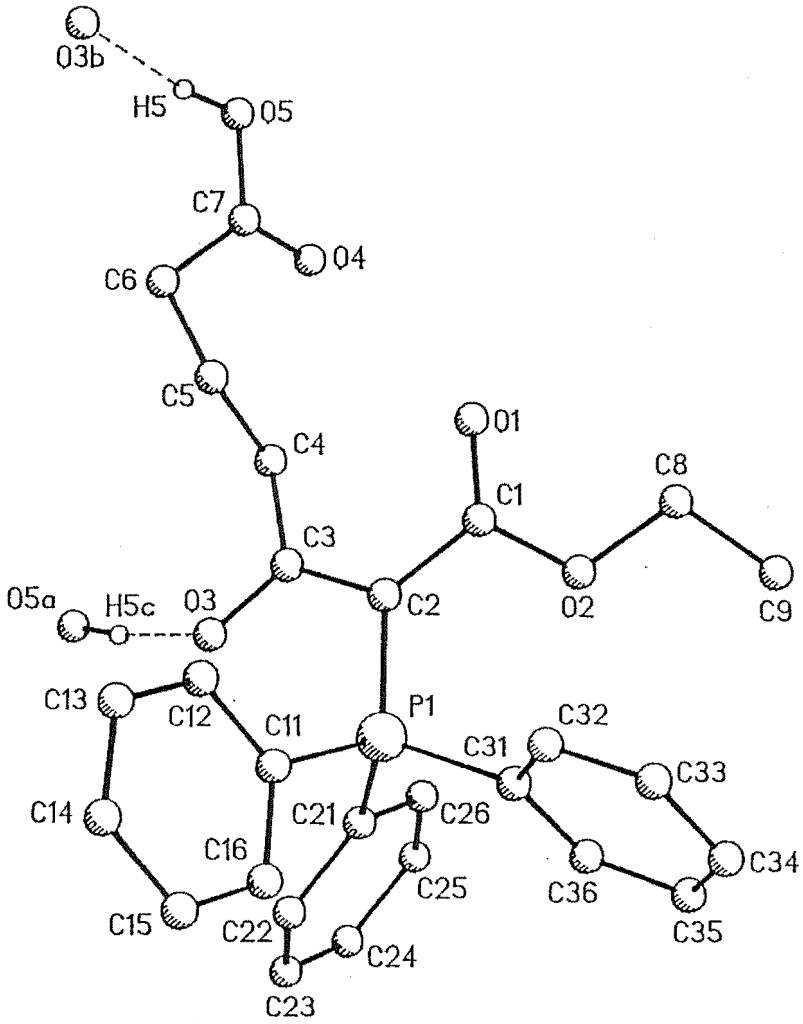

Figure 1.7: Perspective View and Atom Labelling for 1.8(akc). H5 was Inserted at a Calculated Position

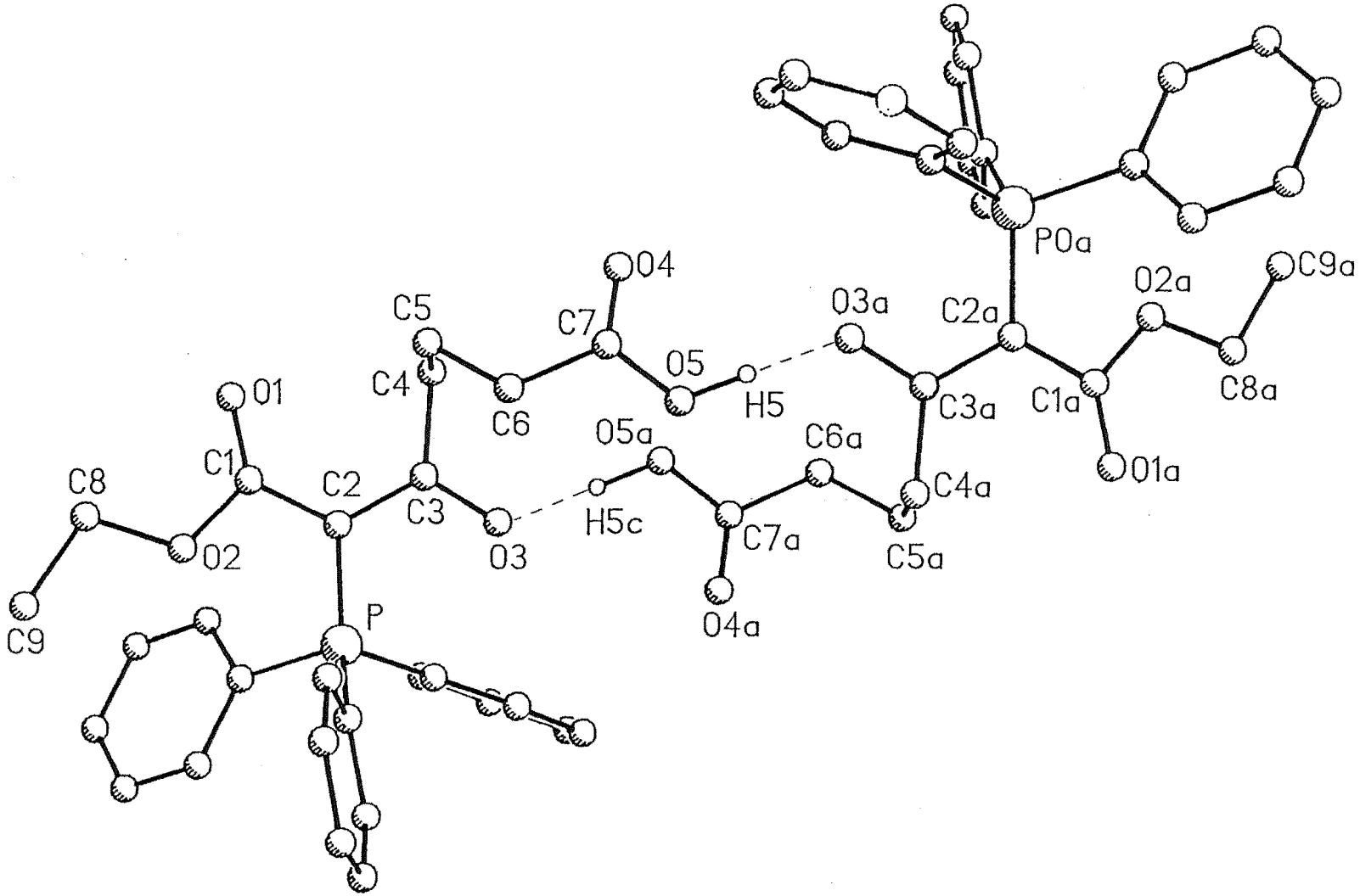

Figure 1.8: Perspective View and Atom Labelling for 1.8(akd) Showing Intermolecular Hydrogen Bonding

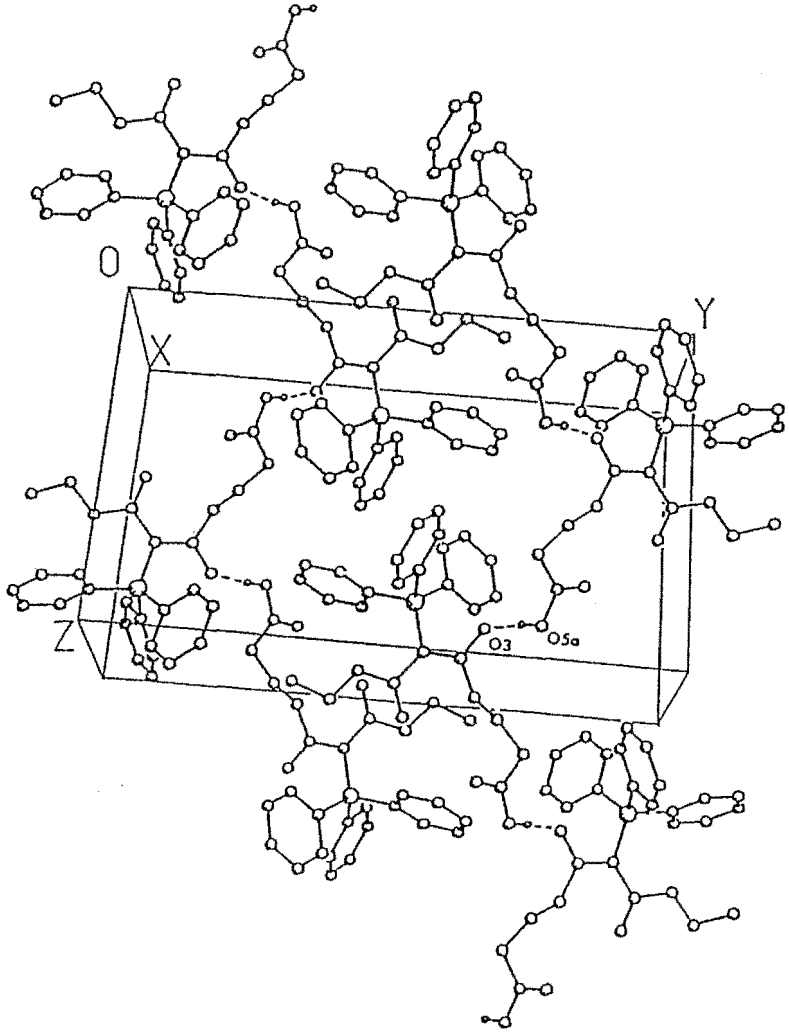

Figure 1.9: Packing Diagram For 1.8(akc) Showing Helices Generated by the Acid Carboxyl to Ketone Hydrogen Bonding.

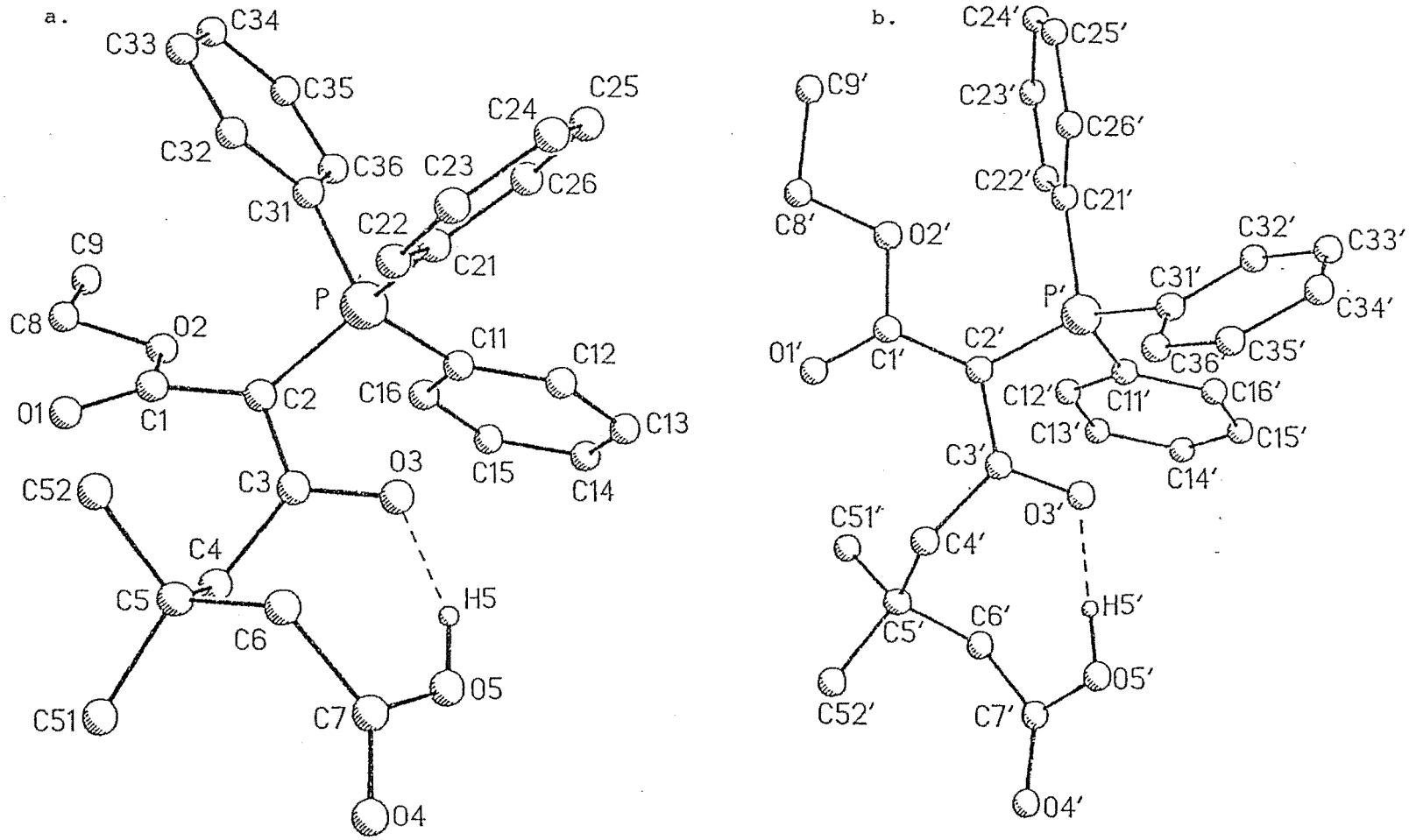

Figure 1.10: Perspective View and Atom Labelling for 1.9(aki) Showing Intramolecular Hydrogen Bonding. Each of the Two Crystallographically Independent Molecules is Shown Individually for Clarity

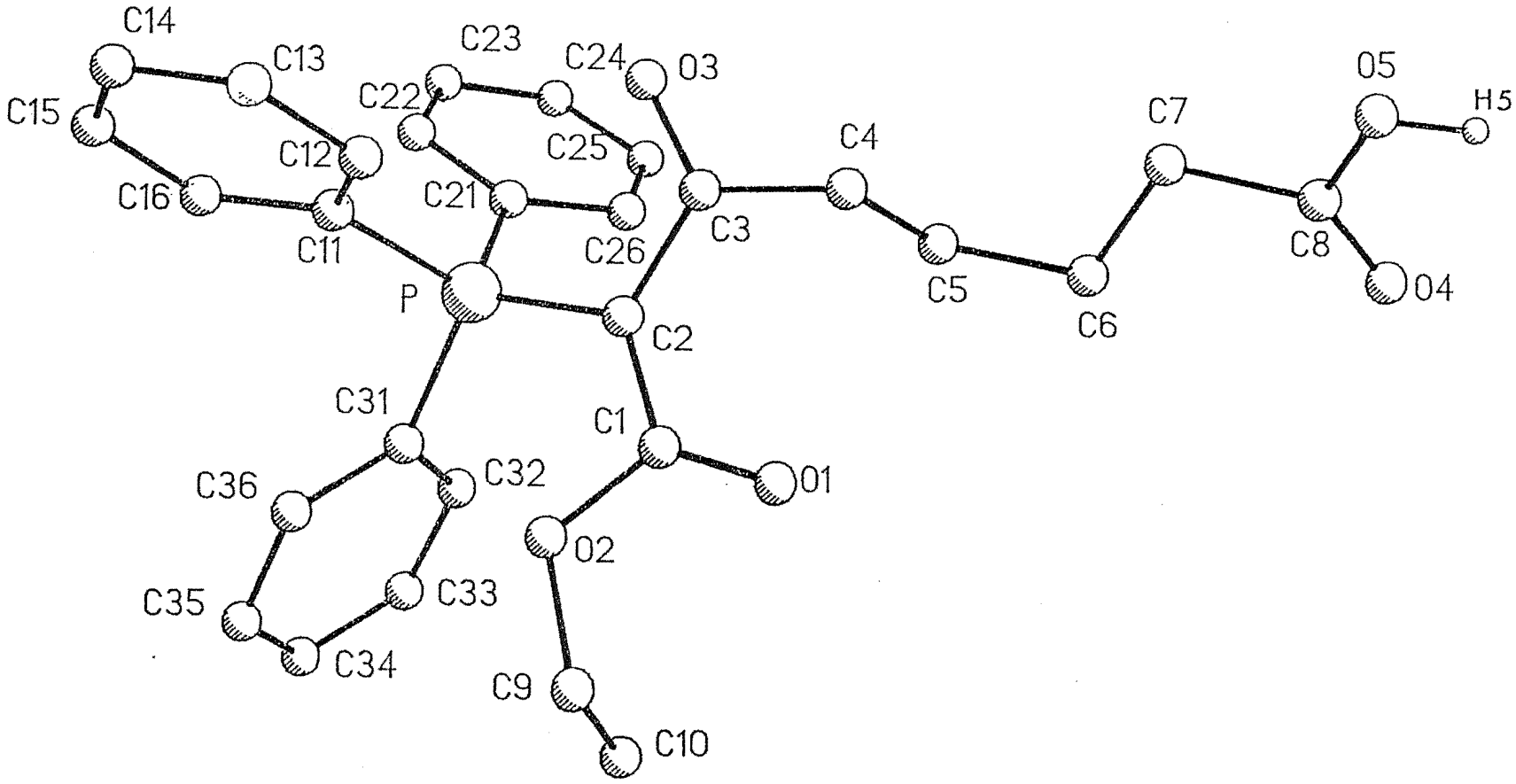

Figure 1.11: Perspective View and Atom Labelling for 1.10(akc) H5 was Inserted at a Calculated Position

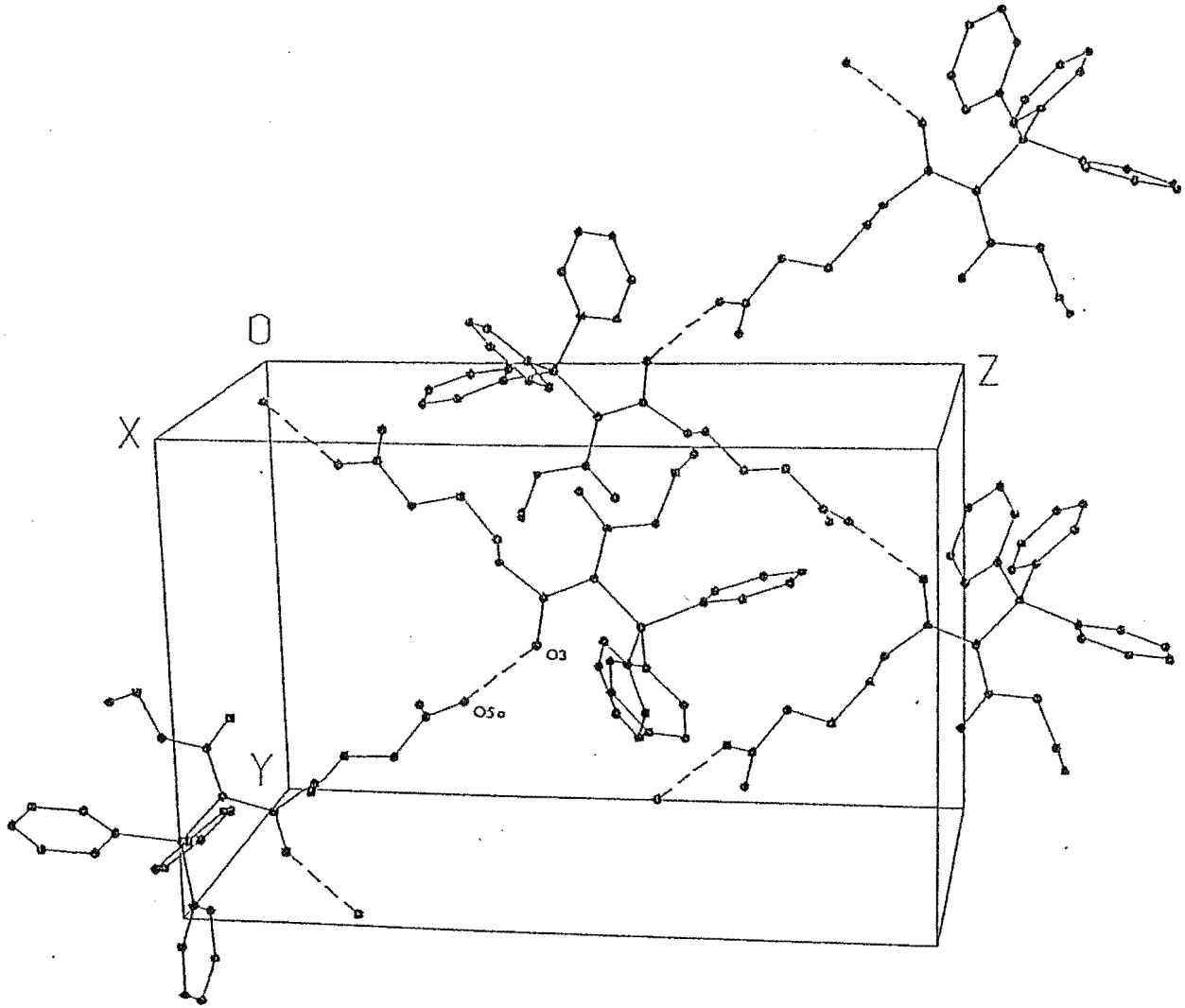

Figure 1.12: Packing Diagram For 1.10(akc) Showing Helices Generated by the Acid Carboxyl to Ketone Hydrogen Bonding.

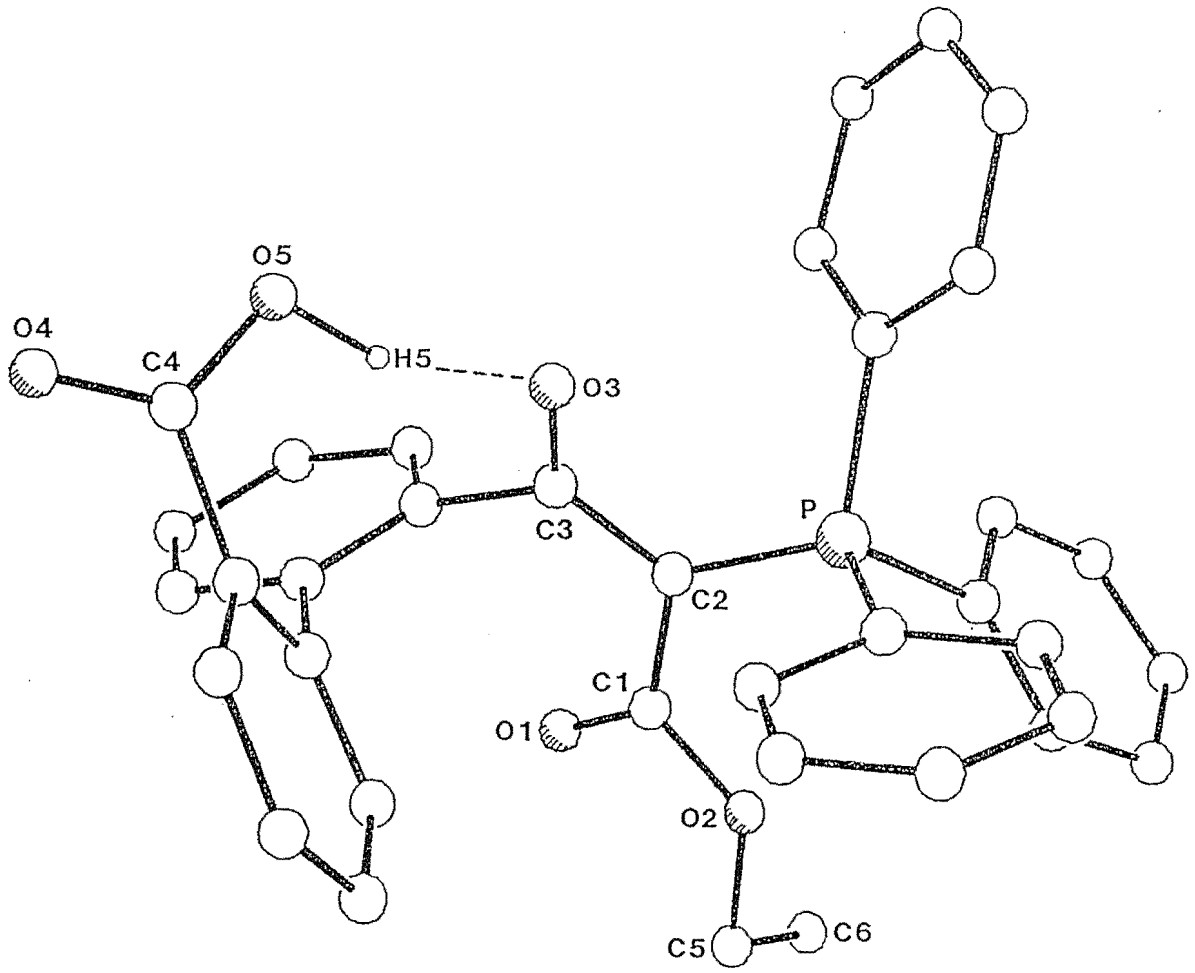

Figure 1.13: Perspective View and Atom Labelling for 1.11(aki) Showing Intramolecular Hydrogen Bonding

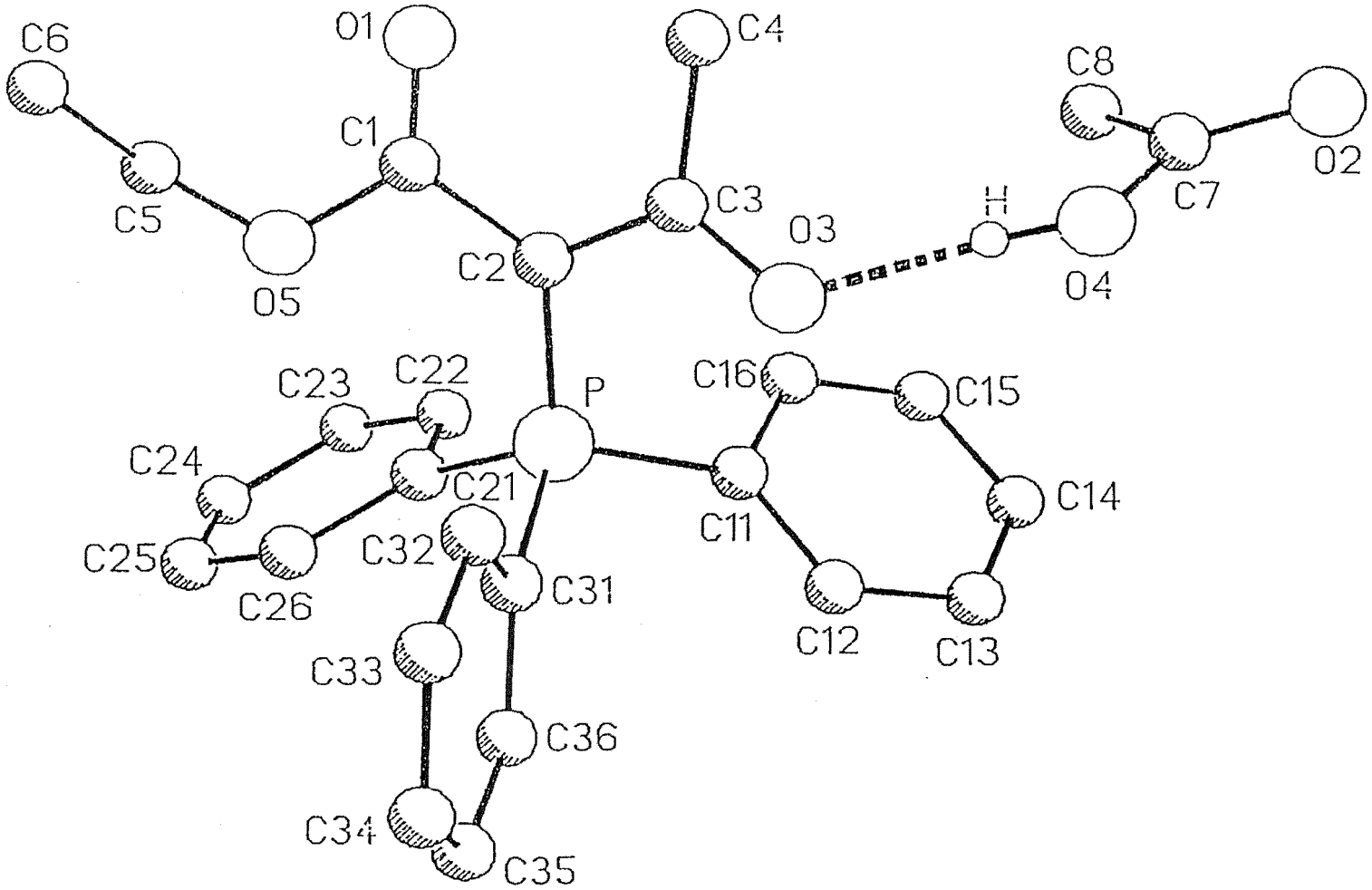

Figure 1.14: Perspective View and Atom Labelling for 1.13 Showing Intermolecular Hydrogen Bonding

Table 1.1. Selected Bond Lengths (Å) and Angles (degrees) for 1.9(aki) and 1.10(akc).

Geometry	Bond	**1.9**(aki)[a]	**1.10**(akc)
Distances	O(5)-H(5)	0.932(24)/0.932(51)	
	O(3)-H(5)[b]	1.670/1.618	
	O(3)-O(5)[c]	2.553/2.549	2.59
Angles	C(1)-C(2)-P	122.1(3)/126.4(4)	122.3(3)
	C(1)-C(2)-C(3)	122.8(3)/124.8(4)	124.1(4)
	C(3)-C(2)-P	114.7(3)/108.7(4)	113.1(3)
	C(2)-C(1)-O(1)	126.2(5)/125.7(5)	127.0(4)
	C(2)-C(1)-O(2)	111.0(4)/114.5(4)	111.6(4)
	C(2)-C(3)-O(3)	118.4(3)/119.8(4)	119.4(4)
	O(3)-C(3)-C(4)	117.8(4)/116.2(5)	119.2(4)
	C(3)-C(4)-C(5)	116.4(4)/113.8(3)	111.7(4)
	C(4)-C(5)-C(6)	113.1(4)/113.8(4)	112.7(5)
	C(5)-C(6)-C(7)	115.0(5)/114.0(3)	116.2(7)
	C(6)-C(7)-O(4)	122.3(5)/123.0(4)	
	C(6)-C(7)-O(5)	115.9(4)/117.2(4)	
	C(6)-C(7)-C(8)		115.1(7)
	C(7)-C(8)-O(4)		122.2(5)
	C(7)-C(8)-O(5)		113.4(5)
	C(7)-O(5)-H(5)	123.9(26)/106.1(27)	
	O(5)-H(5)-O(3)	156.7/175.8	
	C(3)-O(3)-H(5)	152.6/144.7	
Torsion Angles	P-C(2)-C(1)-O(1)	-149.9(5)/168.9(3)	168.2(5)
	P-C(2)-C(3)-O(3)	-0.9(7)/2.9(4)	7.5(6)
	O(4)-C(7)-C(6)-C(5)	-98.7(6)/99.1(5)	
	O(4)-C(8)-C(7)-C(6)		-147.6(6)
	O(1)-C(1)-C(2)-C(3)	38.5(9)/-6.6(6)	-20.9(9)
	O(3)-C(3)-C(2)-C(1)	171.3(5)/179.2(3)	-164.2(5)

a two crystallographically independent molecules (' values given second)
b hydrogen bond
c non-bonded interatomic distance

perhaps expected catemeric form (Figure 1.9) and a second most unusual acid carboxyl to ketone dimer resulting in a sixteen-membered ring (Figure 1.8). Hydrogen bonded rings, other than acid to acid pairing, are usually formed via intramolecular interactions, and it is significant that the vast majority are six-membered. Five-membered rings are rare but observed when linerality of the hydrogen bond is possible. There are few examples of other ring sizes known for simple molecules[1.5]. The sixteen-membered ring reported here is unique with no other examples of large hydrogen bonded rings of this size in simple molecules known to the author. The ketone O(3) to carboxyl O(5a) separation is 2.60Å for both structures and the hydrogen bond O(3)-H(5c)-O(5a) angle is 177.1° for the dimer and 177.5° for the catemer. Two other crystals of **1.8** and a subsequent crystal obtained from a sample recrystalised from ethyl acetate-light petroleum were consistent with the dimeric form unit cell dimensions. No further examples of the catemeric form were obtained. It is interesting to note that the unique sixteen-membered ring appears to form in preference to the expected catemer, even though the hydrogen bond angles (Table 1.2) and lengths for both forms are very similar. Crystal packing must therefore influence the mode of hydrogen bonding adopted. The mode of hydrogen bonding in the keto acid phosphoranes seems to be independent of the solvent of crystallisation. The glutaric derived phosphorane **1.8** crystalised in both a catemeric and a dimeric acid carboxyl to ketone hydrogen bonded form.

The X-ray crystal structure of the keto acid phosphorane **1.9**(aki), derived from 3,3-dimethylglutaric anhydride and crystalised from ethyl acetate-light petroleum, consisted of two well separated crystallographically independent molecules as shown in Figure 1.10. Torsional angles are given for both molecules in Table 1.1. Figure 1.10 shows intramolecular acid carboxyl to ketone hydrogen bonding (aki) resulting in an uncommon eight-membered ring, refer to previous

Table 1.2: Hydrogen Bond Angles (degrees) for Selected Phosphoranes.

Compound	C=O--O	=O--H-O
1.8(akc)	124.0	177.5
1.8(akd)	128.5	177.1
1.9(aki)	113.0/113.7	156.7/175.8

discussion. Ketone O(3) to carboxyl O(5) separation is 2.55/2.55Å and the O(3)-H(5)-O(5) angle is 156.7/175.8°. Presumably the dimethyl substitution makes both the catemeric and dimeric crystal packing observed for **1.8** less favoured. It is well documented that increased acyclic carbon chain substitution favours cyclisation[1.15].

The rigid constraints of the diphenyl group of **1.11** also facilitates solid state intramolecular acid carboxyl to ketone hydrogen bonding as evidenced[1.6] by a ketone O(3) to carboxyl O(5) separation of 2.67Å and an unusually large diphenyl dihedral angle of 99.4° (Figure 1.13). Intramolecular hydrogen bonding in this instance results in a chiral diphenyl as the formation of the bridging ring restricts rotation. The methylene protons at C(5) (Figure 1.13) become diastereotopic and are observed by ^{1}H NMR spectroscopy as a complex signal instead of the otherwise expected quartet for achiral esters. The methylene signal for the methyl ester analogue **1.12** gave a clean quartet, indicating free rotation around the central biphenyl bond on the ^{1}H NMR timescale. The methyl ester **1.12** cannot form the bridging ring via hydrogen bonding and hence is not chiral. The closeness in space of acid carboxyl and ketone groups due to the rigid constraints of a molecule does not necessarily

result in intramolecular hydrogen bonding. For example, the X-ray crystal structure of *cis*-3-acetyl-2,2-dimethylcyclobutane-acetic acid revealed acid carboxyl to ketone catemeric rather than intramolecular hydrogen bonding[1.16] (Figure 1.16).

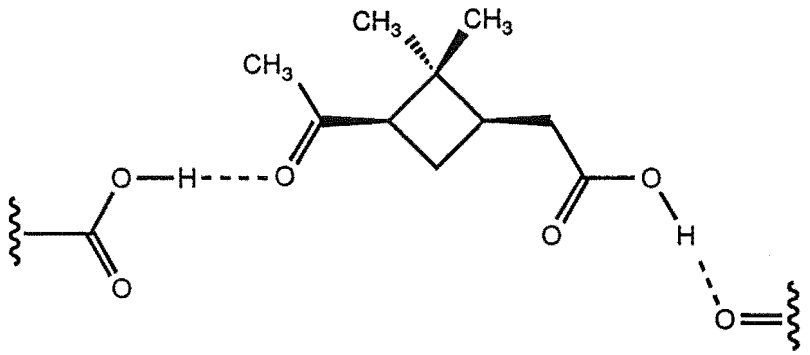

Figure 1.16: *Cis*-3-acetyl-2,2-dimethylcyclobutane acetic acid showing intermolecular Hydrogen Bonding (dashed lines to two other molecules).

The acetic anhydride derived keto acid phosphorane **1.13**[1.12] represents a related intermolecular association between two different molecules. This can be considered an example of a catemer with an infinite carbon chain length between the acid and ketone functionalities (Figure 1.14). The hydrogen bonding in keto acid phosphorane **1.13** would be expected to be optimal as there should be minimal steric interactions between participating groups. This is not supported by the =O--H-O angle of 172.9° and a C=O--O angle of 118.5°, compare the same angles for **1.8**(akc), **1.8**(akd), and **1.9**(aki) (Table 1.2). However, the acid carboxyl group is in the most unusual antiplaner conformation which could account for the deviation from the optimal angles.

The hydrogen bonds in the keto acid phosphoranes **1.7-1.11**, and **1.13** are consistently shorter, on average 1.6Å, and hence stronger, than the normal keto acid hydrogen bond of about 1.7Å[1.14]. It is possible to have

two hydrogen bonds to a carbonyl group if the substituents are small, clearly this is not the case for these phosphoranes, and was not observed.

Extensive delocalisation of the π system of the stabilised phosphorane moiety of **1.7-1.13** is possible. The possible canonical forms to represent this delocalisation are shown in Figure 1.17. The most common geometry, *synplaner* ketone and *antiplaner* ester, is observed in all but the phosphorane **1.12**. Consistent with other phosphoranes previously reported by this research group, the relatively long[1.12] P-C(2), C(1)-O(1), and C(3)-O(3) bond lengths for **1.9**(aki), **1.8**(akc) and **1.8**(akd) and the comparatively short[1.12] C(1)-C(2), and C(2)-C(3) bond lengths in **1.9**(aki), **1.8**(akc), and **1.8**(akd)(Table 1.3), are consistent with extensive phosphorane delocalisation. These bond lengths lay between those of a single and double bond and indicate partial double bond character due to delocalisation of the π system.

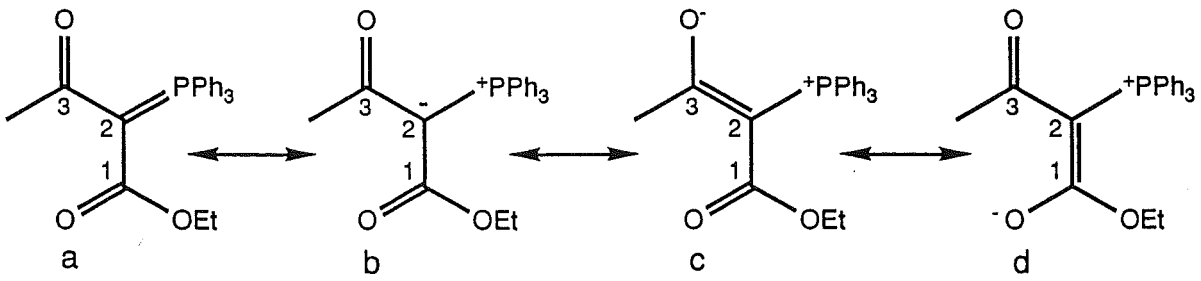

Figure 1.17: Canonical forms of the stabilised keto-phosphorane

The bond angles C(1)-C(2)-P, C(1)-C(2)-C(3), and C(3)-C(2)-P are also consistent with a distorted trigonal geometry about C(2) (Table 1.4). Compounds of the type **1.7-1.14** can exist as either a phosphonium salt or a phosphorane, Scheme 1.1. C(2) is tetrahedral sp^3 for a phosphonium salt, whereas it is trigonal sp^2 in the phosphorane. It has been shown[1.10] that **1.11** exists in solution as the phosphorane and in the solid state a

Table 1.3. Selected Bond Lengths for the Delocalised Phosphorane System.

Compound	P-C2	C1-C2	C2-C3	C1-O1	C3-O3
1.8(akc)	1.749(3)	1.450(4)	1.411(5)	1.213(4)	1.254(4)
1.8(akd)	1.768(2)	1.456(3)	1.416(3)	1.205(3)	1.253(3)
1.9(aki)[a]	1.767(4)	1.473(7)	1.404(6)	1.203(6)	1.280(5)
	1.773(4)	1.440(8)	1.410(8)	1.216(6)	1.282(6)

[a] bond lengths for both crystallographically independent molecules

(Note: Normal bond lengths (Å);P-C 1.86, P=C 1.66*, C-C 1.54, C=C 1.34, C=O 1.2, C-O 1.34. *Bond length for nonstabilised phosphorane.)

Table 1.4. Bond Angles (degrees) Showing the Distorted Trigonal Geometry of Phosphoranes.

	P-C(2)-C(3)	P-C(2)-C(1)	C(1)-C(2)-C(3)
1.8(akc)	112.0(2)	124.2(3)	123.7(3)
1.8(akd)	116.9(2)	119.5(2)	122.8(2)

distorted trigonal geometry about C(2) also indicates a phosphorane structure.

It is interesting to note that the stabilised phosphorane precursor (Figure 1.18) of α-Fluoro-β-keto esters existed in two geometrical isomers, observed by ^{19}F NMR, where the negative charge is localised on the oxygen[1,17]. This phosphorane is similar to those studied in this thesis.

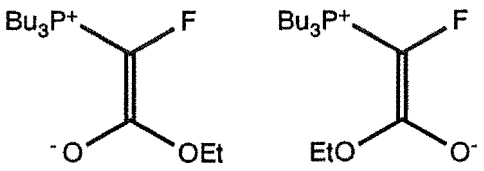

Figure 1.18

However, the added ketone functionality of **1.7-1.13** gives further delocalisation as evidenced by bond lengths (Table 1.3). Previous structural studies[1.17,1.18,1.19] on stabilised ylides have shown that both *cis* and *trans* forms are observed with rapid interconversion in the presence of trace acid[1.19] (Scheme 1.3).

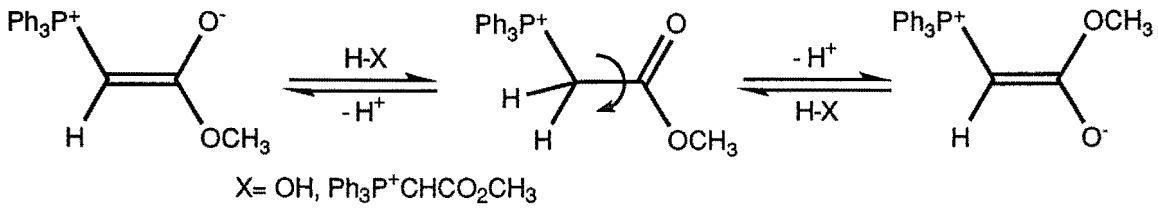

Scheme 1.3

The reactivity of the ylide $Ph_3PCHCO_2CH_3$ in the Wittig reaction is decreased upon removal of trace acid[1.19]. The ylide is most reactive under rapid *cis/trans* interconversion conditions as the negative charge is more available to the reactive carbon centre, resulting in enhanced nucleophilicity. The interconversion of the *cis/trans* forms of the phthalic anhydride derived phosphorane was found to be independent of trace acid. This is due to the presence of an acidic proton which autocatalyses the interconversion[1.19] (Scheme 1.4). The *cis/trans* forms of the ylide $Ph_3PCHCO_2CH_3$ were found to coalesce at 50°C with rigourous exclusion of trace acids either by drying or with addition of butyllithium. We observed the *cis/trans* isomers of $Ph_3PCHCO_2CH_2CH_3$ **0.1** in $CDCl_3$ (not rigourously

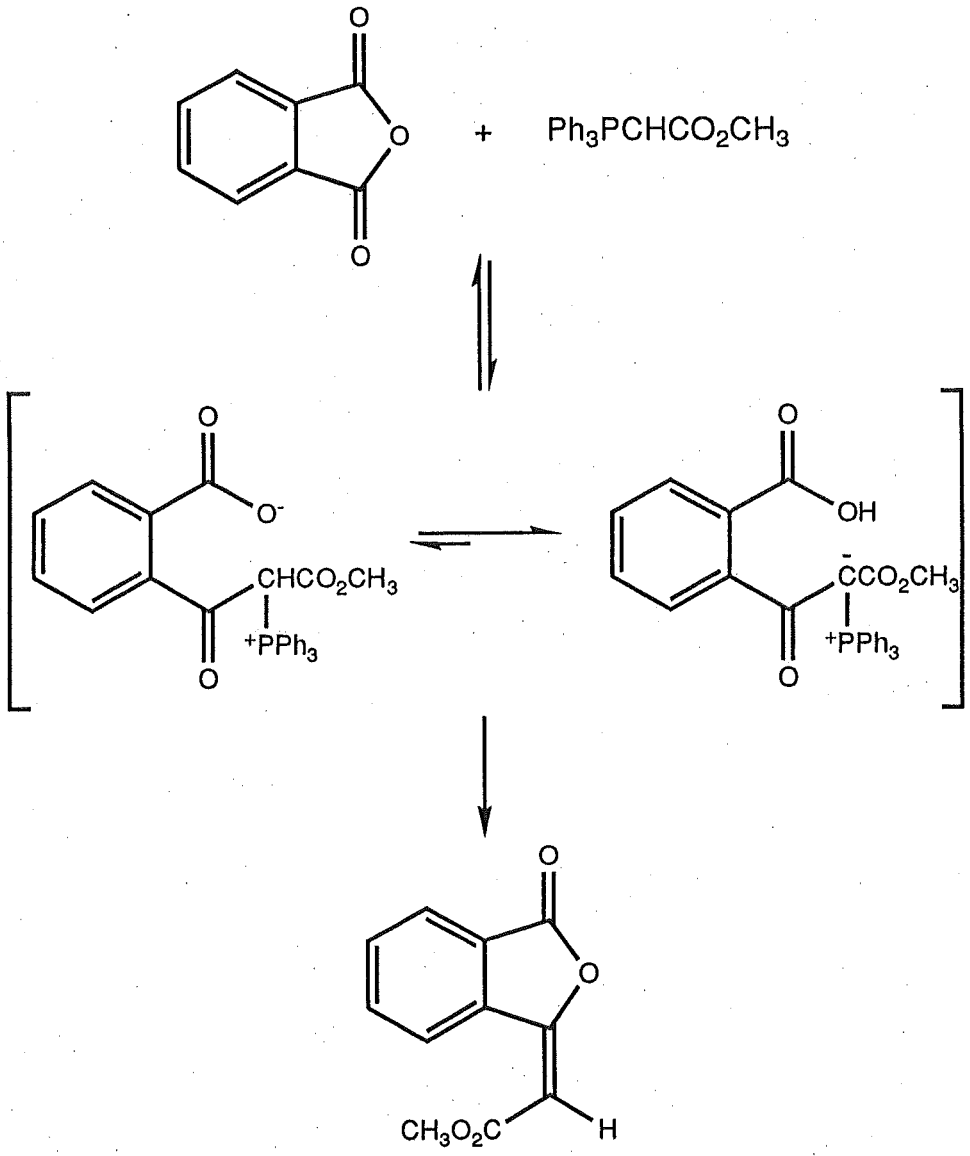

Scheme 1.4

dried) by ^1H and ^{31}P NMR spectroscopy and found a coalescence temperature of -22°C. A solvent effect on the ratio of *cis/trans* isomers has been reported[1.18]. Nonpolar solvents favour the *cis* isomer over the *trans*, whereas the reverse is true for polar solvents. The observed ratio of *cis/trans* isomers for the ylide $Ph_3PCHCO_2CH_2CH_3$ **0.1** in $CDCl_3$ is in agreement with the reported[1.18] value of 1.8.

The common *synplaner* carbonyl geometry for **1.7-1.11**, **1.13**, and **1.14**, and the less common *antiplaner* geometry for the ester of **1.12** is observed in the solid state. The canonical form (c) (Figure 1.17) would

appear to have a significant contribution to the resonance stabilisation, evidenced by the longer C(3)-O(3) bond in comparison with the C(1)-O(1) bond length. The deviation from planarity of the O(1)-C(1)-C(2)-C(3) torsional angle is significantly greater than the deviation for the O(3)-C(3)-C(2)-C(1) torsional angle (Table 1.5), which further supports this. The canonical form (c), with the negative charge localised on O(3), might be expected to enhance the hydrogen bonding basicity, and hence acid carboxyl to ketone hydrogen bonding. However, the C(3)-O(3) bond length of 1.256(4)Å for the acid carboxyl dimer **1.7**(aad) is not significantly shorter than C(3)-O(3) bond lengths in the acid carboxyl to ketone intramolecular hydrogen bonded dimer **1.8**(akd) 1.253(3)Å and catemer **1.8**(akc) 1.254(4)Å. The C(3)-O(3) bond lengths of the acid carboxyl to ketone intramolecular hydrogen bonded **1.9**(aki) and **1.11**(aki), of 1.280(5)/1.282(6) and 1.270Å respectively, are longer than **1.7**(add), **1.8**(akc) and **1.8**(akd). This indicates a possible balance between a greater contribution by the resonance form (c) and a gain in steric strain on forming a large ring. It would appear that chain length and steric considerations are major factors in determining the type of hydrogen bonding.

Some deviation from planarity, about the resonance stabilized phosphorane moiety of **1.7-1.14** is evident from the torsional angles (Table 1.5). The least deviation is evident when the ketone O(3) is not involved in hydrogen bonding as in **1.7**(aad) and **1.14**. However, a significant deviation from planarity is apparent when O(3) is involved in hydrogen bonding as in **1.8-1.11** and **1.13** (Table 1.5). The acid to carbomethoxy intermolecularly hydrogen bonded phosphorane **1.15** is also reported to show a greater deviation from planarity than the *tert*-butyl ester analogue **1.16**[1.20].

Table 1.5:. Magnitude[a] of O(1), O(3) and P deviation from planarity (°) for the stabilized phosphoranes **1.7-1.14**.

Torsion Angle	No H-bonding			Intermol. H-bonding				Intramol. H-bonding	
	1.14	**1.7**(aad)	**1.12**	**1.8**(akd)	**1.8**(akc)	**1.10**(akc)	**1.13**	**1.9**(aki)[b]	**1.11**(aki)
O(1)-C(1)-C(2)-C(3)	3.1	20.5	29.9	20.3	28.5	20.9	26.3	38.5/6.6	22.9
P-C(2)-C(1)-O(1)	9.5	6.4	32.1	9.6	25.2	11.8	27.3	30.1/11.1	18.2
O(3)-C(3)-C(2)-C(1)	4.5	15.4	2.2	14.7	0.2	15.8	7.3	8.7/0.8	30.1
P-C(2)-C(3)-O(3)	1.1	2.8	0.1	4.3	3.1	7.5	8.3	0.9/2.9	10.9
Average	4.6	11.3	16.1	12.2	14.3	14.0	17.3	19.6/5.4	20.5

[a] calculated from respective torsion angles

[b] two crystallographically independent molecules (' values given second)

The extent of deviation from planarity about the resonance stabilized phosphorane within the intermolecular hydrogen bonded examples **1.8**, **1.10** and **1.13**, shows some correlation with increasing carbon chain length between the acid and ketone groups. Intramolecular hydrogen bonding (aki) gives the most significant deviation from planarity as in **1.11** and one of the two crystallographically independent molecules of **1.9** (Figure (1.10a)) (see Section 1.3 for supportive infrared evidence). The second molecule of **1.9** (Figure (1.10b)) compensates for the lack of deviation of phosphorane planarity with an almost linear intramolecular hydrogen bond [O(5)-H(5)-O(3) 175.8°]. The two crystallographically independent molecules of **1.9** vary greatly in bond and torsional angles about the hydrogen bond. The first molecule fits into the pattern of an increase in deviation from planarity of the keto phosphorane moiety for intramolecular hydrogen bonding, see torsional angles (Table 1.5), yet the second molecule has significantly less deviation from planarity. This reflects the fact that intramolecular hydrogen bonding, and the resultant ring, are sufficiently flexible to accommodate two independent conformers. The unusually large ester carbonyl O(1) deviation from planarity for the methyl ester **1.12** [P-C(2)-C(1)-O(1) 32.1°] is misleading since **1.12** is unique in that O(1) is *syn* to P[1.6]. In all the other keto acid phosphoranes O(1) is *anti* to P. The ketone O(3) is *syn* to P in all structures **1.7-1.14**.

A number of other features from the X-ray structures of the keto acid phosphoranes are worth noting. The O(4)-C(7)-C(6)-C(5) torsion angle of -98.7°/99.1° for **1.9**(aki) and the O(4)-C(6)-C(12)-C(11) torsion angle of 128.1° for **1.11**(aki) (Figure 1.11) is consistent with distortion of the *synplanar* arrangement reported for carboxylic acids[1.13], a result of intramolecular hydrogen bonding. The catemeric form of **1.8**(akc) is again unusual in that it too has a large O(4)-C(7)-C(6)-C(5) torsion angle (49.8°). The corresponding torsion angles for **1.7**(aad) -20.6°, **1.8**(akd) 17.6° and **1.10**(akc) -147.6° are closer to the normal *synplanar* arrangement. The

expected[1.13] *synplanar* geometry for the carboxyl group (HO-CO-) is apparent in the structures of **1.7**(aad), **1.8**(akd), **1.10**(akc) while the much less common *antiplanar* arrangement is apparent for the intramolecular hydrogen bonded **1.9** and **1.11** and more surprisingly for **1.13** and **1.8**(akc) (*synplanar* geometry is observed for other reported examples of acid to ketone catemeric hydrogen bonding[1.5]). The catemer **1.10**(akc) has hydrogen bonded helixes of the same handedness along screw axis of axial length 6.8Å. Whereas the catemer **1.8**(akc) has the hydrogen bonded chains situated on an n glide plain of axial length 6.3Å. The normal triphenylphosphoranylidine propeller arrangement is observed in all of the phosphoranes studied.

1.3: Infrared and Raman Spectroscopy of Keto Acid Phosphoranes

Solid state infrared spectroscopy has been used to determine crystalline hydrogen bonding modes where hydrogen bonding produces frequency shifts for both the ketone and carboxylic acid carbonyls[1.5,1.21]. Problems have been encountered with this approach since other factors such as strain and conjugation can contribute to frequency shifts. Recently, a comparison of infrared and Raman spectroscopy has been used to determine the solid state hydrogen bonding patterns in carboxylic acids[1.5,1.21]. We chose to study the infrared and Raman spectra of the keto acid phosphoranes **1.7-1.11** and **1.13** as they represent a closely related series of keto carboxylic acids that give predictable modes of hydrogen bonding. In the past isolated examples and the comparison of structurally dissimilar compounds have been used to rationalise the mode of hydrogen bonding adopted by keto carboxylic acids.

The use of Raman spectroscopy in organic chemistry, although not routine, can be used in combination with infrared spectroscopy to provide information that is otherwise only obtained from X-ray crystallography or neutron diffraction experiments. Raman spectroscopy relies on the principle of an inelastic collision of a photon with a molecule[1.22]. The photon undergoes an energy change to promote or demote the molecule into a higher or lower rotational or vibrational state, respectively. On the other hand, infrared spectroscopy is complementary to Raman in that an absorption phenomenon which changes the molecules rotational or vibrational states. For a molecular vibration to be infrared active it must undergo a change in the dipole moment, but for a molecular vibration to be Raman active it must undergo a change in the polarisability. Carbonyl stretching frequencies of keto acids are ideal for observation due to symmetric and antisymmetric modes of vibration which can be either infrared active or Raman active.

A summary of the solid state infrared and Raman carbonyl stretching frequencies for the keto acid phosphoranes **1.7-1.11** and **1.13** is given in Table 1.6. The ketone carbonyl and the acid hydroxyl, but not the acid carbonyl, are involved in hydrogen bonding in all but **1.7**(aad). The acid carbonyl stretching frequency for **1.7**(aad) is observed at 1705 cm^{-1}, consistent with a normal acid to acid dimer[1.16,1.23], while the same absorption for **1.8-1.11** and **1.13** is observed at a higher frequency but still lower than in gas-phase acid monomers[1.16]. The conjugated ketone and ester carbonyl stretching frequencies for **1.7**(aad), **1.8**, **1.10**(akc) and **1.13** are coincident. The intramolecular hydrogen bonding (aki) in **1.9** and **1.11** disrupts the extended phosphorane conjugation (see earlier for a discussion). The result is a carbonyl absorption shift towards 1700 cm^{-1} and hence three distinct carbonyl absorptions are observed. Consistent with this is the fact that the ester and ketone carbonyl stretching

frequencies are coincident at 1670 cm^{-1} for **1.12**[1,6] which can not display intramolecular hydrogen bonding.

For the centrosymmetric carboxylic acid dimer **1.7**(aad) the vibrational coordinates of the acid carbonyl groups within the hydrogen bonded ring should couple to give both infrared and Raman active modes. The symmetric stretching mode is infrared inactive due to no change in the dipole moment, but Raman active due to a change in the polarisability. The reverse is true for the antisymmetric stretch which is Raman inactive and infrared active. The coupling of the two carbonyls depends on both the symmetry and the alignment of the vibrational modes. The centrosymmetric eight-membered ring of **1.7**(aad) would be anticipated to give strong coupling, and indeed we observe a frequency difference of some 45 cm^{-1} (Table 1.6). Several other acid dimers frequency differences have been reported[1,5], which lie in the range of 30-82 cm^{-1}. The frequency of the ketone remains the same as it is not involved in the hydrogen bonding.

For the low-symmetry, crystalline keto acid phosphoranes **1.9**(aki), **1.10**(akc), **1.11**(aki) and **1.13**, the acid carbonyl stretching frequencies in the Raman spectra are very similar to those in the infrared (Table 1.6). The ketone carbonyl and acid hydroxyl in each of these systems are involved in intermolecular catenation or intramolecular hydrogen bonding and vibrational coupling between the acid carbonyl groups should be weak due to both asymmetry and poor alignment. These frequency differences compare well with reported[1,5] frequency differences for non-acid dimer hydrogen bonded keto acid of 1-10 cm^{-1}.

The infrared and Raman frequencies obtained from a single crystal of the acid carboxyl to ketone hydrogen bonded dimer of **1.8**(akd), although centrosymmetric, differ by only 2 cm^{-1}. The poor coupling of the same order of magnitude as that found in the non-centrosymmetric catemeric species, is a consequence of vibrational alignment and the

Table 1.6: Solid-State Infrared (KBr) and Raman (Glass Capillary) Carbonyl Stretching Frequencies for the Keto Acid Phosphoranes 1.7-1.11, and 1.13

Compound	Infrared (cm^{-1})[a]		Raman (cm^{-1})[a]		Δ (cm^{-1})
	acid	ketone/ester	acid	ketone/ester	for acid
1.7(aad)	1705	1666	1660	1660[b]	45
1.8(akd)	1723	1670	1721	1667	2
1.9(aki)	1726	1675, 1687	1723	1665, 1682	3
1.10(akc)	1719	1677	1716	1671[b]	3
1.11(aki)	1731	1657, 1689	1726	1655, 1689	5
1.13	1735	1676	1727	1674[b]	8

[a] frequencies ± 3 cm^{-1}

[b] acid/ketone/ester carbonyl stretching frequencies coincide

separation (7.379 Å) of the acid carbonyls O(4) and O(4a). A sample of a population of crystalline **1.8** gave identical acid carbonyl stretching frequencies by infrared and Raman spectroscopy to the single dimeric crystal. It is unclear as to the catemeric content of this sample. Unfortunately the Raman and infrared spectra of a single crystal of the catemeric form of **1.8** could not be obtained.

1.4: Summary

The X-ray crystal structure of 3,3-dimethyl-6-ethoxycarbonyl-5-oxo-6-(triphenylphosphoranylidene)hexanoic acid **1.9** and 7-ethoxycarbonyl-6-oxo-7-(triphenylphosphoranylidene)heptanoic acid **1.10** revealed acid to ketone intramolecular and catemeric hydrogen bonding, respectively. Intermolecular hydrogen bonding for the related **1.7**, **1.8** and **1.13** and intramolecular hydrogen bonding for **1.11** are consistent with the length and substitution of acid to ketone carbon chain. Raman and infrared spectroscopy have also been used to differentiate the centrosymmetric and vibrationally coupled acid to acid dimeric hydrogen bonding of the keto acid phosphorane **1.7** from the alternative modes of acid to ketone hydrogen bonding found in **1.8-1.11** and **1.13**.

Synthesis and Bromolactonisation of Keto Acid Phosphoranes

Chapter 2

Synthesis of Succinic Bromo Enol Lactones

2.1: Introduction

Many naturally occurring enol lactones, for example ylidenebutenolides[0.12], have been synthesised using the reaction of an anhydride with a stabilised phosphorane as a key step. Mechanistic studies[2.1] have shown that acyl phosphoranes of the type **0.3** are often observed as intermediates in this reaction. The simplest ylidenebutenolide that has been isolated is protoanemonin **2.1**[0.12]. Other natural ylidenebutenolides have also been isolated, for example freelingyne **2.2**[2.2], the first known acetylenic sesquiterpenoid. Natural ylidenebutenolides have been reported to exhibit biological activity. For example, the potent antibiotic fungal toxin Patulin[0.12]**2.3**, the antibacterial Tetrenolin[2.3] **2.4**, and the compound that is characteristic of butter flavour, Bovolide **2.5**[2.4].

A subclass of the naturally occurring enol lactones, the ynenol lactones[0.12], for example **2.6** and **2.7** possess important biological activity. The ynenol lactone **2.8**[0.12] has a strong growth inhibitory effect on plants. These molecules have also been reported to act as mechanism-based inactivators of specific serine protease enzymes, for example **2.9**[2.5] inhibits

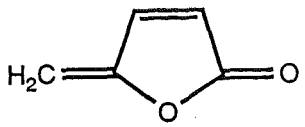

2.1

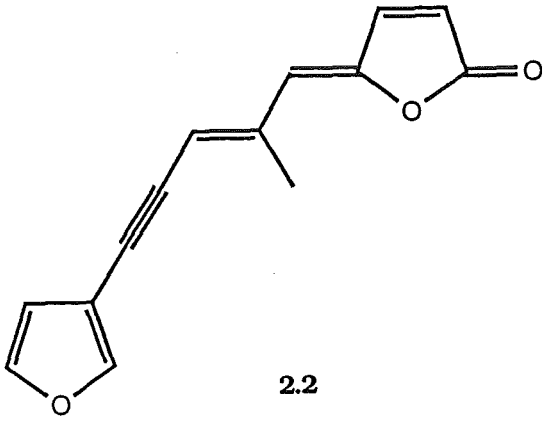

2.2

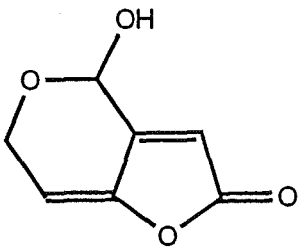

2.3

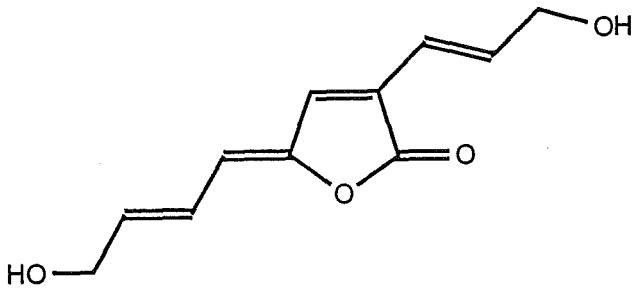

2.4

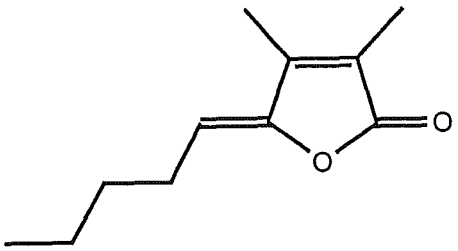

2.5

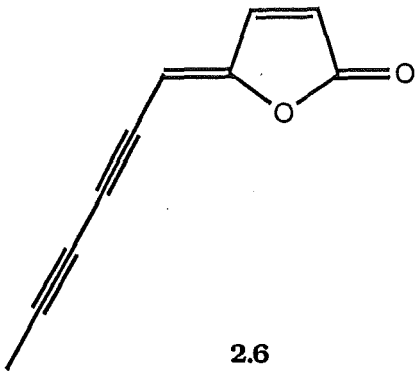

2.6

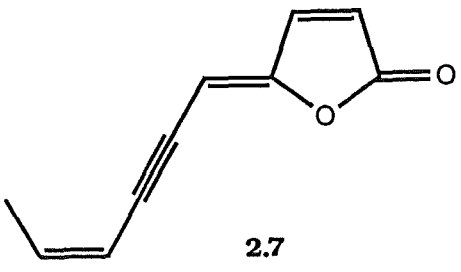

2.7

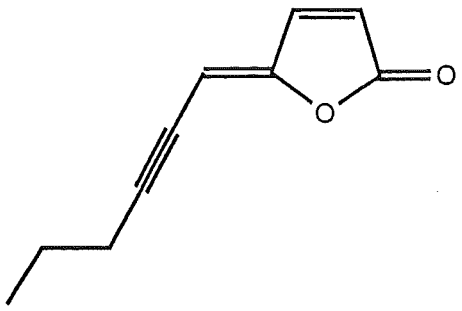

2.8

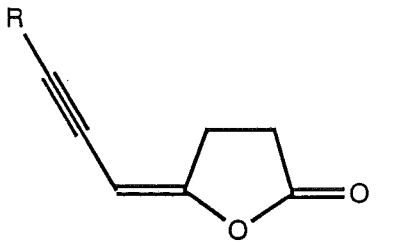

R = H, CH_2Ph, *i*-Pr, *n*-Bu

2.9

Human Leukocyte Elastase.

Halo enol lactones, for example the fimbrolanes[2.6] **2.10**, are another subclass of naturally occurring enol lactones. This class has also been developed to give mechanism-based inactivators of serine proteases[0.14,0.15] (see Introduction for brief discussion).

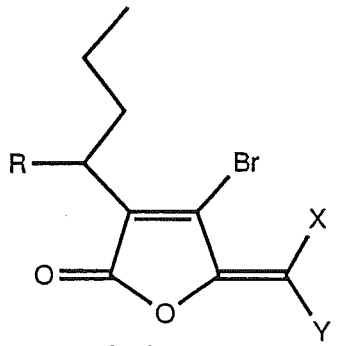

2.10

R = OAc, OH		R = H	
X	Y	X	Y
Br	H	Br	H
H	Br	H	Br
I	H	Br	Br
H	I		
Cl	H		
H	Cl		
Br	Br		

Mechanism-based inactivators show therapeutic potential as they provide a highly specific means of controlling enzyme activity. The cell degradative disease Emphysema has been linked[2.7] to the enzyme Human Leukocyte Elastase which has subsequently been therapeutically targeted by mechanism-based inactivators. In recent years halo enol lactones[0.14,0.15] have gained considerable attention as potential mechanism-based inactivators of the major pancreatic serine proteases, for example

chymotrypsin and the above mentioned Human Leukocyte Elastase. Consequently, halo enol lactones have attracted considerable synthetic interest. A new synthetic approach to halo enol lactones is presented in this Chapter while possible applications to the mechanism-based inactivation of serine proteases are discussed in more detail in Chapter 5.

2.2: Syntheses of Halo enol lactones

There are a number of known syntheses of halo enol lactones. The formation of enol lactones and halo enol lactones from acetylenic acid precursors via mercury mediated lactonisation[0.14] is well established and yields mixtures of *E*- and *Z*-isomers, Scheme 2.1. Both bromo enol lactones and chloro enol lactones **2.11** have been prepared in moderate yield[0.14] using this procedure, Scheme 2.1. The synthesis of halo enol lactones by the direct mercury mediated cyclisation of halo acetylenic acids proves less efficient than the analogous preparation of enol lactones, Scheme 2.1 (R≠halogen). The transition metal complex $[(cycphos)RuCl]_2$[2.8] has been used to produce exclusively *Z*-enol lactones and the corresponding endo isomer as a by-product (itself thought to be biologically active), Scheme 2.2. Direct halogenation of H- enol lactones to produce the corresponding halo enol lactones has yielded limited success[0.14]. Two isolated examples of this are shown in Scheme 2.3, but this procedure has not been proven to be generally applicable (see Section 2.4: New Synthesis of Bromo Enol Lactones).

Several halogenating agents have been used for the halolactonisation of acetylenic acids. N-halosuccinimides[0.14] (bromo, chloro, iodo) yield exclusively the *E*-stereoisomer (Scheme 2.4). Although there is one report of a small amount of the *Z*-isomer being produced for N-iodosuccinimide[0.14]. Iodine itself has proven to be an effective

Scheme 2.1

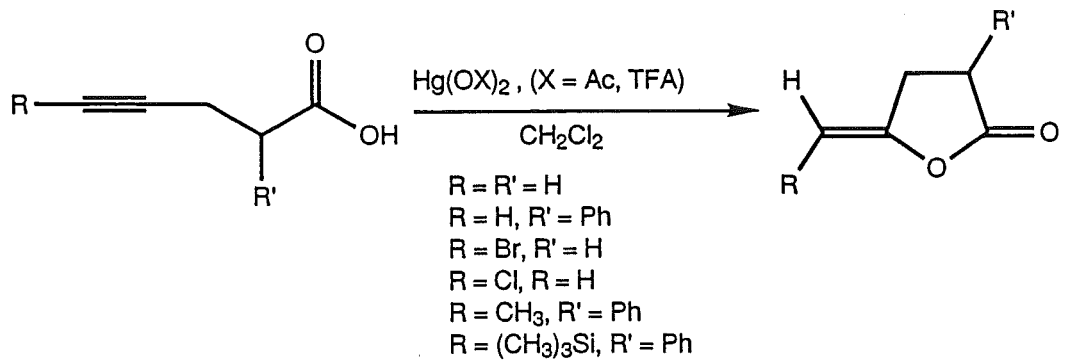

Scheme 2.2

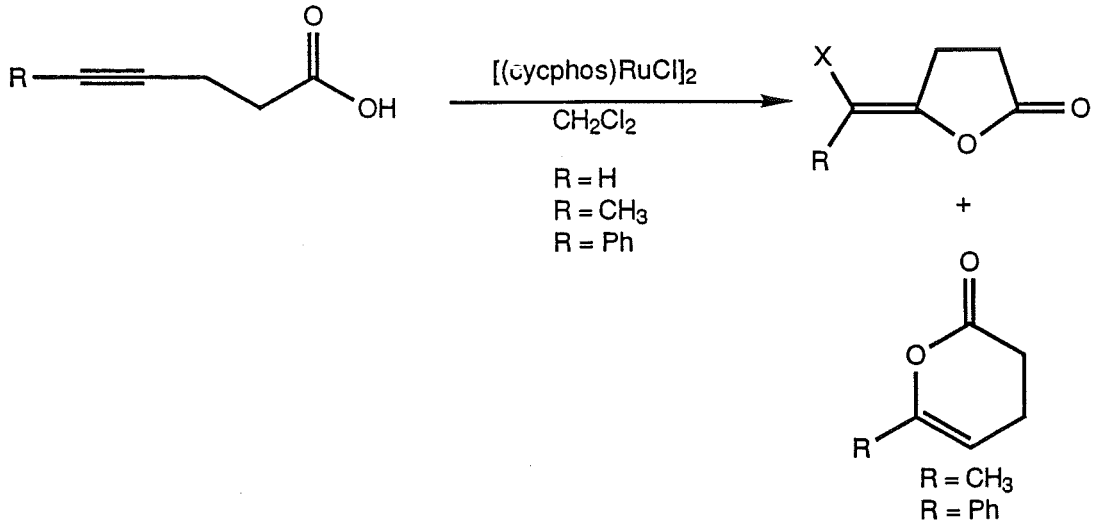

Scheme 2.3

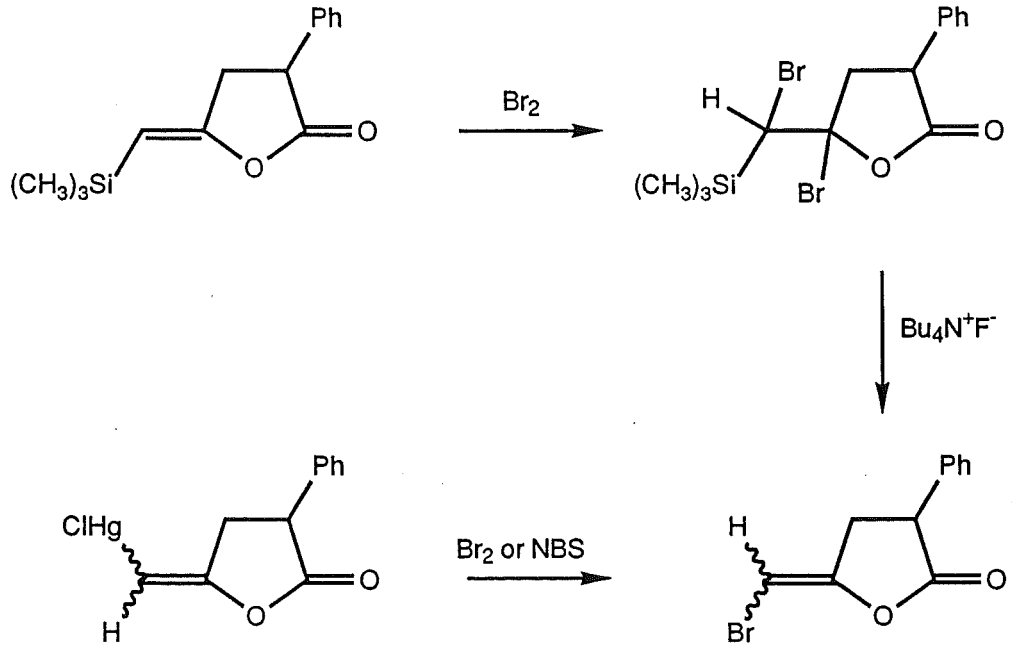

halogenating agent in aqueous conditions[2.9]. The *E*-iodo enol lactone predominates (Scheme 2.5), although only one example has been reported. *E*-iodo(III) enol lactones[2.10] of the type **2.12** have also been prepared using iodosylbenzene (Cl_2IPh) and BF_3-Et_2O (Scheme 2.6). The iodo(III) enol lactones and the normal enol lactones behave similarly in hydrolysis studies. The iodo(III) enol lactones and the iodo enol lactones undergo nucleophilic attack at the lactone carbonyl. Ring opening to reveal an electophilic carbon, is followed by nucleophilic attack (Scheme 2.7). This series of reactions mimics the proposed mechanism of halo enol lactone inactivation of serine proteases[0.13,0.14] (see Introduction, Figure 0.7).

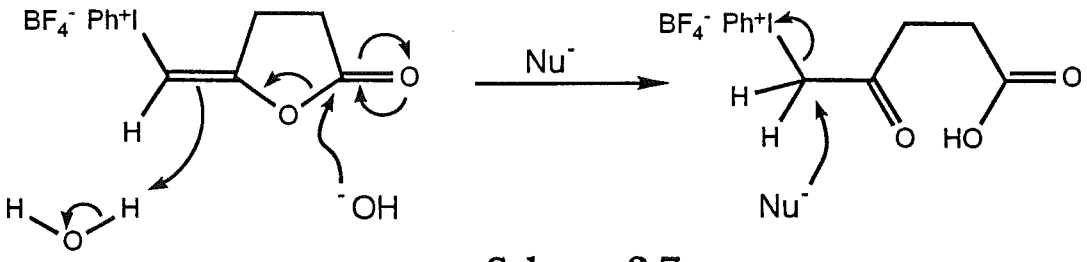

Scheme 2.7

Finally, dehydration of bromo ketone acids[0.14,2.11] has been used to produce *Z*-bromo enol lactones but only on very limited examples (Schemes 2.8 and 2.9).

The disadvantage of these syntheses is that they lack versatility and generality and often give access to only one geometrical isomer. The precursors are also often time consuming and synthetically difficult to prepare. For these reasons we decided to develop a synthesis based on the Wittig anhydride olefination reaction[0.11]. The classical Wittig carbonyl olefination reaction involves the condensation of an aldehyde or ketone with a phosphorus ylide to give an alkene[0.4], Scheme 2.10 and Introduction.

Scheme 2.4

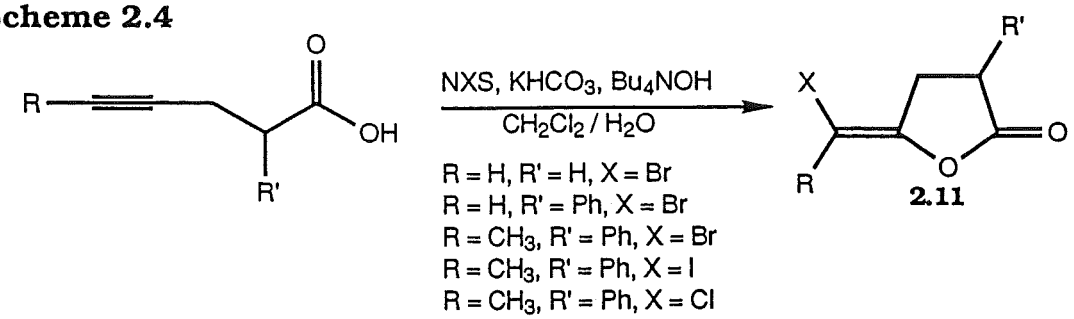

2.11

Scheme 2.5

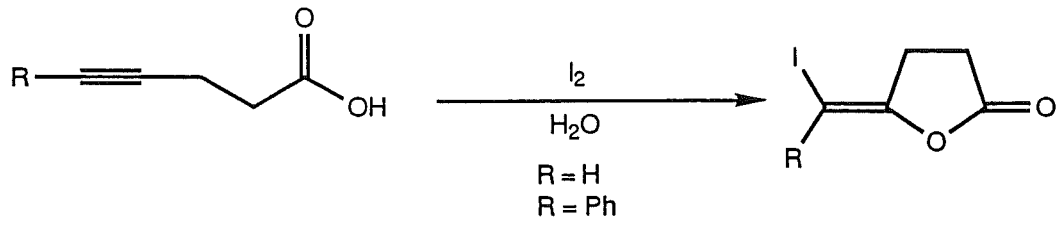

Scheme 2.6

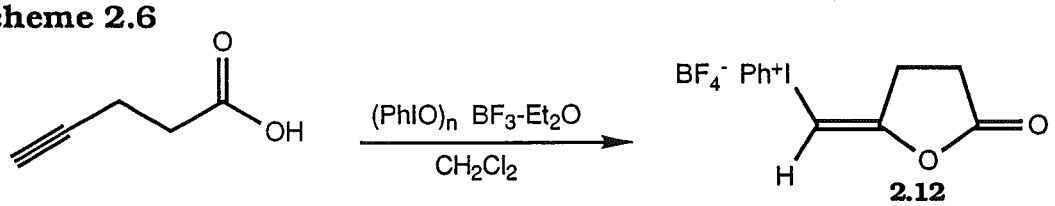

2.12

Scheme 2.8

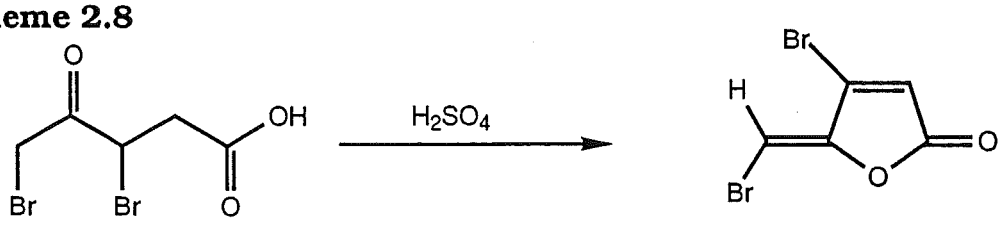

Scheme 2.9

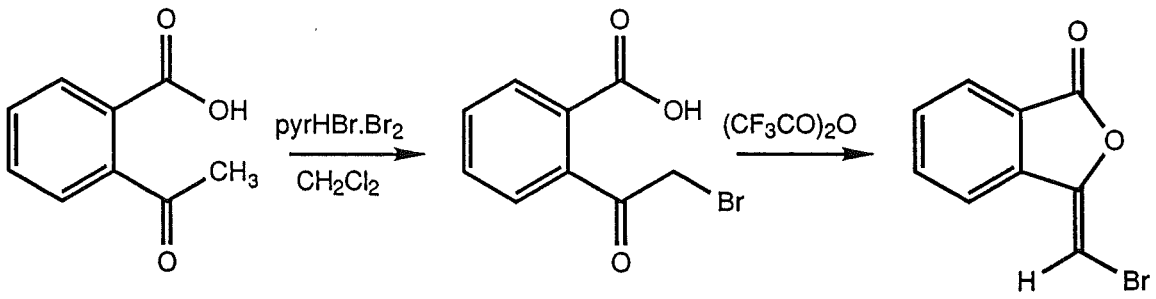

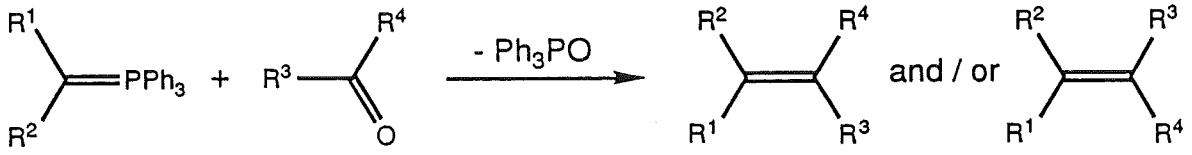

Scheme 2.10

As mentioned in the Introduction, the Wittig reaction has also been extended to several other types of carbonyl containing compounds, for example amides[0.5], anhydrides[0.5], esters[0.5], imides[0.5,2.12] and thiolesters[0.5] (Scheme 2.11a-e). The Wittig reaction between an anhydride and a stabilised ylide to give enol lactones is a viable synthesis that offers the advantages of generality and ease of performance (see Section 2.3.3). The developed procedures have enabled entry into five-, six-, and the previously unknown seven-membered ring halo enol lactones as well as phthalic based examples.

2.3: Wittig Carbonyl Olefination Reaction

The Wittig reaction can be divided into three classes on the basis of the reactivity of the phosphorus ylide. The ylides are classified as stabilised, semistabilised, and nonstabilised, on the basis of the substituent on the nucleophilic carbon (C1), Figure 2.1. For a detailed discussion see Introduction. Stabilised ylides have strongly conjugating substituents, for example X and/or Y = CO_2R, CN, and SO_2Ph, and generally produce *E*-alkenes on reaction with aldehydes and ketones[2.13]. Semistabilised ylides have mildly conjugating substituents, for example phenyl (Ph) or allyl, and often show no stereochemical preference[0.3]. Nonstabilised ylides lack such functionalities and generally produce *Z*-alkenes[2.13]. The greater the ylide stabilisation the lower it's reactivity. The reactivity of the ylide is also

Scheme 2.11

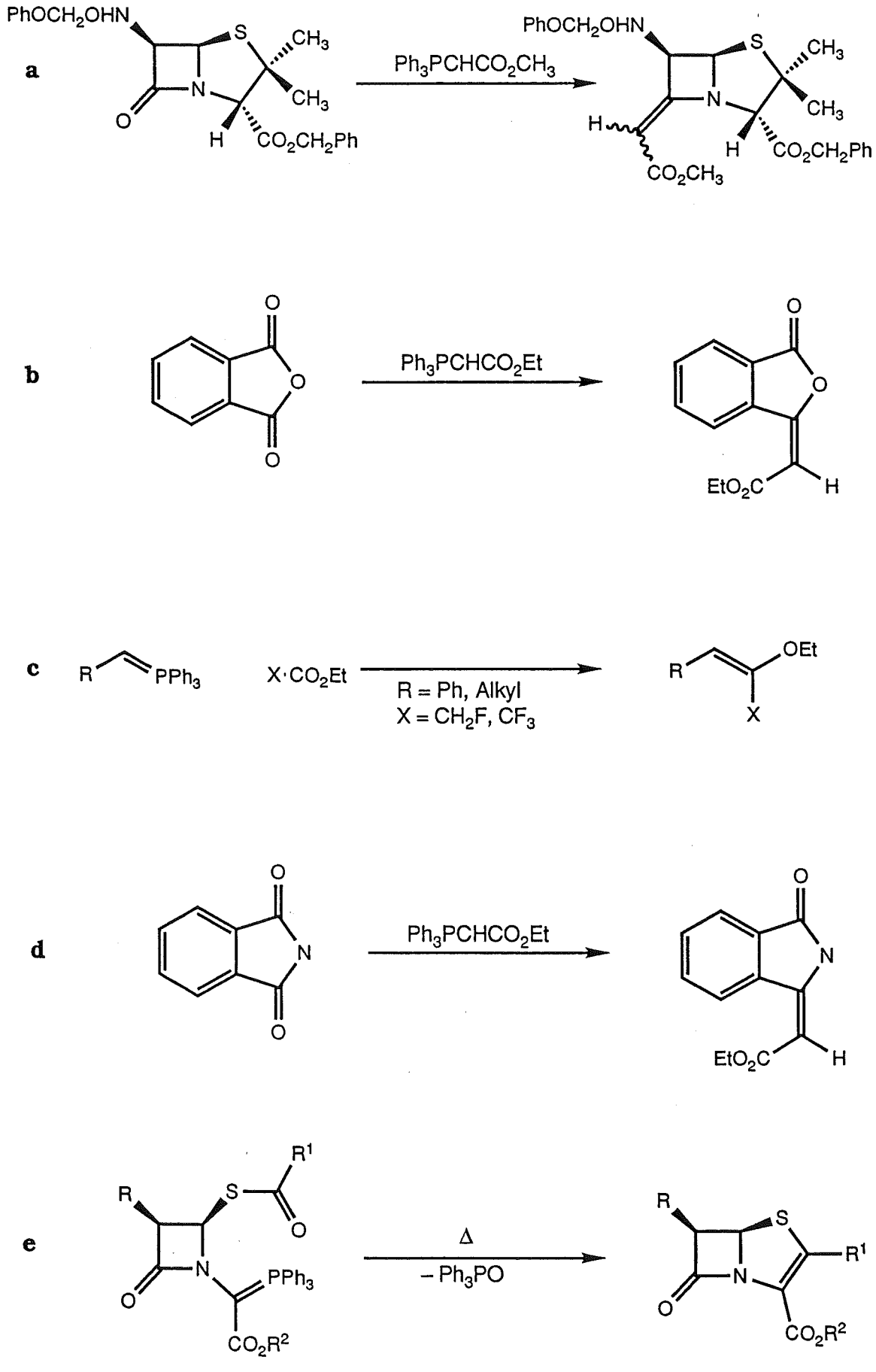
a
PhOCH2OHN
S
CH3
CH3
N
O
H
CO2CH2Ph
Ph3PCHCO2CH3
PhOCH2OHN
S
CH3
CH3
H
N
H
CO2CH2Ph
CO2CH3
b
O
O
O
Ph3PCHCO2Et
O
O
EtO2C
H
c
R
PPh3
X·CO2Et
R = Ph, Alkyl
X = CH2F, CF3
OEt
R
X
d
O
N
O
Ph3PCHCO2Et
O
N
EtO2C
H
e
R1
R
S
O
N
O
PPh3
CO2R2
Δ
– Ph3PO
R
S
R1
N
O
CO2R2

dependent on the substituents on the phosphorus, R^1, R^2, and R^3. The most common ylides have $R^1 = R^2 = R^3 = Ph$.

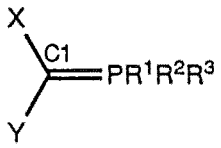

Figure 2.1

2.3.1: Wittig Reaction with Nonstabilised Ylides

The mechanism of the Wittig carbonyl olefination reaction is still under investigation some 38 years after it's discovery[0.4] and is far from totally understood. In particular, the nature of the mechanistic intermediates and the stereocontrol of the reaction are being investigated[0.6]. A number of mechanisms have been proposed for the Wittig reaction ranging from a one electron transfer[2.14] to a concerted [2+2] cycloaddition.

Wittig initially proposed a cyclic four-membered intermediate[0.4] (the oxaphosphetanes **2.15, 2.16** in Scheme 2.12), but subsequently favoured a zwitterionic phosphorus betaine[2.15] (**2.13** and **2.14** in Scheme 2.12) based on experimental evidence. The formation of stable lithium halide - betaine salts[0.6] and the trapping of β-hydroxy phosphonium salts[0.5] with acid at low temperature supported the betaine as an intermediate of the Wittig reaction. However, there is a lack of direct evidence for uncomplexed betaines.

The advent of ^{31}P NMR spectroscopy proved significant in the study of the reaction mechanism and the detection of reaction intermediates. The quadracoordinate phosphorus betaine, and the pentacoordinate phosphorus oxaphosphetane, give vastly different ^{31}P NMR chemical

Scheme 2.12: Classical Wittig Carbonyl Olefination Reaction

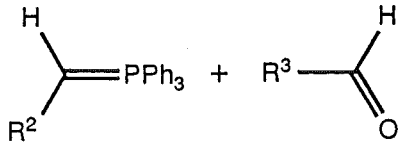

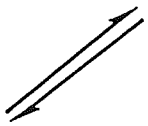

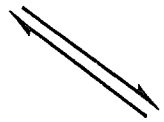

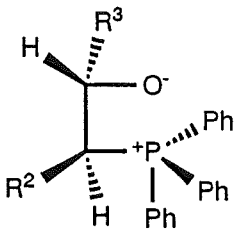

trans betaine
2.13

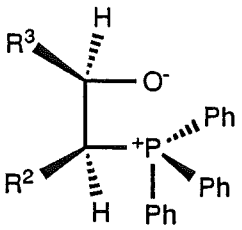

cis betaine
2.14

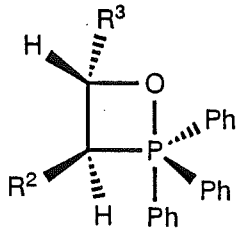

trans oxaphosphetane
2.15

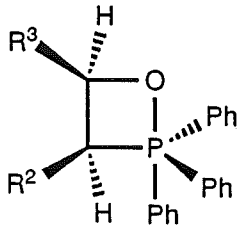

cis oxaphosphetane
2.16

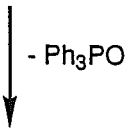

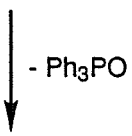

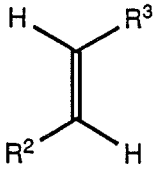

trans olefin

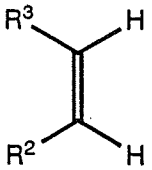

cis olefin

shifts[0.9]. Vedejs[2.16] has demonstrated by low temperature ^{31}P NMR that the oxaphosphetane is the only observable, and therefore the principle, intermediate in the reaction of nonstabilised ylides and aldehydes. Maryanoff[0.5,2.17] has also observed the *cis* and *trans* oxaphosphetanes **2.15** and **2.16** as the only intermediates. These results do not rule out the betaine as an intermediate. Rather, the oxaphosphetane is the only observable intermediate and hence it's decomposition is rate determining. Several model oxaphosphetanes, for example **2.17**[2.18] and **2.18**[2.19], have been synthesised and structure data has been gathered.

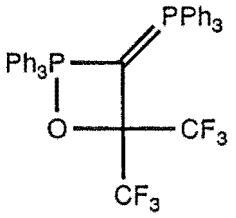

2.17

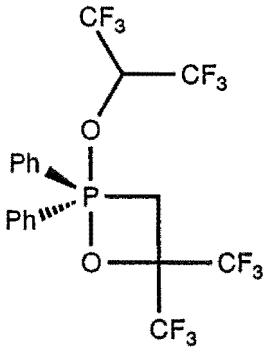

2.18

Bestmann[2.20] postulated an alternative mechanism (Scheme 2.13) in which the oxygen derived from the carbonyl group is thought[2.20] to occupy an apical (axial) position on the phosphorus as in **2.19**. A ligand reorganisation of the subtituents on the phosphorus via psuedorotation[2.21] must take place in order for the elimination of triphenylphosphine oxide to occur. This is related to apical entry/apical departure for nucleophilic substitution reactions at pentacoordinate (trigonal bipyradal) phosphorus[2.20]. The oxaphosphetane **2.20** represents a crucial intermediate in this reaction. Psuedorotation of oxaphosphoranes has been shown to be a dynamic process occurring 10^8 times faster than

Scheme 2.13: Bestmann Mechanism for the Wittig Reaction

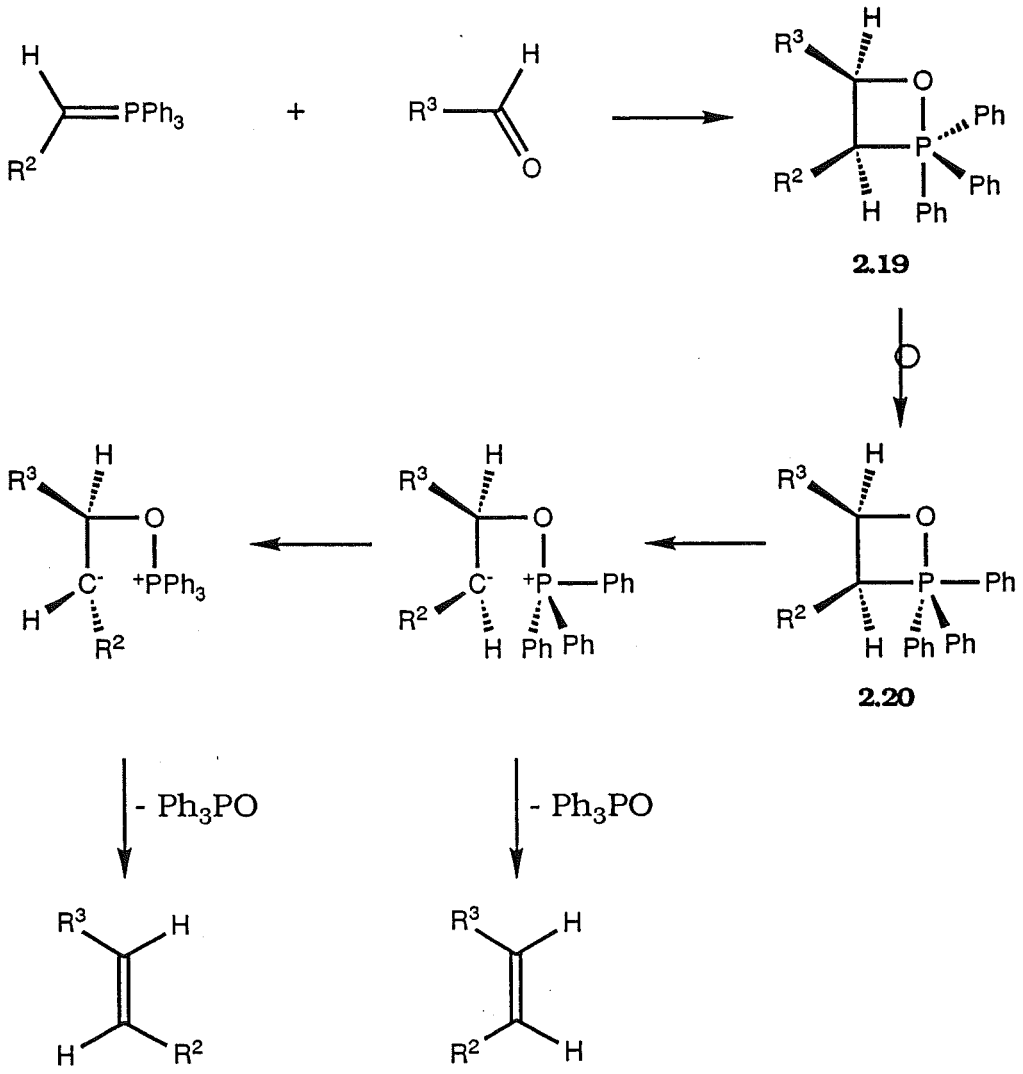

decomposition of the oxaphosphetane[2.16].

Recently, a [2+2] concerted reaction mechanism[2.17] for the Wittig carbonyl olefination reaction has also gathered support. An orthogonal ($\pi 2_s + \pi 2_a$) condensation has been proposed to account for the high *Z*-stereoselectivity (Scheme 2.14) observed for the more reactive nonstabilised ylides.

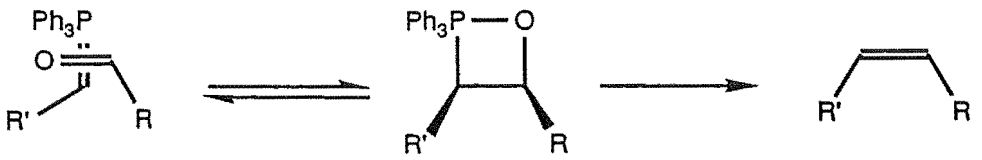

Scheme 2.14

The stereochemistry of the alkenes produced is of great interest and relies on the relative rates of decomposition of the two diastereomeric oxaphosphetanes. This suggests[0.6] that the decomposition of the oxaphosphetanes is a kinetic pathway. The reaction of a nonstabilised ylide with an aldehyde often preferentially produces the thermodynamically less stable *Z*-alkene. This has been attributed to the *cis* disubstituted oxaphosphetanes decomposing faster than the *trans* isomers. The formation of the oxaphosphetane, from the nonstablised ylide and aldehyde, is in principle reversible. To explain the anomalous high *E*-stereochemistry of some nonstabilised ylides with aldehydes, the concept of stereochemical drift[0.6] was introduced. Stereochemical drift was attributed largely to the faster rate of reversal of the *cis* oxaphosphetane to regenerate ylide and aldehyde, relative to the *trans* oxaphosphetane. A sizable portion of the *E*-stereoselectivity observed with trialkylphosphorus ylides and ylides bearing anionic groups is associated with thermodynamic control via reaction reversal. Wittig reactions that experience a significant measure of thermodynamic control are the exception rather than the rule[0.6].

2.3.2: Wittig Reaction with Stabilised Ylides

A number of mechanisms for the reaction of a stabilised ylide with aldehydes have been proposed[0.6]. Mechanistic and kinetic studies have given little evidence for the postulated oxaphosphetane or betaine

intermediates. Kinetic studies have, however, indicated that the rate determining step involves the condensation of the stabilised ylide with the aldehyde. The mechanism for a stabilised ylide reaction is thought to be similar to that of the nonstabilised ylide[0.6]. The initially formed betaine rapidly forms the corresponding oxaphosphetane which then decomposes almost exclusively to the *E*-alkene. The initial ylide attack on the aldehyde is not reversible and hence the stereochemistry could therefore depend on the initial formation of the betaines. Also, inclusion of the Bestmann type intermediate would allow stereochemical equilibrium such that a preferential decomposition of the *trans*-disubstituted oxaphosphetane would explain the high *E*-alkene selectivity[0.6].

A coplaner ($_{\pi}2_{s}$ +$_{\pi}2_{a}$) cycloaddition mechanism[2.22] has also been proposed to account for the high *E*-stereoselectivity observed (Scheme 2.15) for the reaction of a stabilised ylide and an aldehyde. The P-O and C-C bonds form to different extents depending on the aldehyde and phosphorus substitution.

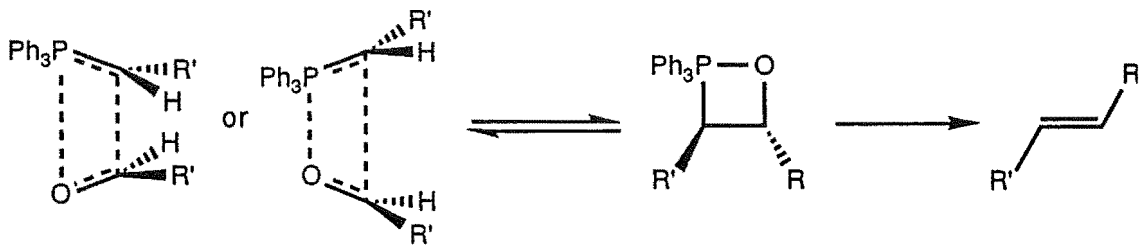

Scheme 2.15

2.3.3: Wittig Anhydride Olefination Reaction

The Wittig reaction between an anhydride and a stabilized ylide has been relatively uninvestigated with regard to its mechanism[2.1,2.23,2.24]. This reaction, unlike the Wittig carbonyl olefination reaction, proceeds via

a stable intermediate phosphorane[2.1]. The formation of the intermediate would indicate that its subsequent reaction is rate determining. The mechanism proposed[2.1] (Scheme 2.16) is similar to the commonly accepted Wittig carbonyl olefination mechanism (Scheme 2.12). However, an alternative ring opening pathway can occur to produce an initial and unstable acyclic phosphonium salt **2.21** which rapidly tautomerises to the more stable phosphorane **2.22**. X-ray crystallography[1.10] and NMR studies[1.10] have shown that the phosphorane **2.22** is the favoured form in the solid and solution phase. The reaction of the ylide **0.1** with succinic anhydride to give the phosphorane **1.7** has been shown to be irreversible[2.1]. Therefore, the stereochemistry of the product enol lactones **2.27** and/or **2.28** must be determined by either the ratio of the initially formed betaines **2.23** and **2.24**, the relative rates of triphenylphosphine oxide loss from the oxaphosphetanes **2.25** and **2.26** or the relative rates of phosphonium salt cyclisation. The reaction (Scheme 2.16) would allow equilibration of the two oxaphosphetanes **2.25** and **2.26**. Therefore, the products might be expected to be those that are thermodynamically most stable, assuming the stability of the product is reflected in the stability of the oxaphosphetanes. Equilibrium studies[2.1] on the product enol lactones have shown this not to be the case. Equilibrium of the oxaphosphetanes would not be possible if the loss of triphenylphosphine oxide was rapid relative to the formation of the oxaphosphetanes. Thus the enol lactone product would not necessarily be the thermodynamically most stable. The ratio of the *E*- and *Z*-enol lactones **2.27** and **2.28** would then be a consequence of the relative amounts of the two oxaphosphetanes **2.25** and **2.26** or betaines **2.23** and **2.24**. The rate of cyclisation of the phosphonium salt to the respective betaine may therefore determine the overall reaction rate. The steric and electronic effects in the two cyclisation transition states would then be

important. The enol lactone product[2.1] obtained from succinic anhydride is exclusively the *E*-stereoisomer **2.27**, which is consistent with the rate of

Scheme 2.16: Mechanism of the Wittig Succinic Anhydride Olefination Reaction

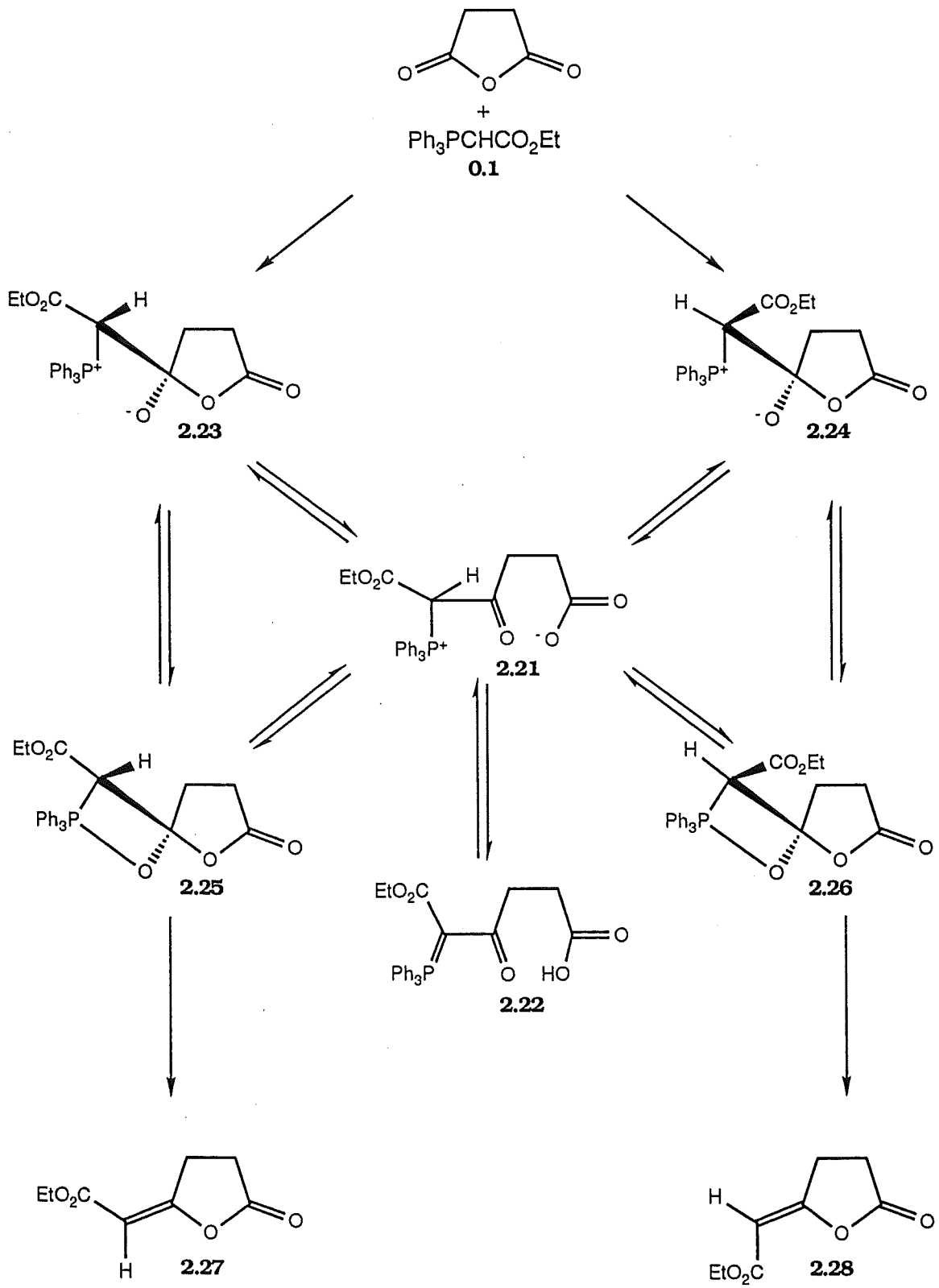

cyclisation of the *E*-transition state **2.29** being faster than the *Z*(**2.30**). The *E*-cyclisation transition state (Figure 2.2) carbonyl would be more open to carboxylate attack than in the corresponding *Z*-transition state, since the ethyl ester sterically hinders the carboxylate approach.

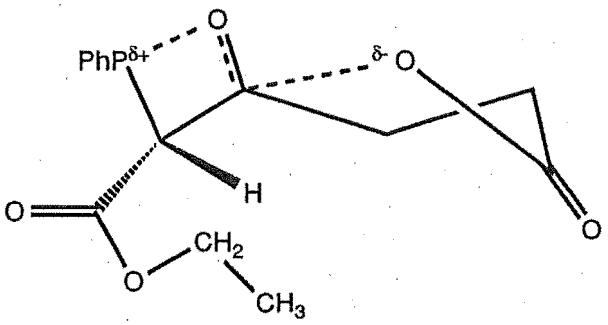

E-transition state **2.29**

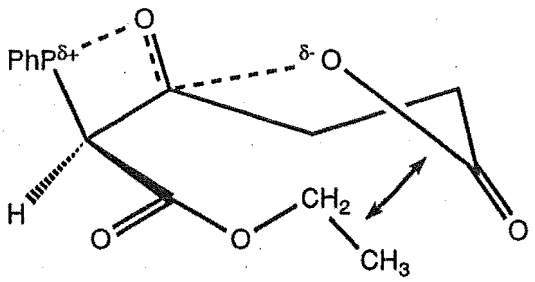

Z-transition state **2.30**

Figure 2.2

2.4: A New Synthesis of Bromo Enol Lactones

The first reported reaction between an anhydride and a stabilised ylide was in 1965 by Chopard[2.25]. Massey-Westrop's group initiated detailed studies of this reaction[0.11] in 1969. The intermediacy of the acylphosphoranes in this reaction has only recently been firmly established. The synthesis of H-enol lactones from these phosphoranes

(see Section 2.3.3) is still being investigated and a significant number of enol lactones[2.1,2.23,2.24,2.26] have been synthesised using this route.

We decided to utilise the established chemistry[2.1] of the phosphorane systems to introduce a halogen into the stabilised ylide, for example $Ph_3PCBrCO_2Et$ **2.31**, and hence into the product enol lactone. The aim was to develop a new general and versatile synthesis of halo enol lactones. Unfortunately the reaction of succinic anhydride with bromo ylide **2.31** did not proceed and gave only starting material. Halo ylides are known[0.3] to be less reactive due to decreased nucleophilicity at C-1, the site of reaction. We reasoned that an independent synthesis of the proposed intermediate phosphonium salt **2.32** would avoid the initial and presumably slow step of ylide attack on the anhydride and hence permit the synthesis of the desired bromo enol lactones (Scheme 2.17). Indeed, the direct introduction of one equivalent of bromine to the succinic derived phosphorane in CH_2Cl_2 gave bromo enol lactones **2.33** and **2.24** in low yield. The same reaction at 0°C with an equivalent of triethylamine present gave a high yield of the bromo enol lactones **2.33** and **2.34**, 77%. The reaction gave both the *E* **2.34** and *Z* **2.33** bromo enol lactone geometrical isomers in a ratio of 7:3, respectively. Interestingly, the brominating agent pyridinium bromide perbromide worked as efficiently in the preparation of bromo enol lactones. Phosphonium salts of the type **2.21** have never been observed but have been implicated[2.1,2.27] in a number of reactions. The bromophosphonium salt **2.32**, if formed, would be expected to cyclise rapidly on the basis of model studies[1.11]. See Section 2.4.3. for a more detailed mechanistic study.

Scheme 2.17 : Mechanism of the Bromolactonisation of the Succinic Derived Phosphorane 2.22

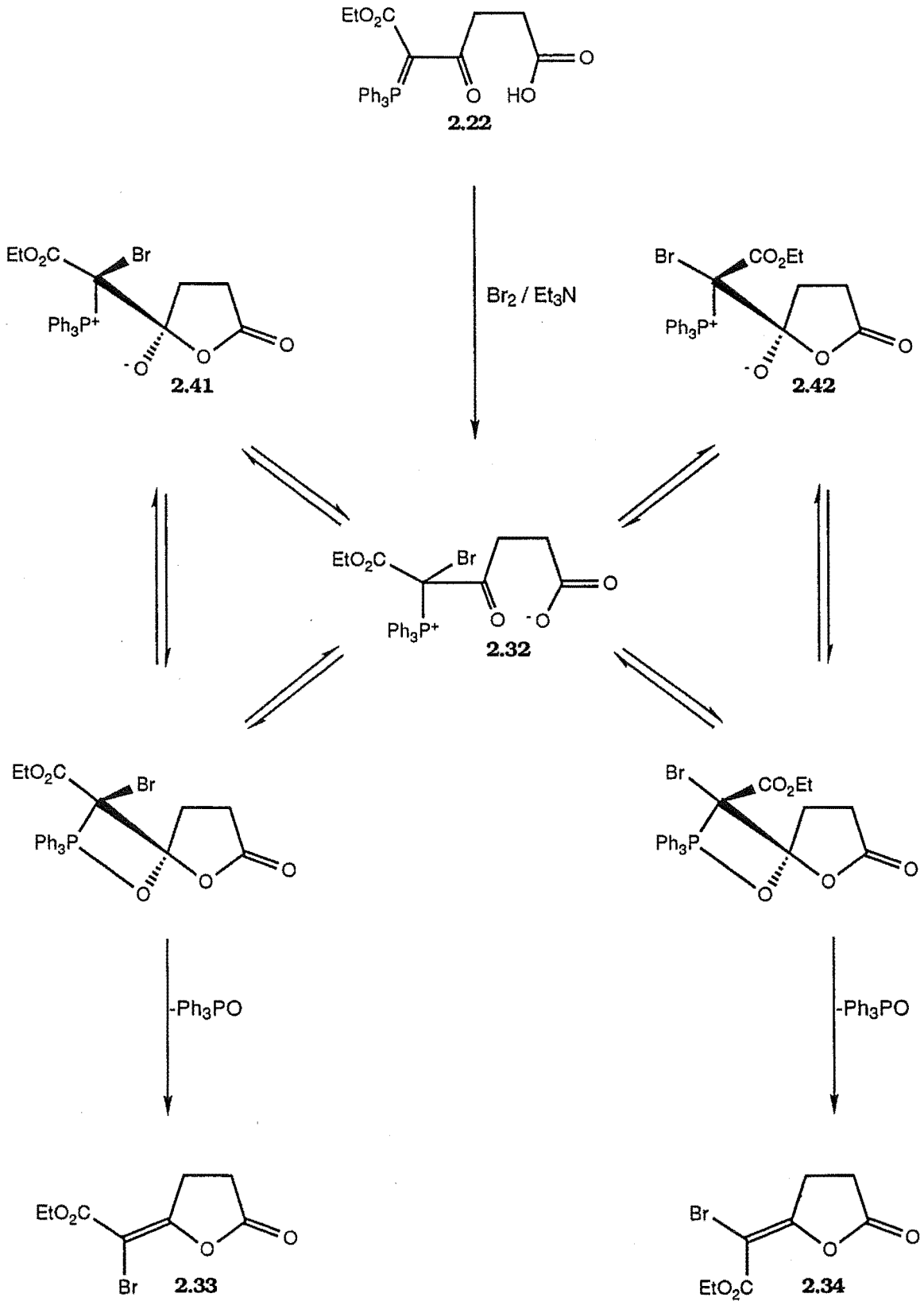

2.4.1: SCOOPY Reaction

The above reaction of the phosphorane **2.21** and Br_2/Et_3N represents an extension of the α-***s***ubstition plus ***c***arbonyl ***o***lefination via β-***o***xido ***p***hosphorous ***y***lides, commonly known as the SCOOPY reaction[2.28], Schemes 2.18, 2.19. The lithium phosphonium salt **2.35**, produced via reaction of the ylide Ph_3PCHR with aldehyde R'CHO followed by treatment with butyllithium, reacts with an electrophile X^+ to produce the phosphonium salt **2.36**. Subsequent loss of triphenylphosphine oxide yields the alkene **2.37**. Examples of the electrophiles X^+ used in this reaction are given in Table 2.1. The fluoridating agent[2.28a] $FClO_3$ and chlorinating agent[2.28a] Cl_2IPh generally produced a mixture of geometrical isomers. The brominating agent[2.28a] Br_2 gave a low yield of the *cis* isomer of **2.27**. It is interesting to note that there is little stereocontrol when R=H, and a high preference for the *cis* halo alkene when R=alkyl. Corey[2.28d] applied the SCOOPY reaction to the synthesis of **2.38**, **2.39**, and **2.40**, Scheme 2.19. Halogenation[2.28d] by Cl_2 gave the *cis* isomer **2.39**, whilst the chlorinating agent Cl_2IPh yielded exclusively the *trans* isomer **2.40**. Bromine and several other brominating agents proved[2.28d] unsuccessful as did Iodine. However, the iodo alkene **2.38** was synthesised[2.28d] using $LiI\text{-}I_2$ (Scheme 2.19). The bromolactonisation reaction reported in this thesis is more subtle than the SCOOPY reaction in that the key intermediates **2.41** and **2.42**, analogous to **2.36**, is only formed following the lactonisation step, Scheme 2.17. The intramolecular attack of the carboxylate anion of **2.32** on the keto carbonyl forms the lactone, and only then the bromophosphonium salts **2.41** and **2.42**, analogous to **2.36**, are formed. The electrophile Br^+ initiates the reaction by brominating the phosphorane C=P to form the bromophosphonium salt **2.32**, where salts of the type **2.21** are known[1.11,2.27] to cyclise rapidly (see Section 2.4.3 for discussion on cyclisation of phosphonium salts).

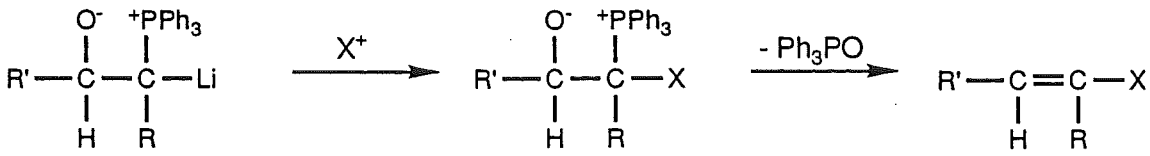

2.35 **2.36** **2.37**

Scheme 2.18: SCOOPY Reaction (Schlosser[2.28a])

Table 2.1: SCOOPY Reaction (Schlosser[2.28a])

Compound	R	R'	Purity *cis/trans*	Agent
4-fluoro*trans* -heptene	nC_3H_7	C_2H_5	>95%	$FClO_3$
ω-fluorostyrene	H	C_6H_5	55:45	$FClO_3$
β-Methyl *cis* -ω-fluorostyrene	CH_3	C_6H_5	>98%	$FClO_3$
ω-chlorostyrene	H	C_6H_5	52:48	$Cl_2IC_6H_5$
β-Methyl *cis* -ω-chlorostyrene	CH_3	C_6H_5	>98%	$Cl_2IC_6H_5$
β-Methyl *cis* -ω-bromostyrene	CH_3	C_6H_5	>90%	Br_2

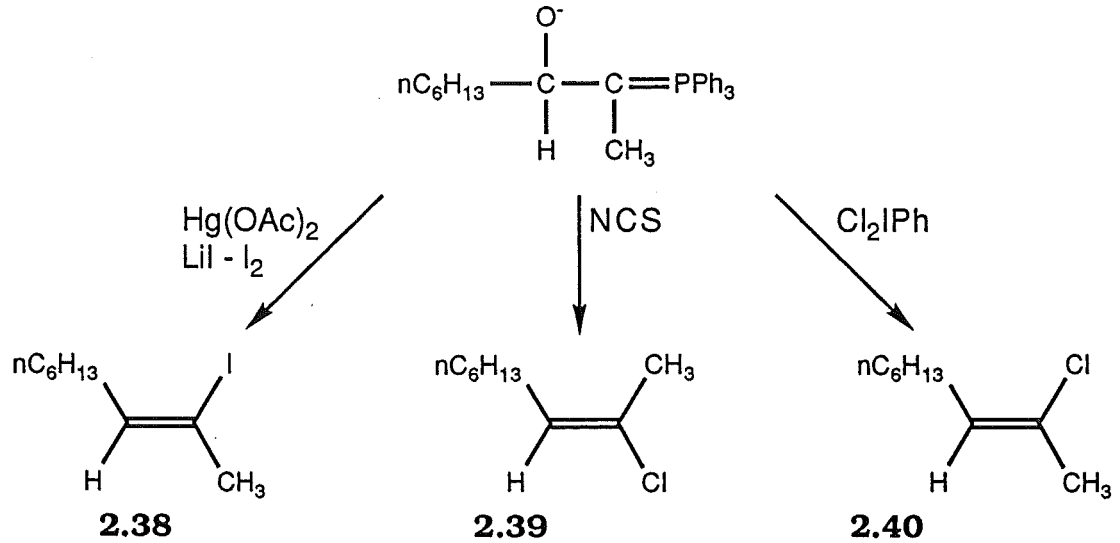

2.38 **2.39** **2.40**

Scheme 2.19: SCOOPY Reaction (Corey[2.28d])

2.4.2: Structure Assignment of Bromo Enol Lactones

The stereochemical assignment of the *E*- and *Z*-bromo enol lactone isomers was initially based on the comparison of the ^{1}H NMR spectra of structurally similar enol lactones[0.14,0.15,2.1,2.24]. The ethyl ester deshields the $(H\text{-}3)_2$ protons, Figure 2.3, when close in space to these protons. For example the $(H\text{-}3)_2$ proton resonance shifts downfield by 0.2-0.4ppm when the ester group is *trans* to the lactone oxygen (Figure 2.3). An allylic coupling constant $J_{H_1}(H\text{-}3)_2$ of 1.5-2.0 Hz is observed when the the ester is *trans* to the lactone oxygen and 0.8-1.0 Hz when it is *cis*. This gives further support to the assignment. NOE measurements[1.10] can also characterise enol lactones configuration when there is a olefinic methyl group present, Figure 2.3. The bromo enol lactones lack an allylic proton or an allylic methyl group on the double bond, and hence the stereochemical assignment is more difficult.

The *E*- and *Z*-bromo enol lactones **2.33** and **2.34** were inseparable by silica column and thin layer chromatography, however, separation was achieved by normal phase HPLC. An X-ray crystal structure of a crystal of the minor isomer (Figure 2.4) was consistent with the initial tentative ^{1}H NMR assignment as drawn in **2.33**. Note that the ester in the *Z*-bromo enol lactone **2.33** is in the same position as the *E*-enol lactone **2.27** due to the introduction of the higher priority bromine atom.

A number of interesting observations are evident from the crystal structure. The common *syn* arrangements[0.14] (S1.3) and (S1.2) (see Chapter 1) is observed for the α,β-unsaturated ester and the ester configurations C7-O4-C6-O3. The expected slight deviation from planarity of the five-membered lactone ring is observed and evidenced by the torsional angles C1-C2-C3-C4 -2.0(7), O2-C1-C2-C3 4.9(11), and O2-C4-C3-C2 -1.5(7). There appears to be very little delocalisation of the α,β-unsaturated system as evidenced by the bond lengths O3-C6 1.212(9), C4-

Figure 2.3: Stereochemical Assignment by ^{1}H NMR Resonance Signals of Enol, Methyl Enol and Bromo Enol Lactones

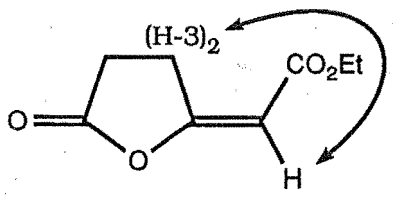

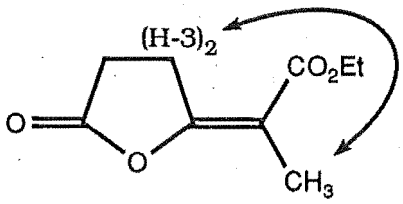

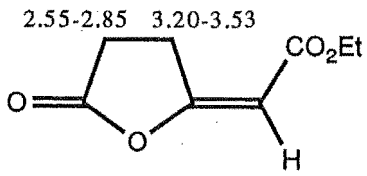

2.27

E

5.85, J=2.0 Hz

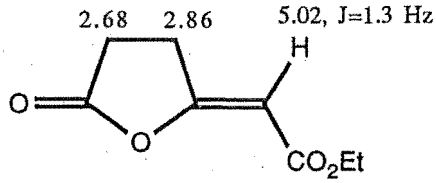

2.28

Z

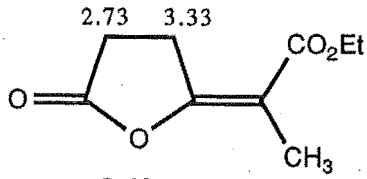

2.43

E

1.91, J=1.8 Hz

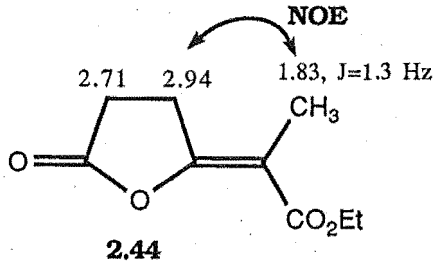

2.44

Z

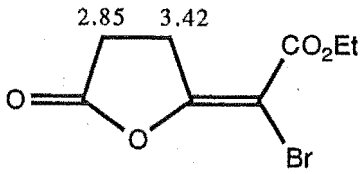

2.33

Z

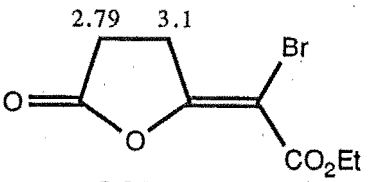

2.34

E

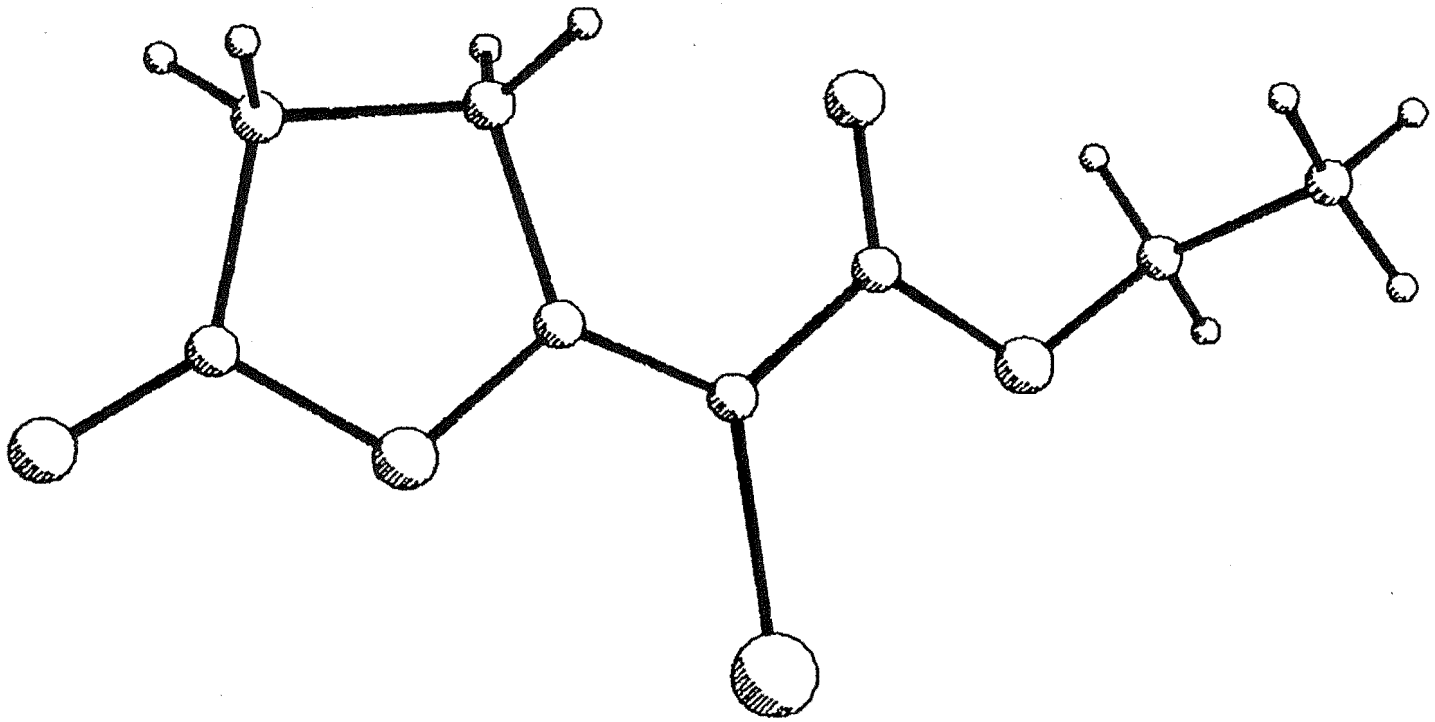

Figure 2.4: Perspective View of *Z*-Succinic Bromo Enol Lactone 2.33.

C5 1.336(10), and C5-C6 1.469(11). The bromine atom and the oxygen atom O3 are not significantly twisted out of the plane of the sp^2 system, with torsional angles of -1.7(9) for O2-C4-C5-Br and of-1.7(11) for C4-C5-C6-O3. Although the bromine atom is quite large it appears to have little effect on the overall geometry.

Molecular mechanics[2.29] (MM2) calculations were carried out on the isomeric bromo enol lactones, **2.33** and **2.34**, in order to determine which isomer represented the thermodynamic product. The *E* **2.34** and *Z* **2.33** structures were both minimised with rotation about the three chain bonds and the ring system. The C7-C8 and C8-C10 bonds required 180° increments as C7 and C8 are sp^2 hybridised carbon atoms, while C10-O11 was rotated in 60° increments. The energy minimisation of the *E*-structure produced 13 conformers having energies within 3Kcal/mol of the minimum energy. Application of the Boltzman distribution[2.29] at 25°C showed that the Boltzman average energy was 23.49Kcal/mol. The four lowest energy conformations are shown in Figure 2.5. The large number of observed conformers reflects the relatively free rotation of the ethyl ester, as there is little interaction with the five-membered ring.

The energy minimisation of the *Z*-structure produced 11 conformers having energies within 3Kcal/mol of the minimum energy, and with a Boltzman average energy of 23.37Kcal/mol. The six lowest energy conformers accounted for 95.42% of the population and the four lowest energy conformers are shown in Figure 2.6. The smaller number of conformers reflects the interaction of the ethyl ester and the five-membered ring. The *E*-structure is the major isomer produced in the reaction of succinic anhydride and ylide **0.1**.

These MM2 calculations were unable to determine whether the kinetic product or thermodynamic product is favoured, as the relative energies are very close. Identical model calculations were carried out on the hydrogen enol lactone systems to determine the reliability of the MM2

Figure 2.5: Four Lowest Energy Conformations of 2.34

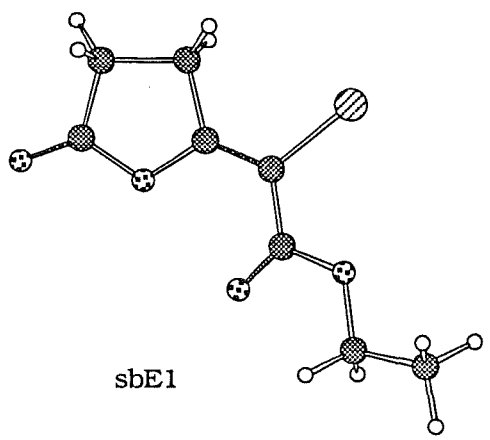

sbE1

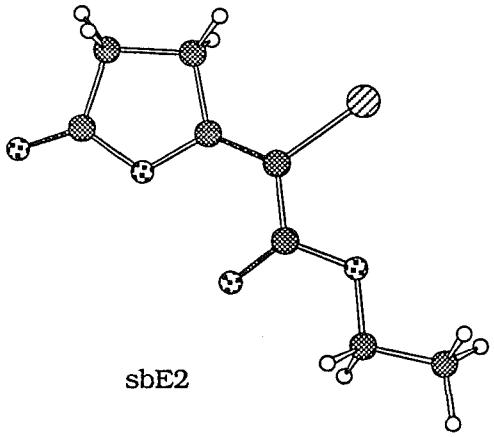

sbE2

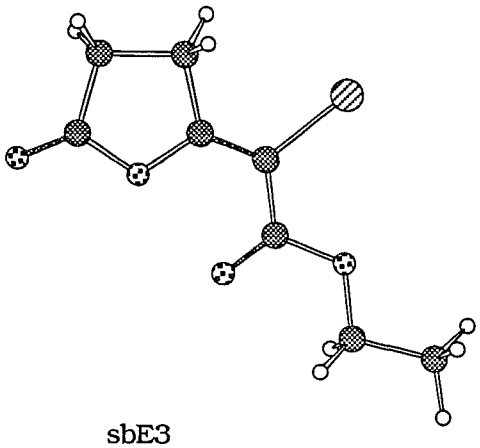

sbE3

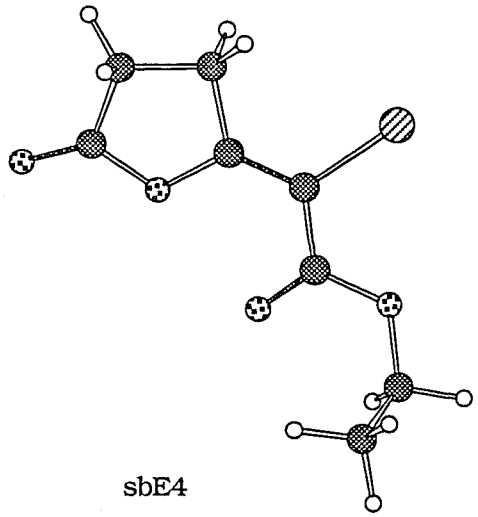

sbE4

Figure 2.6: Four Lowest Energy Conformations of 2.33

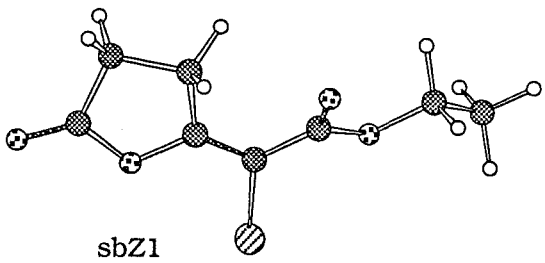

sbZ1

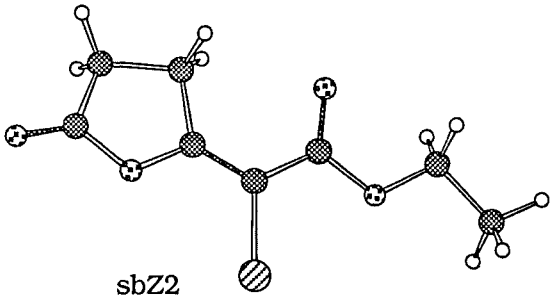

sbZ2

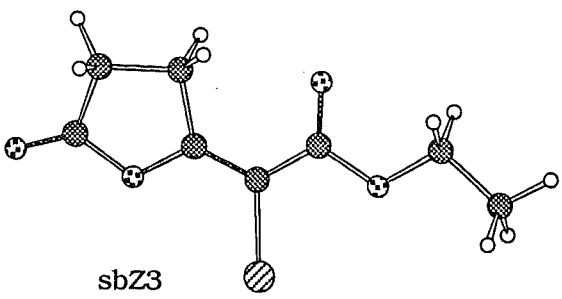

sbZ3

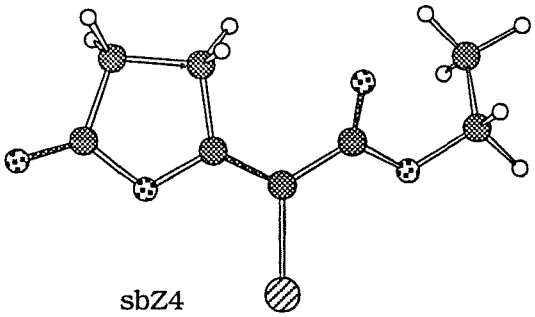

sbZ4

method. The MM2 calculations on the hydrogen enol lactone systems support the experimental equilibrium evidence (the product *E*-enol lactones readily equilibrates to the more stable *Z*-enol lactones with trace TFA[2.1]) that the *Z*-enol lactone **2.28** is thermodynamically more stable with an Boltzman average energy of 17.68Kcal/mol while the *E*-isomer **2.27** has an Boltzman average energy of 18.27Kcal/mol, Table 2.2. The *E*-isomer on application of the Boltzman distribution at 25°C showed that the 4 lowest energy isomers accounted for 99.93% of the population (the four lowest energy conformers of the *E*- and *Z*-structures are shown in Figures 2.7, and 2.8). The small number of conformers reflects the interaction of the ethyl ester and the 5-membered ring and is analogous to the previously discussed *Z*-bromo enol lactone.

The bromolactonisation reaction should preferentially give the kinetic product to be consistent with the proposal that the mechanism of the reaction of a stabilised ylide and a carbonyl system proceeds via kinetic control. These MM2 calculations on the product enol lactones **2.27**, **2.28**, **2.33**, and **2.34** illustrates that the energies of the products may not necessarily reflect the energies of the transition states. Therefore, it is possible to obtain either the kinetic or thermodynamic product via a kinetic pathway depending on the transition states energies for the loss of triphenylphosphine oxide from the oxephosphetanes.

Finally, the crystallographically derived structure was compared with the MM2 calculated bromo enol lactone conformers. Conformers sbz5 and sbz6 are in close agreement with the X-ray structure (0.121Å and 0.166Å average deviation of atoms respectively, Figures 2.9, 2.10). The conformers sbz5 and sbz6, are 0.589 and 0.627Kcal/mol higher in energy respectively than the lowest energy conformation which has an average deviation of atoms of 0.339Å from the crystallographically derived structure.

Figure 2.7: Four Lowest Energy Conformations of 2.27

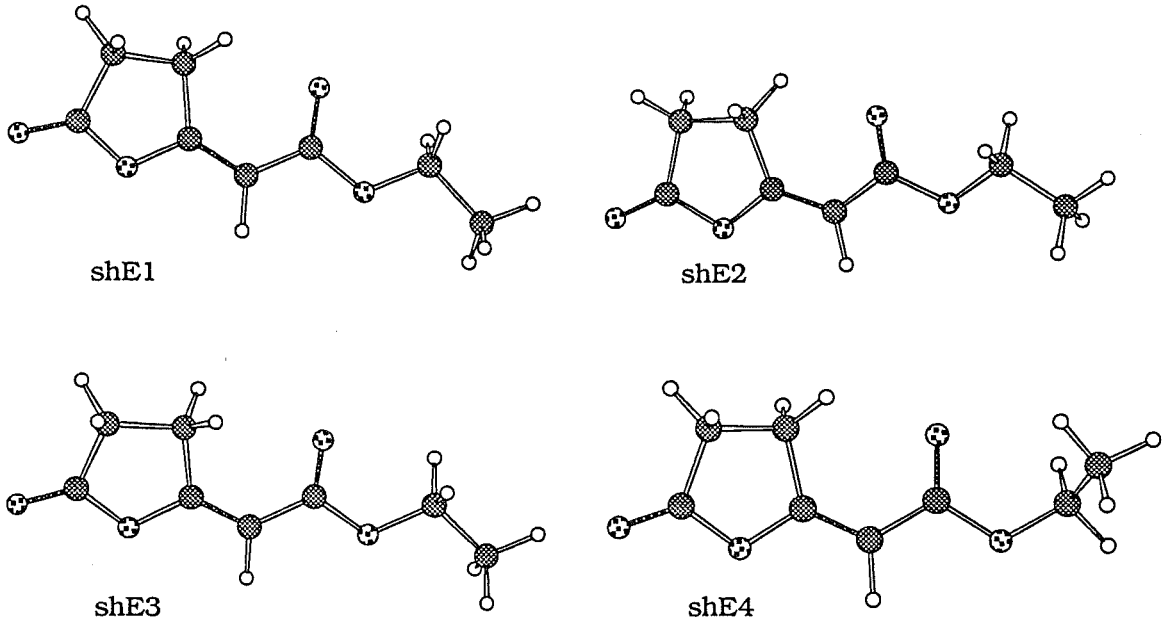

Figure 2.8: Four Lowest Energy Conformations of 2.28

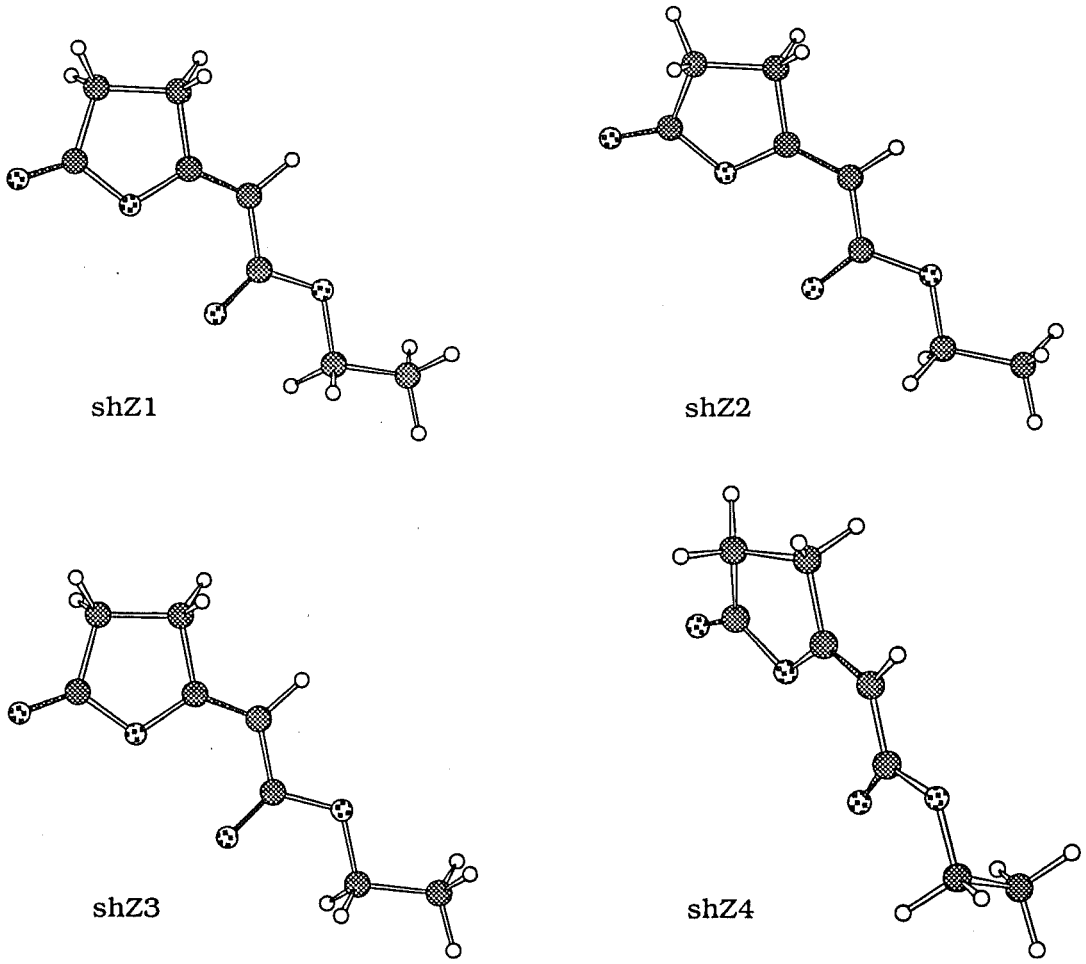

Table 2.2: MM2 Energy Minimisations on Hydrogen and Bromo Enol Lactones 2.27, 2.28, 2.33 and 2.34

System	Conformer%	Energy (Kcal/mol)	Boltzman average Energy (Kcal/mol)
she **2.27**			
	1 = 31.89 %	18.137	18.27
	2 = 28.97 %	18.194	
	3 = 20.29 %	18.407	
	4 = 18.86 %	18.450	
shz **2.28**			
	1 = 17.43 %	17.314	17.69
	2 = 15.97 %	17.366	
	3 = 9.02 %	17.706	
	4 = 8.49 %	17.743	
	5 = 8.29 %	17.757	
	6 = 8.25 %	17.760	
	7 = 7.51 %	17.816	
	8 = 6.64 %	17.890	
	9 = 4.86 %	18.076	
	10 = 4.80 %	18.083	
	11 = 4.42 %	18.132	
	12 = 4.32 %	18.145	
sbe **2.34**			
	1 = 16.71 %	23.119	23.49
	2 = 14.39 %	23.208	
	3 = 10.20 %	23.413	
	4 = 10.05 %	23.422	
	5 = 9.29 %	23.469	
	6 = 8.69 %	23.509	
	7 = 7.64 %	23.586	
	8 = 6.13 %	23.717	
	9 = 4.09 %	23.958	
	10 = 3.65 %	24.027	
	11 = 3.61 %	24.032	
	12 = 2.91 %	24.161	
	13 = 2.64 %	24.219	
sbz **2.33**			
	1 = 27.63 %	23.006	23.37
	2 = 19.54 %	23.213	
	3 = 15.91 %	23.336	
	4 = 12.17 %	23.496	
	5 = 10.41 %	23.589	
	6 = 9.76 %	23.627	
	7 = 1.36 %	24.803	
	8 = 1.06 %	24.951	
	9 = 0.83 %	25.099	
	10 = 0.71 %	25.188	
	11 = 0.63 %	25.260	

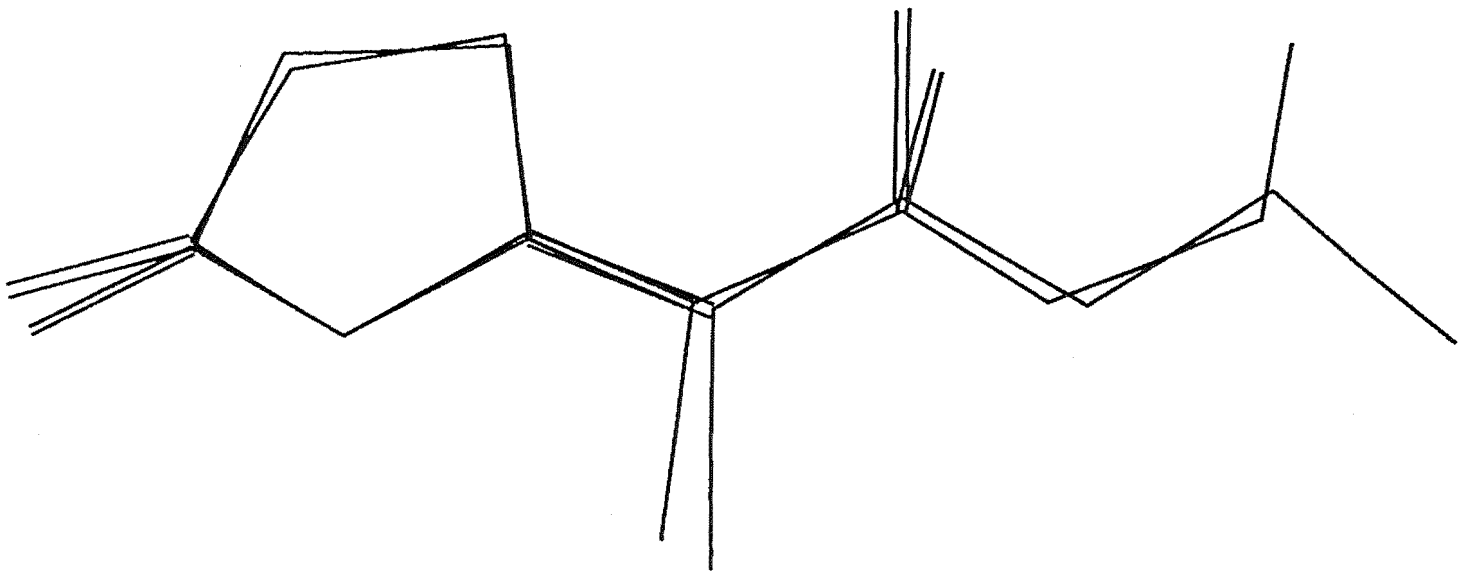

Figure 2.9: Comparison of Conformer SbZ5 with the X-ray Determined Structure for 2.33.

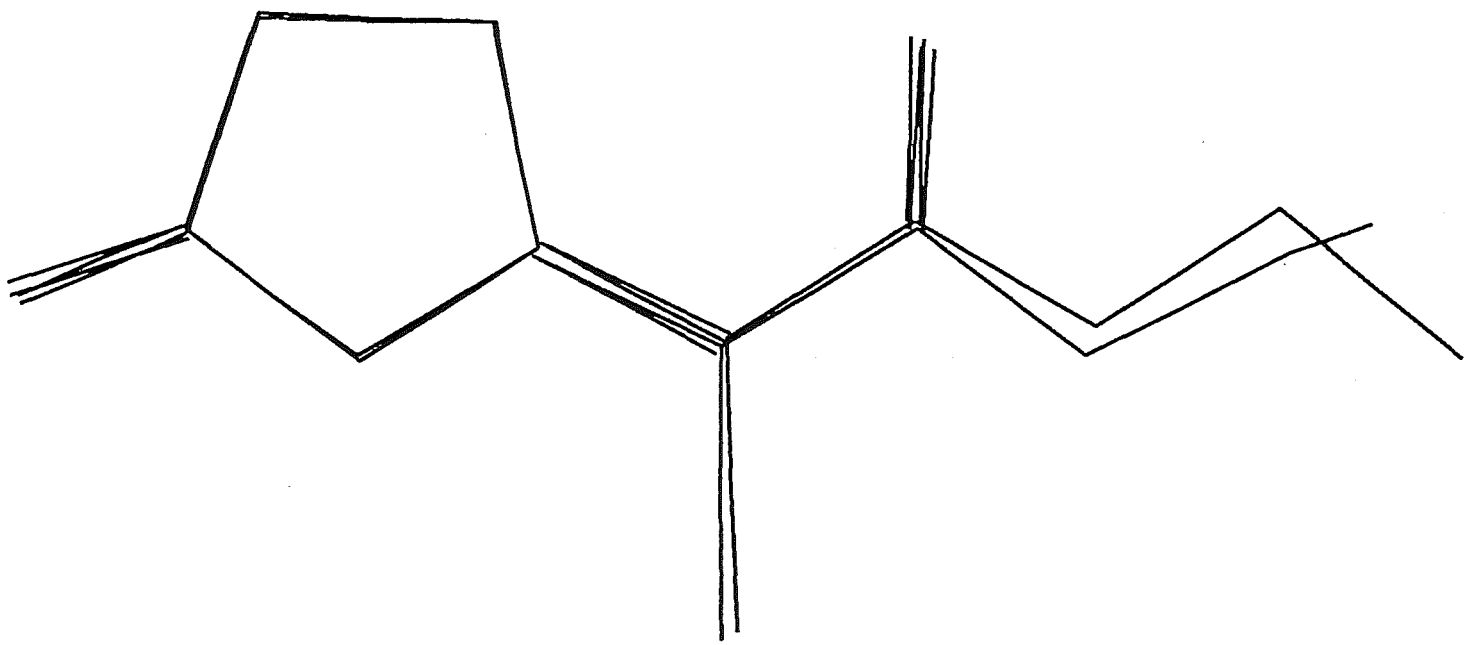

Figure 2.10: Comparison of Conformer SbZ6 with the X-ray Determined Structure for 2.33.

2.4.3: Mechanism of Bromo Enol Lactone Formation

While the reaction of Ph_3PCHCO_2Et with succinic anhydride yields exclusively the *E*-enol lactone **2.27**[2.24], the bromolactonisation of the acyclic intermediate **2.22** yields the bromo enol lactones **2.33** and **2.34** in an *E*:*Z* isomer ratio of 7:3. The formation of the succinic bromo enol lactones from the bromination of the corresponding acyl phosphorane is extremely rapid at 0°C while the alternative formation of hydrogen enol lactone **2.27** requires refluxing in $CHCl_3$ for four hours[2.24]. Therefore, it would appear unlikely that the bromo enol lactone formation occurs via incipient formation of **2.27** followed by bromination. Indeed the attempted bromination of **2.27** under conditions identical to those for the bromolactonisation failed to yield bromo enol lactones.

The proposed mechanism is shown in Scheme 2.17 as discussed earlier. The isolation of the *E*- and *Z*-bromo enol lactones stereoisomers could reflect a change in the cyclisation rates of the two transition states **2.45** and **2.46** (Figure 2.11), or the relative rate of loss of triphenylphosphine oxide from the oxaphosphetanes. The bromine atom in the *Z*-cyclisation transition state may sterically hinder the carboxylate attack on the carbonyl. Alternatively, the decomposition rates of the oxaphosphetanes leading to the *E*- and *Z*-bromo enol lactones might be slowed relative to betaine formation, thus giving time for thermodynamic equilibration. Following the bromolactonisation at low temperature (-40°C) by ^1H NMR failed to detect any intermediates. This is perhaps not surprising as intermediates have not been previously observed in the reaction of a stabilised ylide with a carbonyl containing compound.

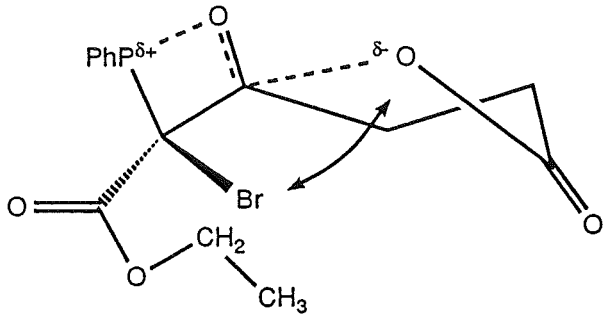

Z-transition state **2.45**

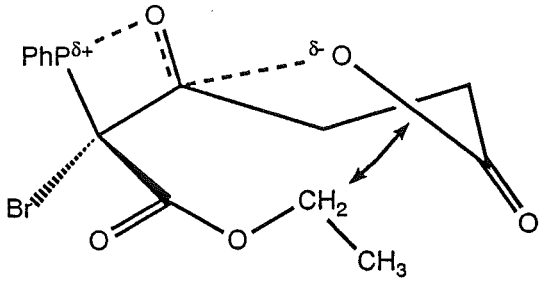

E-transition state **2.46**

Figure 2.11

The initial bromine attack on the nucleophilic carbon centre would form the α-bromo phosphonium salt **2.32**. This would in turn enter the normal Wittig sequence to form the bromo enol lactones **2.33** and **2.34**, Scheme 2.17. However, it is also known[1,9] that acyl phosphonium salts and acyl phosphoranes form allenes when the cyclisation pathway is not possible, for example the methyl ester of **2.47**, see Section 2.4.4.3. An alternative mechanism for the bromolactonisation reaction is therefore evident, Scheme 2.20.

The bromo allene **2.47** would be highly susceptible to nucleophilic attack at the central carbon centre[2,29] (Figure 2.12a). If the nucleophile was the carboxylate anion, the desired bromo enol lactones might form (Scheme 2.20). It was therefore important to study the possibility of allene formation as an intermediate to illucidate the bromolactonisation reaction mechanism.

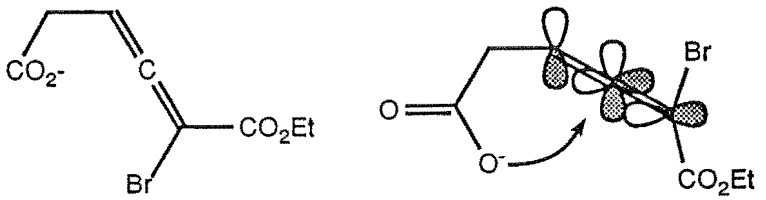

2.47

Figure 2.12a

Scheme 2.20: A Possible Mechanism for an Allene Intermediate in the Formation of Bromo Enol Lactones

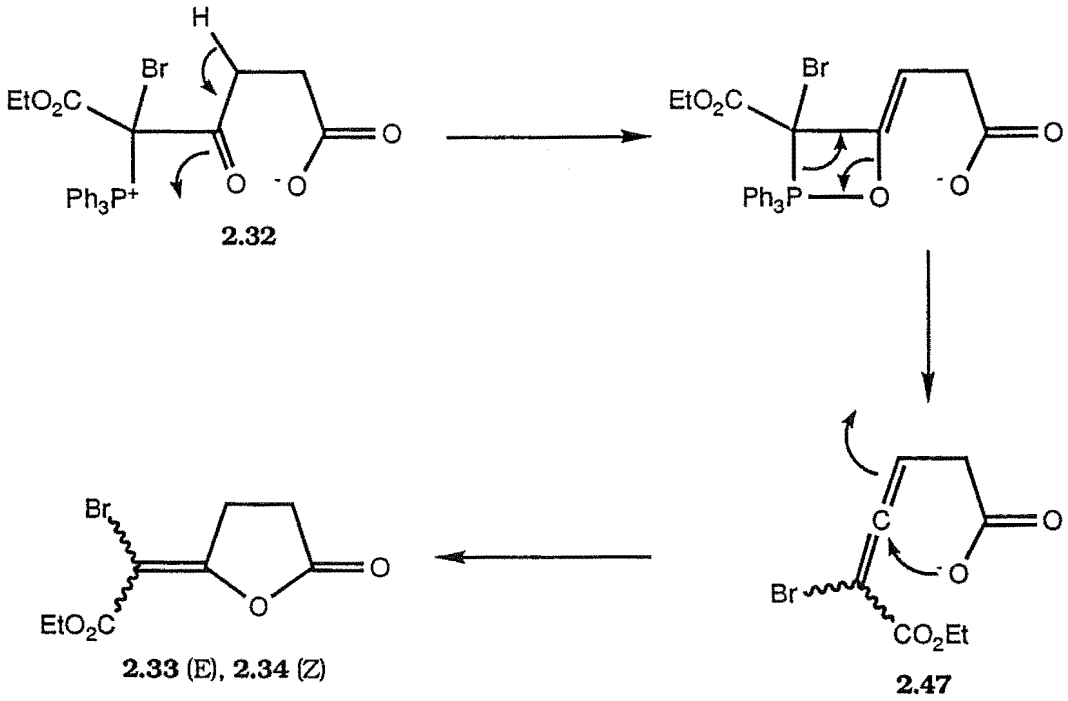

2.4.3.1: Allenes as a Reactive Intermediate.

Several model compounds were synthesised in order to study the bromo allenes[2.30]. The reaction of the acid chlorides **2.48a-d** with one equivalent of the bromo ylide **2.31** and one equivalent of triethylamine in $CHCl_3$ at O°C proceeded rapidly, to the bromo allenes **2.49a-d** quantitatively by ^1H NMR spectroscopy (Table 2.3). This reaction was studied in more

detail to provide further mechanistic information and since it represents a convenient preparation of bromo allenes.

Table 2.3: Bromo Allenes from Corresponding Acid Chlorides

Acid Chloride	Allene
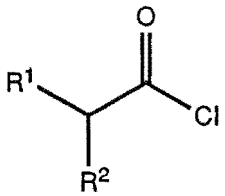	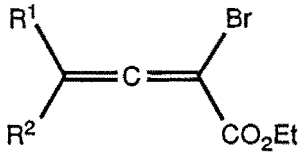
2.48a: $R^1 = R^2 = H$	**2.49a**: $R^1 = R^2 = H$
2.48b: $R^1 = H, R^2 = CH_3$	**2.49b**: $R^1 = H, R^2 = CH_3$
2.48c: $R^1 = R^2 = CH_3$	**2.49c**: $R^1 = R^2 = CH_3$
2.48d: $R^1 = H, R^2 = CH_2CH_3$	**2.49d**: $R^1 = H, R^2 = CH_2CH_3$

The reaction of an acid chloride with a phosphorus ylide to produce acyl phosphoranes[0.10,1.9b,2.32] and acyl phosphonium salts[0.10,1.9b,2.32] is itself synthetically important. A transylidation reaction occurs to produce the phosphonium salts **2.50a-d**, when ylides of the type **2.51a-c** and **0.1** are used, together with the synthetically useful acyl phosphorane **2.52a-d**. Alternatively, the transylidation step can be suppressed by low temperatures or by ylides substituted at C-1, Scheme 2.21. For example, the methyl ylide **2.53** gives the phosphonium salts **2.54a-d**. Treatment of the phosphonium salt with a further equivalent of ylide[2.32c] or with one equivalent of triethylamine[1.9a,2.32e] then yields the desired allenes **2.56a-c** (Scheme 2.22).

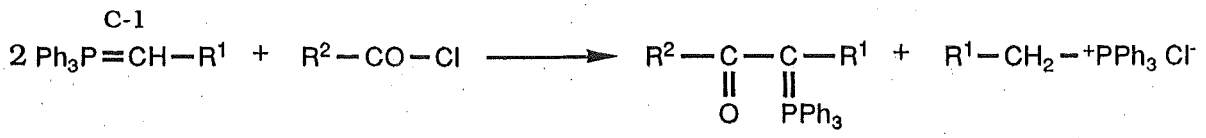

2.51a: R^1 = H
2.51b: R^1 = CH_3
2.51c: R^1 = Ph
0.1: R^1 = CO_2Et

2.52a: R^1 = H
2.52b: R^1 = CH_3
2.52c: R^1 = Ph
2.52d: R^1 = CO_2Et

2.50a: R^1 = H
2.50b: R^1 = CH_3
2.50c: R^1 = Ph
2.50d: R^1 = CO_2Et

Scheme 2.21

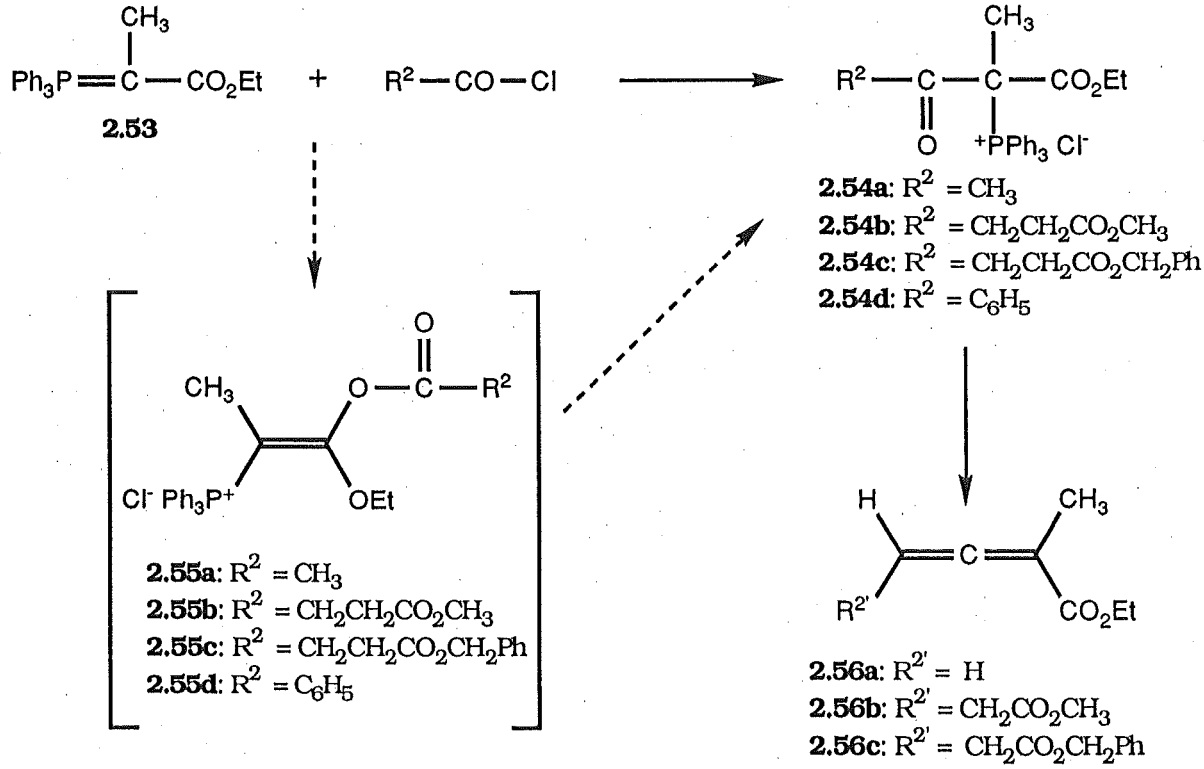

2.54a: R^2 = CH_3
2.54b: R^2 = $CH_2CH_2CO_2CH_3$
2.54c: R^2 = $CH_2CH_2CO_2CH_2Ph$
2.54d: R^2 = C_6H_5

2.55a: R^2 = CH_3
2.55b: R^2 = $CH_2CH_2CO_2CH_3$
2.55c: R^2 = $CH_2CH_2CO_2CH_2Ph$
2.55d: R^2 = C_6H_5

2.56a: $R^{2'}$ = H
2.56b: $R^{2'}$ = $CH_2CO_2CH_3$
2.56c: $R^{2'}$ = $CH_2CO_2CH_2Ph$

Scheme 2.22

Two mechanisms have been postulated for the formation of allenes from acid chlorides and ylides. One mechanism postulates the ketene[2.32] **2.57**, rather than the acid chloride as the species reacting with the ylide (Scheme 2.23). The second suggests that the C-acylated phosphonium salt[2.32] **2.58** gives rise to the allene via the phosphonium salt **2.59** and

subsequent loss of triphenylphosphine oxide (Scheme 2.24). The two mechanisms have the same intermediate phosphonium salt **2.59**. It is known that ketenes are reactive intermediates[2.33] and can form under our conditions, however we have not observed their formation in these reactions. We have observed C-acylated salts of the type **2.58** by using stepwise addition of reagents. The C-acylated phosphonium salts are formed first by the reaction of the acid chloride with one equivalent of ylide. The allene is formed only after further addition of base, one equivalent of triethylamine or another equivalent of ylide. This excludes the ketene mechanism as the ketene will only form if the triethylamine is added before addition to the ylide.

2.4.3.2: Synthesis and NMR of C-acyl and Oacyl Phosphonium Salts

The C-acylated phosphonium salt **2.54a**, analogous to the salt **2.32** proposed as a key intermediate in the bromo enol lactone formation (Scheme 2.20), were detected by ^{1}H NMR spectroscopy in the reaction of acetyl chloride and the bromo ylide **2.31**. The methyl ylide **2.53** was used for model studies since this reaction proceeded more readily and gave cleaner products. The methyl group also provides a convenient ^{1}H NMR resonance for monitoring the reaction. The reaction of the acid chloride **2.48a** and one equivalent of methyl ylide **2.53** in $CDCl_3$ gave complete conversion to the C-acylated phosphonium salt **2.54a** after 60 minutes. However, surprisingly the ^{1}H NMR spectrum revealed an intermediate subsequently assigned as **2.55a**. A quartet at 3.73ppm was initially observed and this diminished with time as a coupled quartet at 4.15ppm, due to the O**CH_2**CH_3 of **2.54a**, appeared. The initial ^{31}P NMR signal observed at 24.2ppm was inconsistent with starting material

Scheme 2.23: Mechanism of the Reaction of a Ketene with an Ylide

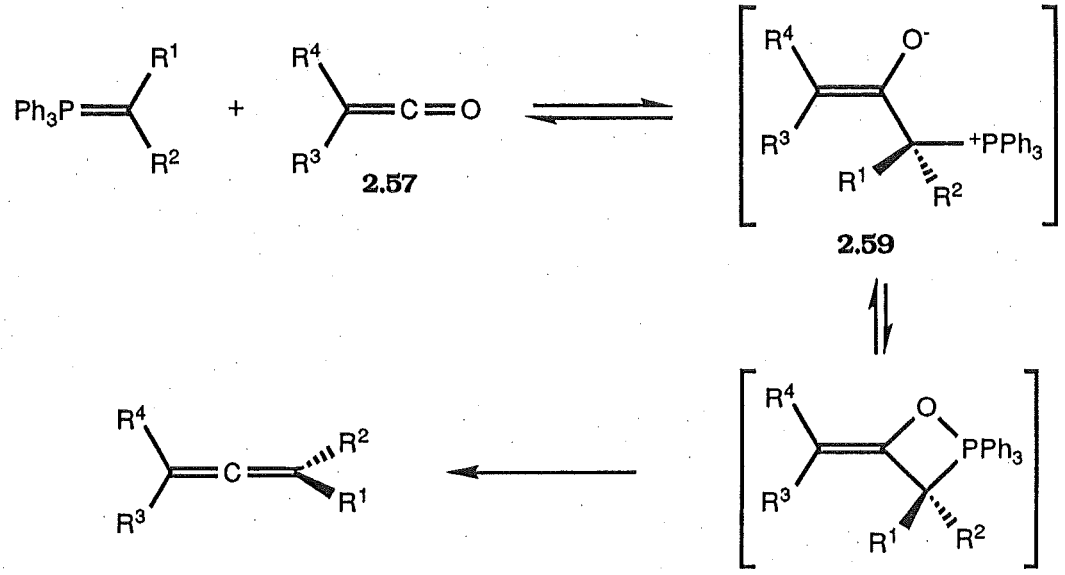

Scheme 2.24: Mechanism of the Reaction of an Acid Chloride with an Ylide

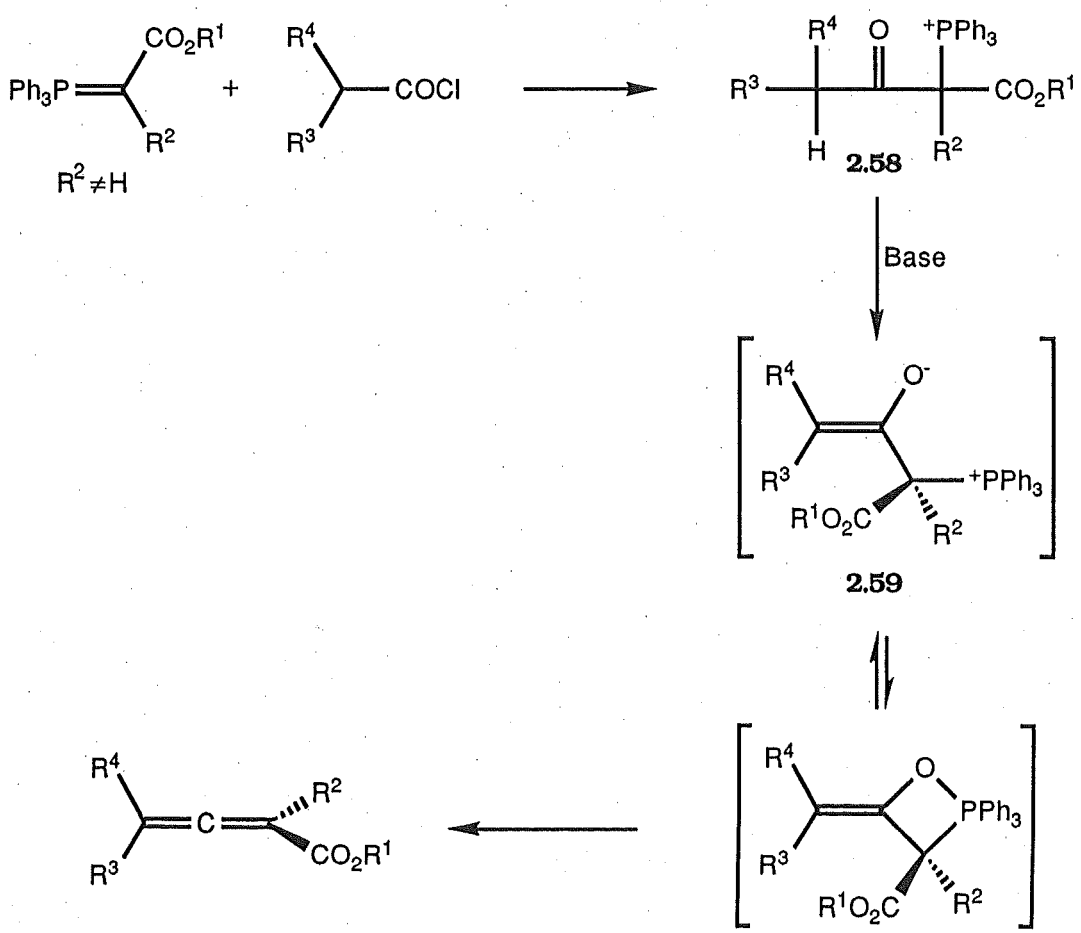

($Ph_3PCCH_3CO_2Et$ 23.3ppm) and with a C-acyl phosphonium salt (**2.54a**, 28.8ppm). The ^{31}P NMR signal disappeared and the expected C-acyl phosphonium salt signal at 28.8ppm appeared with time. The ^{1}H and ^{31}P NMR spectral data are consistent with the formation of the labile O-acylated phosphonium salt **2.55a** which readily rearranges to the C-acylated phosphonium salt **2.54a**.

Tables 2.4 and 2.5 list the ^{1}H NMR and ^{13}C NMR spectral data for the initially formed O-acyl phosphonium salts **2.55** and the ultimately formed C-acyl phosphonium salts **2.54**. The ^{13}C resonances were assigned on the basis of the chemical shifts and ^{13}C-^{31}P coupling constants of previously studied phenyl substituted phosphorus compounds[2.34] and by using low temperature heteronuclear ^{1}H-^{13}C correlation spectroscopy. The suggestion that the intermediate might be of the type **2.60** is inconsistent with the observed ^{13}C NMR spectral data. In particular the ^{13}C-^{31}P coupling constant for C-1 would be expected[0.9] to be smaller than the observed 50Hz for the C-acyl salts. The phosphorus is two atoms removed from C-1 in **2.60**, but the ^{13}C-^{31}P coupling constant is 93Hz. The ^{13}C-^{31}P coupling constant for C-2 not observed in the C-acyl salt **2.54a** is 12Hz. This is consistent with the O-acyl salt **2.55a** and inconsistent with an intermediate of the type **2.60**. Likewise a ^{13}C-^{31}P coupling constant for the CH_3 group of 7.5Hz is only consistent with the O-acyl salt intermediate **2.55a**. The same coupling constant would be expected to be very small or not observed in **2.60**. The ^{31}P chemical shift of the O-acyl salt intermediate **2.55a** is 24.3ppm which is similar to the chemical shift of 23.3ppm observed for the methyl ylide **2.53**. This is also consistent with an O-acyl phosphonium salt as the intermediate since it is structurally similar to the methyl ylide **2.53** and therefore will have a similar ^{31}P chemical shift. Vedejs[2.16] *et al.* has reported evidence against intermediates of the type **2.61** in reversibility studies on aldehydes and the stabilised methyl ylide **2.53**.

Table 2.4: ^{13}C and ^{1}H NMR Characterisation of the C-Acyl Phosphorane[a]

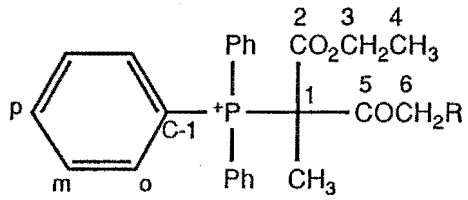

Carbon Chemical Shifts[a]

Compound	C-1	o	m	p	1	1-CH_3	2	3	4	5	6	7	8	9	Ph
2.54a: R = H	117.7 (86.6)	134.6 (10.2)	130.4 (12.8)	135.3 (3.0)	66.3 (50.4)	21.6	166.5	64.8	13.3	201.3 (4.3)	28.7 (2.0)				
2.54b: R = CH_2CO_2Me	116.5 (86.0)	132.9 (10.8)	129.3 (13.2)	134.3	64.8 (50.0)	20.5	164.7	63.8	12.1	201.2 (4.2)	34.2 (1.5)	26.3	171.0	50.6	
2.54c: R = $CH_2CO_2CH_2Ph$	117.7 (85.6)	134.0 (10.0)	130.3 (13.0)	135.3	66.1 (50.0)	21.6	165.9	64.9	13.2	202.1 (4.1)	35.2 (2.1)	27.5	171.5	66.3	127.7 128.0 128.3 135.4
2.54d: R = C_5H_6	117.4 (86.1)	133.8 (9.6)	129.8 (12.7)	134.4 (2.9)	66.8 (49.7)	22.1	166.0	64.5	13.1	208.3	[c]				128-137

Proton Chemical Shift[b]

	PPh_3	1-CH_3	3	4	6	7	9	Ph
2.54a: R = H	7.6 - 8.0	2.20 (d, 17.7)	4.15 (m)	1.10 (t, 7.1)	2.66			
2.54b: R = CH_2CO_2Me	7.6 - 8.0	2.20 (d, 18.0)	4.15 (m)	1.10 (t, 7.2)	3.25 (H_a, m) 3.47 (H_b, m)	2.66 (m)	3.64 (s)	
2.54c: R = $CH_2CO_2CH_2Ph$	7.6 - 8.0	2.11 (d, 16.s)	4.15 (m)	1.04 (t, 7.1)	3.22 (H_a, m) 3.40 (H_b, m)	2.72 (m)	5.06 (ABq, 12.6) 5.09	7.30
2.54d: R = C_5H_6	7.4-8.0	2.27 (d, 18.3)	3.99 (m)	0.98 (t, 7.1)	[c]			7.4-8.0

[a] Chemical shifts in ppm (^{13}C-^{31}P coupling constants in Hz)
[b] Chemical shifts in ppm (multiplicity, Hz)
[c] Benzoyl chloride derivative

Table 2.5: ^{13}C and ^{1}H NMR Characterisation of the O-Acyl Phosphorane[a]

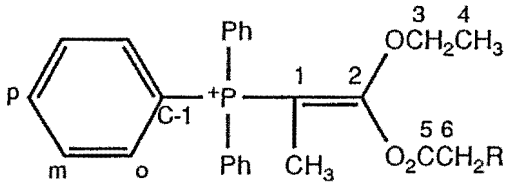

Carbon Chemical Shift[a]

Compound	C-1	o	m	p	1	1-CH_3	2	3	4	5	6	7	8	9	Ph
2.55a: R = H	117.1 (91.7)	132.4 (10.0)	129.1(12.8)	133.9	75.4 (93.5)	12.1 (7.5)	158.6 (12.0)	65.5	12.5	165.0	19.8				
2.55c: R = CH_2CO_2Me	117.7 (91.6)	133.0 (10.4)	129.7 (12.8)	134.4 (2.9)	75.7 (93.4)	12.5 (7.3)	159.3 (12.1)	66.0	12.9	168.1	28.0	27.6	171.9	50.6	
2.55d: R = C_6H_5	118.1 (91.7)	133.2 (10.5)	129.9 (13.2)	134.5 (3.0)	76.5 (93.6)	12.7 (7.2)	160.0 (12.4)	66.1	13.0	161.5	c				127-138

Proton Chemical Shift[b]

	PPh_3	1-CH_3	3	4	6	7	9	Ph
2.55a: R = H	7.40 - 8.00	1.65 (d, 14.5)	3.73 (q, 7.1)	0.53 (t, 7.1)	2.49 (s)			
2.55b: R = CH_2CO_2Me	7.40 - 7.90	1.67 (d, 14.7)	3.79 (q, 7.1)	0.54 (t, 7.1)	3.11 (m)	2.84 (m)	3.70 (s)	
2.55c: R = $CH_2CO_2CH_2Ph$	7.40 - 8.00	1.62 (d, 14.6)	3.75 (q, 7.1)	0.50 (t, 7.1)	3.12 (m)	2.88 (m)	5.13 (s)	7.30
2.55d: R = C_6H_5	7.40-8.00	1.67 (d, 14.3)	3.77 (q 7.1)	0.55 (t, 7.1)	c			7.4-8.0

[a] Chemical shift in ppm (^{13}C-^{31}P coupling constants in Hz)
[b] Chemical shift in ppm (multiplicity, Hz)
[c] Benzoyl chloride derivative

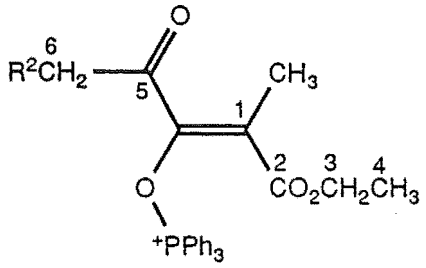

2.60

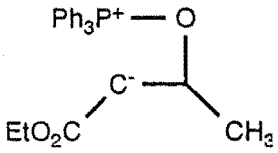

2.61

The ^{13}C NMR spectral data for **2.54b-d** and **2.55b-d** are also consistent with the assigned structures. Importantly, the aromatic C-1 resonance of both sets of compounds occurs in an upfield position characteristic of a phosphonium salt[2.1,2.34] and the expected ^{13}C-^{31}P coupling constants[2.1,2.34] are observed for the phenyl carbons. The ^{13}C NMR signal for C-1 in structures **2.55a-d** is downfield relative to model compounds[2.35].

Ylides of the type **2.53** have been shown to be an equilibrium mixture of *cis* and *trans* enolate forms which show separate ^{1}H, ^{13}C, and ^{31}P NMR signals[2.34,2.35]. We have also observed separate ^{1}H, and ^{31}P NMR signals for the ylide **0.1** (see Chapter 1). Compounds **2.55a-d** would appear to be single isomers by ^{1}H NMR and ^{13}C NMR spectroscopy (-35°C). The configuration of the O-acyl phosphonium salts **2.55a-d** is tentatively assigned as *E*- similar to conformer 1 (Table 2.6) on the basis of the OCH_2CH_3 proton chemical shift. This is based on the reported[2.35] ^{1}H NMR spectrum of the ylide **2.53** shown in Table 2.6.

The broad band decoupled ^{31}P NMR spectra for **2.54a**, **2.54b**, **2.55a**, and **2.55b** (Table 2.7) gave the expected[2.10c] signals for tetracoordinate phosphorus in the range δ20-40 ppm (downfield relative to 85% H_3PO_4). No other intermediates were detected.

Reports of ylide alkylation[2.36], triflations[2.37], and acylations (aromatic acid chlorides only)[2.38] through oxygen have appeared in the literature, but the work in this thesis is unique in that the O-acyl species appear to be

Table 2.6: *Cis* and *trans* ^{1}H NMR Data for 2.53

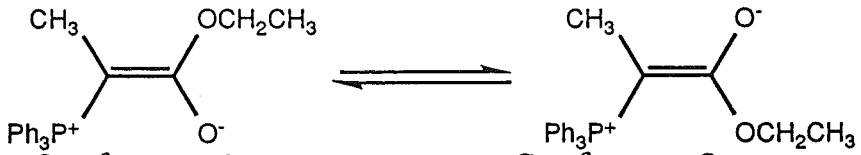

Conformer 1 Conformer 2

^{1}H NMR of conformers (ppm)			
-OC**H**$_2$CH$_3$		-OCH$_2$C**H**$_3$	
Conformer 1	Conformer 2	Conformer 1	Conformer 2
3.70	3.87	0.61	1.13

Table 2.7: ^{31}P NMR Data for Selected C-acyl and O-acyl salts

Compound	^{31}P NMR ($CDCl_3$, δ ppm)
2.54a	36.3
2.54b	36.0
2.55a	24.3
2.55b	24.3

precursors to the C-acyl compounds. The mechanism of this conversion remains uncertain. Presumably it would be intramolecular and we tentatively suggest the mechanism shown in Scheme 2.25.

Scheme 2.25: Possible Intramolecular Mechanism of formation of the C-acylphosphonium salt 2.54 from O-acylphosphonium salt 2.55.

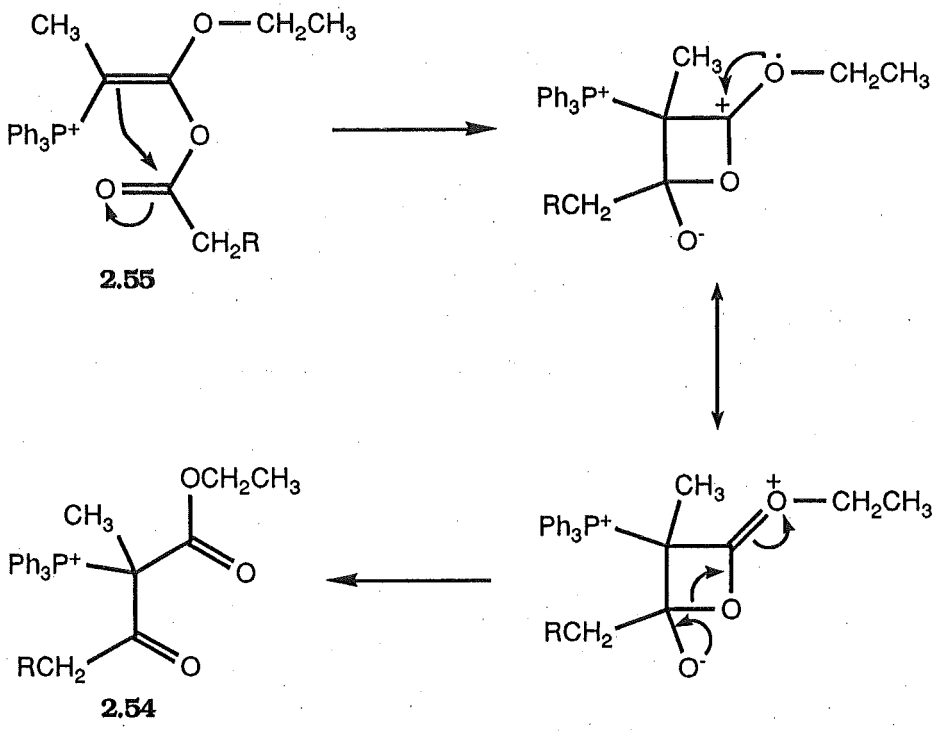

2.4.3.3: Succinic Derived Allenes as Intermediates in the Bromolactonisation Reaction.

It has been shown by this research group[1.11] that allenes form on reaction of the carboxylic protected succinic acid chloride **2.62** with the methyl ylide **2.53** (Scheme 2.26). The C-acyl salt **2.54a**, formed from the methyl ester acid chloride **2.69**, gave the methyl protected allene **2.62** on addition of triethylamine. The benzhydrol protected succinic acid chloride **2.65** similarly gave the C-acyl salt **2.63**. Deprotection of **2.63** with TFA gave enol lactone **2.43**. Neither the benzhydrol protected allene nor the salt **2.64** were observed by ^{1}H NMR spectroscopy. This result is significant as it shows that C-acyl salts are intermediates in the Wittig Anhydride carbonyl olefination reaction.

Scheme 2.26: C-acyl Phosphonium Salts as Intermediates to Enol Lactones

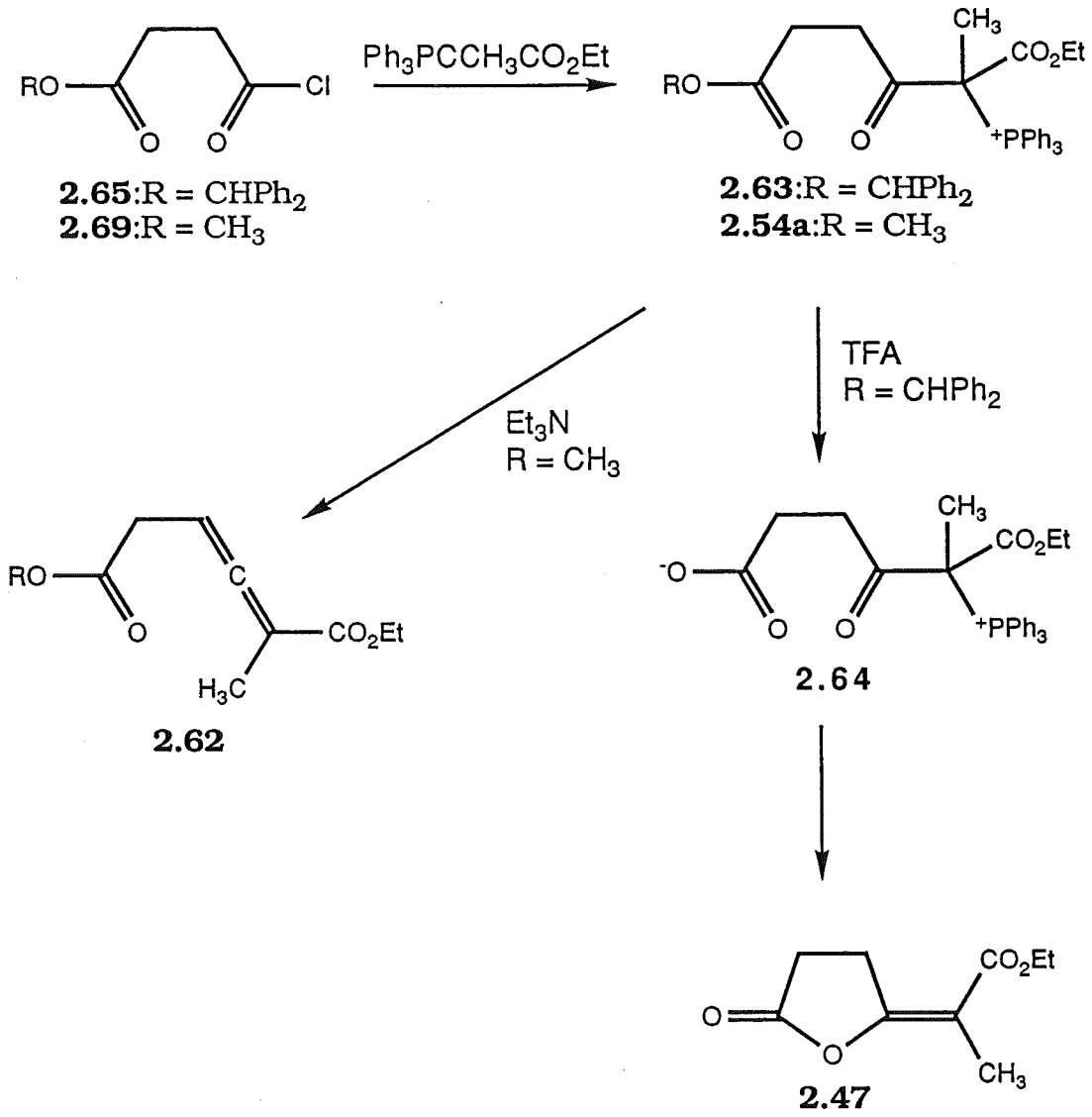

Due to the success in producing alkyl substituted bromo allenes, it was a logical progression to make the bromo allene **2.66**. Deprotection should then either confirm or disprove the intermediacy of allenes in the formation of the bromo enol lactones. The benzhydrol protected succinic derived acid chloride **2.65** was formed from monoprotected succinic acid using a ten-fold excess of oxalyl chloride and dimethylformamide. It was anticipated that the addition of two equivalents of bromo ylide **2.31** would

then yield the bromo allene **2.66**. However, this was not observed. Rather, an unknown compound subsequently shown to be **2.67** (distinctive AB quartet at 6.59ppm and 6.85ppm (16.0 and 39.5Hz, 2H)) was observed by ^{1}H NMR spectroscopy. The proposed structure **2.67** was consistent with the ^{1}H and ^{13}C NMR spectral data. Resonances were observed at 1.33ppm (t, 7.1Hz, $OCH_2C\mathbf{H_3}$) and 4.27ppm (q, 7.1Hz, $OC\mathbf{H_2}CH_3$) and 6.88ppm (s, $OC\mathbf{H}Ph_2$). The methyl ester analogue **2.68** was also observed when the acid chloride **2.69** was used. Here the desired allene **2.70** and the acetylene **2.68** were both observed in a ratio of 50:50, respectively. The ^{1}H NMR spectrum of **2.68** was consistent with the structure **2.67** with an AB quartet at 6.42ppm and 6.74ppm (16.0 and 47.2Hz, 2H) and with the reported ^{1}H NMR spectrum of the known acetylenic diester[2.39] **2.71**. The bromination of the methyl protected phosphorane **2.71** appeared to give acetylene **2.68** but this result was not reproducible.

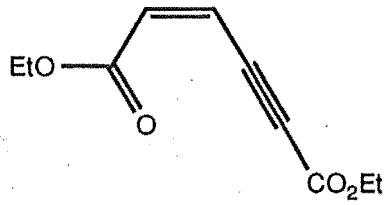

2.71

The ^{1}H NMR of the bromo allene **2.70** was consistent with the previous bromo allenes synthesised with signals at 3.25ppm (d,7.0Hz, $CH_3O_2CC\mathbf{H_2}CHCCBrCO_2Et$) and 5.83ppm (t,7.0Hz, $CH_3O_2CCH_2C\mathbf{H}CCBrCO_2Et$). The methyl ester bromo allene **2.70** could not be selectively deprotected to give the free acid bromo allene, required for mechanistic studies. A possible mechanism for the formation of **2.67** and **2.68** is indicated in Scheme 2.27. The desired bromo allenes **2.66** and **2.70** presumably eliminate HBr to give **2.67** and **2.68** respectively, as

shown in Scheme 2.27. Other literature syntheses[2.39] of acetylenic diesters yield compounds in which the two esters are identical. Our synthesis allows the formation of acetylenic diesters with two different ester groups.

There is no direct evidence for allenes as intermediates in the bromolactonisation reaction. The fact that the acetylene **2.66** was isolated from the reaction of acid chlorides and bromo ylide **2.31** and not in the bromolactonisation reaction would suggest that the bromo allenes are unlikely to be intermediates in the bromolactonisation reaction. The reaction of acid chlorides with the bromo ylide gave no evidence of enol lactones whereas the analogous salt work did[1.11]. The fact that the bromo acylphosphonium salt **2.32** was not observed in the bromolactonisation does not necessarily imply that it is not formed. Rather, it could simply be a consequence of the fact that bromo salts such as **2.32** and the methyl substituted analogue cannot be stabilised by the presumably rapid phosphonium salt-phosphorane rearrangement, or perhaps oxaphosphetane formation and fragmentation are faster with **2.32** than with **2.21**.

Bromo phosphonium salt **2.32** was not detected at low temperture (-35°C) in the reaction of the acylphosphorane **2.22** and bromine. The reactive C-acyl bromo phosphonium salt **2.32** may rapidly enter the normal Wittig sequence or much less likely proceed via a bromo allene to yield bromo enol lactones. The C-acyl methyl analogues **2.64** have been synthesised independently[1.11] and have been shown to rapidly form the methyl enol lactone **2.43**. The C-acyl bromo phosphonium salts should react similarly to form bromo enol lactones. The *E*-stereochemical preference of the products cannot be readily explained by an allene mechanism. The nucleophilic attack indicated in Figure 2.13 is favoured over that indicated in Figure 2.12b due to the steric demands of the ester and the bromine.

Scheme 2.27: Formation of Allenes and Acetylenes

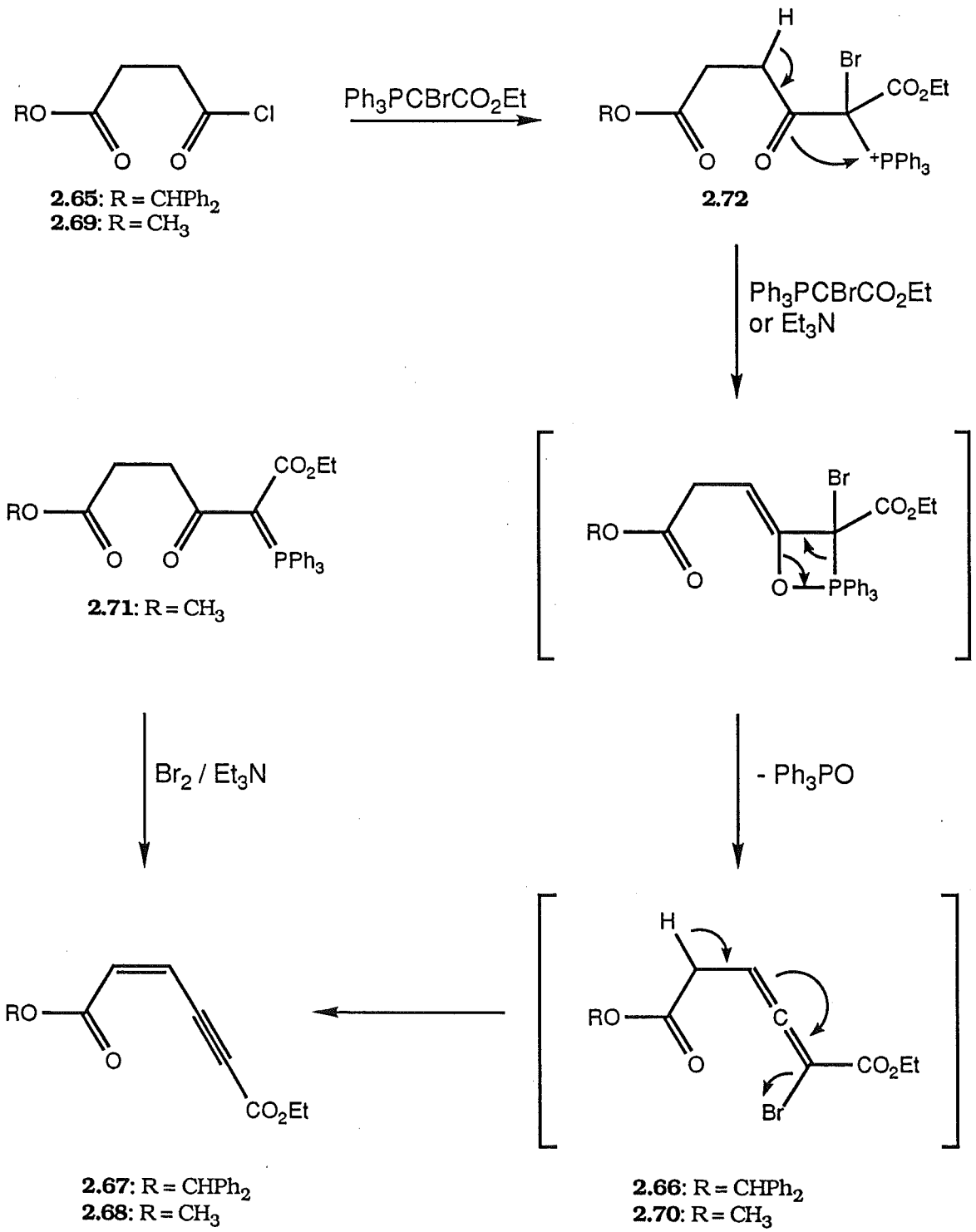

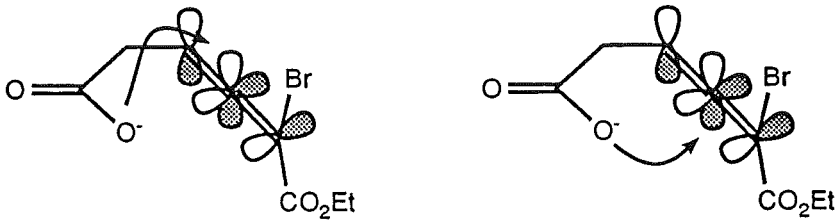

attack from above attack from below

Figure 2.12b

The negative charge in **2.74** would be stabilised by the electron withdrawing nature of the bromine and ethyl ester group. The analagous species produced from an intramolecular attack of the carboxylic acid in the methyl allene **2.63**, however, would not be stabilised to the same degree.

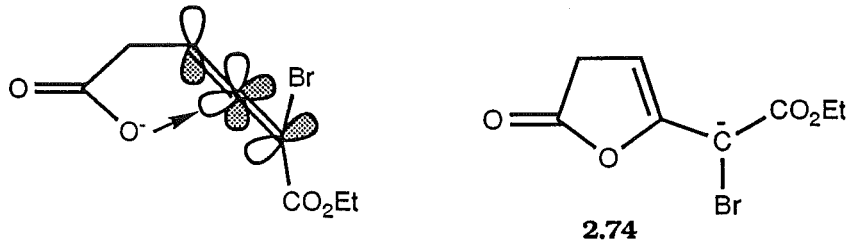

2.74

Figure 2.13

The reaction of larger ring anhydrides with ylides has also been investigated by this research group[1.11,2.40]. The six-membered glutaric series (see Chapter 3) and the seven-membered adipic and diphenic series have been investigated with regard to the bromolactonisation reaction. Adipic anhydride forms the phosphorane **2.75** on reaction with ylide **0.1** and under the bromolactonisation conditions yields the bromo allene **2.76** and the brominated phosphorane **2.77**[1.11]. The formation of **2.76** would perhaps support allenes as intermediates to the enol lactones. However **2.76** did not yield the corresponding bromo enol lactones on heating. The

bromo allenes would therefore appear to be derived from an alternative pathway to bromo enol lactone formation. Both these reactions appear to proceed via a common phosphonium salt intermediate **2.78**. The two products **2.76** and **2.77**

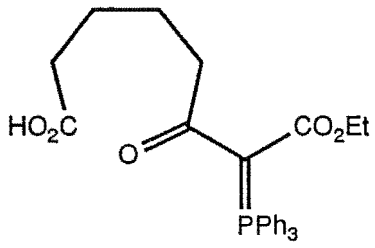

2.75

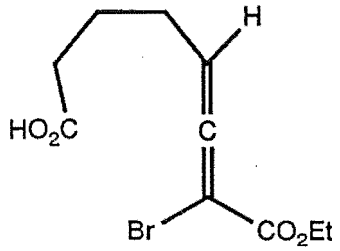

2.76

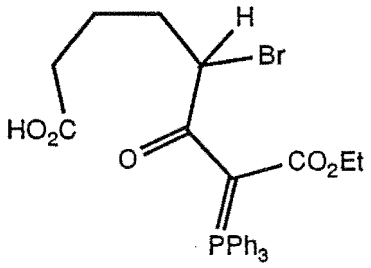

2.77

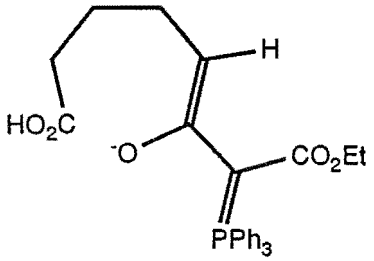

2.78

are formed from competing electrophilic addition of bromine to **2.78**. The failure of the seven-membered ring to cyclise to enol lactone is not surprising as it requires an unfavourable entropy change. This is further evidenced by the failure in formation of the methyl enol lactone from the reaction of adipic anhydride and the methyl ylide **2.53**. Rather, the methyl allene **2.79** forms and does not cyclise.

The diphenic series was subsequently investigated[1.11] since the two phenyl rings lock the proposed phosphonium salt **2.80** in a conformation favourable to cyclisation. Treatment of the phosphorane **2.81**, isolated from

the treatment of diphenic anhydride with ylide **0.1**, under the bromolactonisation conditions gave the *E*- and *Z*-bromo enol

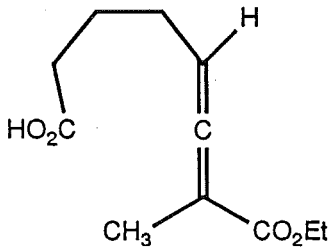

2.79

lactones **2.82** and **2.83** in a ratio of 37:63 respectively[1.11]. This represents a reversal of the stereochemical preference observed in the succinic series. The diphenic phosphorane cannot form a bromo allene as it has no enolisable proton. Again, this suggests that bromo allenes are not intermediates to the bromo enol lactones.

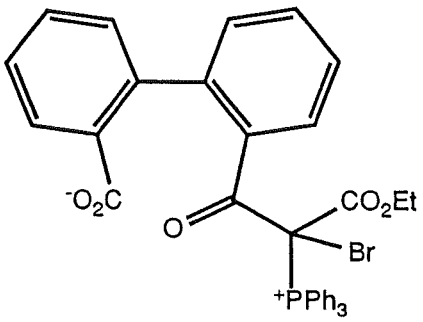

2.80

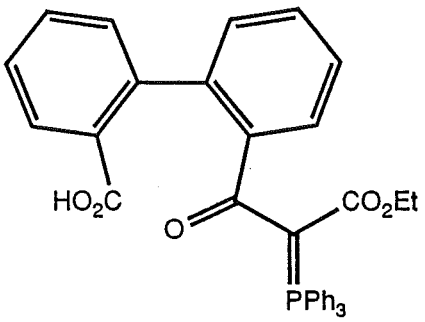

2.81

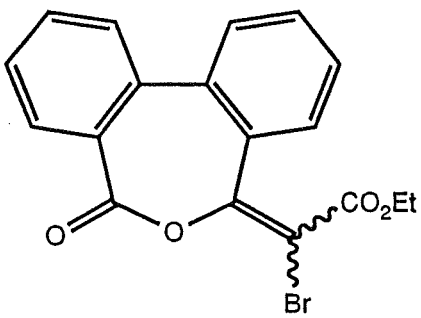

2.82 (*E*), **2.83** (*Z*)

The five-membered phthalic series was also investigated (see Chapter 4). The phthalic phosphorane, which also cannot form a bromo allene without disruption of aromaticity, gave a similar reversal of stereochemical preference. Perhaps, although unlikely, there are actually two mechanisms involved. The reaction could proceed via a bromo allene intermediate if there is an enolisable proton. However, if there is no enolisable proton, the reaction would proceed via the normal Wittig sequence.

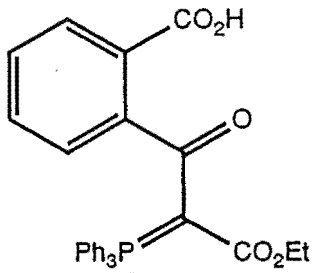

4.17

2.5: Summary

The reactions in this Chapter are summarised in the general Schemes 2.28 and 2.29. The C-acylphosphonium salt, Scheme 2.28, is the key intermediate in the formation of allenes, acetylenes, enol lactones, and bromo enol lactones. The C-acylphosphonium salts can be synthesised by the reaction of the ylide **0.1** with either an anhydride or an acid chloride. Stable C-acyl phosphonium salts may be produced by using substituted ylides **2.31** and **2.53**.

Scheme 2.28: General Scheme A: Summary of Reactions of Anhydrides, Phosphonium salts, and Phosphoranes in Chapter 2

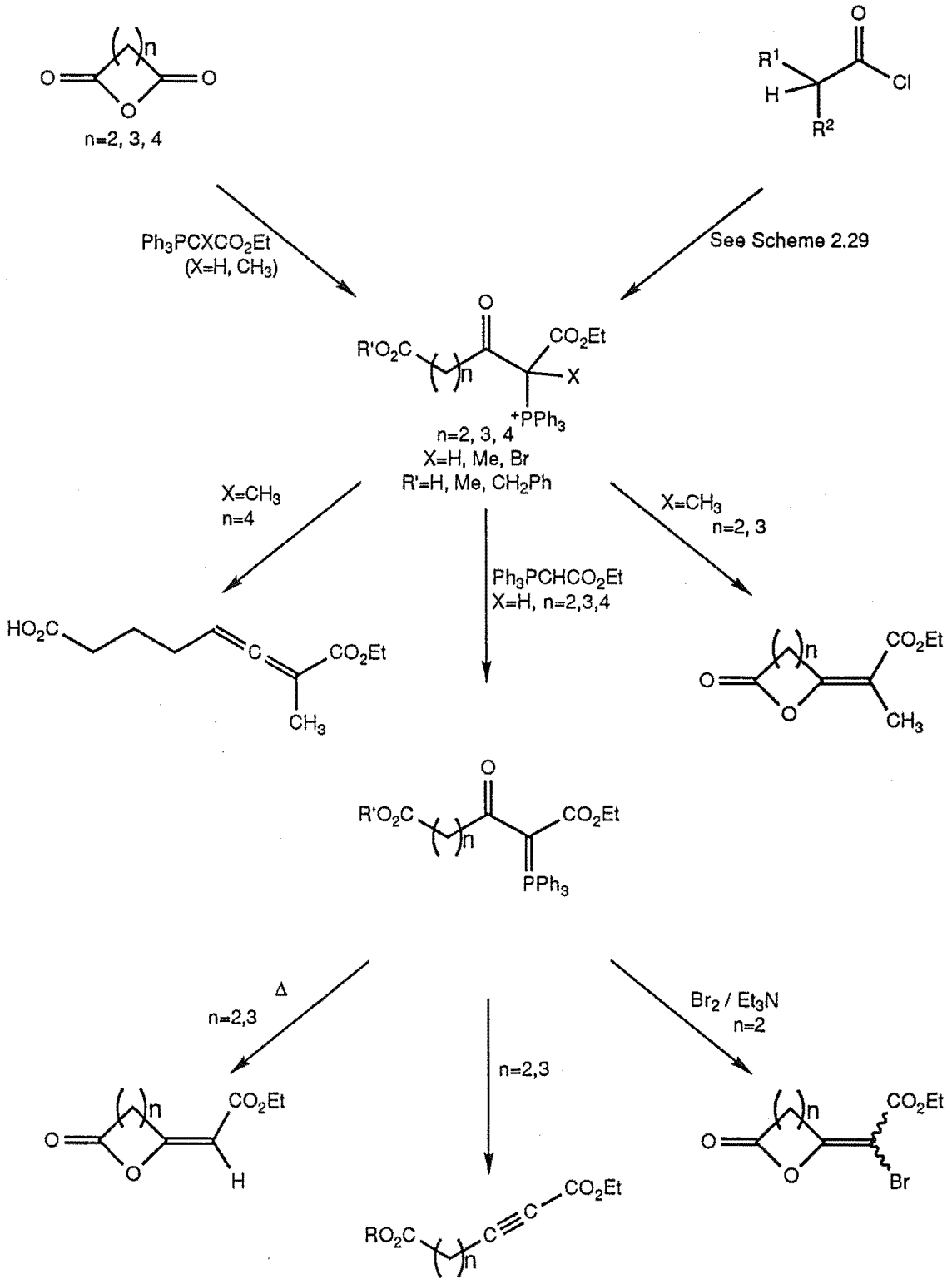

Scheme 2.29: General Scheme B: Summary of Acid Chloride Reactions with Ylides Ph_3CXCO_2Et (X=H, Br, CH_3) in Chapter 2

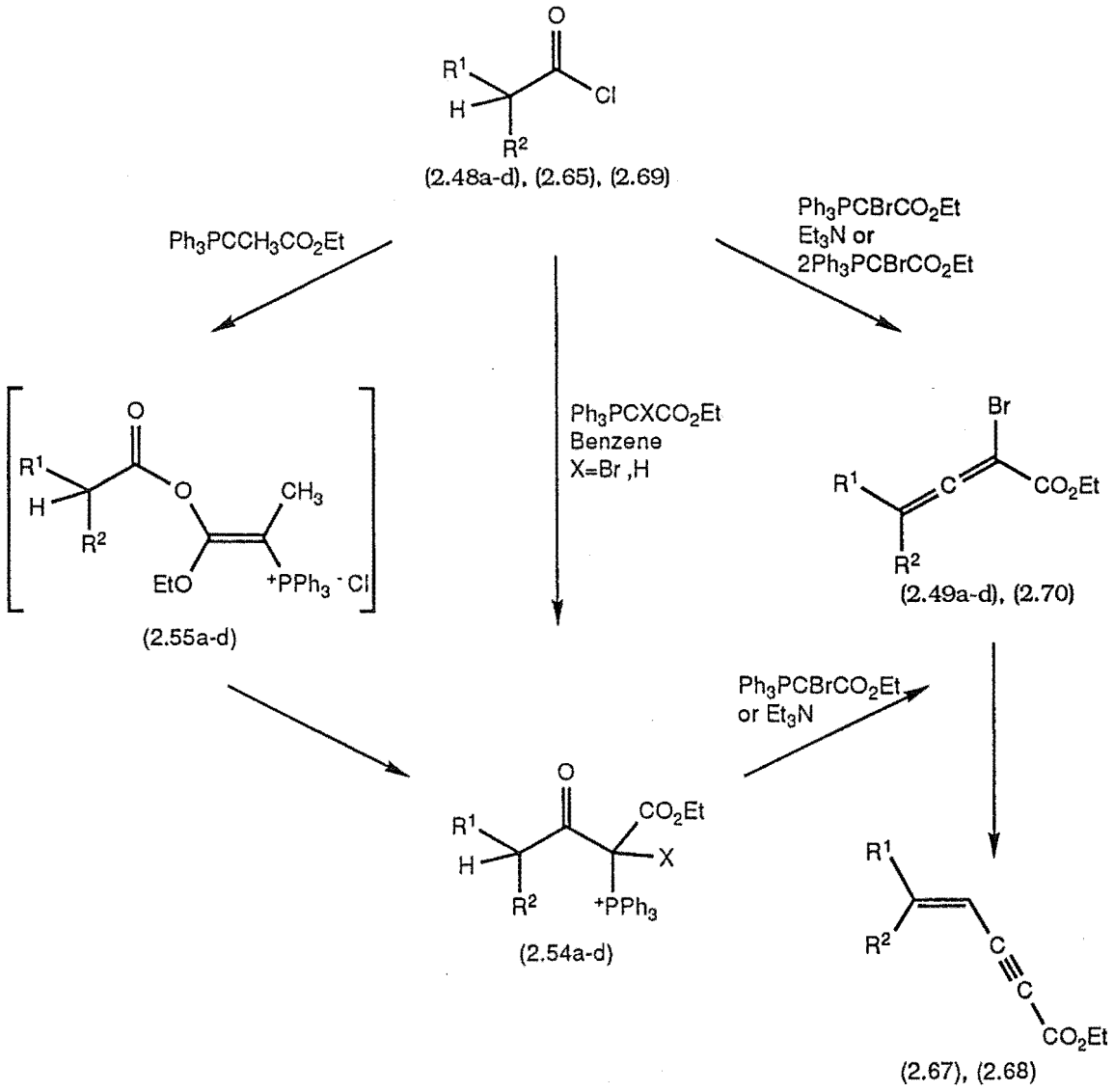

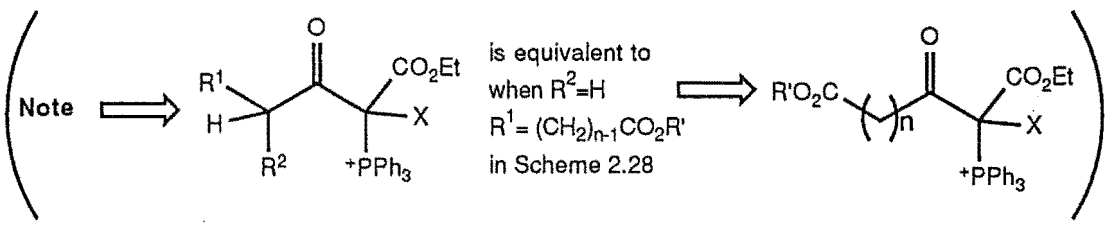

Chapter Three

Synthesis of Glutaric Bromo Enol Lactones

3.1: Introduction

Six-membered halo enol lactones, for example **3.1**, and related compounds are mechanism-based inactivators of chymotrypsin[0.14] and other serine proteases[3.1]. Chymotrypsin catalysed hydrolysis of amides and esters and the mode of enzyme inactivation by halo enol lactones are

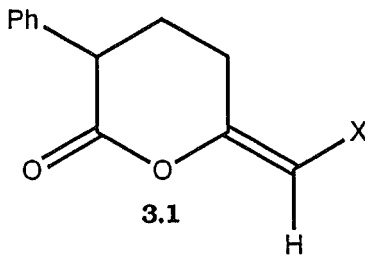

3.1

discussed in detail in Chapter 5 and the Introduction. Six-membered enol lactones are more effective inhibitors[3.2] than five-membered examples as revealed by a higher binding constant K_i, a measure of the affinity of a substrate interaction with the enzyme. The higher affinity of the larger ring examples reflects a better "fit" to the active site. Molecular modelling[3.3] and computer graphics studies[3.3] on chymotrypsin and it's interactions with bromo enol lactones are consistent with the six-membered ring lactones binding with a higher affinity (see Chapter 5).

The overall inactivation rate constants for the inactivation of chymotrypsin depends almost exclusively on the ring size of the inhibitors. The six-membered lactones have 100-200 higher activity than the five-membered[3.2] as mechanism-based inactivators. This may reflect that in the acyl enzyme species, the chain bearing the alkylating group derived from the six-membered ring lactone, Figure 0.6, provides better access to the site of alkylation than the analogous shorter chain derived from the five-membered halo enol lactones.

Although six-membered halo enol lactones are generally better inactivators of chymotrypsin, the five-membered halo enol lactones are of great use in inactivation structure activity relationship studies, as it is easier to modify the substitution.

The strategies adopted for the synthesis of six-membered halo enol lactones are similar to those for the five-membered halo enol lactones discussed in Chapter 2. Halolactonisation of the corresponding acetylenic acids[0.14] is the most widely used procedure, Schemes 3.1, 3.2, and 3.3. A route based on the photoisomerisation of diones[3.4] gives both *E*- and *Z*-isomers, Scheme 3.4. These syntheses have similar disadvantages as those outlined in Chapter 2. The precursors are often time consuming and difficult to prepare, and the syntheses lacks versatility.

The six-membered hydrogen enol lactone **3.2** and the methyl enol lactone **3.3** have been synthesised[2.24] in low yield via the Wittig anhydride olefination reaction. This synthesis is similar to that discussed for the succinic series, Chapter 2, Scheme 2.16. Glutaric anhydride is less reactive than succinic anhydride and only reacts with ylide Ph_3PCHCO_2Et **0.1** under reflux in $CHCl_3$ to form the isolatible acylphosphorane **1.8**, Scheme 3.5. This phosphorane is more stable to cyclisation than the corresponding succinic derived phosphorane **1.7**. In contrast to the succinic series, the *E*-enol lactone **3.2** is the sole stereoisomer obtained[2.24] and this slowly isomerises to the endo product **3.4**. p-Toluenesulphonic

Scheme 3.1

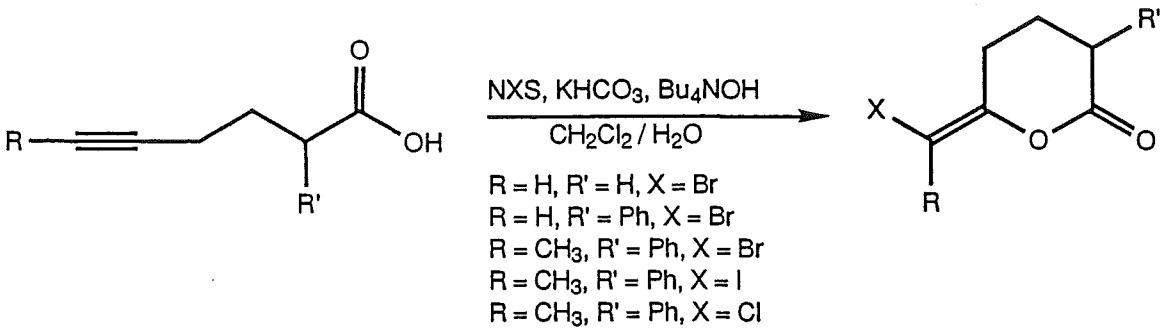

Scheme 3.2

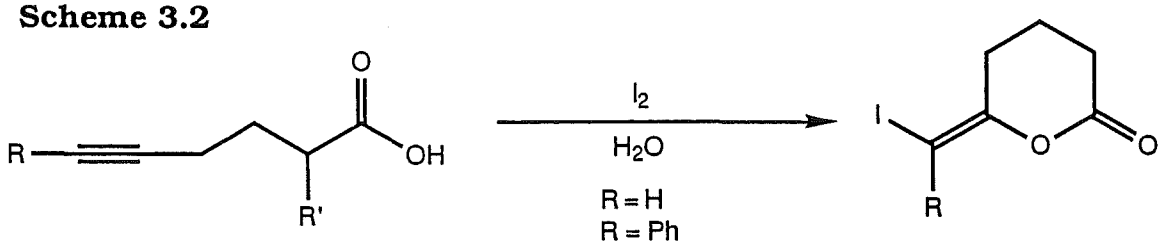

Scheme 3.3

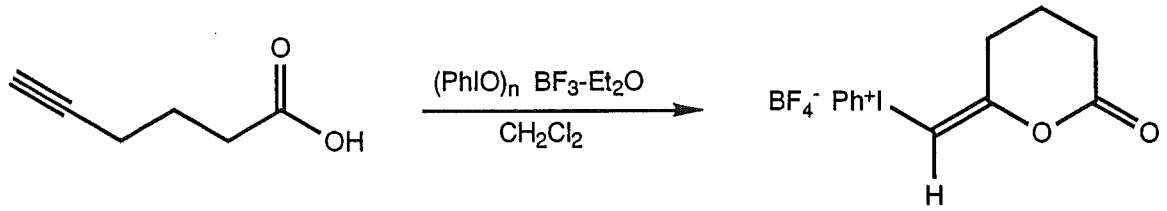

Scheme 3.4

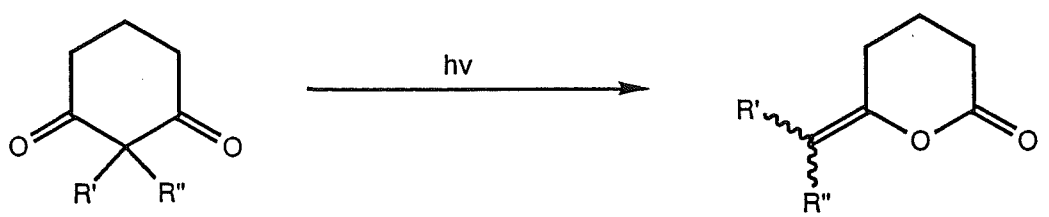

Scheme 3.5 : Mechanism of the Wittig Anhydride Olefination Reaction of Glutaric Anhydride

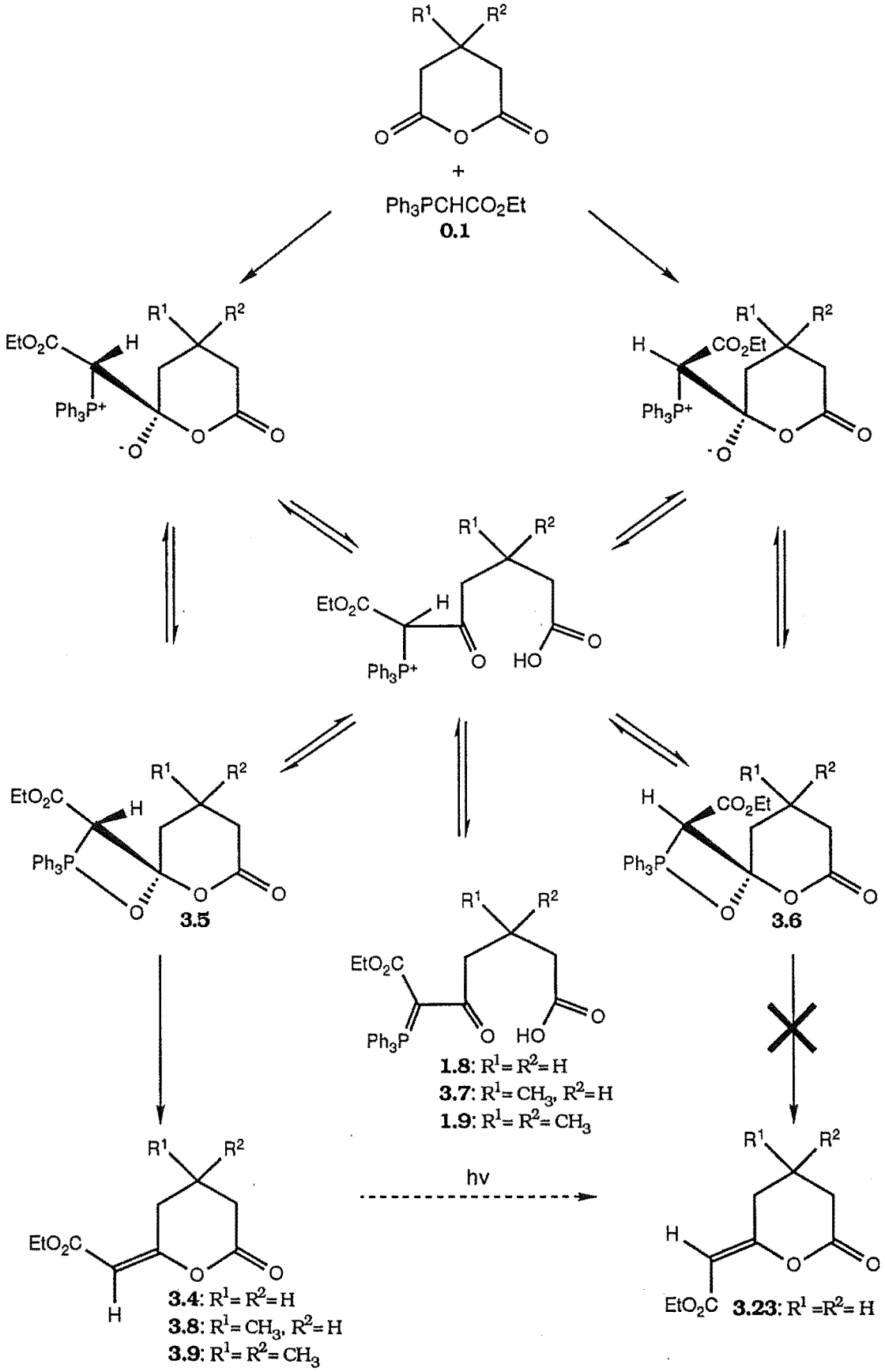

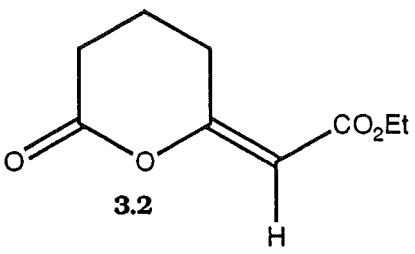

3.2

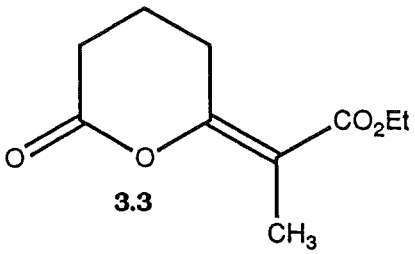

3.3

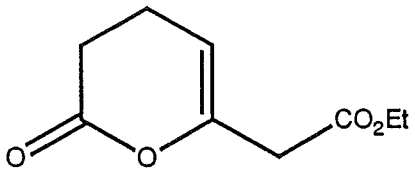

3.4

acid has been shown[2.24] to catalyse this isomerisation.

The formation of the enol lactone **3.2** is less efficient than for the corresponding succinic example, with only 40% formation[2.24b] after 168 hours refluxing in $CHCl_3$. The rate determining step is not the formation of the acylphosphorane **1.8**, but rather the cyclisation and subsequent loss of triphenylphosphine oxide. Thus the stereocontrol must again be due to either the difference in the cyclisation rates of the two transition states (Figure 3.1), or the rate of elimination of triphenylphosphine oxide from the two oxaphosphetanes **3.5** and **3.6**, Scheme 3.5.

The 3-methyl and 3,3-dimethyl phosphoranes[2.1] **3.7** and **1.9**, respectively, cyclise more rapidly and in higher yield than the unsubstituted glutaric phosphorane **1.7**, Table 3.1. This represents an example of the *gem* dimethyl effect[1.15] whereby increased substitution on an acyclic precursor increases the rate of cyclisation. The *E*-enol lactones **3.2**, **3.8**, and **3.9** are obtained as the sole products when using phosphoranes **1.8**, **3.7** and **1.9**. The *Z*-enol lactones are obtainable[2.24] by

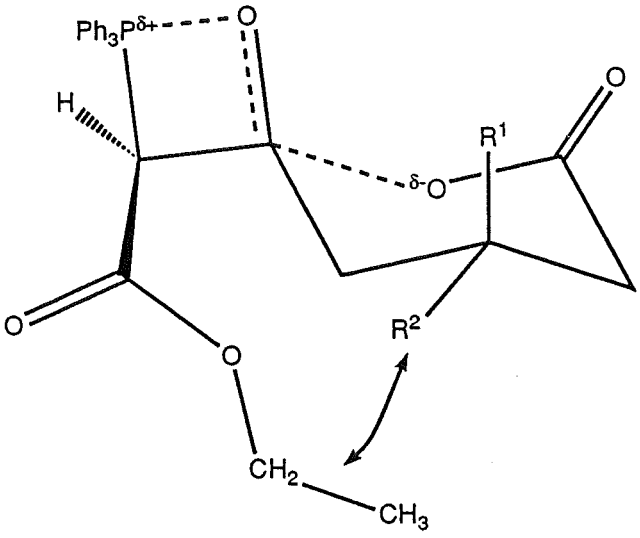

E-transition state

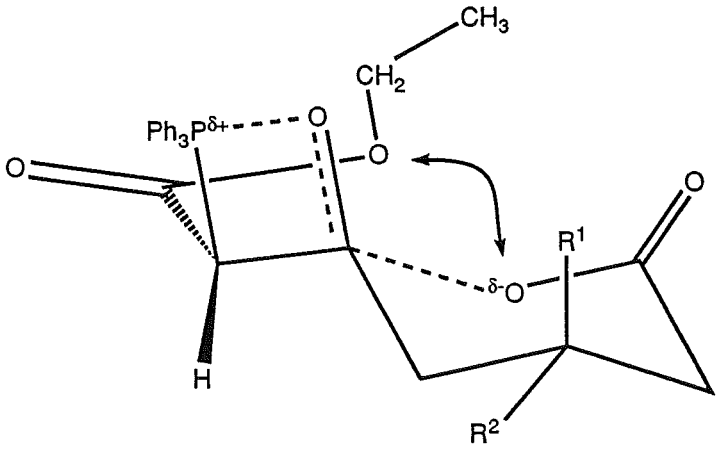

Z-transition state

(Interactions are greater in the *Z*-transition state than in the *E*-transition state)

Figure 3.1

UV induced isomerisation of the corresponding *E*-enol lactones.

The synthesis of large ring enol lactones (n>2, Figure 3.2) via the phosphorane route is difficult (see Chapter 2 for detailed discussion). In summary, the adipic anhydride derived acylphosphorane **1.10** does not cyclise to the hydrogen enol

Table 3.1: Gluaric Acylphosphorane Formation

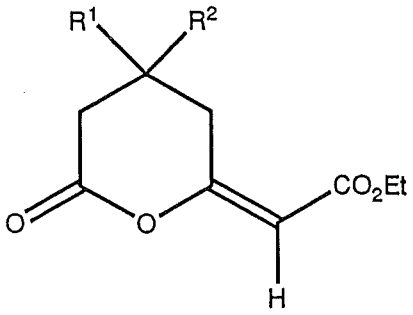

Time	% Enol Lactone Present		
	$R^1=R^2=H$ **3.2**	$R^1=CH_3$, $R^2=H$ **3.5**	$R^1=R^2=CH_3$ **3.6**
1hr	0	10	15
24hrs	30	60	65
168hrs	40	50	85

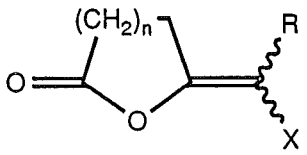

Figure 3.2

lactone even on prolonged heating[1.11]. Similarly, adipic anhydride does not form the methyl enol lactone **3.10** on reaction with the methyl ylide **2.53**, but rather gives the methyl allene **3.10** and other acyclic products[1.7], Scheme 3.6. Similarly, the adipic derived phosphorane **1.10** also does not form bromo enol lactones under the modified SCOOPY bromolactonisation conditions, but rather forms the bromo allene **2.78** and the bromo phosphorane **2.76**. The long chain (n=3, Scheme 3.6) cyclisation is

unfavourable due to entropy factors. Cyclisation is however favourable if the acylphosphorane is forced to adopt a conformation that brings the carboxylate nucleophile close to the keto phosphorane electrophile. For example, bromolactonisation of the diphenic derived phosphorane **1.11** yields the *E*- and *Z*-bromo enol lactones **2.81** and **2.82**, respectively. The two aromatic rings of **1.11** create a barrier to free rotation about the central bond and thus allows the nucleophilic carboxylate to cyclise on bromination. The diphenic derived phosphorane **1.11** does not cyclise to give H enol lactones possibly due to hydrogen bond stabilisation (see Chapter 1). However, diphenic anhydride does react with the more reactive methyl ylide **2.53** to form the corresponding methyl enol lactone.

Adipic and nonanedioic anhydride (n=4 and n=7 respectively) react with methyl ylide **2.53** to yield the allenes[1.7] **3.11** and **3.12**, Scheme 3.6. The mechanism of the reaction of anhydrides with the methyl ylide **2.53** may proceed via two pathways[1.7,1.11]. Firstly, the reaction may proceed without ring opening to form the methyl enol lactone which readily rearranges to the more stable acyclic products (Scheme 3.6). Much more likely, the reaction proceeds via a phosphonium salt (Scheme 3.6). Phosphonium salts of this type have been shown[1.11] to be intermediates in the formation of methyl enol lactones (see Chapter 2).

3.2: Synthesis of Glutaric Bromo Enol Lactones

The Wittig anhydride olefination reaction was investigated as a viable synthesis of six-membered halo enol lactones. The methodology discussed in Chapter 2, for the formation of five-membered halo enol lactones, was applied to the glutaric series. The bromo ylide **2.31** did not react with glutaric anhydride directly. This is not surprising as glutaric anhydride is less reactive than succinic anhydride, due to the lack of inherent ring

Scheme 3.6 : Possible Mechanisms for Allene Formation from Large Ring Anhydrides

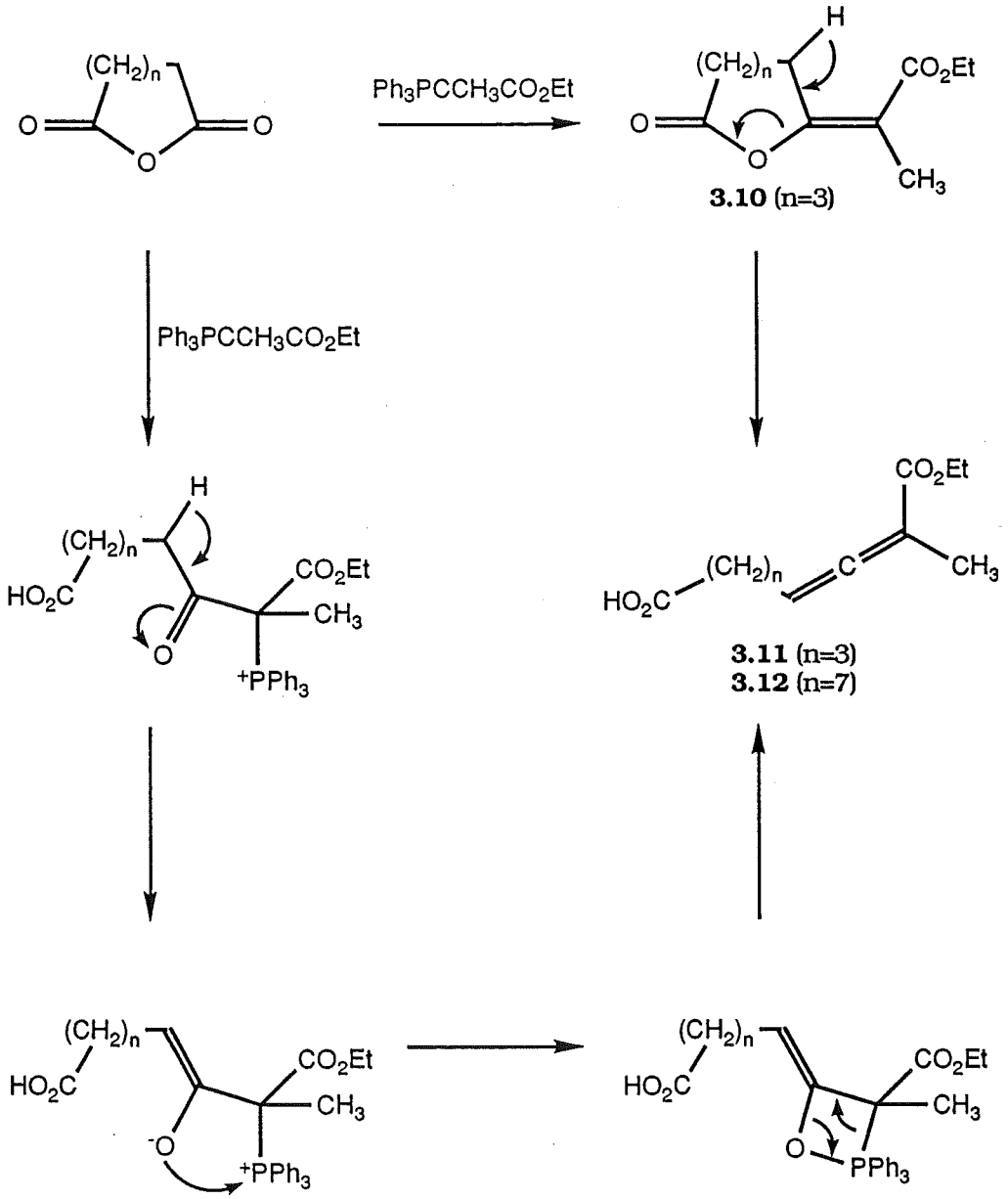

strain.

The phosphoranes **1.8** and **1.9** were prepared by reacting the corresponding anhydrides with the ylide Ph_3PCHCO_2Et in $CHCl_3$ under reflux for one hour[2.1]. The ^{31}P and ^{1}H NMR spectroscopy signals for the phosphoranes were characteristic[2.1] (Table 3.2[2.1]).

The bromolactonisation conditions, outlined in Chapter 2, were applied to these phosphoranes, Scheme 3.7. Solutions of each of the phosphoranes **1.8**, **3.7**, and **1.9** were separately cooled to O°C in CH_2Cl_2 under a nitrogen atmosphere. One equivalent of triethylamine, followed by one equivalent of bromine, were added and after 30 minutes at O°C the solutions were allowed to warm to room temperature. The reactions were instantaneous, as evidenced by the decolourisation of the bromine. The bromolactonisation of the phosphoranes **1.8**, **3.7**, and **1.9** gave both *E* (major) and *Z* (minor) stereoisomers (Table 3.3). A small amount of the endo product **3.19** was also obtained from the reaction of glutaric phosphorane **1.8**. The amount of the endo isomer **3.19** increased with time.

Table 3.2: ^{1}H NMR and ^{31}P NMR Spectroscopy Signals of Acylphosphoranes 1.8, 3.7, 1.9

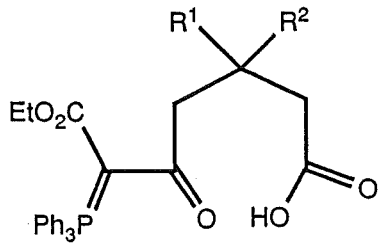

Compound	$O_2CH_2CH_3$	$O_2CH_2CH_3$	PPh_3
1.8: $R^1=R^2=H$	0.65	3.65	17.2
3.7: $R^1=CH_3$, $R^2=H$	0.66	3.65	17.6
1.9: $R^1=R^2=CH_3$	0.65	3.66	17.5

Scheme 3.7: Mechanism of the Bromolactonisation Reaction of Glutaric Derived Phosphoranes 1.8, 3.7, and 1.9.

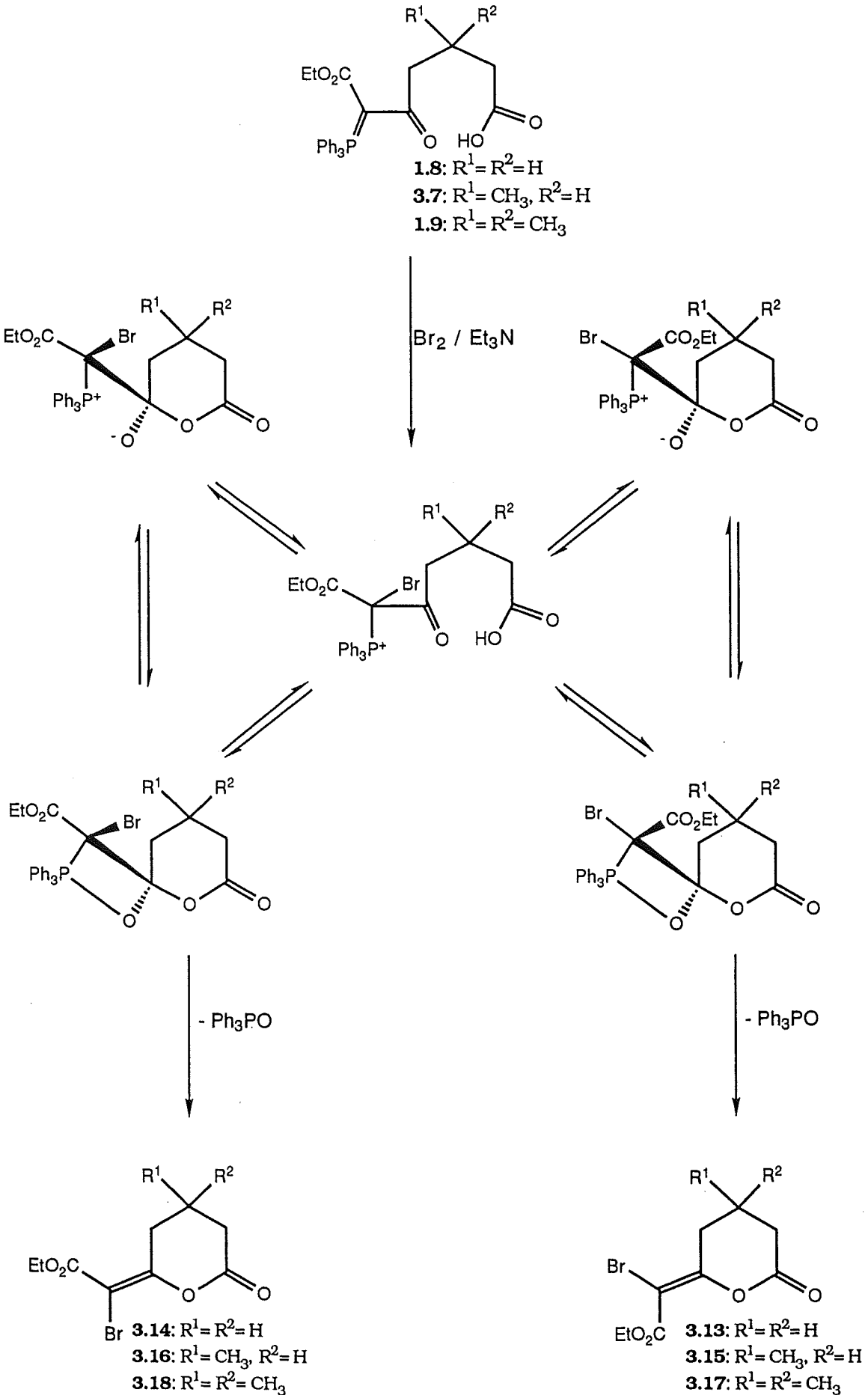

3.2.1: Mechanism of Formation of Glutaric Bromo Enol Lactones.

Stereocontrol in the bromolactonisation of the glutaric derived phosphoranes is greater than in the succinic derived phosphoranes. The *E*- and *Z*-stereoisomeric bromo enol lactones derived from the glutaric phosphoranes **1.8**, **3.7**, and **1.9** revealed a high *E*- preference (90-95%) while the *E*- and *Z*-stereoisomeric bromo enol lactones from the succinic phosphorane **1.7** were obtained in a ratio is 7:3, respectively. This suggests that with increased ring size the steric and electronic interactions in the transition states (Figure 3.3) have

Table 3.3: *E*- and *Z*-Glutaric Bromo Enol Lactones: Stereochemical Preferences and Yields

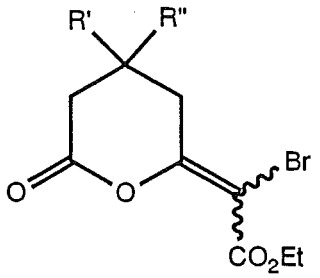

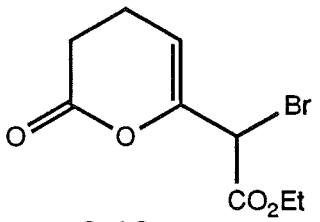

3.19

Bromo enol lactones	***E* (%)**	***Z* (%)**	***Endo***	**Total Yield**
Glutaric	82	10	8	85%
R'= R"= H	**3.13**	**3.14**	**3.19**	
3-Methyl glutaric	85	15	0	91%
R'= H, R"= CH_3	**3.15**	**3.16**		
3,3-Dimethyl glutaric	88	12	0	86%
R'= R"= CH_3	**3.17**	**3.18**		

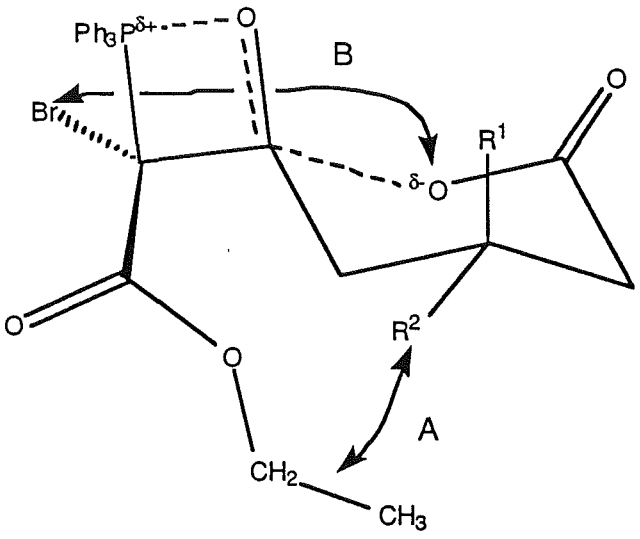

Z-transition state

Interactions are greater in B than in A

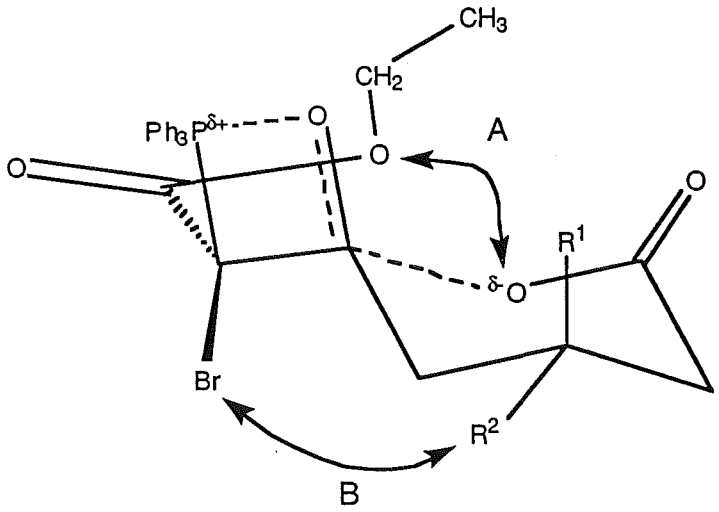

E-transition state

(Interactions are greater in the *Z*-transition state than in the *E*-transition state)

Figure 3.3

more influence. The increased flexibility of the carboxylic group, due to the increased alkyl chain length of the glutaric system, allows greater interaction with the ester functionality (Figure 3.3).

The protected acid chloride **3.20** was reacted with the bromo ylide **2.31** in an attempt to prepare the allene **3.21**, a protected form of a possible reaction intermediate. It was reasoned that the undesired elimination of HBr from the allene **3.21** to give the acetylene **3.22** might

not occur as readily as in the succinic series. Unfortunately the reaction of **3.20** did not form the allene **3.21** or the acetylenic compound **3.22**, similar to **2.67**.

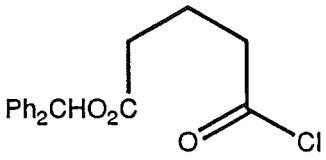

3.20

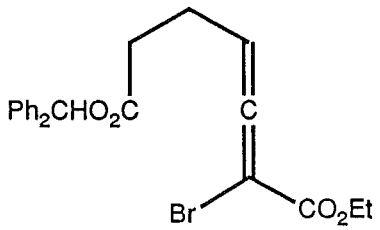

3.21

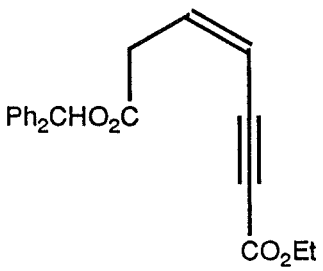

3.22

3.2.2: Structure Assignment and MM2 Calculations of Glutaric Bromo Enol Lactones

The bromo enol lactones **3.13-18** were assigned on the basis of ^{1}H and ^{13}C NMR spectral data. The *E*- and *Z*-stereochemical assignment was based on a comparison of the ^{1}H NMR spectra of structurally similar enol lactones[0.14,0.15,3.2] and the succinic bromo enol lactones reported in Chapter 2 (Table 3.4a-c). The $(H\text{-}3)_2$ proton resonance is shifted downfield by 0.2-0.5 ppm when the ester group is *trans* to the lactone oxygen (Figure 2.3).

Molecular mechanics[2.29] (MM2) calculations were carried out on the isomeric bromo enol lactones **3.13** and **3.14** and the endo product **3.19** in order to determine thermodynamic stabilility. Both the *E* **3.13** and *Z* **3.14** isomers were minimised with rotation of the three chain bonds and the ring system. The C6-C7 and C7-O3 bonds required 180° increments as C6 and C7 are sp^2 hybridised, O3-C8 was rotated in 60° increments. The endo product was minimised with rotation of the chain bonds and the ring system. The bonds C5-C6, C6-C7, O3-C8 required 60° increments and the bond C7-O3 required 180° increments.

Table 3.4a: ^{1}H NMR of *E*-Glutaric Bromo Enol Lactones

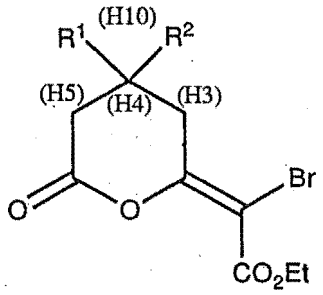

	^{1}H NMR signals(ppm)			
Compound	(H5)	(H4)	(H3)	(H10)
3.13 $R^1 = R^2 = H$	2.67, t, 6.5	1.97, m	2.80, t, 6.5	-
3.15 $R^1 = H, R^2 = CH_3$	2.70, dd, 2.6, 15.5 2.30, m	2.3, m	3.05, dd, 2.6, 15.5 2.30, m	1.12, d, 6.1
3.17 $R^1 = R^2 = CH_3$	2.47, s	-	2.65, s	1.12, s

Table 3.4b:^{1}H NMR of *Z*-Glutaric Bromo Enol Lactones

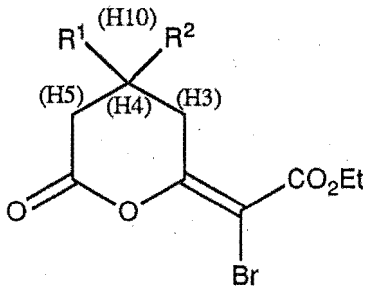

	^{1}H NMR signals			
Compound	(H5)	(H4)	(H3)	(H10)
3.14 $R^1 = R^2 = H$	2.71, t, 6.4	1.96, m	3.16, t, 6.4	-
3.16 $R^1 = H, R^2 = CH_3$	2.79, dd, 1.9, 17.2 2.33, dd, 10.4, 17.2	2.17, m	3.53, dd, 10.4, 17.4 2.82, ddd, 1.9, 4.3, 17.2	1.12, d, 6.6
3.18 $R^1 = R^2 = CH_3$	2.53, s	-	3.01, s	1.10, s

Table 3.4c:^{1}H NMR of *E*-Glutaric Enol Lactones

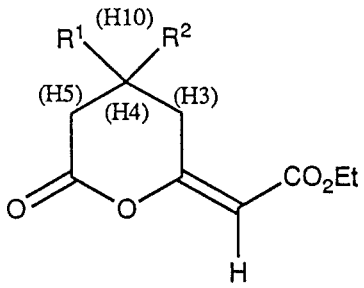

Compound	^{1}H NMR signals (H5)	(H4)	(H3)	(H10)
3.2 $R^1 = R^2 = H$	1.80 - 3.00, m		3.25, dt	-
3.5 $R^1 = H, R^2 = CH_3$	2.00 - 3.00, m		3.58	1.10
3.6 $R^1 = R^2 = CH_3$	2.45, s	-	3.02, s	1.10, s

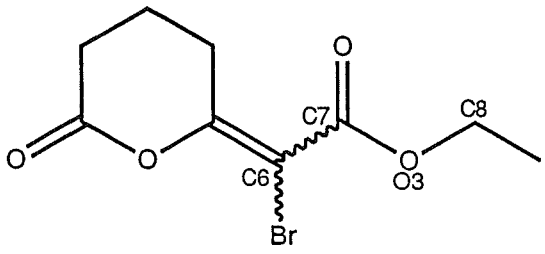

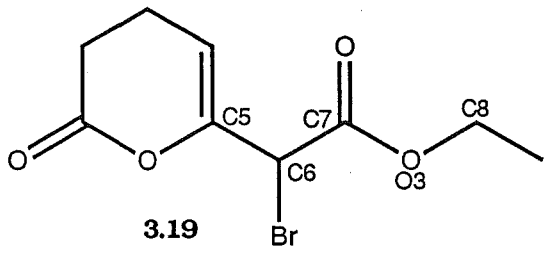

3.19

Energy minimisation of the *E*-structure produced 38 isomers having energies within 3Kcal/mol of the minimum energy. Application of the Boltzman distribution at 25°C showed that the 10 lowest energy isomers accounted for 42.19% of the population and that the Boltzman average energy was 25.25Kcal/mol (Table 3.5). The energy minimisation of the *Z*-structure produced 26 conformers having energies within 3Kcal/mol of the minimum energy. Application of the Boltzman distribution at 25°C

showed that the 10 lowest energy isomers accounted for 81.32% of the population and that the Boltzman average energy was 24.68Kcal/mol (Table 3.5) (the four lowest energy conformers for the bromo enol lactones **3.13** and **3.14** are in Figure 3.4).

The *E*-enol lactone **3.13**, calculated to be thermodynamically less stable than the *Z*-enol lactone **3.14**, is produced in the reaction of glutaric anhydride and ylide **0.1**. The MM2 calculations suggest that the kinetic product is favoured over the thermodynamic *Z*-isomer. This is consistent with the MM2 calculations and experimental evidence[2.24] given in Chapter 2.

The experimentally observed[2.24] thermodynamically stable endo product **3.19** (see 3.1: Introduction) was found on minimisation to have a significantly lower Boltzman average energy of 16.33Kcal/mol. 80 conformers having energies within 3Kcal/mol of the minimum energy (Table 3.5) (the four lowest conformers are in Figure 3.5).

The large number of conformers observed in the glutaric systems, compared to the succinic systems (see Chapter 2), is due to the increased number of conformations of the six-membered ring. The very large number of conformers of the endo system is a reflection of the free rotation of the side chain.

Model calculations were also carried out on the *E*- and *Z*-hydrogen enol lactone systems **3.2** and **3.23** to determine the reliability of the MM2 method (Table 3.5). The results are predictable and similar to the succinic series in that the *Z*-enol lactone is the thermodynamically more stable isomer yet the *E*-enol lactone is exclusively observed experimentally (the four lowest energy conformers for the enol lactones **3.2** and **3.23** are in Figure 3.6).

Figure 3.4: Four Lowest Energy Conformers of 3.13 and 3.14.

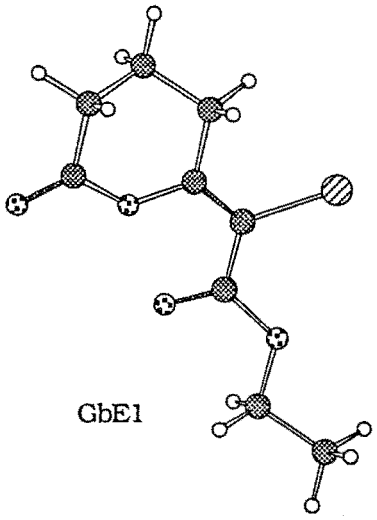

GbE1

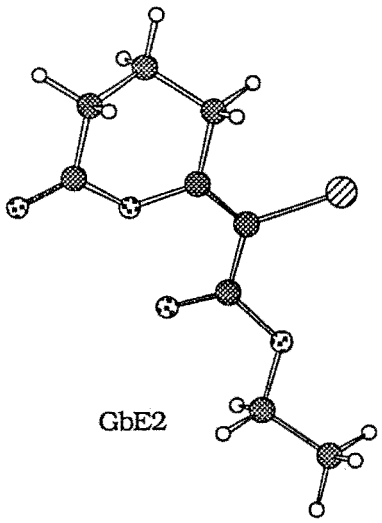

GbE2

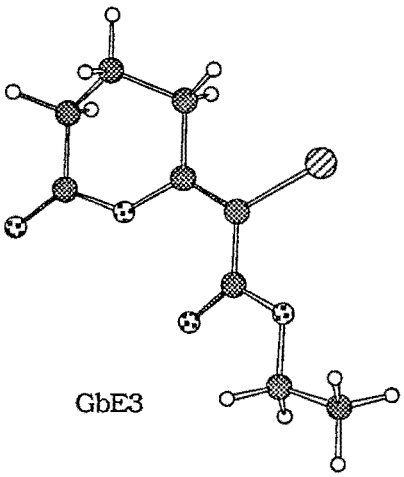

GbE3

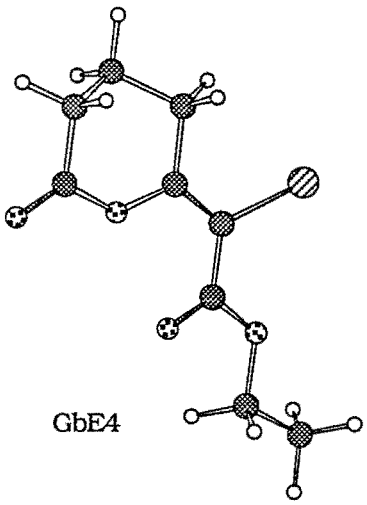

GbE4

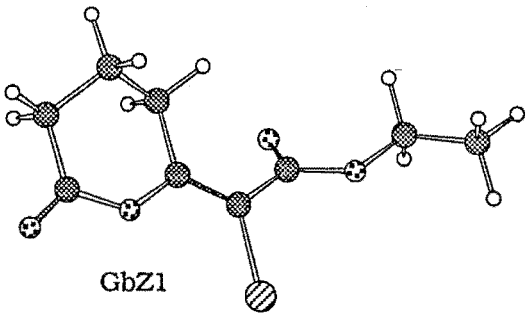

GbZ1

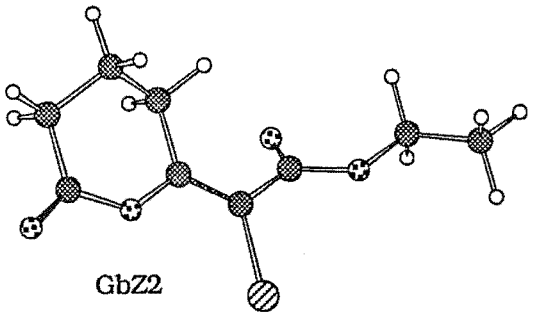

GbZ2

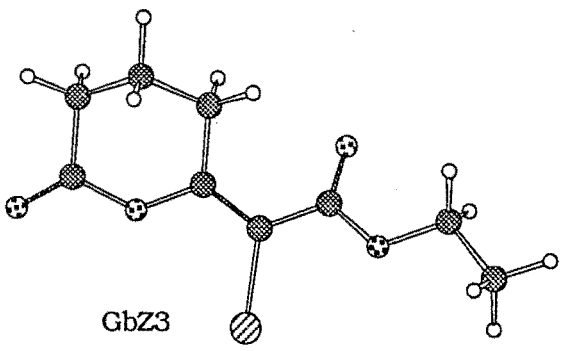

GbZ3

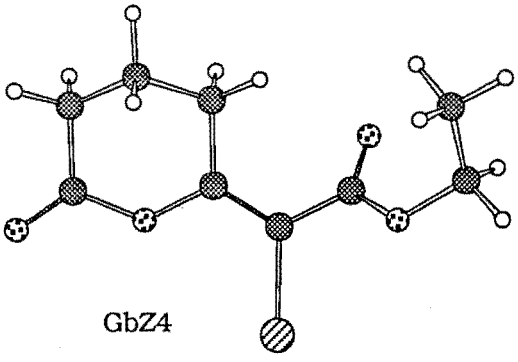

GbZ4

Figure 3.5: Six Lowest Energy Conformers of 3.19.

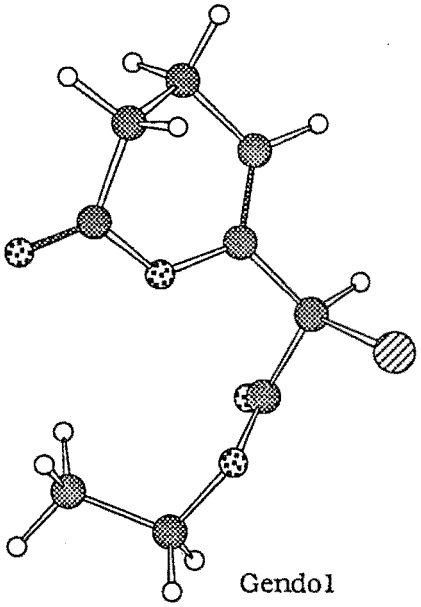

Gendo1

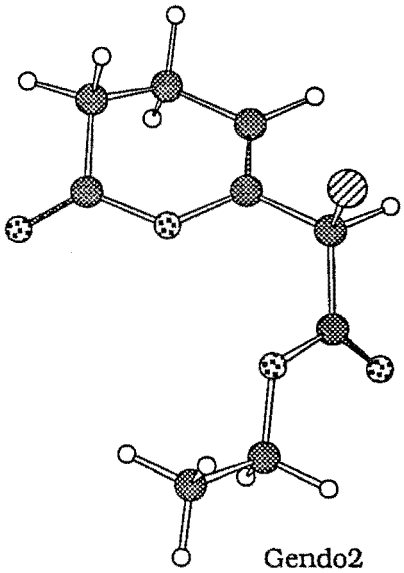

Gendo2

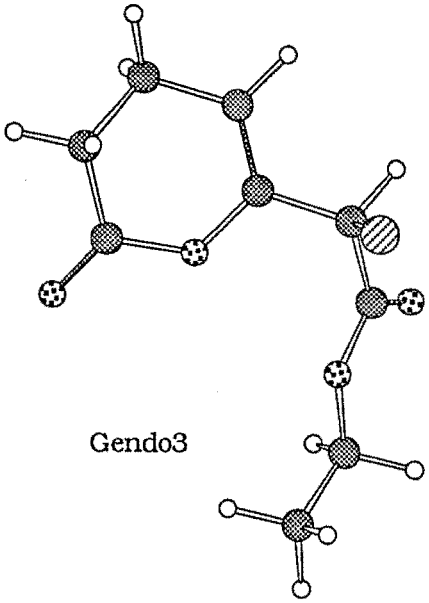

Gendo3

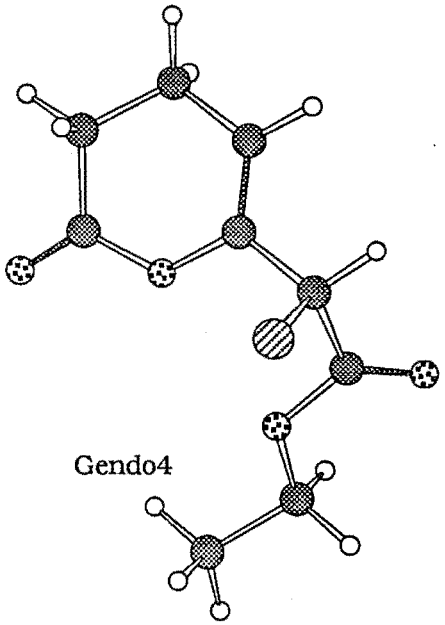

Gendo4

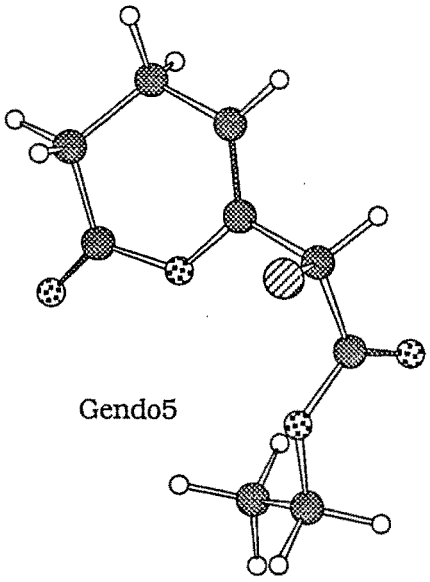

Gendo5

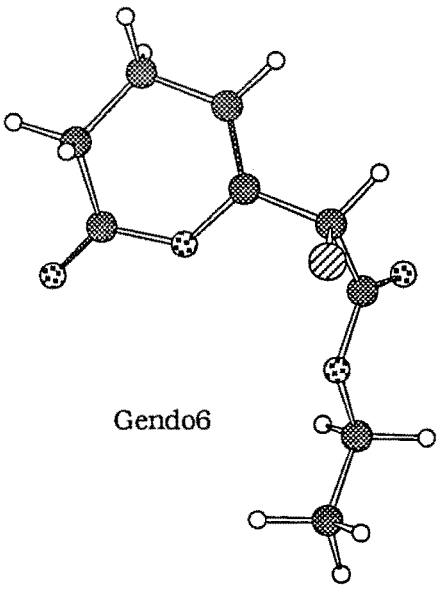

Gendo6

Figure 3.6: Four Lowest Energy Conformers of 3.2 and 3.23.

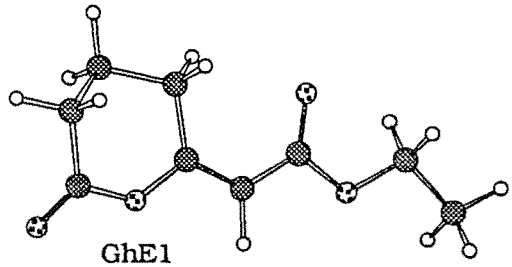

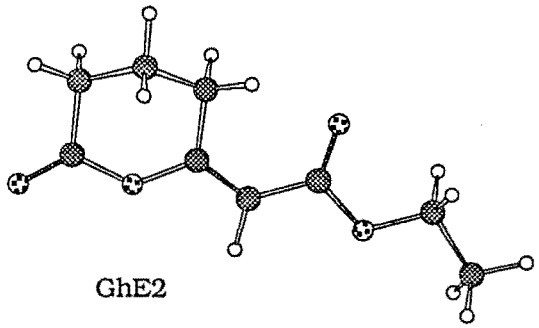

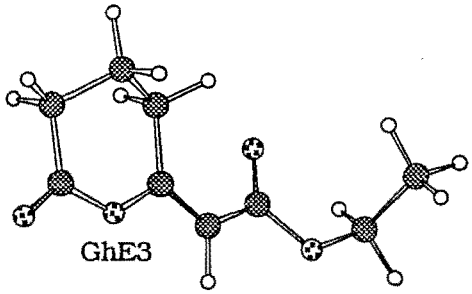

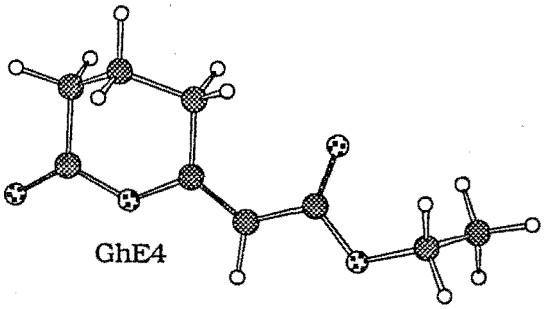

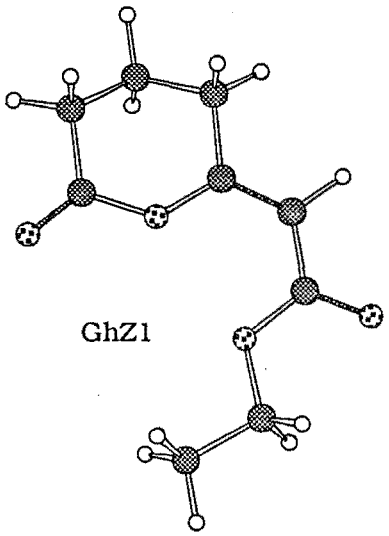

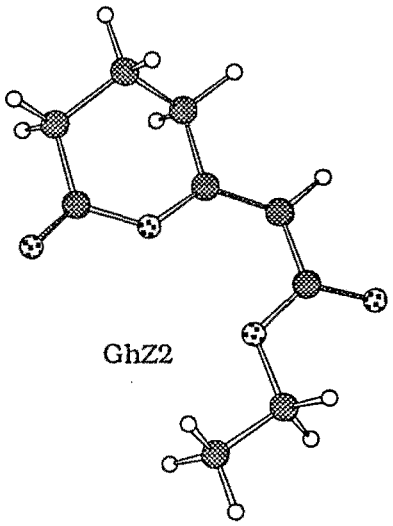

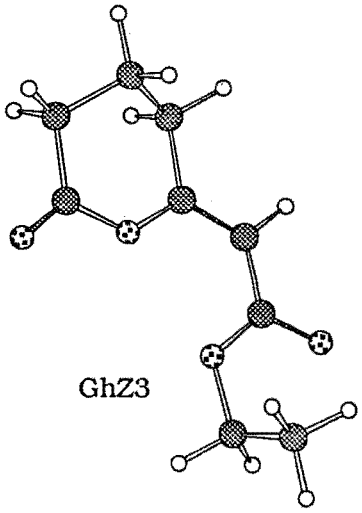

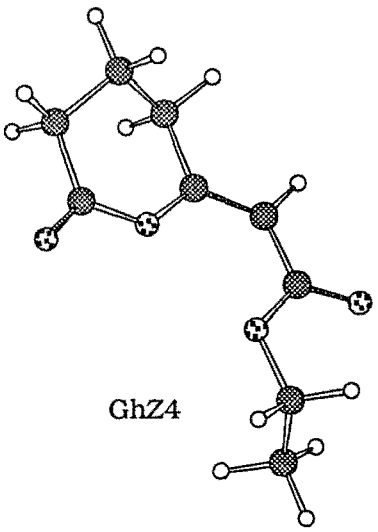

Table 3.5: MM2 Energy Minimisations on Glutaric Hydrogen and Bromo Enol Lactones 3.2, 3.23, 3.13, and 3.14 and Endo isomer 3.19

System	Conformer%	Energy (Kcal/mol)	Boltzman average Energy (Kcal/mol)
gbe **3.13**			
	1 = 5.78%	24.845	25.25
	2 = 5.42%	24.883	
	3 = 4.50%	24.994	
	4 = 4.40%	25.007	
	5 = 3.99%	25.066	
	6 = 3.97%	25.069	
	7 = 3.67%	25.115	
	8 = 3.60%	25.127	
	9 = 3.57%	25.132	
	10 = 3.29%	25.180	
gbz **3.14**			
	1 = 10.69%	24.322	24.68
	2 = 10.66%	24.323	
	3 = 10.34%	24.342	
	4 = 7.80%	24.510	
	5 = 7.77%	24.512	
	6 = 7.77%	24.513	
	7 = 7.29%	24.550	
	8 = 7.18%	24.559	
	9 = 6.58%	24.612	
	10 = 5.24%	24.747	
gendoBr **3.19**			
	1 = 5.18%	15.689	16.33
	2 = 5.01%	15.709	
	3 = 4.46%	15.778	
	4 = 4.19%	15.815	
	5 = 4.10%	15.829	
	6 = 3.98%	15.846	
	7 = 3.93%	15.853	
ghe **3.2**			
	1 = 14.49%	19.537	19.95
	2 = 14.47%	19.538	
	3 = 10.63%	19.722	
	4 = 9.98%	19.760	
	5 = 9.18%	19.809	
	6 = 8.88%	19.829	
	7 = 8.79%	19.835	
ghz **3.23**			
	1 = 15.63%	17.554	18.00
	2 = 14.45%	17.601	
	3 = 7.76%	17.972	
	4 = 7.65%	17.980	
	5 = 7.63%	17.982	
	6 = 7.61%	17.983	

3.3: Summary

The bromolactonisation reaction has been extended to include six-membered rings. Greater stereocontrol than in the succinic series is observed in the formation of the glutaric bromo enol lactones. There is a preference for the *E*-bromo enol lactones of ≈ 85%. This is consistent with the succinic series which has a *E*-stereoisomer preference of 70%.

Chapter Four

Synthesis of Phthalic Bromo Enol Lactones

4.1: Introduction

Phthalic derived enol lactones are also biologically[0.12] and commercially[4.1] important. For example, the main source of celery odour and flavour in the perfumery and flavour industries is the naturally occurring alkylidene phthalides[4.1] **4.1** and **4.2**. The natural compound[0.12] **4.3** has been found to be an inhibitor of root geotropism.

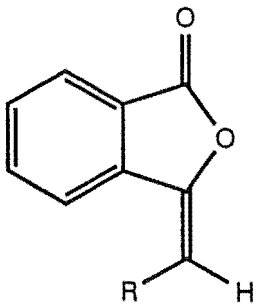

4.1: R = *i*-Pr
4.2: R = *i*-Bu

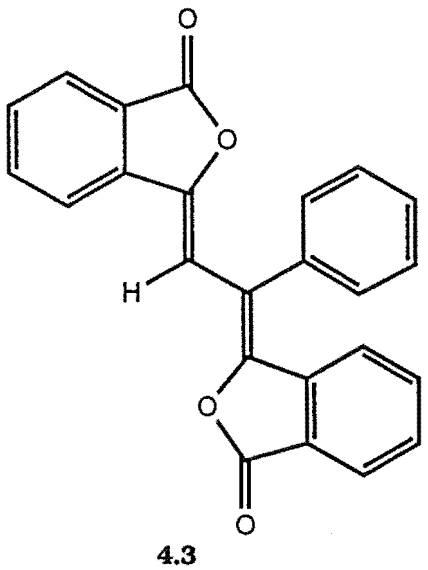

4.3

The alkylidene phthalides are of interest as potential mechanism-based inactivators of serine proteases due to the presence of the aromatic ring. Chymotrypsin, a typical serine protease, cleaves a peptide on the

carboxyl side of an aromatic amino acid. The closely related isocoumarins (benzopyran-1-ones) **4.4** and **4.5** have been shown[2.40] to be mechanism-based inactivators of chymotrypsin. The mode of inactivation[0.16] envolves the enzyme hydrolysis of the lactone **4.4** to reveal a reactive acyl chloride (Scheme 4.1) that then acylates a nearby nucleophile, thus blocking the active site and inactivating the enzyme.

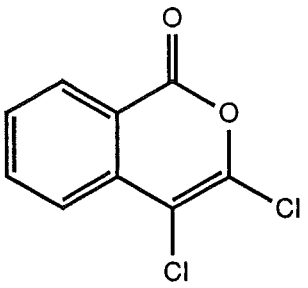

4.4

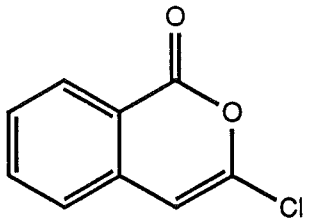

4.5

It has been shown[2.40] by this research group that the bromo lactones **4.6**, **4.7**, and **4.8** also inactivate chymotrypsin. The probable mode of inactivation of **4.6**, **4.7**, and **4.8** differs from **4.4** in that enzyme catalysed hydrolysis releases a reactive electrophilic alkylating α-halo ketone, which can alkylate an active site nucleophile, thus inactivating the enzyme. Work in this research group[2.40] has also shown that the halo enol lactones **4.9**, **2.81**, and **2.82** inactivate chymotrypsin. Since **4.9**, **2.81**, and **2.82** have aromatic rings in a similar position to the alkylidene phthalides it was thought that the introduction of a halo enol moiety in the alkylidene phthalides may produce potent mechanism-based inactivators.

Few syntheses of halo alkylidene phthalides have been reported in the literature. The only general synthesis[4.2] relies on the halogenation of the phthalide followed by loss of HBr to form the bromo enol lactone **4.10**, Scheme 4.2. Both the *E*- and *Z*-stereoisomers are formed, when R=H or propyl, Scheme 4.2. The synthesis of the alkylidene phthalides **4.11** is

Scheme 4.1: Inactivation of a Serine Protease by Isocoumarin 4.4

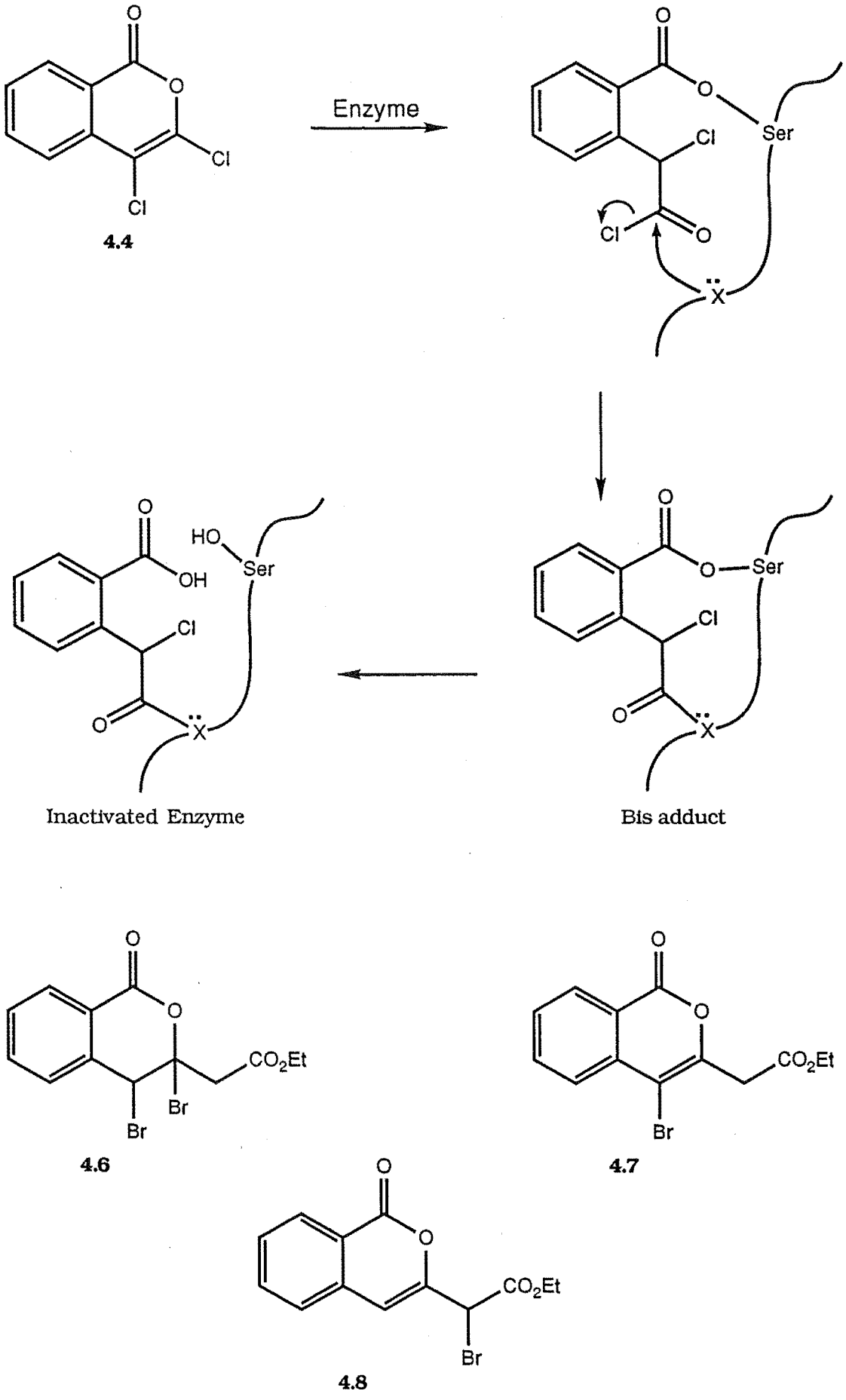

4.4

4.6

4.7

4.8

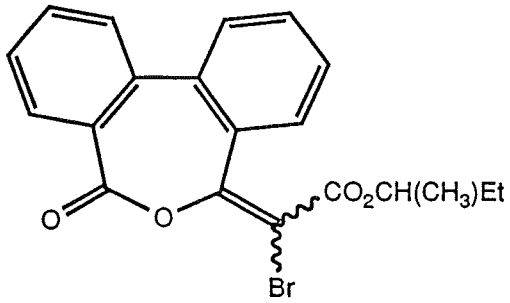

4.9

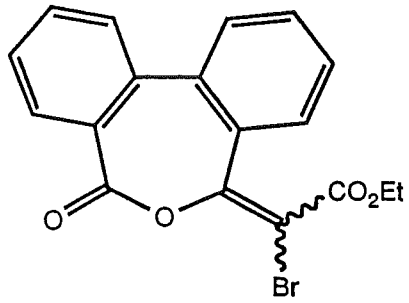

2.81, 2.82

crucial to the above synthesis, and is also of interest in the synthesis of natural compounds. Few general syntheses for the formation of alkylidene phthalides have been reported. The photoisomerisation of diones[4.3] **4.12** to alkylidene phthalides **4.11** gives both the *E*- and *Z*-stereoisomers in low yield (combined yields of around 50%), Scheme 4.3. A Wittig olefination reaction has been utilised in two ways[4.4] to produce hydrogen alkylidene phthalides. Firstly, a direct reaction[4.4] to form the phthalide phosphorus ylide, and subsequent reaction with an aldehyde gave the *E*-phthalic enol lactones (Scheme 4,4). The second method[2.1] uses of the Wittig anhydride

Scheme 4.2:

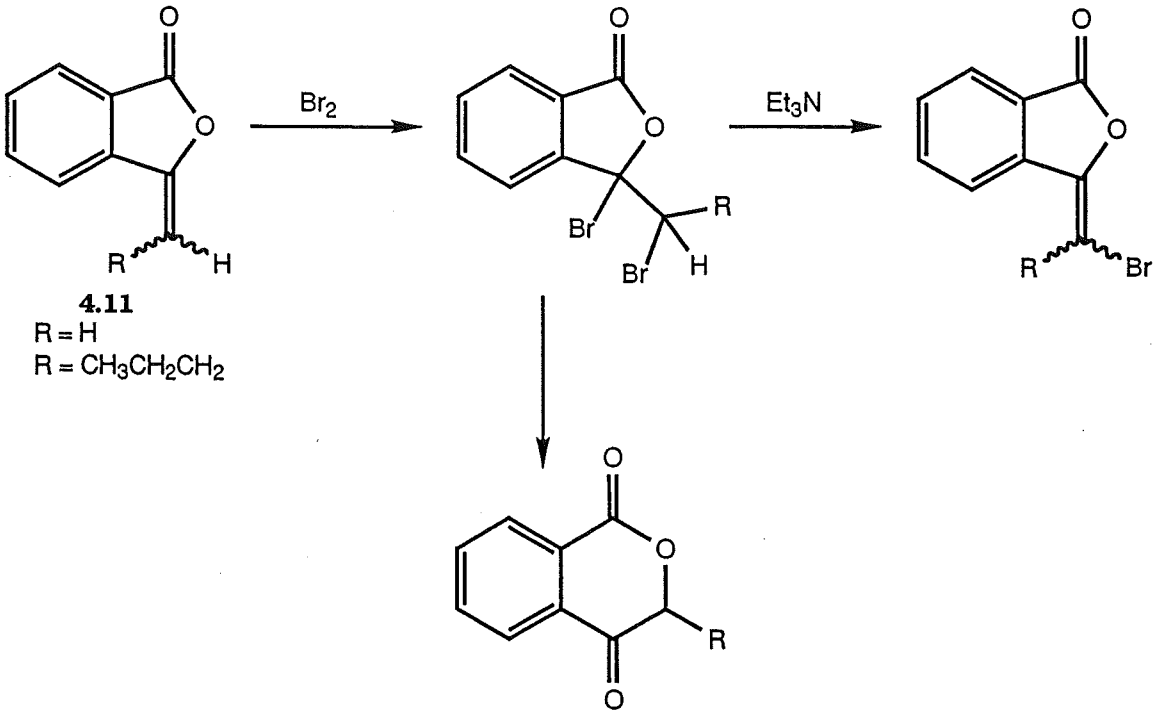

4.11
R = H
R = $CH_3CH_2CH_2$

Scheme 4.3:

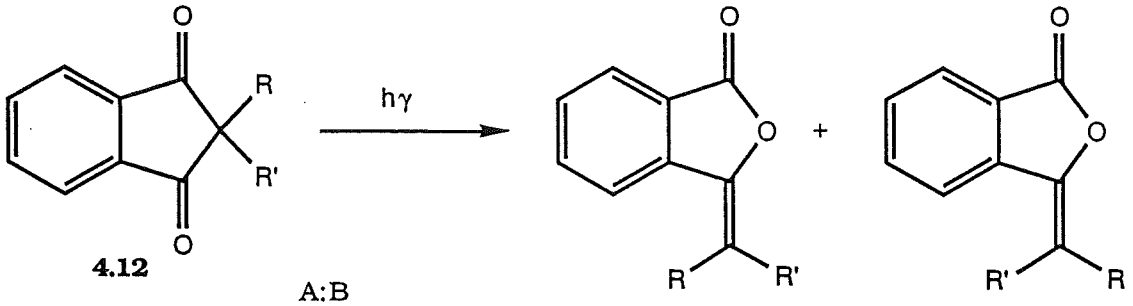

4.12 **A** **4.11** **B**

	A:B
R=Ph R'=H	43:7
R=Ph R'=CH_2Ph	11:32
R=Ph R'=CH_3	11:43
R=Ph-OMe(p) R'=H	69:0

Scheme 4.4

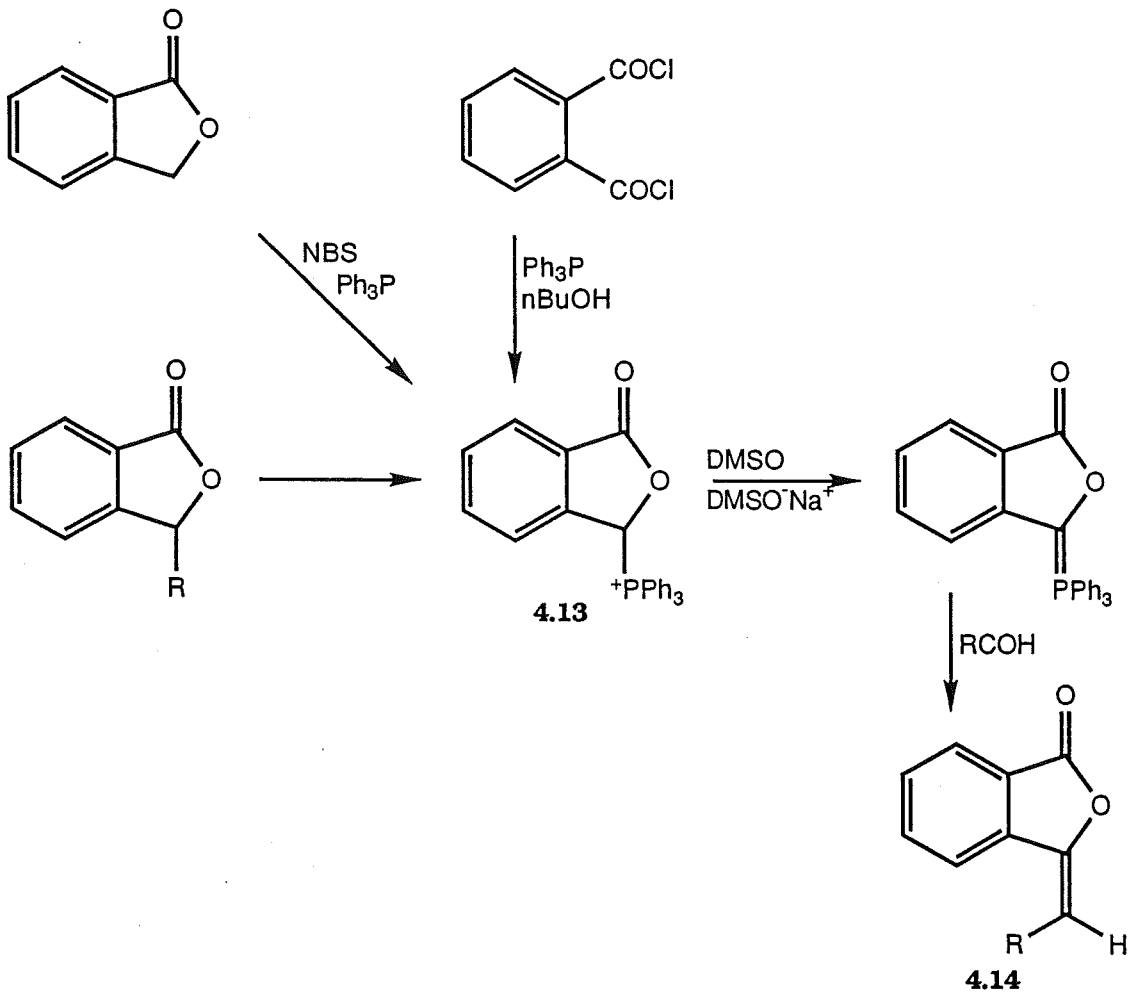

4.13 **4.14**

olefination reaction to produce the phthalic enol lactones **4.15** and **4.16** from phthalic anhydride, Scheme 4.5. We decided to extend this existing chemistry to produce phthalic bromo enol lactones.

The synthesis of phthalic enol lactones via a Wittig anhydride olefination reaction has been studied by Massy Westropp[2.1] *et al.* and others[4.5]. The reaction between phthalic anhydride and the hydrogen ylide **0.1** gives the *E*- and *Z*-enol lactones **4.15** and **4.16** (Scheme 4.5) in a ratio of 9:1, respectively[2.1]. The high *E*-stereoselectivity is consistent with the succinic and glutaric based examples discussed in Chapters 2 and 3. The intermediate phosphorane **4.17** (Scheme 4.5) is observed (80% at O°C) but is too reactive to be isolated[2.1]. The overall mechanism is similar to that of the succinic and glutaric series, except that the initial reaction of phthalic anhydride and ylide **0.1** to give **4.17** is reversible. The *E*-stereoisomeric preference can be explained by unfavourable steric and electronic interactions of the carboxylate anion and the ethyl ester in the transition state **4.18** leading to the *Z*-stereoisomer, Figure 4.1. These interactions are absent in the transition state **4.19** leading to the *E*-stereoisomer, Figure 4.1.

4,5-dichloro phthalic anhydride gave an enhanced rate of intermediate formation and decreased rate of subsequent cyclisation[2.1]. This observation is consistent with an increase in electrophilicity of the carbonyl anhydride due to the chloro electron withdrawal and a decrease in nucleophilicity of the carboxylate group of **4.20**, Figure 4.2 (R^3=Cl, R^4=H, R^5=H, R^6=Cl). The opposite effects are observed with electron donating methyl groups in the 4,5 position[2.1] **4.21**, Figure 4.2 (R^3=H, R^4=CH_3, R^5=CH_3, R^6=H).

The 3,6 dimethyl substituted phthalic anhydride[2.1] **4.22**, Figure 4.2 (R^3=CH_3, R^4=H, R^5=H, R^6=CH_3) gives a decreased rate in the formation of the intermediate **4.23** due to the expected decrease in electrophilicity of the carbonyl anhydride and an increase in nucleophilicity of the carboxylate group of **4.23**.

Scheme 4.5 : Mechanism of the Wittig Phthalic Anhydride Olefination Reaction

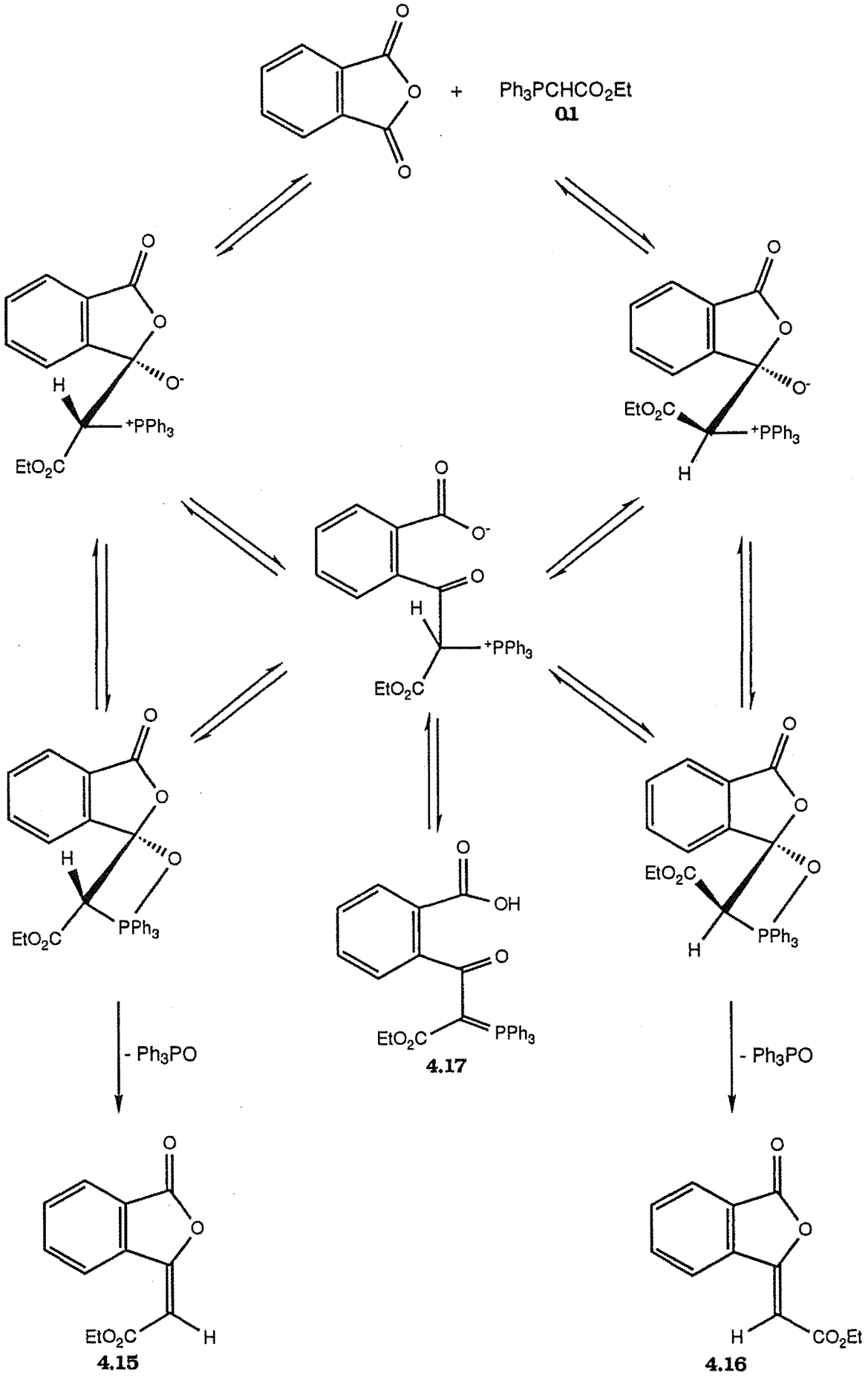

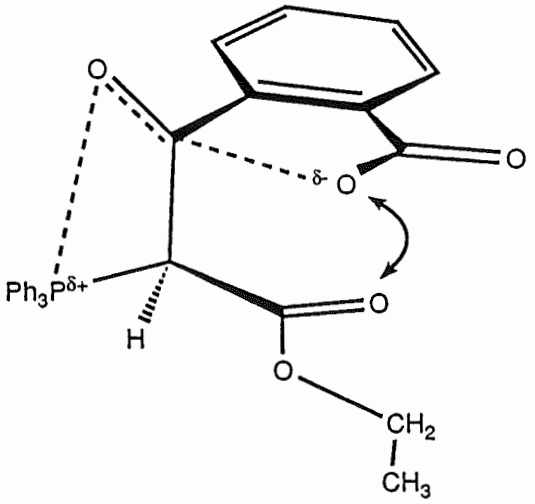

Z-transition state **4.18**

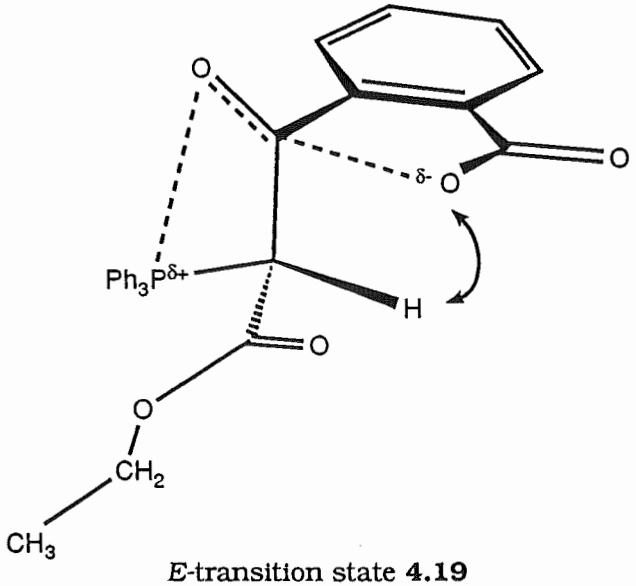

E-transition state **4.19**

Figure 4.1

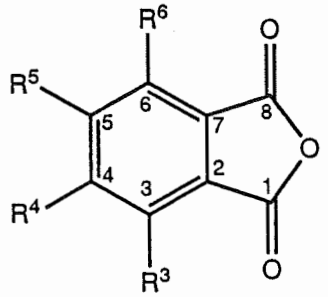

Figure 4.2

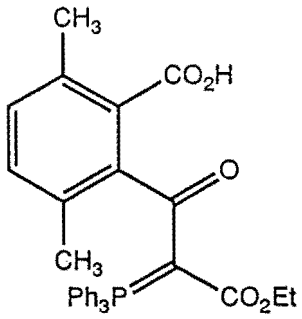

4.23

Steric interaction between the 3 and 6 methyl groups and the ylide dictate the stereocontrol. This steric effect is evident with an *E*- to *Z*-enol lactone product ratio of 1:15, respectively. The high *Z*-stereoselectivity is opposite to the normal *E*- stereoselectivity observed in succinic and glutaric anhydrides. The steric effect of 3,6 methyl substitution on betaines and/or oxaphosphetanes (**4.23** and **4.24**, Figure 4.3) formation is greater than the steric and electronic effects involved in the lactone cyclisation.

For monosubstituted phthalic anhydrides[4.5], the regioselectivity of attack of the ylide on the anhydride depends largely on the electronic effects of the substituent. Electron withdrawing groups, such as NO_2 and CO_2Me, in the 3 position of the aromatic ring direct the ylide attack to the 1-carbonyl. Steric interaction between the 3-substituent and the ethyl ester in the transition states, Figure 4.4, results predominantly in the *Z*-enol lactone formation (Figure 4.2). Minor attack also occurred at the 8-carbonyl and gave predominance of the *E*-stereoisomer, as there is no steric interaction with the 3-substituent. Electron donating substituents in the 3 position of the aromatic ring, such as CH_3 and NMe_2, direct the ylide attack to the 8-carbonyl, with a predominance of *E*-enol lactones.

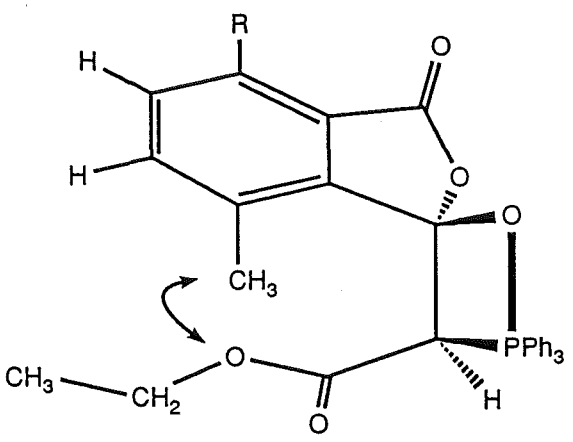

E-oxaphosphetane **4.23**

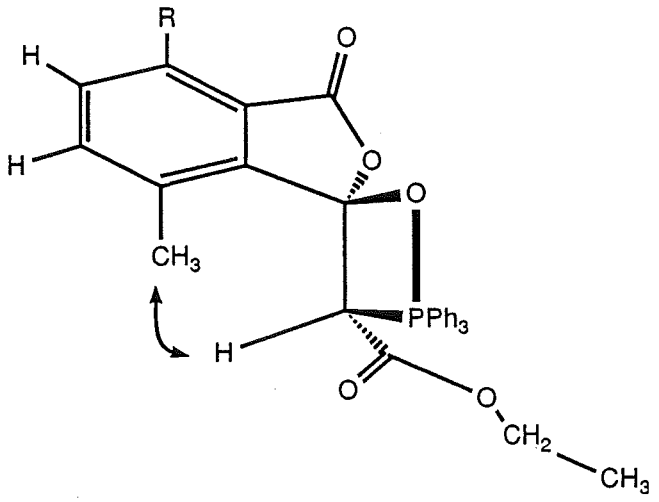

Z-oxaphosphetane **4.24**

Figure 4.3

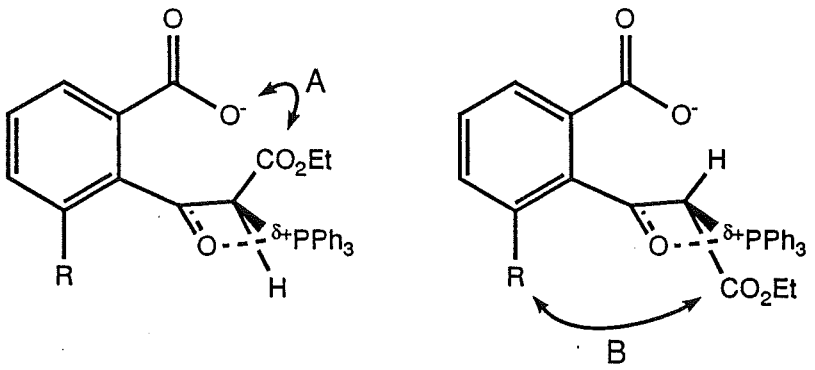

Steric effect B is greater than steric and electronic effects A

Figure 4.4:

4.2: Synthesis of Phthalic Bromo Enol Lactones

The *E*- and *Z*-phthalic bromo enol lactones **4.25** and **4.26** were prepared in two ways using different entry points into the Wittig anhydride olefination reaction, Scheme 4.6. Phthalic anhydride is more reactive than succinic and glutaric anhydride and it reacted directly with the bromo ylide **2.31** at 60°C for 2 hours in $CHCl_3$ to form the *E*- and *Z*-bromo enol lactones **4.25** and **4.26** in a ratio of 7:13, respectively. The reaction was shown to have gone to completion by the disappearance of the triplet and quartet of the bromo ylide in the ^1H NMR spectrum of the reaction mixture. The products were isolated in 87% yield by radial chromatography on a 2mm silica gel plate eluting with CH_2Cl_2. Partial separation of the two stereoisomers was achieved with one fraction containing a mixture of **4.25** and **4.26** and a second fraction containing pure **4.26**.

The second entry into the Wittig anhydride olefination reaction is based on the bromolactonisation reaction developed in Chapters 2 and 3. The reaction of phthalic anhydride and the ylide **0.1** proceeds via the phosphorane **4.17** (Scheme 4.5). The ring opened phosphorane intermediate **4.17** is characterised by ^1H NMR signals for the ethyl ester quartet at 3.56ppm and triplet at 0.72ppm. An unusual upfield shift of ≈0.5 ppm for the triplet and quartet signals of the ethyl ester is typical[2.1] for acyclic phosphoranes. At low temperatures (0°C) the acyclic phosphorane intermediate **4.17** was observed by ^1H NMR spectroscopy, but proved too reactive to isolate. The intermediate **4.17** (65% after 30 minutes at 0°C in $CDCl_3$) was therefore reacted under the modified SCOOPY bromolactonisation conditions, Scheme 4.6. One equivalent of triethylamine followed by one equivalent of bromine was added and instantaneous decolourisation of the bromine was observed. The *E*- and *Z*-bromo enol lactones **4.25** and **4.26** were isolated by radial chromatography in a ratio of 7:13 respectively and in a combined yield of 55% (85% based

Scheme 4.6 : Mechanism of the Wittig Phthalic Anhydride Olefination Reaction and Bromolactonisation of the Phthalic Derived Phosphorane

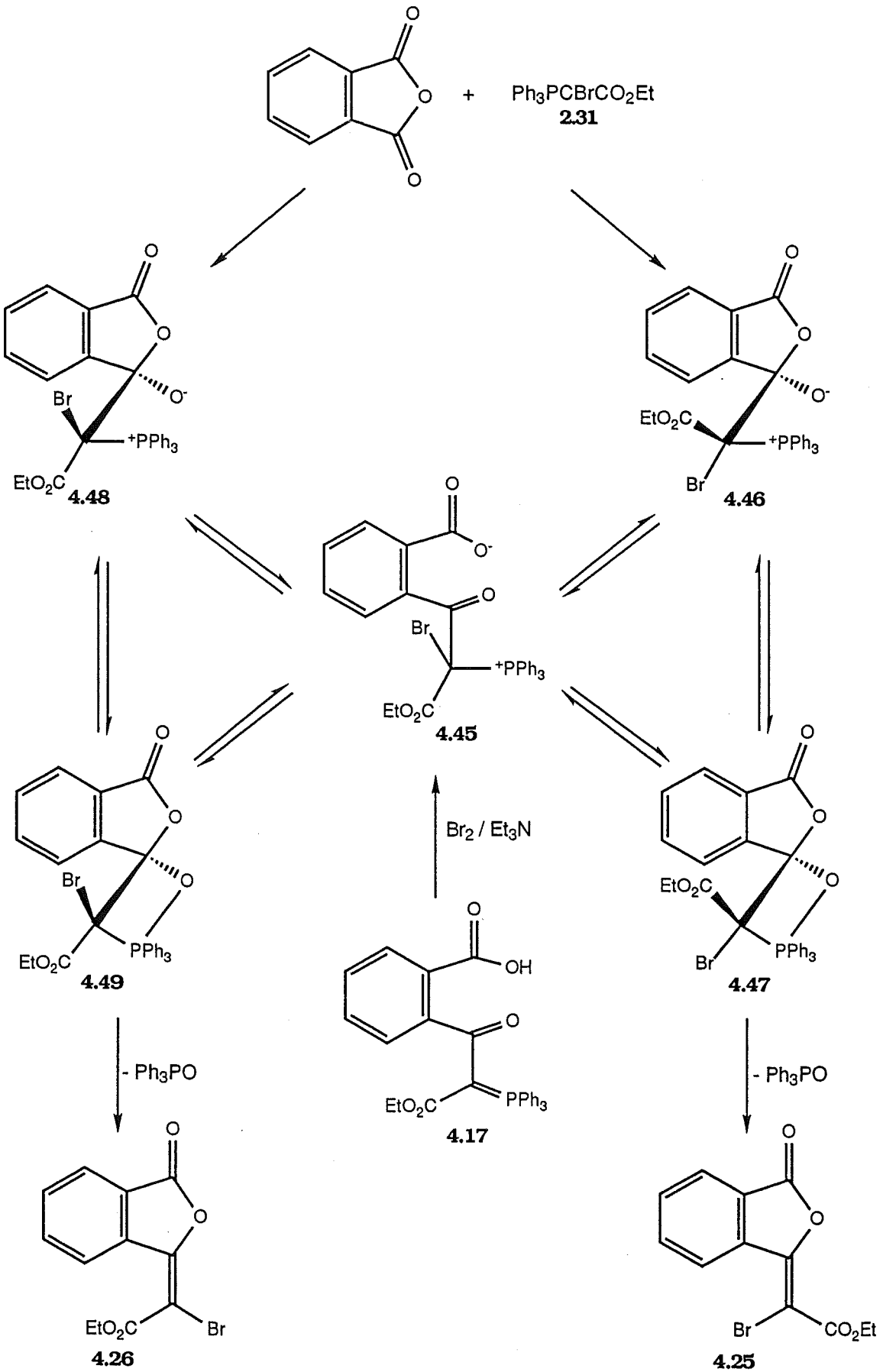

on the amount of intermediate **4.17**). The magnitude of stereoisomeric preference for the *Z*-bromo enol lactone **4.26** is the same as that obtained in the direct Wittig anhydride olefination reaction with the bromo ylide **2.31**, and hence a common mechanism is likely.

The effect of phthalic anhydride substitution on the reaction with ylide **0.1** is consistent with the steric and electronic effects discussed in the introduction (Section 4.1). The reaction of 3-methylphthalic anhydride[4,5] and ylide **0.1** proceeds rapidly, without the observation of acyclic intermediates **4.27** and **4.28**, to form enol lactones **4.29**, **4.30**, and **4.31**. The reaction may therefore proceed without ring opening. The reaction of 3-methylphthalic anhydride with one equivalent of bromo ylide **2.31** at room temperature for 4 hours in CH_2Cl_2 yielded the major products **4.32** and **4.33** and a small amount of **4.34**. The regioselectivity of these reactions is governed by the initial ylide attack on the anhydride. The methyl substituent directs the attack of the ylide to the 8-carbonyl (Figure 4.2).

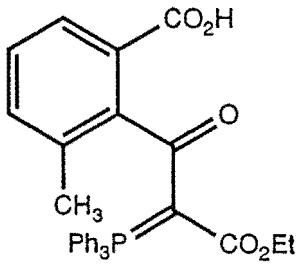

4.27

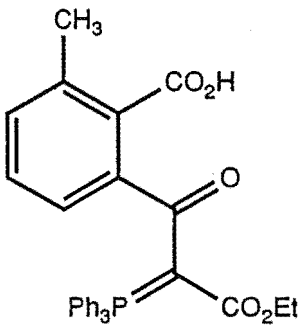

4.28

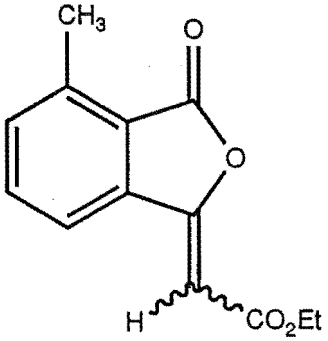

4.29(*E*), 4.30(*Z*)

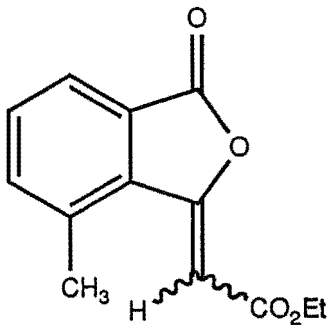

4.30(*Z*)

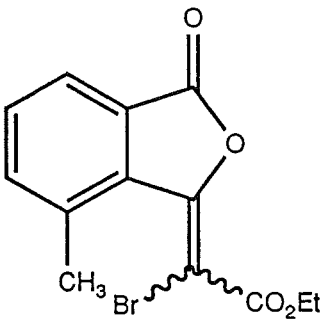

4.34(*Z*)

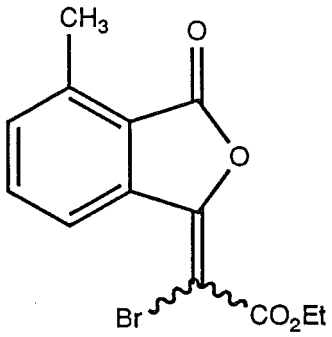

4.32(*Z*), 4.33(*E*)

The reaction of 3-nitrophthalic anhydride with the ylide **0.1** yielded the expected[4.5] acyclic intermediate phosphoranes **4.35** and **4.36**, which did not cyclise at room temperature to the enol lactones **4.37**, **4.38**, **4.39**, and **4.40**. This observation is consistent with an increase in the rate of intermediate formation, and decrease in the rate of subsequent cyclisation due to the electron withdrawing

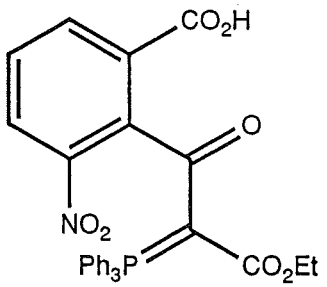

4.35

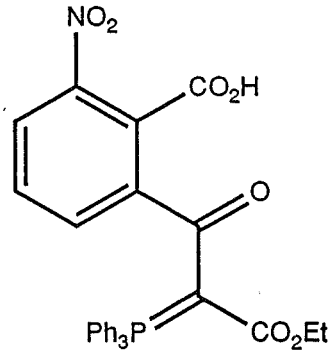

4.36

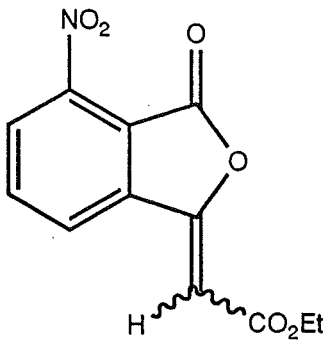

4.37(*E*), 4.38(*Z*)

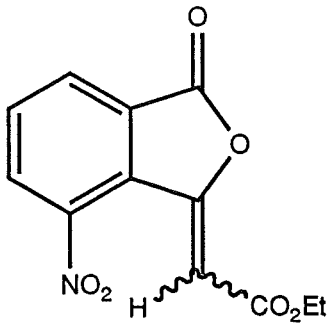

4.39(*Z*), 4.40(*E*)

nature of the nitro group. The modified SCOOPY conditions were applied to this phosphorane. The bromolactonisation reaction appeared to give bromo enol lactones **4.41**, **4.42**, **4.43**, and **4.44**, in a total yield of 74%. The bromo enol lactones were inseparable by radial and high performance liquid chromatography. Tentative assignment of the configuration of **4.43**, and **4.44** was achieved by comparison of the ^1H NMR spectra of the known enol lactones **4.37**, **4.38**, **4.39**, and **4.40** (Section 4.2.2).

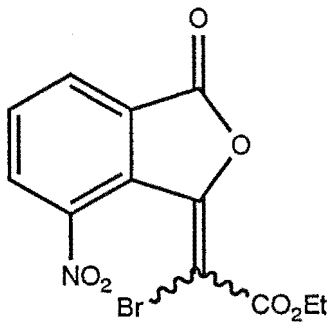

4.41(*Z*), 4.42(*E*)

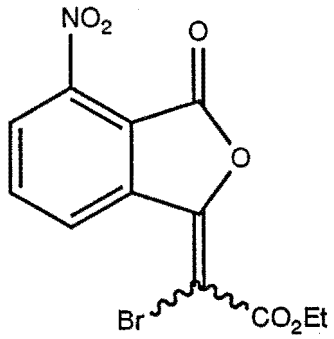

4.43(*Z*) , 4.44(*E*)

The 3-nitrophthalic anhydride was also reacted with the bromo ylide **2.31**, in $CHCl_3$ at reflux for 12 hours, to form the bromo enol lactones **4.41**, **4.42**, **4.43**, and **4.44**. The solvent was evaporated under reduced pressure and the residue was purified by radial chromatography on a 2mm silica gel plate eluting with CH_2Cl_2. The ratio of bromo enol lactones **4.41**, **4.42**, **4.43**, and **4.44** was the same as for the bromolactonisation reaction. The regioselectivity is consistent with the electronic nature of the substituted nitro group. The 3-nitro group's electronic effect overcomes steric interaction of the nitro group and the ethyl ester in the transition states and results in a predominance of attack on the 1-carbonyl. This is consistent with the reaction of the hydrogen ylide and 3-nitrophthalic anhydride (see 4.1: Introduction).

4.2.1: Mechanism of Phthalic Bromo Enol Lactone Formation

The mechanism of the bromolactonisation is thought to proceed via the bromophosphonium salt **4.45** which can cyclise and eliminate triphenylphosphine oxide to form the bromo enol lactones **4.25** and **4.26**. The reaction of phthalic anhydride and ylide **0.1** is reversible (see 4.1: Introduction). However, the bromolactonisation reaction is unlikely to proceed via reversible phthalic anhydride and bromo ylide **2.31** formation. The bromolactonisation reaction occurs instantaneously at O°C, whereas the reaction of bromo ylide **2.31** with phthalic anhydride takes 2 hours at 40°C. Bromo ylide was not observed in the reaction mixture obtained from treatment of with bromine and triethylamine. The different reaction conditions used to form the bromo and hydrogen enol lactones (instantaneous at 0°C and 2 hours at 40°C, respectively) would suggest that bromo enol lactone formation via incipient formation of enol lactones **4.15** and **4.16** followed by bromination is unlikely.

The effect of the bromine atom is to reduce the stereoselectivity observed. There is still a preference, although diminished, for the ethyl ester to be *trans* to the lactone oxygen (*Z*-transition state Figure 4.5). The *Z*-stereopreference for the phthalic derived bromo enol lactones is opposite to that of succinic and glutaric derived bromo enol lactones. This may be due to the close proximity of the nucleophilic carboxylate anion and the electrophilic carbonyl in the aromatic ring of phthalic anhydride. The bromide atom may have an unfavourable interaction with the carboxylate in the transition state to the *E*-betaine **4.46** and/or *E*-oxaphosphetane **4.47** relative to the *Z*-betaine **4.48** and/or *E*-oxaphosphetane **4.49**. The effect of the 3-substituent of the aromatic ring on the bromo betaine and/or bromo oxaphosphetane is not as great as in the nonbrominated case.

The *E*- and *Z*-bromo enol lactones **4.25** and **4.26** were formed in the same stereoisomeric ratio of 7:13 respectively, in both the direct reaction

of the bromo ylide **2.31** on phthalic anhydride, and also in the indirect bromolactonisation of the intermediate acylphosphorane. This would suggest a common mechanism with different entry points. The initial attack of the bromo ylide on phthalic anhydride must be rate determining, as no subsequent intermediates are observed in the bromolactonisation reaction. The product ratio is dependent either on the relative rates of cyclisation of the acyclic bromophosphonium salt **4.45** to form the isomeric betaines **4.46** and **4.48** or oxaphosphetanes **4.47** and **4.49**,

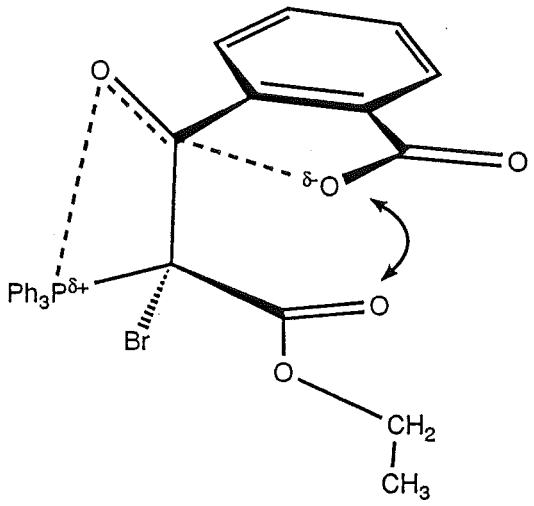

E-transition state

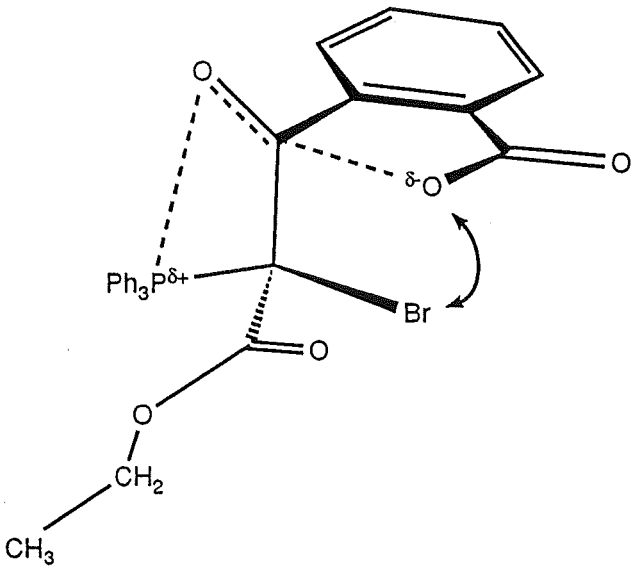

Z-transition state

Figure 4.5

or alternatively, the elimination of triphenylphosphine oxide from the oxaphosphetanes **4.47** and **4.49**. Rapid equilibrium must exist between the cyclic betaines, **4.46** and **4.48**, and oxaphosphetanes, **4.47** and **4.49**, and the acyclic bromophosphonium salt **4.45** to account for the observed stereopreference of the bromo enol lactones **4.25** and **4.26**.

An allene type mechanism (see Chapter 2) is unlikely for phthalic anhydride as there is no enolisable proton α to the carbonyl. This is analogous to the diphenic derived bromo enol lactones **2.81** and **2.82**. The *E*- and *Z*-diphenic derived bromo enol lactones **2.81** and **2.82** form in a ratio of 37:63 respectively. The same stereopreference, although not as large, is observed for the diphenic system[1,11] as the phthalic derived bromo enol lactones **4.25** and **4.26**.

4.2.2: Structure Assignment of Phthalic Bromo Enol Lactones.

The configuration of phthalic derived enol lactones is traditionally assigned on the basis of the chemical shift of the proton of the aromatic ring closest to the enol double bond (either H-6 or H-3 depending on the numbering system, Figure 4.2). This proton is shifted downfield in the *Z*-enol lactone due to the close proximity of the ester. However, in the bromo enol lactones **4.25** and **4.26**, the bromine also exhibits a deshielding effect resulting in a similar downfield shift. The H-6 proton signals for **4.25** and **4.26** are at 8.67ppm and 8.59ppm, respectively. Therefore, it was difficult to assign the configuration on the basis of the ^{1}H NMR spectrum. An X-ray crystal structure of the pure major isomer, separated by radial chromatography, was determined to fully characterise the configuration of the bromo enol lactones **4.25** and **4.26**, Figure 4.6.

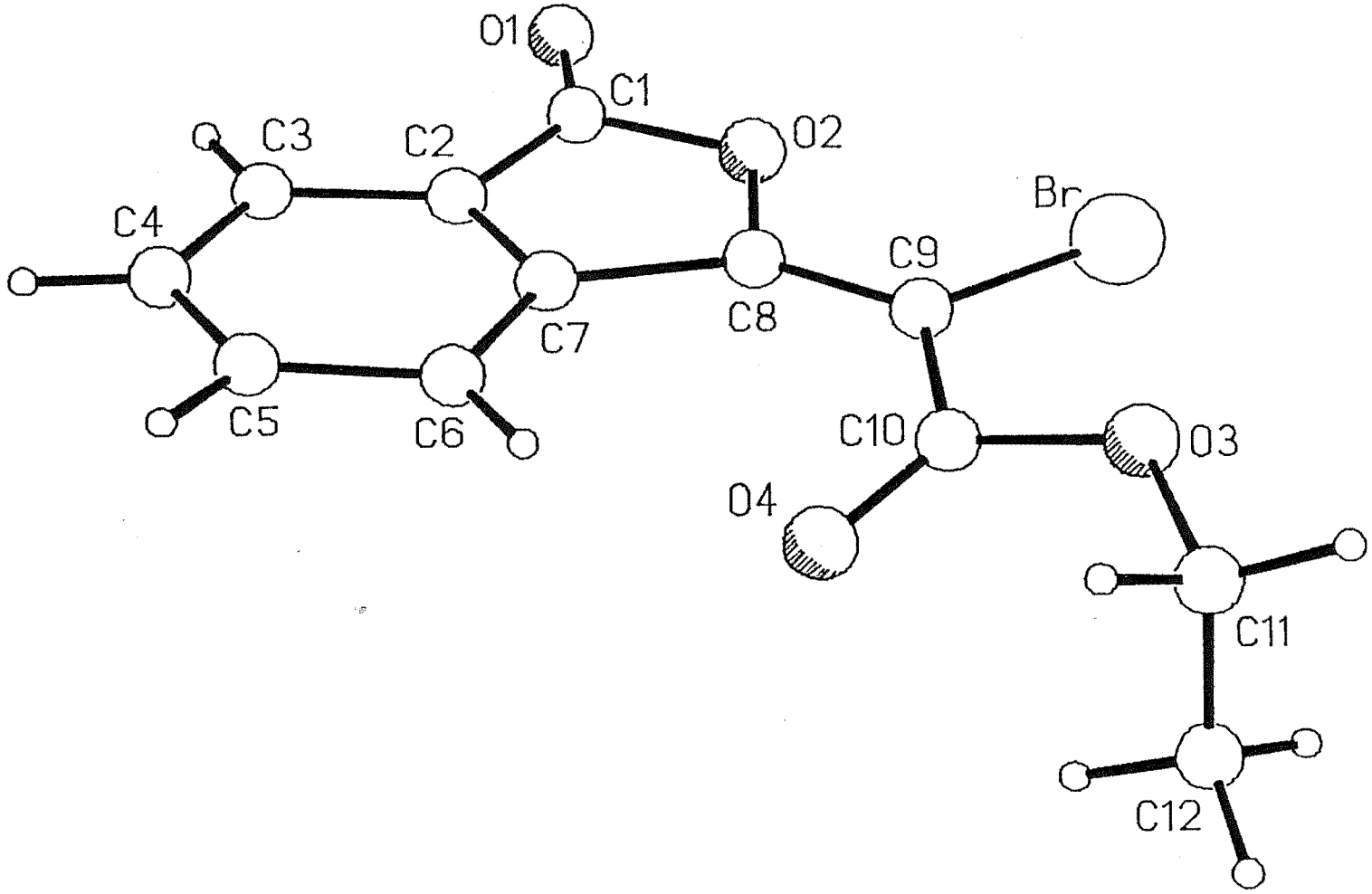

Figure 4.10: Perspective View and Atom Labelling of Z-Phthalic Bromo Enol Lactone 4.26.

A number of interesting observations are evident from the crystal structure. The common syn arrangement[1,13] is observed for both the α,β-unsaturated ester C11-O3-C10-O4 and the ester configurations C11-O3-C10-O4. The deviation from planarity of the five-membered lactone ring is greater than the succinic example **2.33** (see Chapter 2) even though the C2-C7 bond has partial double bond character. This deviation is evidenced by the torsional angles of C1-C2-C7-C8 -6.0(7), O2-C1-C2-C3 176.1(13), and C8-O2-C1-C2 4.9(15). There appears to be very little delocalisation of the α,β-unsaturated system, evidenced by the bond lengths O3-C6 1.193(9), C4-C5 1.343(10), and C5-C6 1.477(11). The bromine atom and O4 are twisted out of the plane of the sp^2 systems, with torsional angles of O2-C8-C9-Br -9.7(9) and C8-C9-C10-O4 -169.2(11) respectively. The steric interaction between the C7 proton and the carbonyl C10-O4 forces the carbonyl out of the plane of the ring. This results in a twisting of the C8-C9 double bond as evidenced by the C7-C8-C9-C10 and O2-C8-C9-Br torsional angles of 12.8° and -9.7(9)°, respectively.

The structural assignment of the 3-methylphthalic bromo enol lactones **4.32**, **4.33**, and **4.34** and 3-nitrophthalic bromo enol lactones **4.41**, **4.42**, **4.43**, and **4.44** was difficult without the diagnostic H-3 proton. The bromo enol lactones **4.32**, **4.33**, **4.34**, **4.41**, and **4.42** were tentatively assigned by comparison of the ^1H NMR of known[4,5] 3-methyl and 3-nitro phthalic enol lactones, Table 4.1.

Molecular mechanics[2,29] (MM2) calculations were again carried out on the isomeric phthalic bromo enol lactones **4.25** and **4.26** in order to determine thermodynamic stability. Both the *E* **4.25** and *Z* **4.26** structures were minimised with rotation about the three chain bonds. The C9-C10 and C10-O3 bonds required 180° increments, as C9 and C10 are sp^2 hybridised carbon atoms. O3-C11 was rotated in 60° increments. Unlike the succinic example (see Chapter 2) the ring system is essentially planer due to the sp^2 carbon centres, and was minimised in the normal MM2

Table 4.1: ^{1}H NMR of Enol Lactones 4.29, 4.30, 4.31, 4.37, 4.38, 4.39, and 4.40, and Bromo Enol Lactones 4.25, 4.26, 4.32, 4.33, 4.34, 4.41, and 4.42

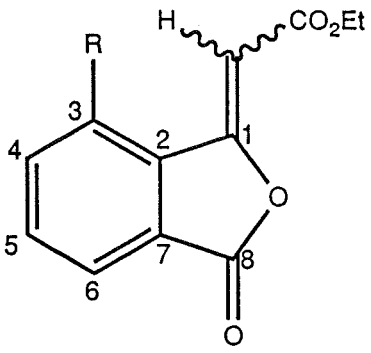

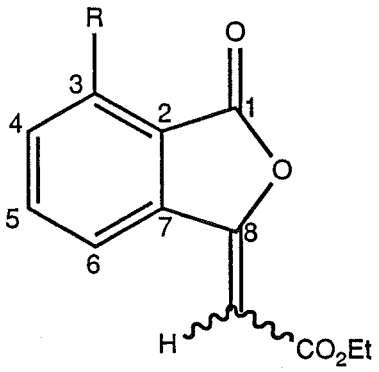

3-Methyl and 3-Nitro Phthalic Enol lactones[4,5] **4.29**, **4.30**, **4.31**, **4.37**, **4.38**, **4.39**, and **4.40**

E/Z	R	(H4)	(H5)	(H6)	(H)	(CH_3)
4.29 *E*-1	CH_3	7.45	7.68	8.91	6.09	2.68
4.30 *Z*-1	CH_3	7.4 - 7.7			5.83	2.67
4.37 *E*-1	NO_2	7.9 - 8.1		9.40	6.27	-
4.38 *Z*-1	NO_2	nr	nr	nr	6.40	-
4.31 *Z*-8	CH_3	nr	nr	nr	5.91	2.59
4.39 *E*-8	NO_2	8.30	7.89	8.42	6.62	-
4.40 *Z*-8	NO_2	nr	nr	nr	6.40	-

Phthalic, 3-Methyl, and 3-Nitro Phthalic Bromo enol lactones **4.25**, **4.26**, **4.32**, **4.33**, **4.34**, **4.41**, and **4.42**

E/Z	(H3)	(H4)	(H5)	(H6)	(CH_3)
4.25	8.02	7.76	7.84	8.67	-
4.26	7.96	7.68	7.78	8.59	-
4.32 *E*-8	-	7.48	7.68	8.49	2.74
4.33 *Z*-8	-	7.43	7.62	8.39	2.72
4.34 *E*-1	-	7.45	7.67	8.90	2.72
4.41 *Z*-1	-	8.08	7.94	8.93	-
4.42 *E*-1	-	8.12	8.01	9.01	-

force field. The energy minimisation of the *E*-structure produced 3 conformers (Figure 4.7) having energies within 3Kcal/mol of the minimum energy. Application of the Boltzman distribution at 25°C showed that the Boltzman average energy was 48.55Kcal/mol. The energy minimisation of the *Z*-structure produced 6 conformers having energies within 3Kcal/mol of the minimum energy (the four lowest energy conformers are shown in Figure 4.7). Application of the Boltzman distribution at 25°C showed that the Boltzman average energy was 48.07Kcal/mol and that the 5 lowest energy conformers accounted for 99.25% of the population.

From these MM2 calculations it is unclear whether the kinetic or thermodynamic product is favoured as the energies are so close. This is inspite of the fact that the ethyl ester orientation is opposite to that in the hydrogen enol lactone systems. Identical model calculations were carried out on the hydrogen enol lactones **4.15** and **4.16** to determine the reliability of the MM2 method. These calculations support the experimental evidence (see 4.1: Introduction) that the *Z*-enol lactone **4.16** is thermodynamically more stable. The *Z*-structure produced 3 conformers (Figure 4.8) with a Boltzman average energy of 38.53Kcal/mol. The *E*-enol lactone **4.15** has an Boltzman average energy of 44.19Kcal/mol, Table 4.2. Application of the Boltzman distribution at 25°C on the *E*-structure showed that the 6 lowest energy conformers accounted for 96.91% of the population (the four lowest energy conformers are shown in Figure 4.8). The kinetic *E*-enol lactone is the product obtained from the reaction of phthalic anhydride and ylide **0.1** (see 4.1: Introduction).

MM2 calculations on the 3-methyl phthalic systems reveal that the methyl substituent interacts with the bromine atom and the ethyl ester to increase the Boltzman average energy. The energy minimisation of the *E*-structure **4.34** produced 8 conformers having energies within 3Kcal mol^{-1} of the minimum energy (the four lowest energy conformers are shown in Figure 4.9). Application of the Boltzman distribution at 25°C showed that

the Boltzman average energy was 56.96Kcal/mol. The energy minimisation of the corresponding *Z*-structure **4.50** produced 6 conformers having energies within 3Kcal/mol of the minimum energy (the four lowest energy conformers are shown in Figure 4.9). Application of the Boltzman distribution at 25°C showed that the average energy was 53.78Kcal/mol. The energy minimisation of the *E*-structure **4.32** was performed to establish that no noticeable increase in energy due to interaction of the methyl substituent and the bromine atom was evident. The calculations produced 6 conformers having energies within 3Kcal/mol of the minimum energy. Application of the Boltzman distribution at 25°C showed that the Boltzman average energy was 48.89Kcal/mol, a value not significantly different from the unsubstituted *E*-phthalic bromo enol lactone **4.25** (48.55Kcal/mol). The *E*- and *Z*-3-methyl phthalic examples **4.34** and **4.50** are significantly higher in energy than the unsubstituted phthalic examples **4.25** and **4.26**. This is due to the steric interaction of the methyl substituent and the bromine atom and the ethyl ester. The major methyl phthalic bromo enol lactones **4.32** and **4.33**, produced on the reaction of the bromo ylide **2.31** and 3-methyl phthalic anhydride, occur via reaction at the less sterically hindered 8-carbonyl. The minor isomer **4.33**, the thermodynamically less stable product, is produced via reaction on the more hindered 1-carbonyl. Steric interactions between the ethyl ester and bromine with the methyl substituent obviously play a significant part in this reaction. The 3-nitro phthalic bromo enol lactones **4.41**, **4.42**, **4.43**, and **4.44** were not modelled as the parameters for the nitro group were not readily available.

The crystallographically derived structure was compared with the MM2 calculated bromo enol lactone conformers. Conformers pbz1 and pbz3 are in the closest agreement with the x-ray structure with 0.82Å and 0.84Å average deviation of atoms respectively (Figure 4.10 shows pbz1 comparison to X-ray structure). The MM2 calculations did not produce a

Figure 4.7 : Lowest Energy Conformations of 4.25 and 4.26.

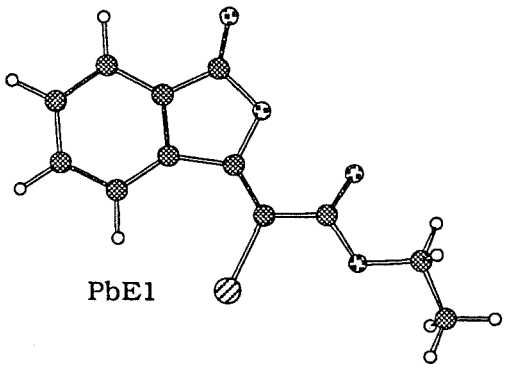

PbE1

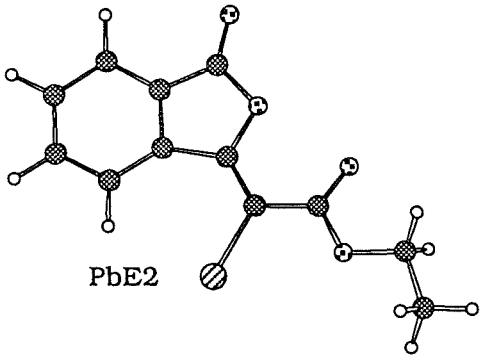

PbE2

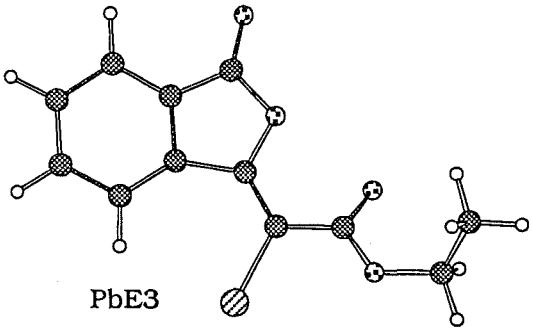

PbE3

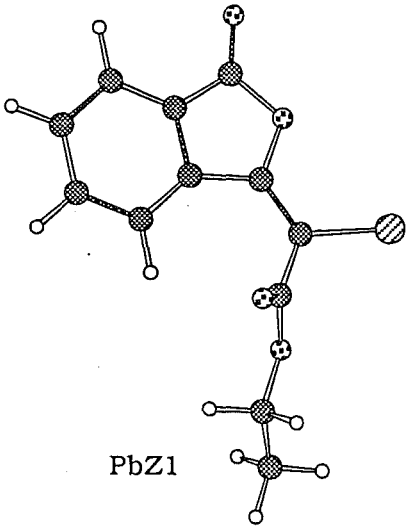

PbZ1

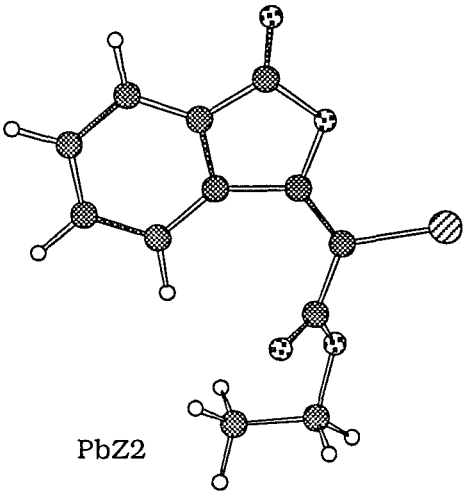

PbZ2

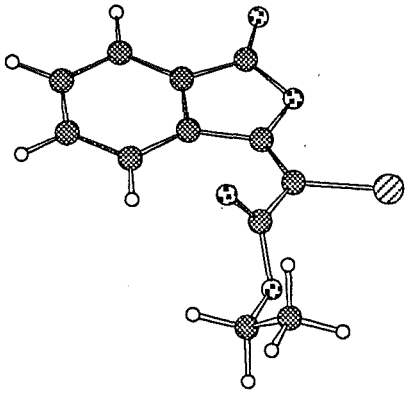

PbZ3

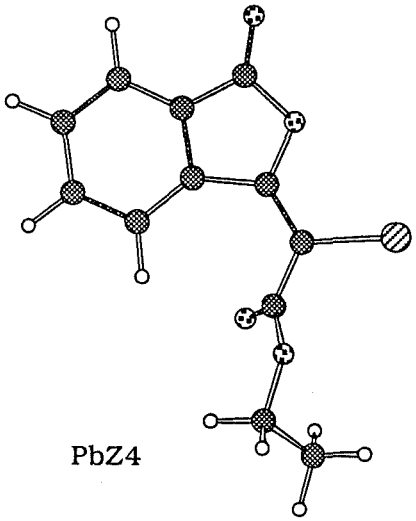

PbZ4

Figure 4.8: Lowest Energy Conformers of 4.15 and 4.16

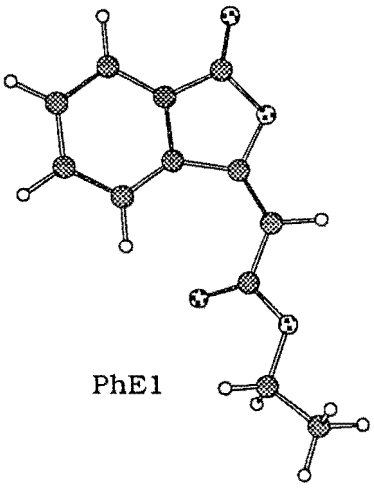

PhE1

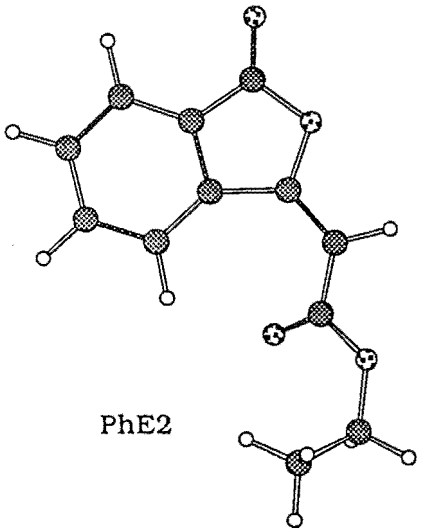

PhE2

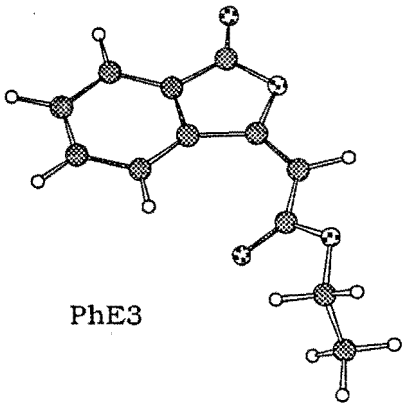

PhE3

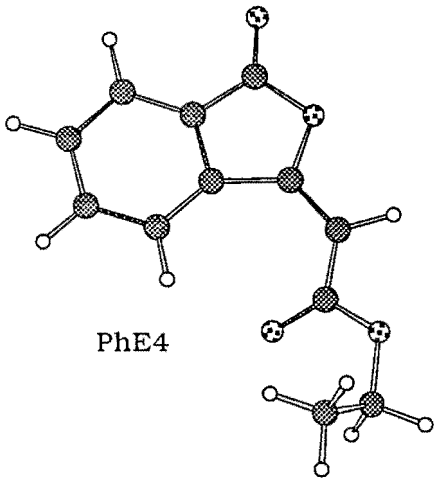

PhE4

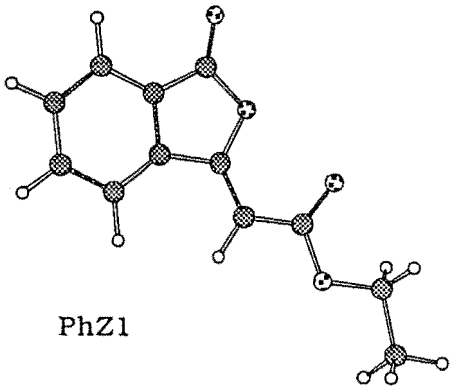

PhZ1

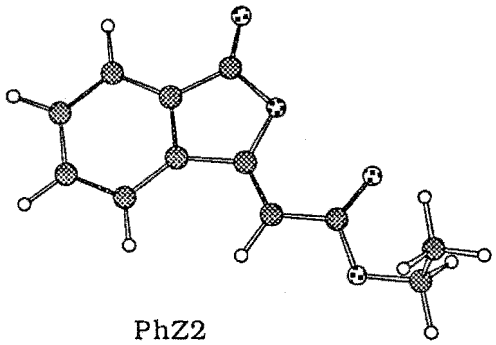

PhZ2

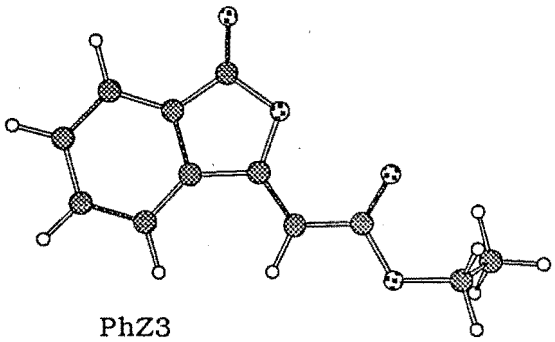

PhZ3

Figure 4.9: Four Lowest Energy Conformers for 4.34(m1pbE) and 4.50(m1pbZ).

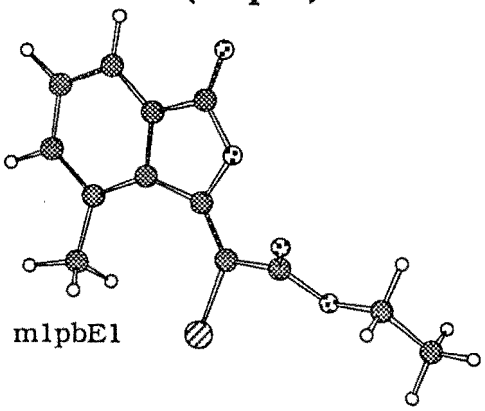

m1pbE1

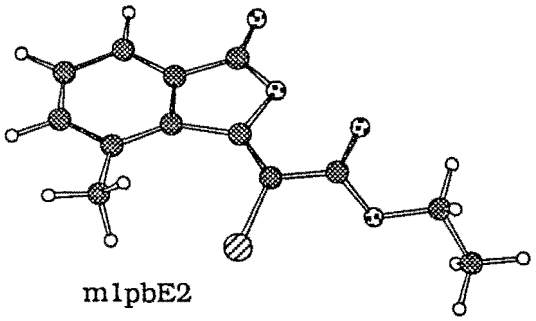

m1pbE2

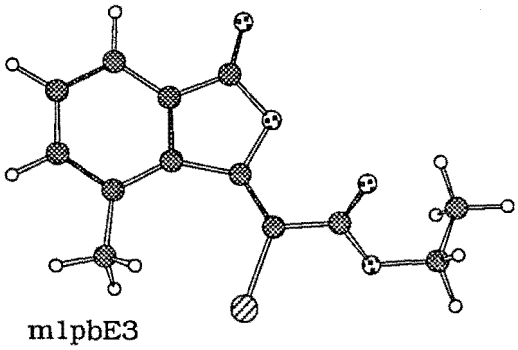

m1pbE3

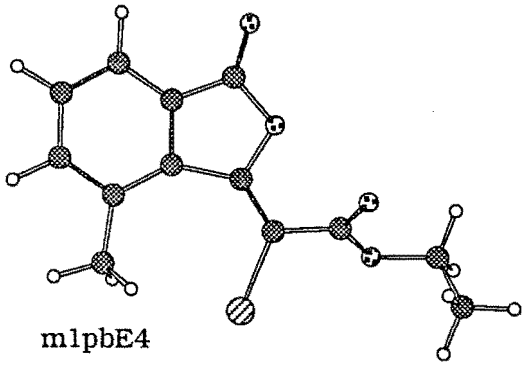

m1pbE4

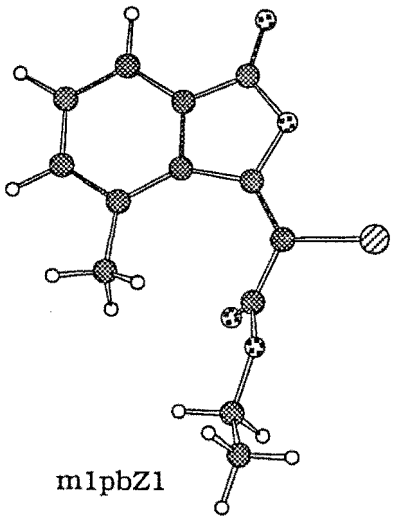

m1pbZ1

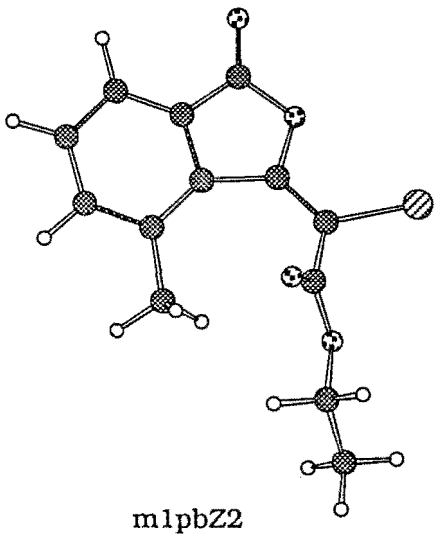

m1pbZ2

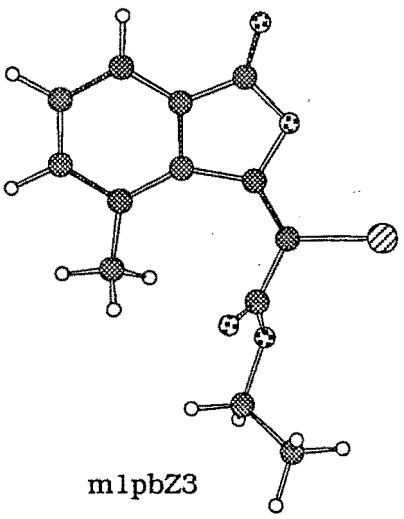

m1pbZ3

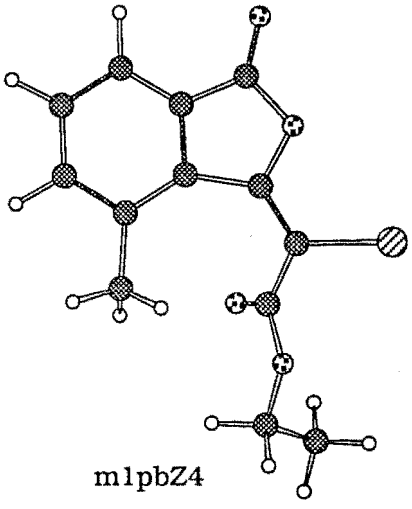

m1pbZ4

Table 4.2: MM2 Calculations on Phthalic Systems.

System	Conformer%	Energy (Kcal/mol)	Boltzman Average Energy (Kcal/mol)
phE **4.15**			
	1 = 21.74%	43.980	44.19
	2 = 21.64%	43.983	
	3 = 15.93%	44.166	
	4 = 15.23%	44.193	
	5 = 12.22%	44.324	
	6 = 10.19%	44.433	
	7 = 0.95%	45.846	
	8 = 0.95%	45.848	
	9 = 0.54%	46.189	
	11 = 0.22%	46.732	
phZ **4.16**			
	1 = 43.29%	38.390	38.53
	2 = 28.46%	38.640	
	3 = 28.25%	38.645	
pbE **4.25**			
	1 = 46.78%	48.376	48.55
	2 = 29.95%	48.642	
	3 = 23.27%	48.793	
pbZ **4.26**			
	1 = 28.91%	47.842	48.07
	2 = 18.63%	48.104	
	3 = 17.50%	48.141	
	4 = 17.33%	48.147	
	5 = 16.88%	48.162	
	6 = 0.75%	50.021	
m8pbE **4.32**			
	1 = 36.11%	48.562	48.89
	2 = 22.07%	48.856	
	3 = 21.34%	48.876	
	4 = 10.10%	49.323	
	5 = 5.20%	49.719	
	6 = 5.18%	49.720	
m1pbE **4.50**			
	1 = 24.01%	56.702	56.96
	2 = 19.54%	56.825	
	3 = 17.52%	56.890	
	4 = 14.53%	57.002	
	5 = 10.02%	57.224	
	6 = 9.61%	57.248	
	7 = 4.60%	57.687	
	8 = 0.17%	59.666	
m1pbZ **4.34**			
	1 = 28.41%	53.611	53.78
	2 = 27.65%	53.627	
	3 = 20.95%	53.793	
	4 = 15.61%	53.968	
	5 = 7.08%	54.440	
	6 = 0.30%	56.319	

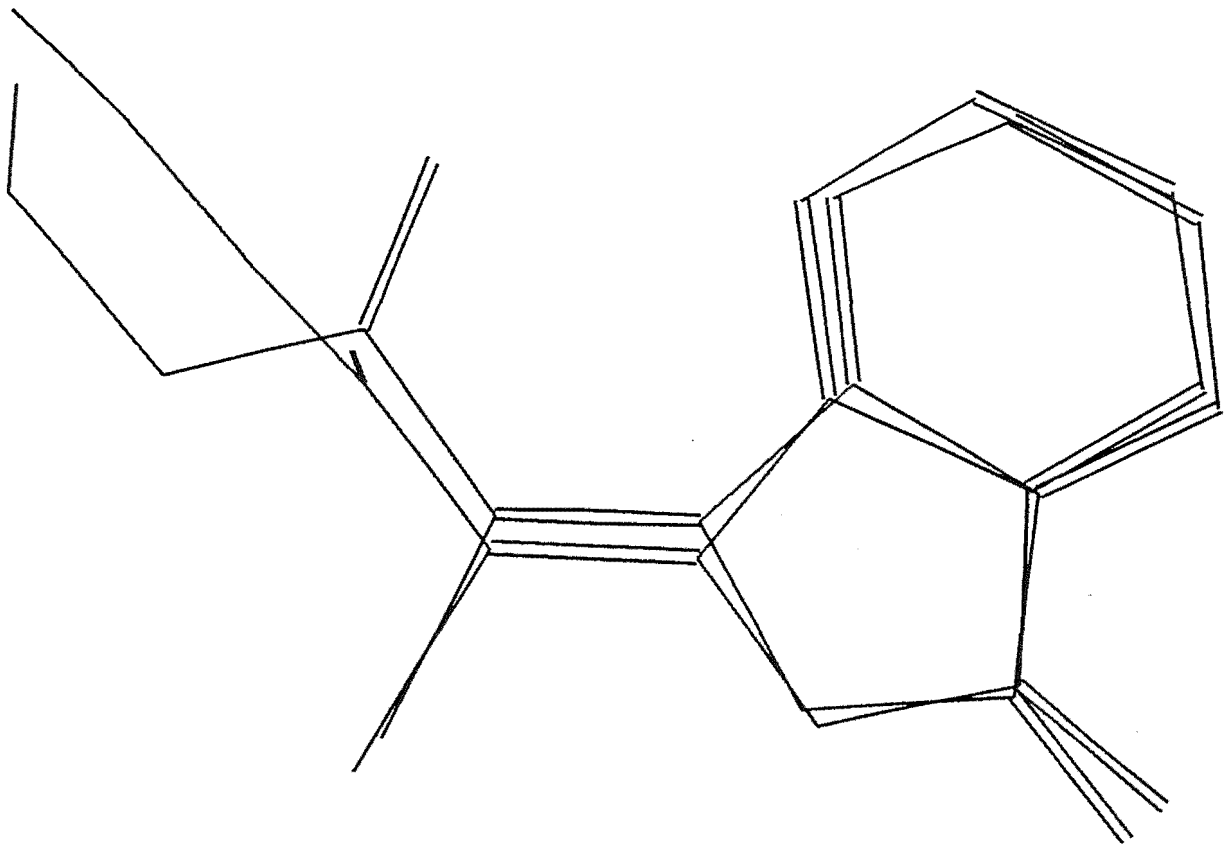

Figure 4.10: Comparison of Conformer PbZ1 with the X-ray Determined Structure for 4.26.

conformer that was identical to the crystallographically derived structure. This is not surprising as the ethyl ester side chain in the crystal structure is not in an energy minima which is possibly due to the crystal packing forces.

4.3: Summary

The synthesis of phthalic bromo enol lactones **4.25** and **4.26** was achieved by direct reaction of phthalic anhydride with the bromo ylide **2.31**, and by the bromolactonisation of the acylphosphorane **4.17**. Similar stereocontrol observed for both these reactions suggests a common mechanism. These reactions were extended to include phthalic anhydrides that were substituted with methyl and nitro groups, to yield the methyl phthalic and nitro phthalic bromo enol lactones **4.32**, **4.33**, **4.34**, **4.41**, **4.42**, **4.43**, and **4.44**.

Chapter 5

Extending the Bromolactonisation Reaction to Amino Acid Analogues

5.1 Introduction

Halo enol lactones have been developed[0.15,3.2,5.1] as potential mechanism-based inactivators of proteases. Therefore, it is useful to incorporate the strategies of drug design into a discussion on halo enol lactones. The key feature of a mechanism-based inactivator is that it is a substrate with latent reactivity. The halo enol lactone inactivator should therefore have enzyme recognition features incorporated into the molecule. Chymotrypsin cleaves a peptide on the carbonyl side of an amino acid that has an aromatic residue, such as phenylalanine (see Introduction). Therefore, it is important to incorporate an aromatic substituent into the molecule for chymotrypsin recognition. The position of the aromatic substituent is important for two reasons. Firstly, it dictates whether or not the molecule is oriented correctly to enable a fit into the active site, and secondly that following catalysis, the revealed latent reactive α-halo ketone is suitably positioned for nucleophilic attack.

Katzenellenbogen *et al.* has synthesised[5.1] several aromatic substituted halo enol lactones **5.1a-d** and **5.2a-b** and tested them for mechanism-based inactivation of chymotrypsin. He found that the aromatic substituent must be in the α position (with respect to the carbonyl) for mechanism-based inactivation. It was observed[5.1] that in terms of potency, a napthal group was superior to the phenyl group, iodo

was twice as good as bromo, and six-membered lactone rings were 20-40 times better than five-membered rings.

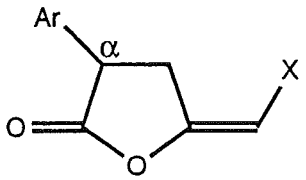

5.1

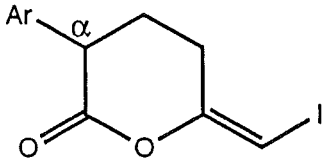

5.2

Ar	X
a:1-Np	I
b:Ph	I
c:1-Np	Br
d:Ph	Br

The halo enol lactones[5.1] **5.3**, **5.4**, and **5.5** with a β or γ aromatic substituent are competitive inhibitors and reversible inactivators. This change in inhibitor activity illustrates the high sensitivity of the enzyme active site to molecular shape and electrostatic interactions.

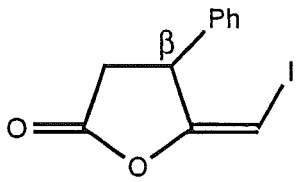

53

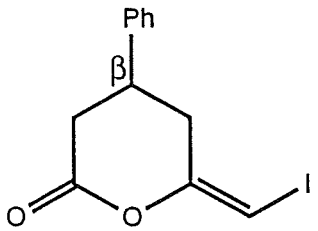

54

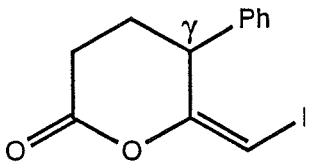

55

Molecular mechanics calculations[3.3] on the active site of chymotrypsin and on the β-aromatic halo enol lactones **5.3** and **5.4** have been useful in the rationalisation of the forementioned structure activity relationships. The calculations were used to test the validity of the proposed mechanism of inactivation (see Introduction). Conformational analyses were performed[3.3] at three levels. Firstly, on the Michealis complex, which measures the effectiveness of the substrates binding (K_I). Secondly, on the acylenzyme intermediate, which determines which

nucleophilic residues can attack the released reactive electropositive α-halo ketone, and thirdly, on the final bis adduct, which assesses the stability of the enzyme-inactivator complex and gives an estimate of the enthalpy of alkylation. The results of these calculations are in good agreement with experimental observations[5.1]. The naphthal substituent gives 5Kcal/mol more stabilisation of binding than the phenyl substituent in the Michealis complex, and the six-membered ring lactones bind with 3Kcal/mol more stabilisation than the five-membered rings in the Michealis complex. The His-57 residue in the acylenzyme intermediate is more accessible by 10Kcal/mol for nucleophilic attack than the next most likely candidate, Met 192.

The natural substrate of chymotrypsin is a polypeptide, so the inclusion of a correctly positioned amine functionality to further mimic an amino acid was examined. The racemic halo enol lactone **5.6** has been synthesised but no inhibition data has been reported[5.1], Scheme 5.1. The synthesis of **5.6**, by the standard halolactonisation of the corresponding acetylenic acid, occurred in a yield of 7-21% depending on the synthetic route[5.1]. The precursor acetylenic acid **5.7** was synthesised in 5 steps in a yield of 31%. The bromolactonisation synthesis that we have developed based on the Wittig reaction enables the stereocontrolled inclusion of recognition features, such as the aromatic and amine substituents (see Sections 5.2, 5.3, and 5.4).

The reaction of ylide Ph_3PCHCO_2Et **0.1** with asymmetrically substituted anhydrides forms the basis of this work and is briefly discussed at this point. Two rationales have been proposed to explain which carbonyl is preferentially attacked. The first of these is based on the Bürgi-Dunitz rule[5.2] which states that a nucleophile attacks a carbonyl at an angle of 110-120° (Figure 5.1). A nucleophile must therefore approach the carbonyl of a lactone or anhydride across the ring.

Scheme 5.1

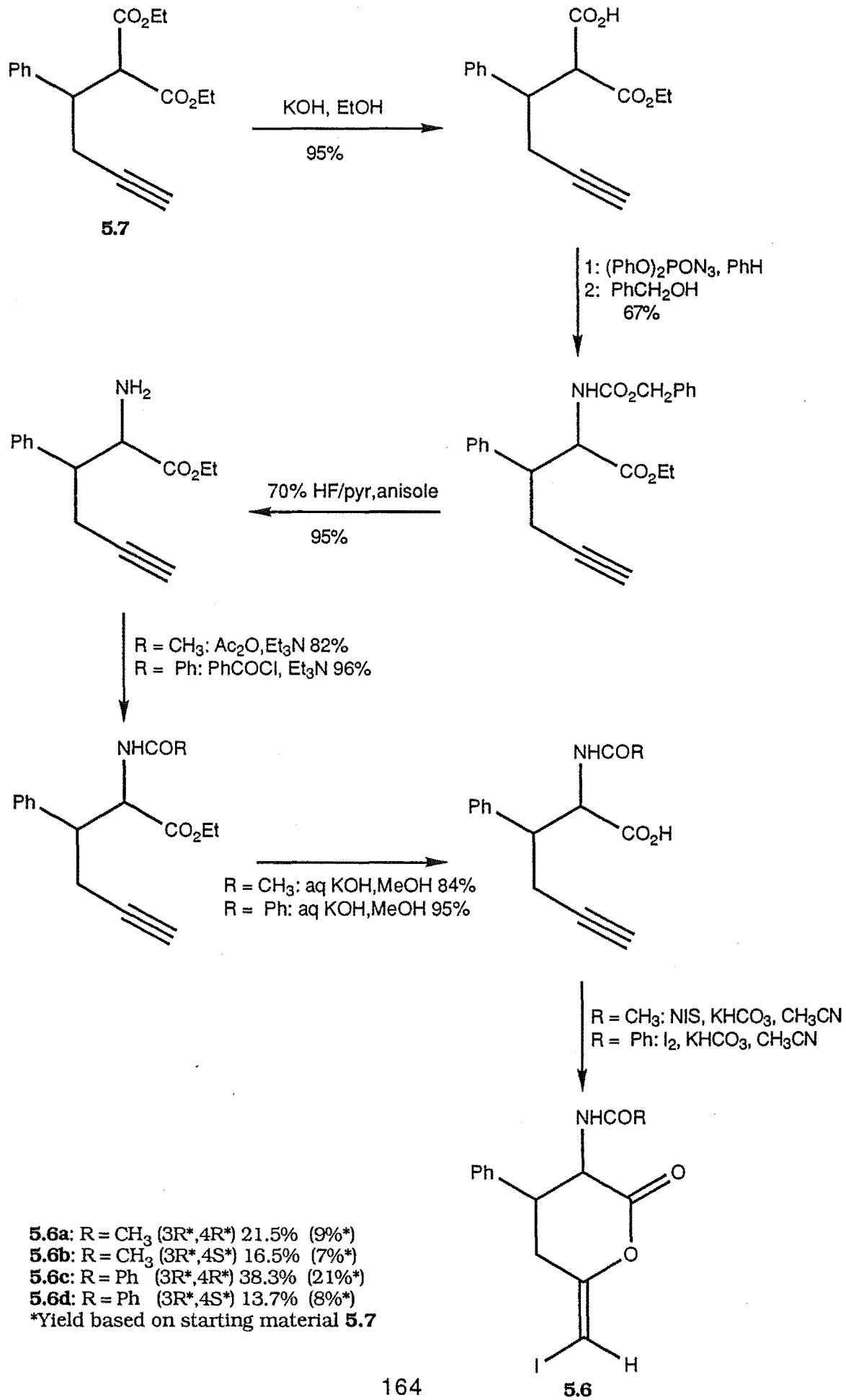

5.6a: R = CH_3 (3R*,4R*) 21.5% (9%*)
5.6b: R = CH_3 (3R*,4S*) 16.5% (7%*)
5.6c: R = Ph (3R*,4R*) 38.3% (21%*)
5.6d: R = Ph (3R*,4S*) 13.7% (8%*)
*Yield based on starting material **5.7**

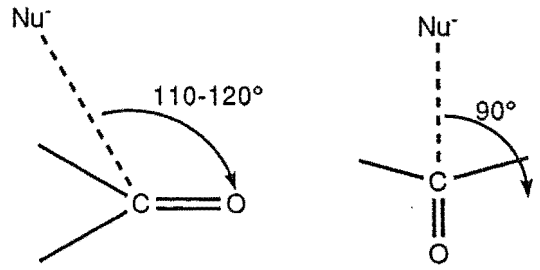

Figure 5.1: Nucleophilic attack on a carbonyl

For an asymmetrically substituted anhydride the most unhindered pathway for the nucleophile would therefore be at the apparently most hindered α-carbonyl (Figure 5.2:pathway A).

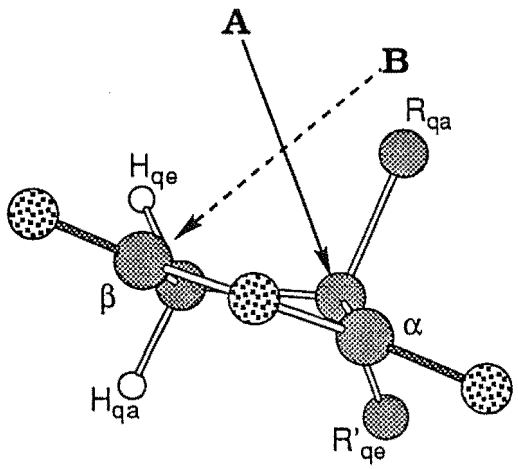

Figure 5.2: Pathways for Nucleophilic Attack on Asymmetric Anhydrides.
Pathway A: Reaction at most hindered carbonyl via unhindered pathway; Pathway B: Reaction at unhindered carbonyl via the most hindered pathway.
(α = α-carbonyl to the substituents R_{qa}, R'_{qe}
β = β-carbonyl to the substituents R_{qa}, R'_{qe}
qe = quasiequatorial, qa = quasiaxial)

This rationale has been used to explain stereoselective borohydride reductions of *gem*-disubstituted succinimide[5.3] and succinic anhydride derivatives. However, the reaction of *gem*-disubstituted succinic anhydrides with the ylide **5.8** at the alternative carbonyl does not support this rationale, but rather may support an alternative cycloaddition [2+2] mechanism[2.22]. Monosubstituted succinic anhydrides react with the ylide at both carbonyls depending on the ring substitution. It is known[5.4] that substituted succinic anhydrides favour a nonplanar conformation, with the

alkyl and aryl groups preferring to be in a quasiequatorial position and therefore the regioselectivity due to steric interaction with the nucleophile will not be as large.

The second rationalisation of ylide attack on asymmetrically substituted anhydrides has been formulated by Kayser[5.5] *et al.* This is based on previous studies[5.5] on metal hydrides and *ab initio* calculations and represents an extension of the Bürgi-Dunitz rule. Metal hydrides react regioselectively with *gem*-disubstituted succinic anhydrides favouring, almost exclusively, reduction of the most hindered α-carbonyl, Figure 5.3.

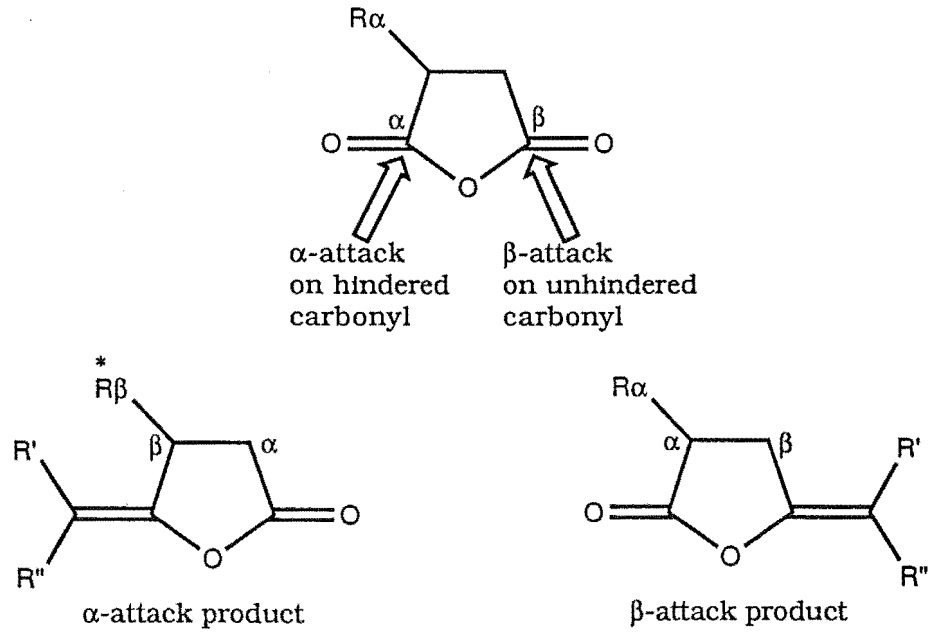

Figure 5.3: Nucleophilic Attack on an Asymmetric Anhydride

This observation supports the Bürgi-Dunitz hypothesis of nucleophilic attack on the most hindered α-carbonyl[5.5]. Monosubstituted succinic anhydrides generally gave a mixture of the two regioisomers, although reduction occurs preferentially at the most hindered carbonyl. The

following four factors, postulated[5.5] for metal hydride systems, have also been used to explain proposed regiocontrol on ylide attack, 1: the intrinsic reactivity of the carbonyl group; 2: a chelating or complexation effect; 3: antiperiplanar effect; and 4: steric congestion. The intrinsic reactivity of the carbonyl depends on the electronic nature of the substituents, for example the reactivity will increase if an electron withdrawing substituent is near the carbonyl. The chelating or complexation effect is related to a proposed charge donor complex that may form if an electron donator, near the carbonyl, stabilises the charge on the phosphorus betaine intermediate (Figure 5.4). This has been used[5.6] to rationalise the 100% α–regioselectivity observed for the reaction of methoxy succinic anhydride and ylide **0.1**.

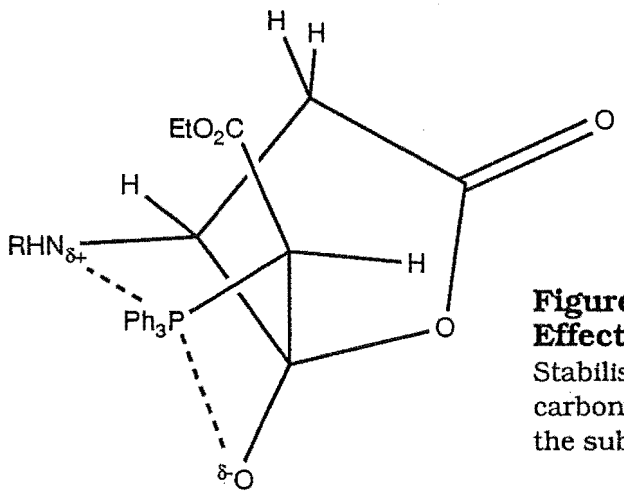

Figure 5.4: Chelation or Complexation Effect.
Stabilisation of the phosphorus by the carbonyl and electron donation from the substituent amine

The antiperiplanar effect[5.7] essentially states that there is greater stabilisation of the transition state if the σ^*_{C-X} antibonding orbital is low in energy, Figure 5.5. The C-C bond antiperiplanar to C-H- is favoured over a C-H as σ^*_{C-C} is lower in energy than σ^*_{C-H} , thus an alkyl substituent in the quasiaxial position will stabilise attack of a nucleophile on that carbonyl. Increased antiperiplanarity of the C-X bond and the nucleophile in the

transition state essentially represents the pyramidalisation of the carbonyl group. The antiperiplanar effect is more obvious in more flexible systems that can easily adopt an antiperiplanar geometry. For example, this effect explains the regio and stereoselectivity of asymmetric diesters[5.7] and diacids where reduction occurs at the most hindered site. Steric

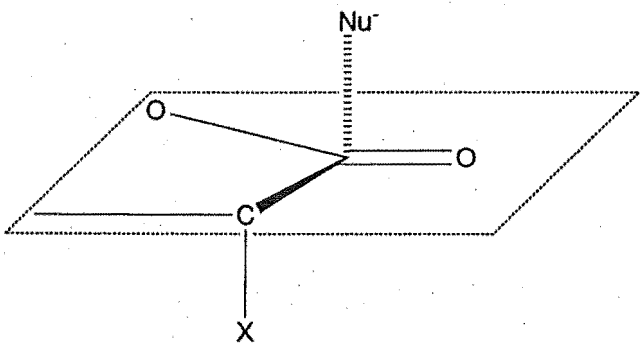

Figure 5.5: Antiperiplanar Geometry

congestion refers to the influence of a bulky ylide on addition to substituted succinic anhydrides[5.5]. For example, the *Z*-enol lactone is formed when there is steric hindrance in the intermediate leading to the alternative *E*- enol lactone (Figure 5.6 and Chapter 2).

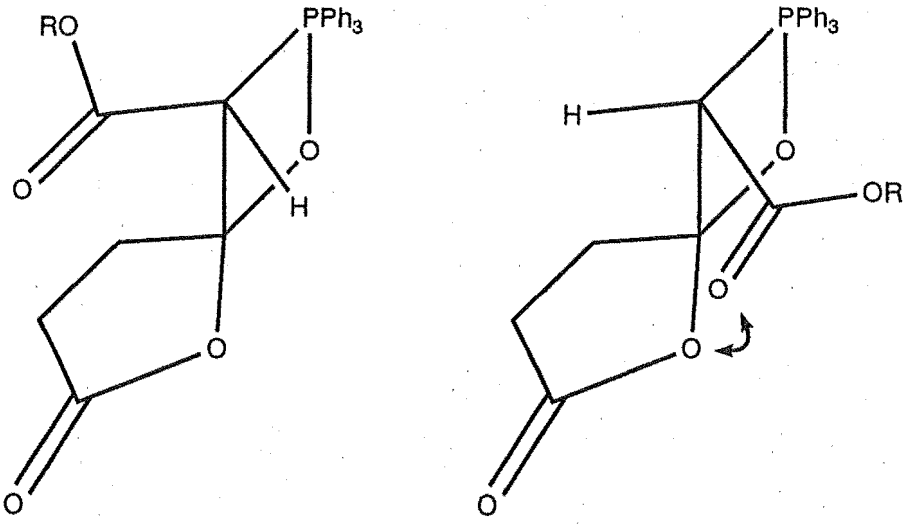

Figure 5.6

Any effort to attribute a single factor for the regiocontrol of reactions of substituted succinic anhydrides is futile. The above features act in concert to give the overall regiocontrol.

The reactions of succinic, glutaric, and phthalic anhydrides discussed in Chapters 2, 3, and 4, respectively are important in the development and understanding of the stereochemical preference in the bromolactonisation reaction. The succinic and glutaric bromo enol lactones represent simple amino acid analogues. The scissile peptide bond of the natural substrate is mimicked by the lactone moiety (Figure 5.7).

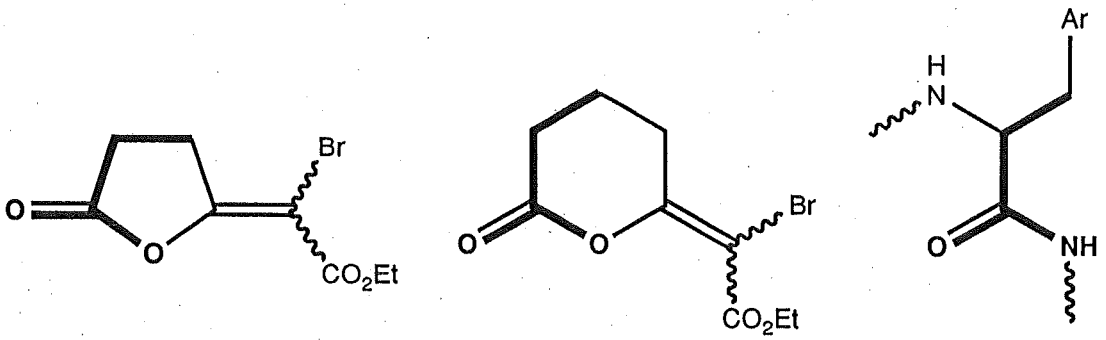

2.33 , 2.34 **3.13 , 3.14** Natural substrate

Figure 5.7

The phthalic bromo enol lactones are better analogues of phenylalanine as they contain an aromatic ring. However, the phthalic bromo enol lactones lack a CH_2 link to the phenyl group, (Figure 5.8). The bromolactonisation reaction has therefore been extended to synthesise bromo enol lactones that are more sophisticated amino acid analogues.

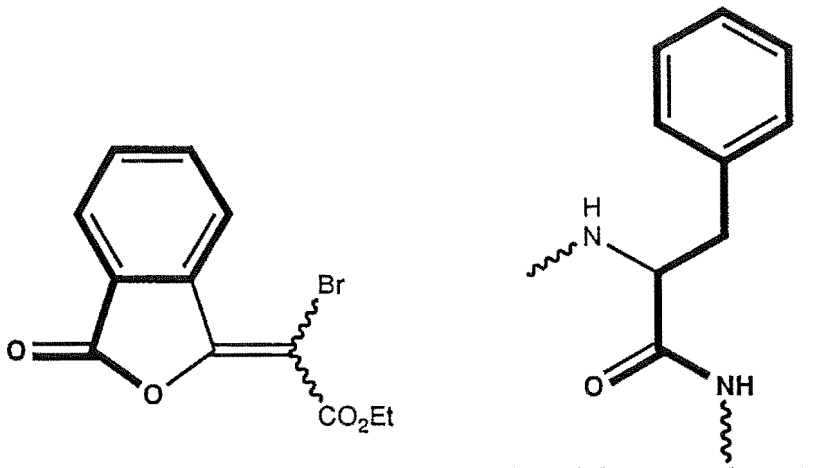

4.25, 4.26 Phenylalanine substrate

Figure 5.8

5.2 3-Phenyl Glutaric Bromo Enol Lactones

The 3-phenyl glutaric bromo enol lactones **5.9** and **5.10** are of interest as they incorporate the exact carbon connectivity of the natural substrate of chymotrypsin, for example phenylalanine (Figure 5.9).

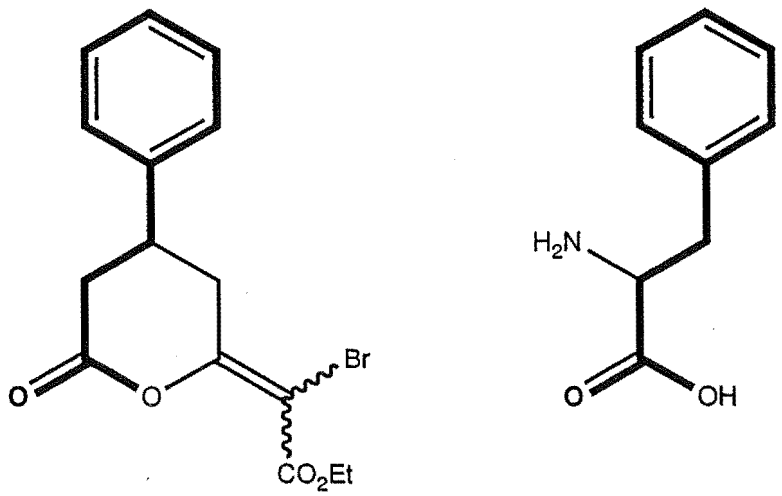

5.9, 5.10 Phenylalanine

Figure 5.9

3-Phenyl glutaric halo enol lactones, for example **5.4,** have been shown to be reversible inhibitors of chymotrypsin (see 5.1: Introduction).

Previous syntheses[5.1] of racemic 3-phenyl glutaric bromo enol lactones have been based on the well established halolactonisation of acetylenic acids.

The bromolactonisation reaction that we have developed is ideally suited to the synthesis of 3-phenyl glutaric bromo enol lactones as 3-phenyl glutaric anhydride is readily available, and symmetric.

The reaction of prochiral 3-phenyl glutaric anhydride with a stabilised ylide is previously unreported, Scheme 5.2. 3-Phenyl glutaric anhydride **5.11** was refluxed with ylide Ph_3PCHCO_2Et **0.1** (1.1 equiv) in $CHCl_3$ for 1 hour. The resulting acylphosphorane **5.12**, characterised by ^1H NMR spectroscopy, slowly formed the enol lactone **5.13** at room temperature (3% after 6 hours). A characteristic downfield shift of 0.5ppm was observed for the ethyl ester quartet and triplet. The *E*-enol lactone **5.13** formation was complete after refluxing **5.12** in $CHCl_3$ for 24 hours. Neither the *Z*-enol lactone **5.14** nor the endo isomer **5.15** were observed. The previously unknown *E*-enol lactone **5.13** was purified by radial chromatography to give an isolated yield of 86%. A complete ^1H NMR assignment of **5.13** was achieved using decoupling and COSY[5.8] experiments, Figure 5.10. The proposed[5.9] "sofa" conformation of the glutaric ring (Figure 5.11), essentially planar with only the 3-carbon out of the ring plane, leads to some interesting proton-proton coupling discussed below.

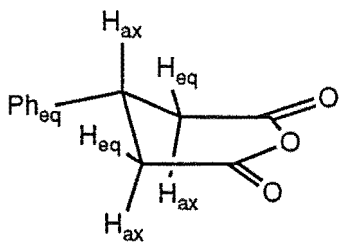

Figure 5.11: Sofa conformation of Glutaric Anhydride

Scheme 5.2: Phenyl Glutaric Anhydride reaction with Ylide 0.1 and Formation of Bromo enol lactones 5.9 and 5.10.

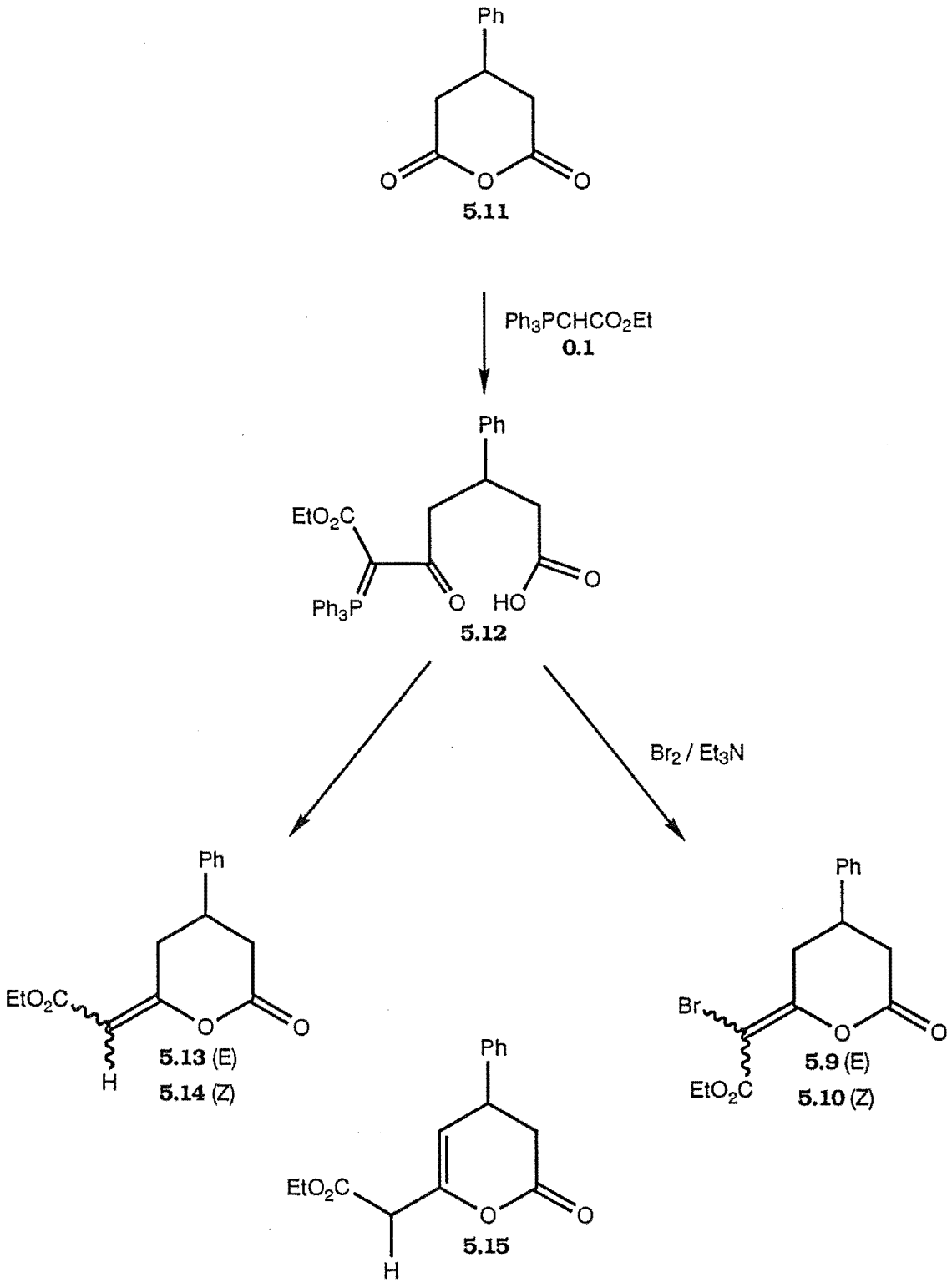

Figure 5.10: COSY Experiment on 5.13 Showing Allylic Coupling of H27 to H25, and Coupling of H22, H23, H24, H25, and H26.

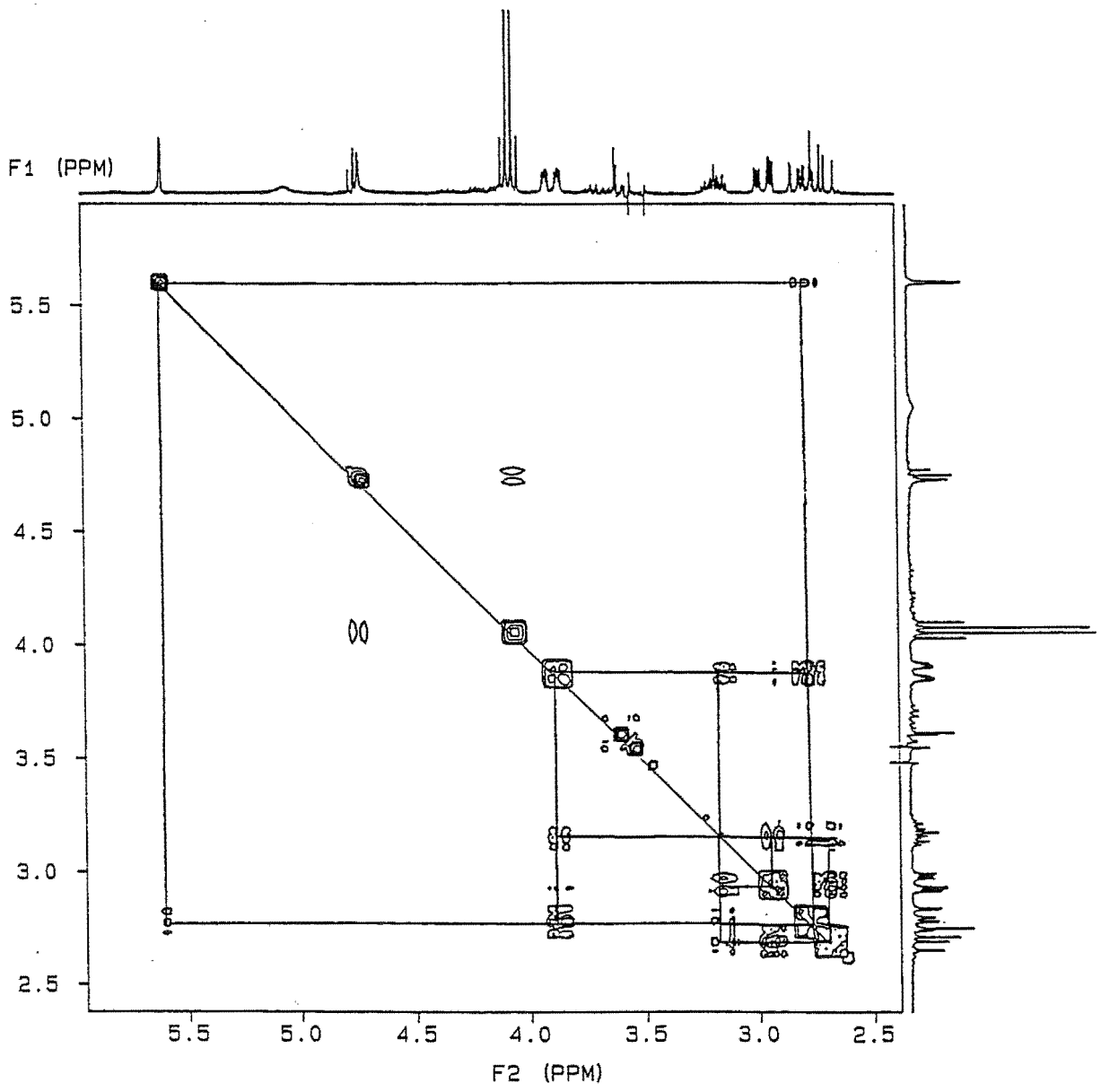

The magnitude of allylic coupling constants has traditionally been used to determine the configuration of enol lactones (see Chapter 3). Allylic coupling is also useful in determining the conformation of protons on the allylic carbon. Allylic coupling[5.10] is at a maximum of about 3Hz when the allylic dihedral angle is 90° or 270° and at a minimum for angles of 0° and 180°. The ^{1}H NMR spectrum of the *E*-enol lactone **5.13** shows that the olefinic proton is coupled to only one of the allylic protons. The ^{1}H NMR spectrum is also consistent with H25 being axial (Figure 5.12), hence giving maximum allylic coupling to H27 and an upfield chemical shift relative to H26. H26 is deshielded 1ppm (relative to H25) by the ester carbonyl. The lack of allylic coupling to H27 is also consistent with H26 being equatorial (O° dihedral angle). The geminal protons H25 and H26 are both coupled to H24 which is subsequently coupled to the geminal protons H22 and H23.

The magnitude of the observed allylic coupling constant of 2.8Hz was consistent with the *E*-stereochemistry. The ^{1}H NMR chemical shift and the coupling constant of the allylic proton H27 to H25 are in good agreement with those of the known *E*-enol lactone **5.16**, Table 5.2.

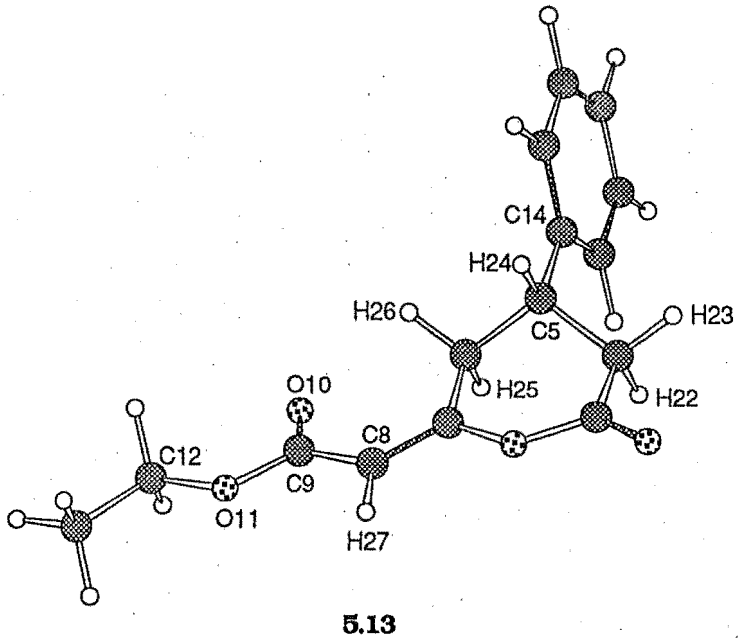

5.13

Figure 5.12

MM2 calculations[2.29] were used to further investigate the geometry of the six-membered ring and to compare the calculated and experimentally determined coupling constants. The *E*-enol lactone **5.13** six-membered ring, and bonds C8-C9, C9-O11 (180° increments), O11-C12 (60° increments), and C5-C14 (30° increments) were minimised, and vicinal coupling constants were calculated within MODEL[2.29]. Energy minimisation of the *E*-structure produced 19 conformers having energies within 3Kcal/mol of the minimum energy. Application of the Boltzman distribution at 25°C showed that the 4 lowest energy conformers accounted for 42.9% of the population and that the Boltzman average energy was 31.90Kcal/mol. The orientation of a phenyl substituent on the glutaric anhydrides has been reported to favour an equatorial position by 0.6-1.2Kcal/mol. The MM2 calculation is consistent with this as the first 14 conformers have the phenyl group in the equatorial position. Previous calculations[5.9] on 3-phenyl glutaric anhydride systems have also reported that the equatorial phenyl ring prefers to be in a planar rather than perpendicular position by 3.8Kcal/mol, due to the phenyl ortho hydrogens interacting with the axial and equatorial hydrogens of the glutaric ring. The MM2 calculation in this study is not consistent with this as all conformers have the phenyl group in the perpendicular position (the six lowest energy conformations are shown in Figure 5.13). The calculated and experimental coupling constants are in good agreement (Table 5.1) and clearly show the ring to be in a sofa conformation.

The bromolactonisation of the acylphosphorane **5.12** shows the same stereocontrol as previously studied glutaric and 3-substituted glutaric derived acylphosphoranes (see Chapter 3). 3-Phenyl glutaric anhydride **5.11** and ylide **0.1** (1.1 equiv) were refluxed in $CHCl_3$ for 1 hour. The stirred solution containing the phosphorane **5.12** was then cooled to 0°C and triethylamine (1 equiv), followed by bromine (1 equiv), were added. After 30 minutes the solution was allowed to warm to room temperature

Table 5.1:MM2 Energy Minimisation and Coupling Constants for 3 -Phenyl Glutaric Hydrogen Enol Lactone (5.13)

Conformer%	Energy (Kcal/mol)	J(25,24)[1]	J(26,24)[1]	J(24,23)[1]	J(24,22)[1]	J(27,26)[2]	J(27,25)[2]
		Coupling constant in Hz (dihedral angle)					
1 = 13.13 %	31.604	12.348 (177)	3.434 (58)	2.713 (63)	12.326 (177)	-0.17 (37.9)	-2.52 (-81.9)
2 = 12.23 %	31.646	12.358 (178)	3.226 (59)	2.733 (63)	12.321 (177)	-0.22 (38.5)	-2.51 (-81.3)
3 = 12.16 %	31.650	12.328 (176)	3.599 (57)	2.666 (63)	12.315 (177)	-0.42 (41.6)	-2.43 (-77.8)
4 = 11.40 %	31.689	12.355 (178)	3.288 (59)	2.691 (63)	12.310 (176)	-0.47 (42.4)	-2.40 (-77.8)
5 = 7.37 %	31.949	12.328 (176)	3.549 (57)	2.530 (64)	12.245 (174)	0.06 (34.3)	-2.57 (-85.9)
6 = 6.62 %	32.012	12.345 (177)	3.405 (58)	2.637 (64)	12.277 (175)	-0.13 (37.3)	-2.53 (-82.4)
7 = 6.41 %	32.032	12.321 (175)	3.596 (57)	2.610 (64)	12.266 (175)	-0.02 (35.5)	-2.57 (-85.4)
8 = 6.16 %	32.056	12.346 (177)	3.400 (58)	2.699 (63)	12.294 (176)	-0.36 (40.7)	-2.46 (-79.0)
9 = 5.14 %	32.164	12.346 (178)	3.000 (61)	2.838 (62)	12.350 (178)	-0.36 (40.6)	-2.46 (-79.0)
10 = 4.93 %	32.188	12.356 (179)	3.111 (60)	2.771 (63)	12.342 (178)	-0.19 (38.2)	-2.52 (-81.6)
11 = 4.88 %	32.195	12.352 (179)	3.080 (60)	2.844 (62)	12.351 (179)	-0.09 (36.7)	-2.54 (-83.0)
12 = 4.24 %	32.278	12.360 (179)	3.245 (59)	2.750 (63)	12.339 (178)	-0.11 (37.0)	-2.53 (-82.5)
13 = 4.14 %	32.292	12.360 (179)	3.276 (59)	2.760 (63)	12.340 (178)	-0.18 (38.0)	-2.52 (-81.7)
14 = 0.30 %	33.859	1.485 (73)	5.551 (43)	3.115 (58)	3.025 (59)	-0.30 (39.8)	-2.48 (-79.9)
15 = 0.30 %	33.862	1.418 (74)	5.686 (42)	3.205 (58)	2.940 (60)	-0.75 (-46.3)	-2.20 (71.4)
16 = 0.23 %	34.020	12.082 (170)	4.784 (49)	3.365 (58)	12.359 (178)	-0.87 (-48.3)	-2.12 (69.5)
17 = 0.14 %	34.332	1.268 (76)	6.019 (41)	4.148 (52)	2.240 (65)	0.05 (-34.5)	-2.55 (83.5)
18 = 0.11 %	34.432	1.779 (69)	4.950 (47)	4.220 (51)	2.287 (65)	0.00 (-35.2)	-2.54 (82.9)
19 = 0.10 %	34.491	1.904 (68)	4.754 (48)	3.824 (54)	2.605 (62)	-0.16 (-37.1)	-2.49 (80.6)
The Boltzmann averaged energy and coupling constants are:							
	31.90461	12.242	3.380	2.710	12.221	-0.17	-2.48
Experimental Coupling Constants							
		12.4	4.1	2.7	12.2	0.00	2.8

[1]: Vicinal coupling constants were calculated in Model.

[2]: Allyllic coupling constants were calculated by using the formula $1.3\cos^2\phi - 2.6\sin^2\phi \quad (0 \le \phi \le 90)$

$-2.6\sin^2\phi \quad (90 \le \phi \le 180)$

Figure 5.13: Six Lowest Energy Conformers of 5.13

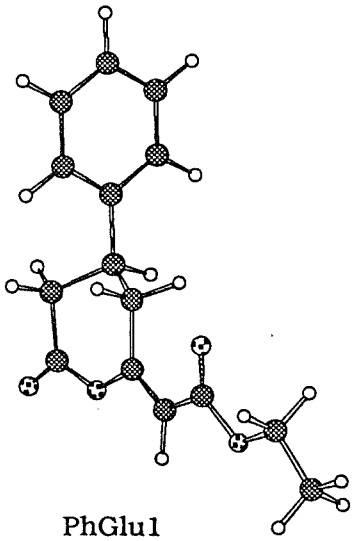

PhGlu1

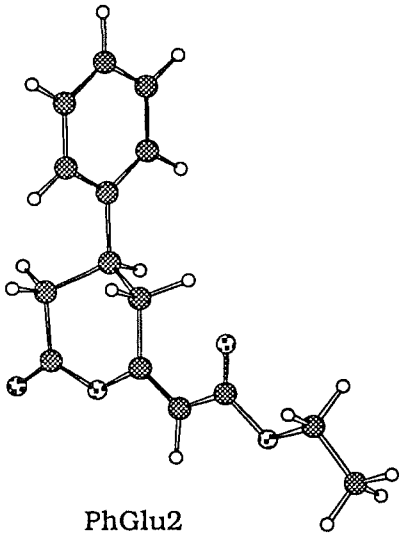

PhGlu2

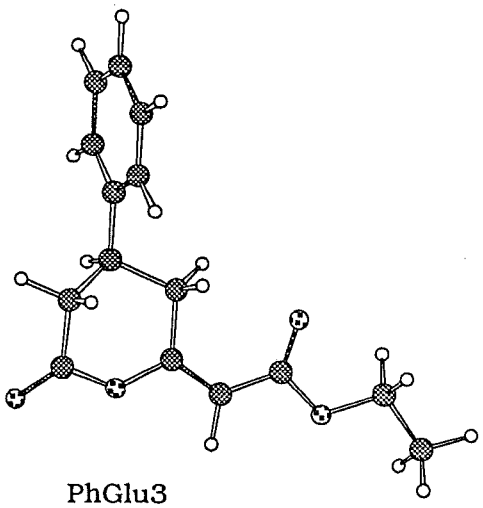

PhGlu3

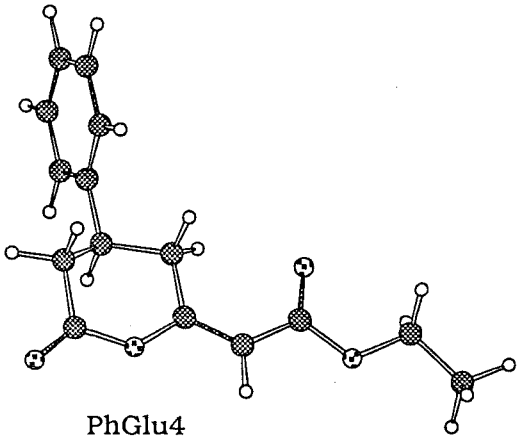

PhGlu4

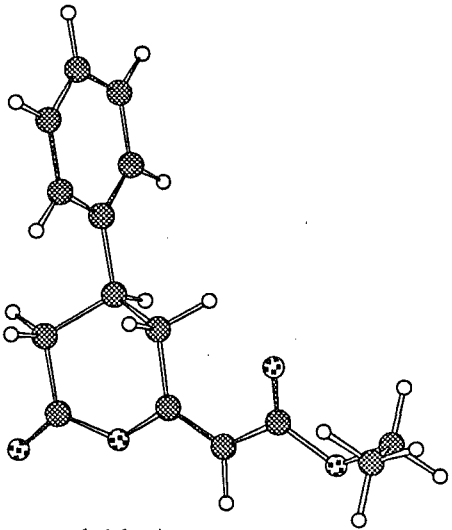

PhGlu5

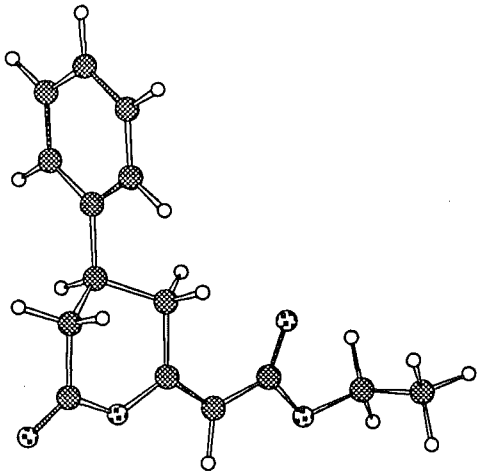

PhGlu6

and the solvent was removed and the residue purified by radial chromatography. The *E*- and *Z*-bromo enol lactones **5.9** and **5.10** were formed in a ratio 86:14 (72%), Scheme 5.2.

The *E*- and *Z*-stereoisomeric ratio of 86:14 is similar to the previously studied substituted glutaric bromo enol lactones, see Chapter 4. The 3-phenylglutaric bromo enol lactones **5.9** and **5.10** are racemic as reaction is equally likely at either face of the prochiral 3-phenylglutaric anhydride.

The ^{1}H NMR spectra of *E*- and *Z*-bromo enol lactones were assigned by comparison of the ^{1}H NMR spectra of *E*-enol lactone **5.13**, the known bromo enol lactone **5.16**, and the previously prepared bromo enol lactones **3.15** and **3.16**, see Chapter 3, Table 5.2. The ^{1}H NMR chemical shifts for the ring protons (H22, H23, H24, H25, and H26) of *Z*-bromo enol lactone **5.10** are in good agreement with the signals for the *E*-enol lactone **5.13**, Table 5.2. Also, the ^{1}H NMR chemical shifts for the ring protons (H22, H23, H24, H25, and H26) of *E*-bromo enol lactone **5.9** are in good agreement with the signals for the known *E*-bromo enol lactone **5.16**, Table 5.2. The deshielding effect of the *trans* lactone oxygen, is observed. The ^{1}H NMR assignment is also consistent with the 3-methyl glutaric bromo enol lactone **3.15**, Table 5.2. A Homonuclear two dimensional J resolved NMR experiment[5.8] resolved the signals for overlapping multiplets.

Table 5.2

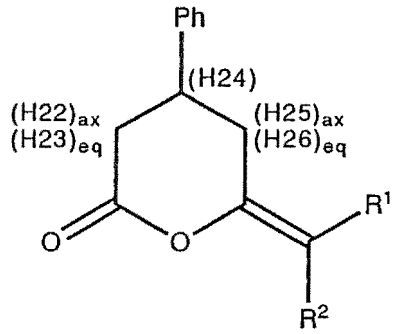

^{1}H NMR signals

Compound	(H22)	(H23)	(H24)	(H25)	(H26)	(H27)
5.9: R^1=Br, R^2=CO_2Et	2.72,dd,12.4,17.1	2.98,ddd,2.2,4.2,17.0	3.3,m	2.79,dd,12.0,17.0	3.3,m	-
5.10: R^1=CO_2Et, R^2=Br	2.82,dd,11.6,23.2	3.32,ddd,2.2,4.6,17.4	3.28,m	2.90,dd,11.6,23.0	3.89,ddd,2.2,4.2,17.1	-
5.13: R^1=CO_2Et, R^2=H	2.80,dd,12.2,22.5	3.05,dd,2.7,4.1,22.3	3.26,m	2.89,ddd,2.3,12.4,20.3	3.98,ddd,2.4,4.0,20.3	5.71,d,2.8
5.16: R^1=Br, R^2=H	2.75,m3.2,m	3.2,m	2.75,m		3.2,m	6.0,d,3
3-methyl glutaric bromo enol lactones (see Chapter3)						
3.15: R^1=Br, R^2=CO_2Et	2.70, dd, 12.6, 15.5	3.05, dd, 2.6, 15.5	2.3, m	2.30, m	2.30, m	-
3.16: R^1=CO_2Et, R^2=Br	2.33, dd, 10.4, 17.2	2.79, dd, 1.9, 17.2	2.17, m	2.82, ddd, 1.9, 4.3, 17.2	3.53, dd, 10.4, 17.4	-

5.3 Phenyl Succinic Bromo Enol Lactones

The reaction of phenyl succinic anhydride **5.17** with the ylide Ph_3PCHCO_2Et **0.1** and the bromolactonisation of the intermediate phosphoranes **5.18** and **5.19** were also investigated as a means of developing better amino acid analogues. The carbon connectivity of the resulting α-bromo enol lactones **5.20** and **5.21** incorporate that of the natural substrate, phenylalanine, Figure 5.14.

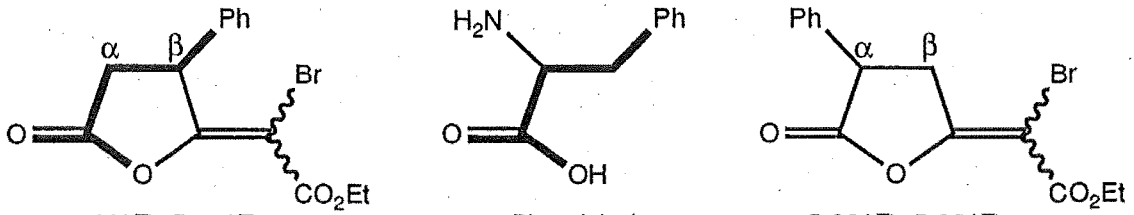

5.20(*E*), **5.21**(*Z*) Phenylalanine **5.22**(*E*), **5.23**(*Z*)

Figure 5.14

This is important as the position of the aromatic ring is crucial to the recognition of the molecule by chymotrypsin as a substrate[5.1] (see 5.1: Introduction). Phenyl succinic anhydride also introduces asymmetry and leads to the possibility of reaction at both carbonyls (see 5.1: Introduction) to give the α- and β-pairs of bromo enol lactones **5.22**, **5.23**, and **5.20**, **5.21**, respectively. When the aromatic ring in a halo enol lactone is in the β-position, directly analogous to phenylalanine, the halo enol lactones are competitive inhibitors, rather than mechanism-based inactivators. The opposite applies when the aromatic ring is in the α-position (see 5.1: Introduction).

While these investigations were underway, the reaction of substituted phenyl succinic anhydrides with the stabilised ylide $Ph_3PCHCO_2CH_3$ **5.24** was reported by Kayser[5.6] *et al.*. The reactions of phenyl and paramethoxy phenyl succinic anhydride with the stabilised

ylide **5.24** were reported[5,6] to produce the α,β-unsaturated lactones **5.25**, **5.26**, **5.27**, and **5.28**. However, the α,β-unsaturated products **5.25** and **5.26** obtained are different to the products obtained in our investigation. A comparison of the ^{1}H NMR spectrum of the paramethoxy phenyl succinic lactones **5.27** and **5.28** (Table 5.3) with the phenyl succinic enol lactones **5.29** and **5.30** (Table 5.5) clearly shows that the products are different (note, ^{1}H NMR data for the phenyl succinic products **5.25** and **5.26** was reported[5,6] to be identical to **5.27** and **5.28**). This anomaly is possibly due to the different reaction conditions used in the cyclisation of the acyl phosphoranes **5.18** and **5.19**. Kayser[5,6] used THF at reflux for 20 hours, while in our study the reaction involved $CHCl_3$ at reflux for 6 hours. Kayser stated[5,6] that the usual enol lactones **5.29** and **5.30** were not observed, rather a rapid isomerisation of the *exo* double bond occurs.

Table 5.3: Kayser[5,6] *et al.* α,β-unsaturated Products

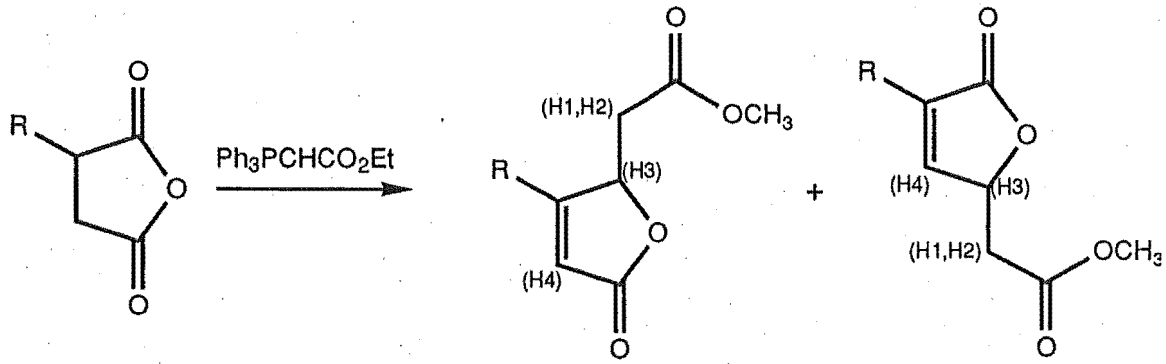

R=Ph — **5.25** (68%) — **5.26** (32%)
R=p-$CH_3OC_6H_4$ — **5.27** (50%) — **5.28** (50%)

^{1}H NMR signals of **5.27** and **5.28**

Compound	H1	H2	H3	(H4)
5.27 R = p-$CH_3OC_6H_4$	2.68,dd,7.2,16.4	2.91,dd,7.0,16.4	5.39,td,7.0,7.2,16	7.54,d,1.6
5.28 R = p-$CH_3OC_6H_4$	2.50,dd,9.4,17.5	2.92,dd,2.6,16.5	5.88,ddd,1.3,2.6,9.4	6.20,d,1.3

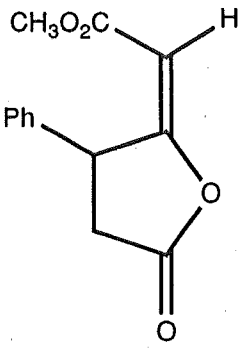

5.29

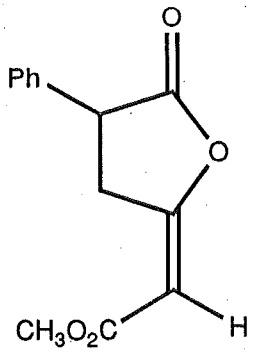

5.30

The report states that the two lactones **5.25** and **5.26** derived from phenyl succinic anhydride **5.17** were inseparable by chromatography and were characterised from the hydrogenation products of the double bond. It should be noted that the hydrogenation products for the enol lactones **5.29** and **5.30** would be identical to those for **5.25** and **5.26**. The ^1H NMR data reported for the two paramethoxyphenyl succinic lactones **5.27** and **5.28** was unclear in the assignments.

A closer examination of the reaction of phenyl succinic anhydride with the ylide Ph_3PCHCO_2Et **0.1** in $CHCl_3$ revealed that the two intermediate acylphosphoranes **5.18** and **5.19** formed in a ratio of 62:38 after 60 minutes (total ^1H NMR yield of 44%), Scheme 5.3. The acylphosphoranes **5.18** and **5.19** cyclised slowly to form the enol lactones **5.31** and **5.32** with standing at room temperature (5% after 90 minutes) thus preventing completion of the acylphosphorane formation, Scheme 5.4. Attempted separation of the acylphosphoranes **5.18** and **5.19** by low temperature (0°C) radial chromatography was unsuccessful. The isomeric phosphoranes **5.18** and **5.19**, in $CHCl_3$, at reflux, gave complete formation of the enol lactones **5.31** and **5.32** after 6 hours, Scheme 5.4. The α and β-enol lactones, **5.31** and **5.32**, formed in a ratio of 62:38.

Scheme 5.3: Reaction of Phenyl Succinic Anhydride with Ylide 0.1

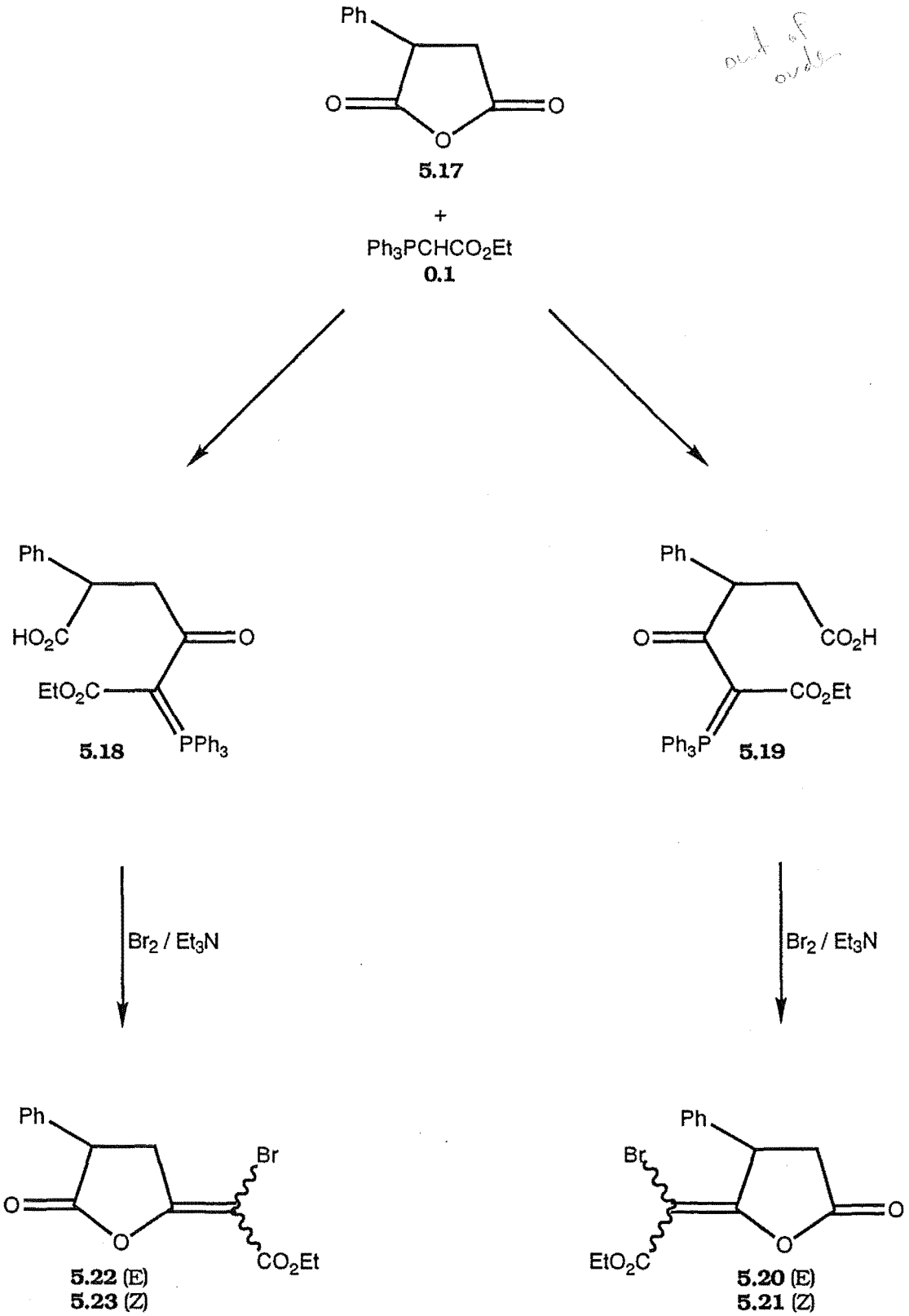

Scheme 5.4: Phenyl Succinic Anhydride Reaction with Ylides 0.1 and 2.53

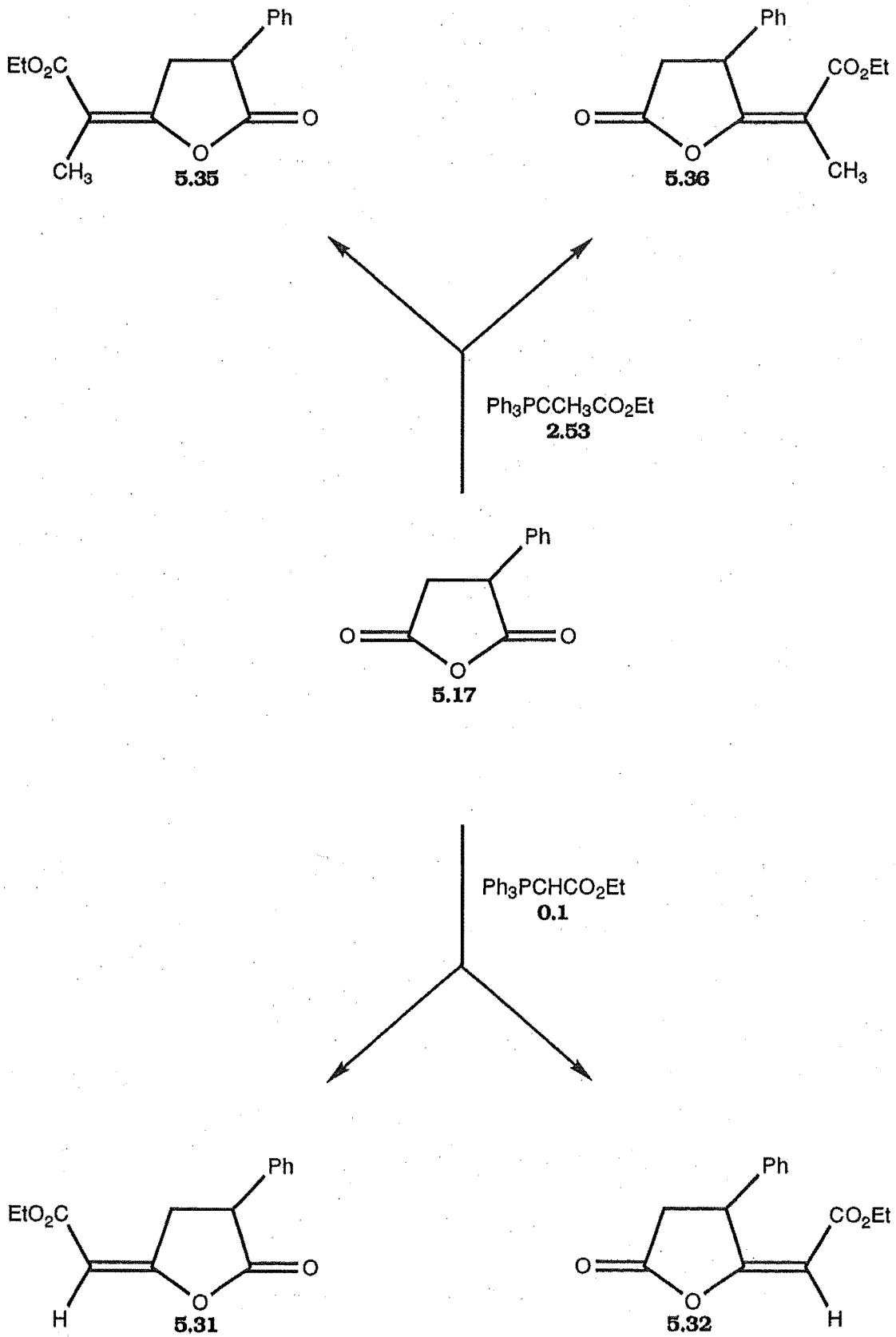

Purification by radial chromatography gave a total yield of 55%. Separation of the enol lactones was achieved by HPLC.

Two trial reactions were set up to complete the investigation on the reaction of phenyl succinic anhydride and the ylide **0.1**. The first, using the same conditions as Kayser reported (THF at reflux), and the second, extending the time of our conditions ($CDCl_3$ at reflux). Both reaction conditions were monitored by ^1H NMR spectroscopy. We found that the α,β-unsaturated products **5.33** and **5.34** formed under identical conditions to Kayser. However, even after 60 hours, three times longer than Kayser's[5.6] conditions, the precusor enol lactones **5.31** and **5.32** were still observed. In THF, the α,β-unsaturated products **5.33** and **5.34** built up to about 60%, with 40% of the enol lactones **5.31** and **5.32**, Table 5.5. The rearrangement of the α–enol lactone **5.31** to give **5.33** was faster than the corresponding rearrangement with β–enol lactone **5.32** to **5.34**. Under extended reflux in $CDCl_3$ (60 hours), the α,β-unsaturated products **5.33** and **5.34** were observed to build up to a maximum of 25%, with 75% of the enol lactones **5.31** and **5.32**, Table 5.5. A possible explanation for the increased formation of the α,β-unsaturated products **5.33** and **5.34** in THF, versus $CDCl_3$, is that THF can stabilise a carbocation intermediate, whereas $CDCl_3$ will stabilise a carbanion intermediate. The isomerisation of the *exo* double bond is presumed to go through a carbocation intermediate.

The ylide $Ph_3PCHCO_2CH_2CH_3$ **0.1**, used in this study is different to that used in Kaysers[5.6] investigation ($Ph_3PCHCO_2CH_3$ **5.24**), although both would be expected to behave similarly. The ^1H NMR spectra of the reactions of the ylide **0.1** are more diagnostic than ylide **5.24** due to the characteristic ethyl ester signals (versus the methyl ester singlet). The change to the ylide **0.1** may affect the position of the thermodynamic equilibrium to give both the the α,β-unsaturated products **5.33** and **5.34** and the enol lactones **5.31** and **5.32**. However, it is surprising that Kayser did not observe any enol lactones or acylphosphoranes.

Bromolactonisation of the two acyl phosphoranes **5.18** and **5.19** with triethylamine and bromine gave the bromo enol lactones **5.20**, **5.21**, **5.22**, and **5.23** in a ratio of 24:12:55:9 respectively, Scheme 5.3. The resulting crude bromo enol lactones were purified by radial chromatography to give a total yield of 38% (the yield is 86% when based on the acylphosphorane). Separation of the bromo enol lactones was achieved by HPLC using a 10mm semi preparative cyano column.

Table 5.4: THF and $CHCl_3$ Conditions for the Reaction of Phenyl Succinic Anhydride and Ylide 0.1.

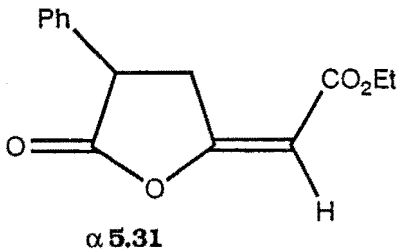

α **5.31**

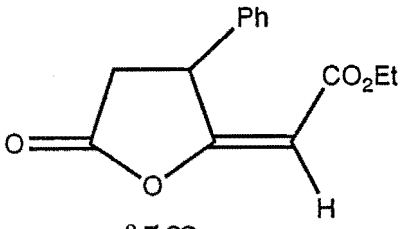

β **5.32**

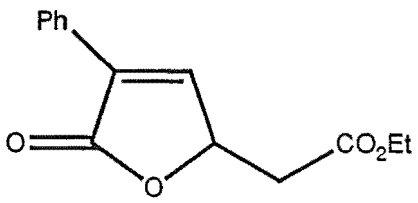

A **5.33**

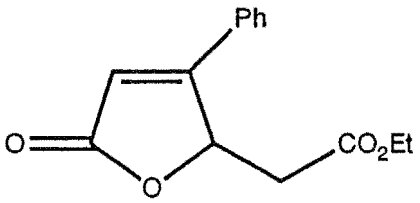

B **5.34**

Time	Solvent	A	B	α	β	A+B	α+β	A%	α%	A+α
12hrs	$CDCl_3$	16	4	63	17	20	80	80	79	79
	THF	34	20	33	13	54	46	63	72	67
20hrs	$CDCl_3$	17	8	56	19	25	75	68	75	73
	THF*	36	20	31	13	56	44	64	70	67
40hrs	$CDCl_3$	18	7	51	24	25	75	72	68	69
	THF	49	12	25	14	61	39	80	64	74
60hrs	$CDCl_3$	18	6	55	21	24	76	75	72	73
	THF	43	16	20	21	59	41	73	49	63

* Kayser 's[5.6] Conditions

The reaction of phenyl succinic anhydride and methyl ylide **2.53** was also investigated to allow a comparison of chemical shifts and coupling patterns in the hydrogen enol lactones **5.31** and **5.32** and the bromo enol lactones **5.20**, **5.21**, **5.22**, and **5.23**. The reaction of phenyl succinic anhydride with ylide **2.53**, $CHCl_3$ at reflux for 6 hours, gave the α- and β-methyl enol lactones **5.35** and **5.36** in a ratio of 74:26 respectively, Scheme 5.4.

The reactions of methyl ylide **2.53** with phenyl succinic anhydride gave the same regio and stereoselectivity as observed for the ylide **0.1**. The chemical shifts and coupling patterns of methyl enol lactones are very similar to the corresponding hydrogen enol lactones. Homoallylic coupling is evident in the methyl resonance, and the multiplicity of this signal is indicative of the regioselectivity of ylide attack.

5.3.1: Structure Assignment of Phenyl Succinic Enol Lactones

The methyl enol lactones **5.35** and **5.36** were assigned as α and β respectively on the basis of the multiplicity of the homoallylic coupling of the vinyl methyl protons and by comparison of chemical shifts and coupling constants of known[5.1] compounds **5.37** and **5.38**. There is very good agreement between the chemical shift and coupling constants for the H1 proton of **5.31** and the α-*E*-methyl enol lactone **5.35**, Table 5.5a. A comparison of the ^{1}H NMR spectral data of the known[5.1] compound **5.39** with β-*E*-methyl enol lactone **5.36**, also shows a very good agreement in the chemical shifts and coupling constants for the H2 and H3 protons, Table 5.5b.

The enol lactones **5.31** and **5.32** were assigned as α and β, respectively, on the basis of the multiplicity of the allylic coupling of the

Table 5.5a

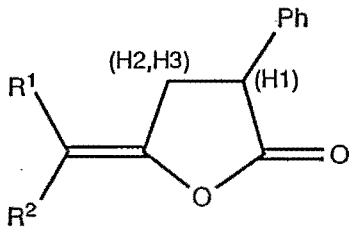

Compound	^{1}H NMR signals (H1)	(H2)	(H3)	Olefinic H
5.20: R^1 = Br, R^2= CO_2Et	4.08,dd,6.9,10.2	3.21,dd,6.9,18.7	3.63,dd,10.3,18.7	-
5.21: R^1= CO_2Et, R^2 = Br	4.15,dd,6.7,11.1	3.48,dd,6.7,19.1	3.95,dd,10.5,19.1	-
5.31: R^1= CO_2Et, R^2 = H	4.05,dd,6.3,10.5	3.49,ddd,2.3,6.3,16.8	3.92,ddd,2.1,10.5,16.8	5.79,t,2.1
5.35: R^1= CO_2Et, R^2 = CH_3	4.05,dd,6.4,10.2	3.45,ddq1.5,6.4,17.1	3.89,ddq,1.5,10.2,17.1	2.96,t,1.5
5.37: R^1= Br, R^2 = H	4.00,dd,7,9	3.20,ddd,1.5,9,17	3.60,ddd,1.5,9,17	6.02,d,2
5.38: R^1= Br, R^2 = CH_3	3.98,dd,7,10.0	3.18,ddq,2,7,17	3.58,ddq,2,10,17	2.34,m

Table 5.5b

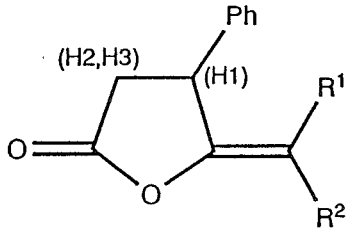

Compound	^{1}H NMR signals (H1)	(H2)	(H3)	Allylic H
5.22: R^1 = Br, R^2= CO_2Et	4.54,dd,3.0,10.1	2.73,dd,3.0,18.7	3.26,dd,10.1,18.7	-
5.23: R^1= CO_2Et, R^2 = Br	5.10,dd,2.3,10.1	2.75,dd,2.3,18.3	3.20,dd,10.0,18.5	-
5.32: R^1= CO_2Et, R^2 = H	5.06,ddd,1.8,2.7,10.1	2.67,dd,2.7,18.4	3.19,dd,10.1,18.4	5.81,d,1.8
5.36: R^1= CO_2Et, R^2 = CH_3	5.05,ddq,1.5,2.2,10.0	2.64,dd,2.2,18.2	3.22,dd,10.0,18.2	2.98,d,1.5
5.39: R^1= I, R^2 = H	4.33,ddd,2.0,3.4,10.5	2.69,dd,3.5,18.0	3.24,dd,10.5,18.0	6.00,d,2.0

olefinic proton. The ^{1}H NMR signal for the olefinic proton in **5.32** appeared as a doublet which indicates that it is allylically coupled to a single proton, (H1, Table 5.5b), thus the enol moiety is in the α-position. This coupling is also observed in the signal for H1 as well as the normal ABX coupling (H1 is further coupled by 1.8Hz to the olefinic proton). The olefinic proton resonance in **5.31** appeared as a triplet which indicates that it is coupled to two protons, (H2 and H3, Table 5.5a), thus the enol moiety is in the β-position. The coupling is also observed in the signals for H2 and H3, as apart from the normal ABX couplings, these are further coupled by 2.1Hz. The magnitude of the allylic coupling constants supports the assignment of *E*-stereochemistry to both enol lactones. A comparison of the ^{1}H NMR spectra of the known[5.1] compound **5.37** and α-*E*-methyl enol lactone **5.35** with the α-*E*-enol lactone **5.31** shows a very good agreement in the chemical shifts and coupling constants for the H2 and H3 protons, Table 5.5a. The ^{1}H NMR spectral data of the known[5.1] compound **5.39**, and β-*E*-methyl enol lactone **5.36** and β-*E*-enol lactone **5.32**, are also in very good agreement in terms of the chemical shift and coupling constants for the H1 proton, Table 5.5.

The assignment of the regio and stereochemistry of the bromo enol lactones **5.20**, **5.21**, **5.22**, and **5.23** was also achieved by comparison of the ^{1}H NMR data with that of known[5.1] compounds **5.37**, **5.38**, and **5.39** and the enol lactones **5.31** and **5.32**, Table 5.5a,b. The α-*E*-bromo enol lactone **5.20** and the known bromo enol lactones **5.37** and **5.38** gave almost identical chemical shifts and coupling constants for H1, H2, and H3. The α-*Z*-bromo enol lactone **5.21** has almost identical chemical shifts and coupling constants as the α-*E*-enol lactone **5.31** for H1, H2, and H3. The characteristic upfield shift of 0.55ppm for H1 of α-*Z*-bromo enol lactone **5.21** relative to the α-*E*-bromo enol lactone **5.20** supports the *E* assignment of configuration. The chemical shifts and coupling constants of H1, H2, and H3 in β-*E*-bromo enol lactone **5.22** and the known iodo enol lactone **5.39**,

are almost identical. Similar comparison can be made for the β-*Z*-bromo enol lactone **5.23** and the β-*E*-enol lactone **5.32**. The characteristic upfield shift of 0.27ppm and 0.32ppm is observed for H2, H3.

5.3.2: Regioselectivity of Ylide **0.1** Attack on Phenyl Succinic Anhydride **5.17**

The reaction of phenyl succinic anhydride with ylides **0.1** and **2.53** is not particularly regioselective. There is a slight preference for attack at the β-carbonyl as evidenced by α:β product ratios of 62:38, 60:40, and 74:26 for the acylphosphoranes **5.18** and **5.19**, enol lactones **5.31** and **5.32**, and methyl enol lactones **5.35** and **5.36**, respectively. This observation is consistent with the fact[5.5] that other monosubstituted succinic anhydrides tend to undergo reaction at both carbonyls, with some preference for β-attack. The reaction of methyl and *gem*-dimethyl succinic anhydrides with the ylide **0.1** gives 100% α-attack, while the reaction of methyl succinic anhydride with the methyl ester ylide **5.24** is reported by Kayser[5.6] *et al.* to give 57% α-attack. The reaction of phenyl succinic anhydride with the methyl ester ylide **5.24** has also been reported by Kayser[5.6] *et al.* to give 68% α-attack, opposite to the regioselectivity observed in our study (64% β-attack). The different products (see earlier discussion) and product ratios must be due to the different ylide **5.24** used in their studies Kayser[5.6] *et al.* heated the reagents under reflux in THF for 20 hours, whereas the initial study used $CHCl_3$ at reflux for 6 hours. The reaction of phenyl succinic anhydride and the ylide **0.1** in THF or $CDCl_3$ at reflux, under identical (to Kaysers study) and extended conditions gave predominantly β-attack (63-79%, Table 5.4, A+α, note β-attack produces the α-products). This is in contrast to the Kayser study and it is surprising

that the methyl ester ylide **5.24** behaves so differently to the ethyl ester ylide **0.1**.

The preference for β-attack is not consistent with the Bürgi-Dunitz hypothesis[5.2] as β-attack results in the reaction at the less hindered β-carbonyl via the most hindered pathway. Although the steric hindrance is only from an axial proton with a monosubstituted succinic ring, Figure 5.2. Alternatively, the result might support the alternative concerted [2+2] mechanism[2.22].

The formation of only *E*-enol lactones is consistent with previous[2.24] reactions of the ylide **0.1** and anhydrides. The results of the phenyl substituted examples are consistent with the theory[5.6] that the electron deficient carbonyl will lie over the electron rich phenyl ring promoting the *E*-stereoisomer, Figure 5.15.

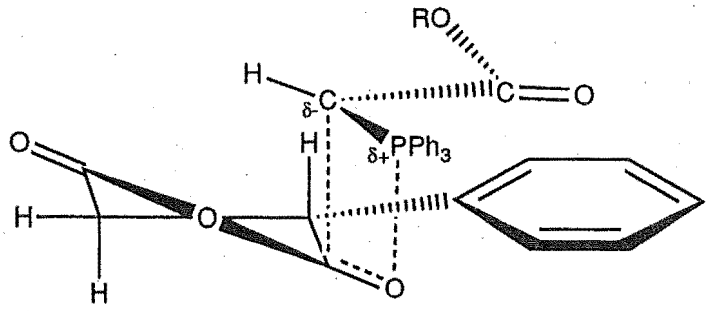

Figure 5.15

The preference for *E*-stereochemistry in the bromolactonisation reaction is evidenced in the formation of α-(*E*:*Z*) and β-(*E*:*Z*) bromo enol lactones in a ratio of 85:15 and 67:33, respectively. This suggests that the phenyl ring has little steric and electronic influence on the transition states, see Chapter 2 for a discussion of the bromolactonisation reaction. The effect of the phenyl group on the thermodynamic stability of the bromo enol lactones **5.20**, **5.21**, **5.22**, and **5.23** was determined by MM2 calculations.

Molecular mechanics[2.29] (MM2) calculations were carried out on the bromo enol lactones 5.20, 5.21, 5.22, and 5.23 in order to determine which is thermodynamically more stable. All structures were minimised with rotation of the four chain bonds and the ring system. The C7-C8 and C8-O10 bonds required 180° increments as C7 and C8 are sp^2 hybridised carbon atoms, O10-C11 was rotated in 60° increments, and C5-C13, or C4-C13 in 30° increments as it is a sp^2-sp^3 bond.

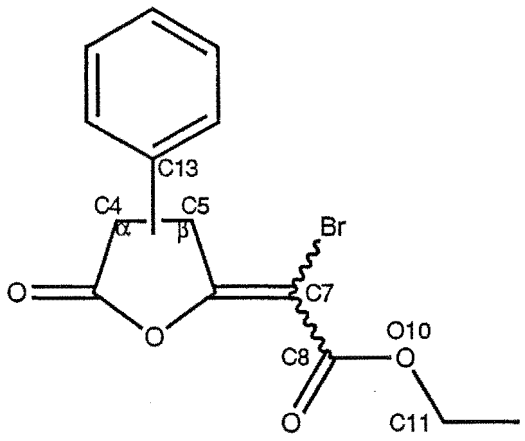

The energy minimisation of the α-*E*-structure **5.20** and α-*Z*-structure **5.21** produced 104 and 98 conformers, respectively, having energies within 3Kcal/mol of the minimum energy. Application of the Boltzman distribution at 25°C showed that the 10 lowest energy conformers for the α-*E*-structure **5.20** and α-*Z*-structure **5.21** accounted for 32.5% and 31.5% of the population and that the Boltzman average energy was 35.94Kcal/mol and 36.05Kcal/mol, respectively, Table 5.6. The energy minimisation of the β-*E*-structure **5.22** and β-*Z*-structure produced 36 and 65 conformers, respectively, having energies within 3Kcal/mol of the minimum energy. Application of the Boltzman distribution at 25°C in these cases revealed that the 10 lowest energy conformers for the β-*E*-structure **5.22** and β-*Z*-structure **5.23** accounted for 50.9% and 62.4% of the population and that

the Boltzman average energy was 35.60Kcal/mol and 34.55Kcal/mol, respectively, Table 5.6. The four lowest energy conformers for each structure are shown in Figures 5.16a-d. From the MM2 calculations it is apparent that there is little difference thermodynamically between all four isomers. However, the Boltzman average energies of the bromo enol lactone structures **5.20** and **5.21**, where the phenyl group is in the α-position, are opposite to the normal trend in the previously studied systems, although the difference in energies is slight. The *Z*-bromo enol lactone structure is thermodynamically more stable in the succinic and glutaric examples, see Chapters 2 and 3.

The bromo enol lactones **5.20** and **5.21** have a large number of conformers which reflects the free rotation of the ethyl ester and the phenyl ring. The bromo enol lactones **5.22** and **5.23** follow the normal trend of the *Z*-structure being the more thermodynamically stable, although again the difference in energies is slight. The β-bromo enol lactone structures have a smaller number of conformers which reflects the interaction of the ethyl ester and the phenyl ring and hence a decrease in bond rotation.

Table 5.6: MM2 Energy Minimisations on Phenyl Succinic Bromo Enol Lactones 5.20, 5.21, 5.22, and 5.23.

System	Conformer%	Energy (Kcal/mol)	Boltzman average Energy (Kcal/mol)
PsαE **5.20**			
	1 = 4.24%	35.311	35.94
	2 = 4.03%	35.341	
	3 = 3.88%	35.364	
	4 = 3.77%	35.381	
	5 = 3.61%	35.406	
	6 = 2.62%	35.598	
	7 = 2.62%	35.599	
	8 = 2.60%	35.602	
	9 = 2.57%	35.609	
	10 = 2.54%	35.616	
PsαZ **5.21**			
	1 = 5.93%	35.364	36.05
	2 = 3.14%	35.744	
	3 = 3.04%	35.762	
	4 = 2.95%	35.781	
	5 = 2.84%	35.803	
	6 = 2.78%	35.817	
	7 = 2.78%	35.817	
	8 = 2.72%	35.829	
	9 = 2.70%	35.834	
	10 = 2.64%	35.847	
PsβE **5.22**			
	1 = 6.93%	35.181	35.60
	2 = 6.87%	35.186	
	3 = 6.06%	35.261	
	4 = 5.95%	35.272	
	5 = 4.37%	35.456	
	6 = 4.32%	35.463	
	7 = 4.28%	35.468	
	8 = 4.05%	35.502	
	9 = 4.04%	35.503	
	10 = 4.01%	35.508	
PsβZ **5.23**			
	1 = 8.03%	34.071	34.55
	2 = 7.94%	34.078	
	3 = 7.94%	34.078	
	4 = 7.49%	34.113	
	5 = 6.56%	34.192	
	6 = 5.66%	34.280	
	7 = 5.64%	34.282	
	8 = 5.45%	34.303	
	9 = 4.56%	34.409	
	10 = 3.16%	34.628	

Figure 5.16a: Four Lowest Energy Conformers of 5.20.

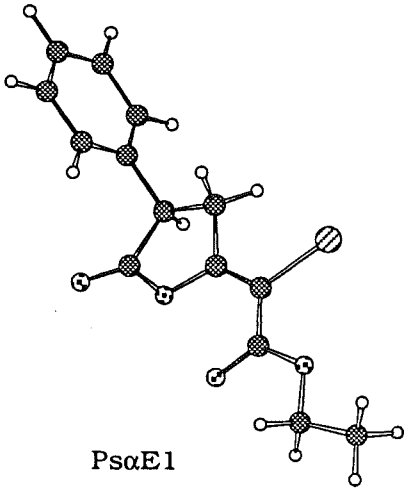

PsαE1

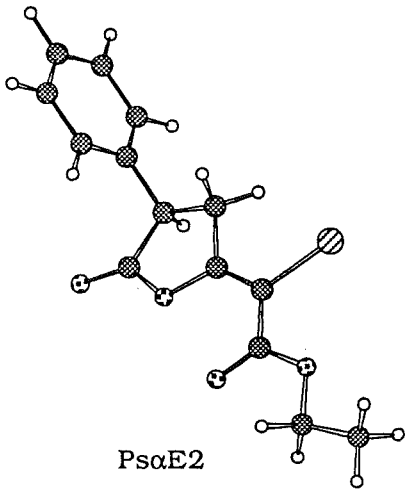

PsαE2

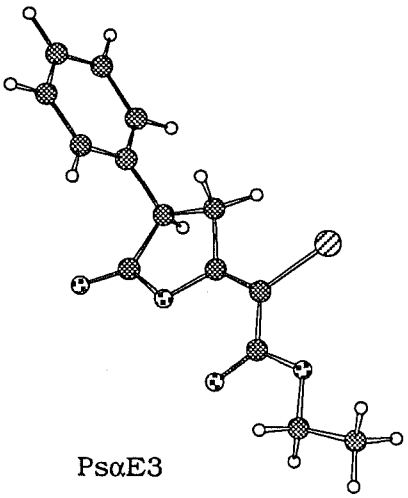

PsαE3

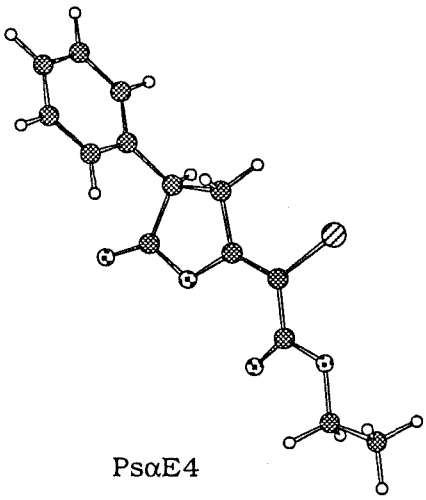

PsαE4

Figure 5.16b: Four Lowest Energy Conformers of 5.21.

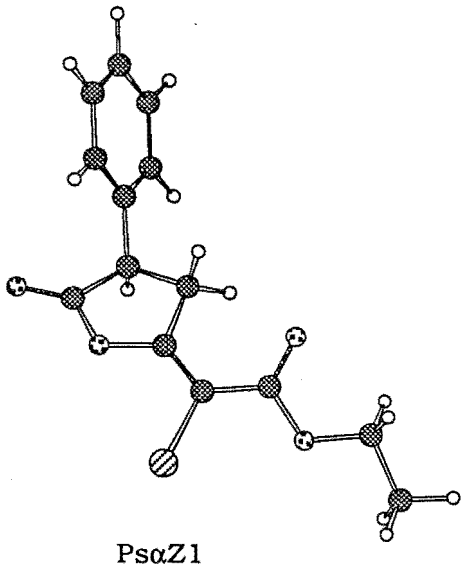

PsαZ1

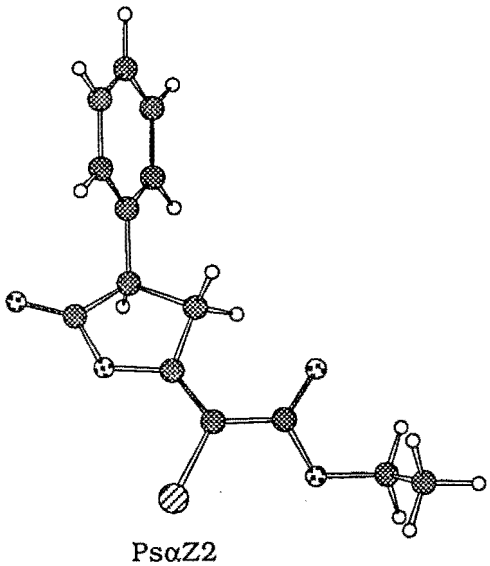

PsαZ2

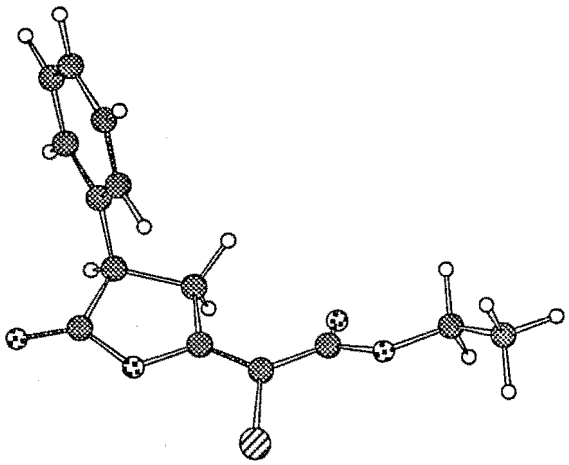

PsαZ3

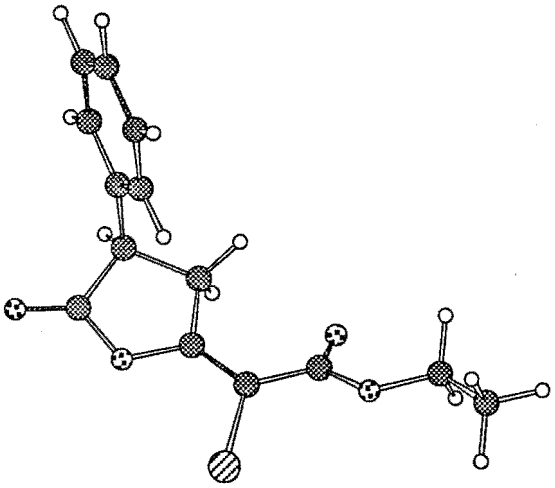

PsαZ4

Figure 5.16c: Four Lowest Energy Conformers of 5.22.

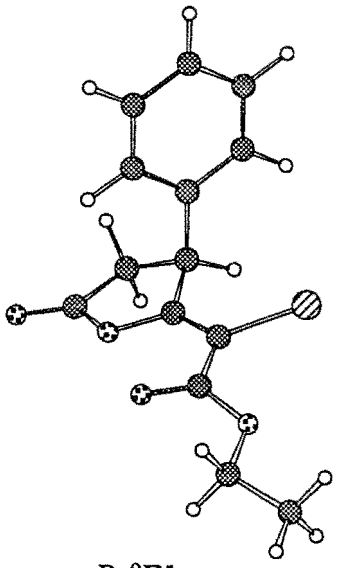

PsβE1

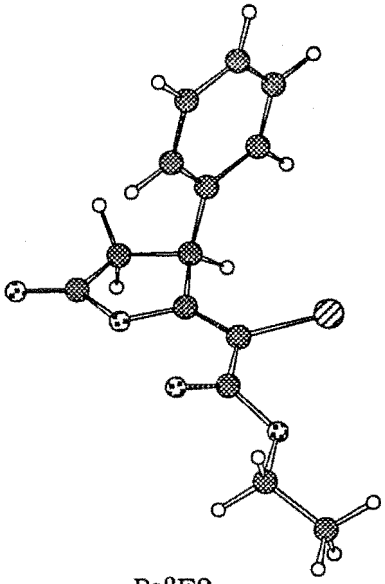

PsβE2

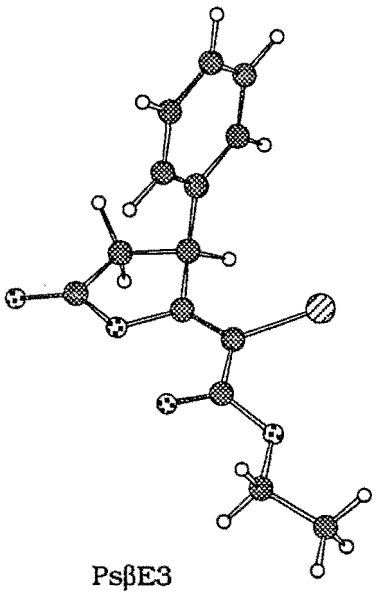

PsβE3

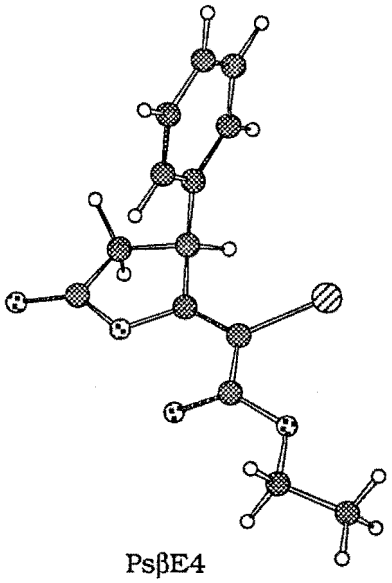

PsβE4

Figure 5.16d: Four Lowest Energy Conformers of 5.23.

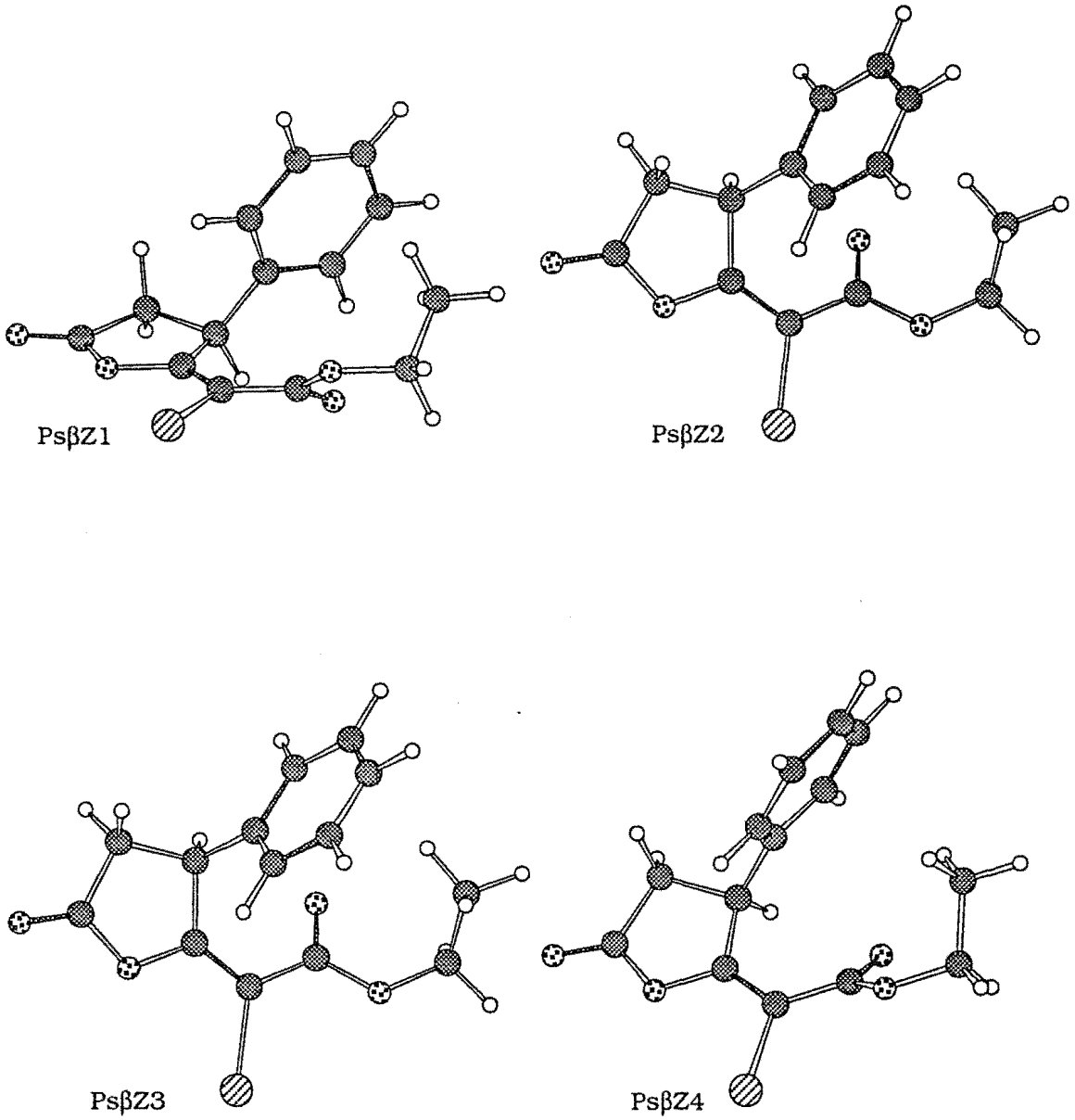

5.4 Amino Acid Analogues Containing a Natural Amino Acid

Mechanism-based inactivators usually mimic the natural amino acid substrate of the enzyme (see 5.1: Introduction). With this in mind, the inclusion of the amine functionality in halo enol lactones has been reported[5.1]. The racemic five-membered halo enol lactones **5.40**, **5.41**, and **5.42** were synthesised[5.1] using the halolactonisation of a substituted acetylenic acids in 5, 5, and 8 steps and in 18.8%, 33.7%, and 18% yields respectively (Schemes 5.5a, 5.5b, and 5.6).

Interestingly, the activity of the halo enol lactones **5.40**, **5.41**, and **5.42** as mechanism-based inactivators of chymotrypsin was less[5.1] than that for simple halo enol lactones **5.1** and **5.2**. However, the halo enol lactones **5.40**, **5.41**, and **5.42** would be expected to have greater specificity for chymotrypsin. As the halo enol lactones **5.40**, **5.41**, and **5.42** were racemic mixtures when tested, a partial explanation for the reduced activity is that enzymes are highly sensitive to the chirality of the substrate. However, other factors for example, the positioning of the scissile peptide bond, may contribute to the low activity. The bromolactonisation reaction allows the required retention of chirality by using a natural amino acid as a starting material.

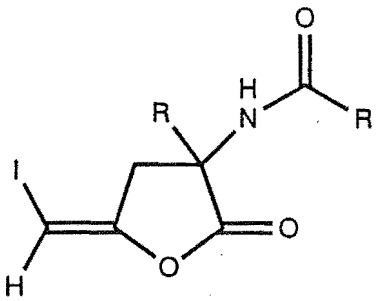

	R	R'	Yield*
5.40	H	Ph	67
5.41	Ph	Ph	60
5.42a	$PhCH_2$	CH_3	52
5.42b	$PhCH_2$	$.CF_3CO_2H$	59

*from the corresponding acetylenic acid

Scheme 5.5a:

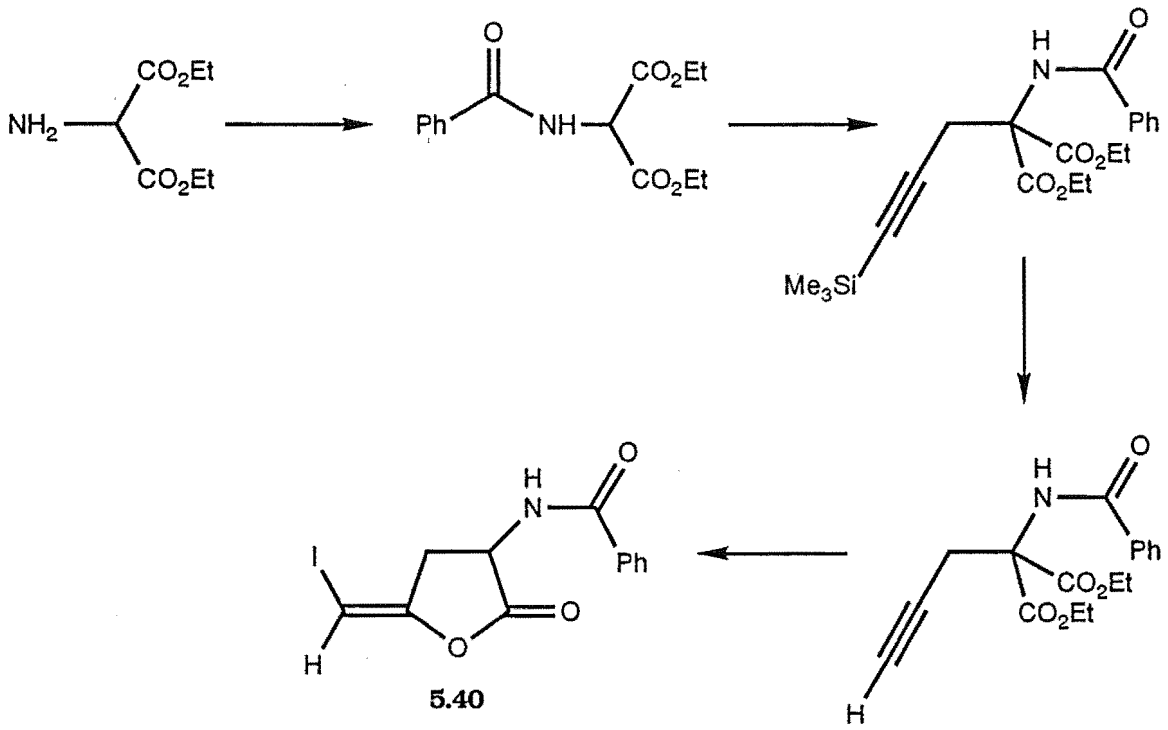

Scheme 5.5b:

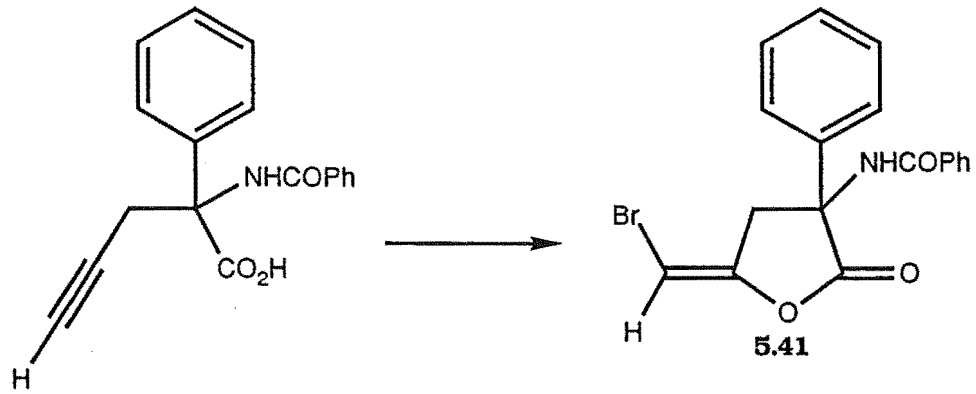

Scheme 5.6

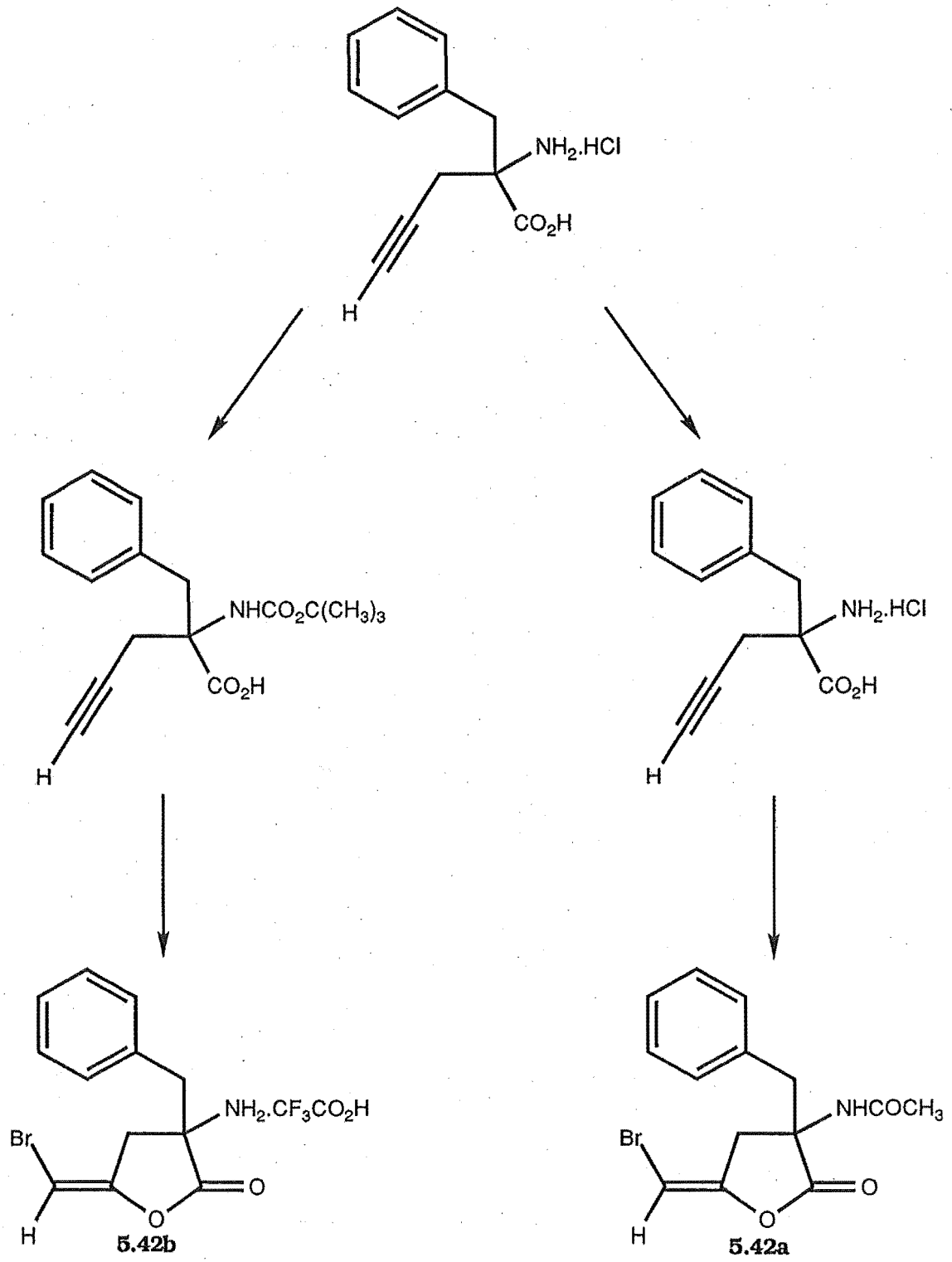

5.4.1 N-Acetyl Aspartic Bromo Enol Lactones

The bifunctional nature of amino acids often requires syntheses to be performed in a specific order using suitable protecting groups. The

protecting group, as the name implies, blocks the reaction at either the amino or acid moiety, while the desired reaction occurs at the unprotected centre. Ideally the protecting group should be easily added, inert to the further reactions, and easily removed in such a way that the unprotected product is uneffected by the removal conditions. Acyl based protecting groups for the amino moiety of amino acids are important since the new amide bond mimics the normal peptide bond in a polypeptide substrate. The simplest acyl protecting group is the acetyl group. Acetyl protecting groups are not suitable for lactone containing molecules since the protected bromo enol lactones would not survive the basic catalysed removal conditions. However, it is a convenient group in that anhydrides can be synthesised by dehydration of a diacid using the same reagents, for example acetic anhydride or acetyl chloride, that will acetylate the primary amine group.

L-Aspartic acid **5.43** is an ideal starting material as the natural chirality and the recognition features of the amine moiety are present. The α-bromo enol lactones derived from L-aspartic acid would include the natural amine recognition feature, Figure 5.17. As L-aspartic acid is asymmetric the entry into β-bromo enol lactones is possible.

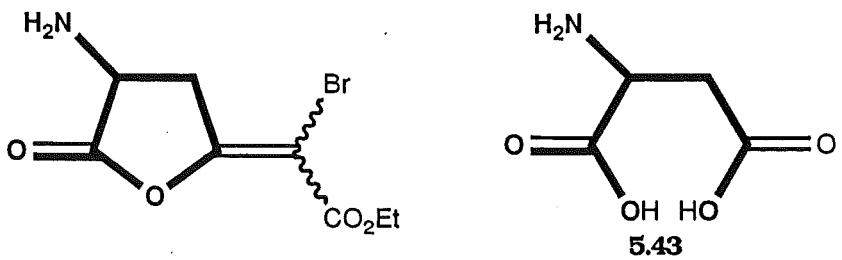

5.43

Figure 5.17

The Wittig Anhydride Olefination approach required an anhydride. The reaction of L-aspartic acid with acetic anhydride or acetyl chloride did

not form N-acetyl aspartic anhydride **5.48**. However, the more reactive trifluoroacetic anhydride readily reacted with aspartic acid to form N-trifluoroacetyl L-aspartic anhydride[5.11]. The reactions of N-trifluoroacetyl L-aspartic anhydride with the ylide Ph_3PCHCO_2Et **0.1** did not yield the desired phosphoranes (see Chapters 2, 3, and 4) probably due to the presence of the reactive trifluoroacetyl amide that leads to undesired alternative reactions.

The more stable N-acetyl L-aspartic anhydride **5.48** was, however, finally synthesised[5.12] by acylation the HBr salt of L-aspartic anhydride with acetic anhydride. The reaction of N-acetyl aspartic anhydride and ylide **0.1**, in $CDCl_3$, formed the two phosphoranes **5.49** and **5.50** in a ratio of 80:20, Scheme 5.7. The reaction was conveniently followed by ^1H NMR spectroscopy and it was found that the phosphorans **5.49** and **5.50** built up to a maximum of 80% after 90 minutes. $CHCl_3$ at reflux for 48 hours then gave the α- and β-hydrogen enol lactones **5.51** and **5.52** in a ratio of 58:42, Scheme 5.8. Purification by radial chromatography and gave a total yield of 68%.

The bromolactonisation reaction relies on the acylphosphorane as the starting material. Unfortunately the separation of the acylphosphoranes from the starting materials by chromatography was unsuccessful. The bromolactonistion reaction on the mixture of starting material and acylphosphoranes would theoretically give all four isomers **5.44**, **5.45**, **5.46**, and **5.47**, Scheme 5.7. There is also the added problem that amino acids have been reported[5.13] to be brominated in the α-position under similar brominating conditions. The phosphoranes **5.49** and **5.50** did however appear to form bromo enol lactones **5.44**, **5.45**, **5.46**, and **5.47**, under bromolactonisation conditions. The phosphoranes **5.49** and **5.50** were allowed to build up to a total maximum of 20% from the reaction of N-acetyl aspartic anhydride and ylide **0.1**, at room temperature (2 hours), in $CHCl_3$. The solution was then cooled to 0°C and treated with

Scheme 5.7: Reaction of N-Acetyl Aspartic Anhydride with Ylide 0.1

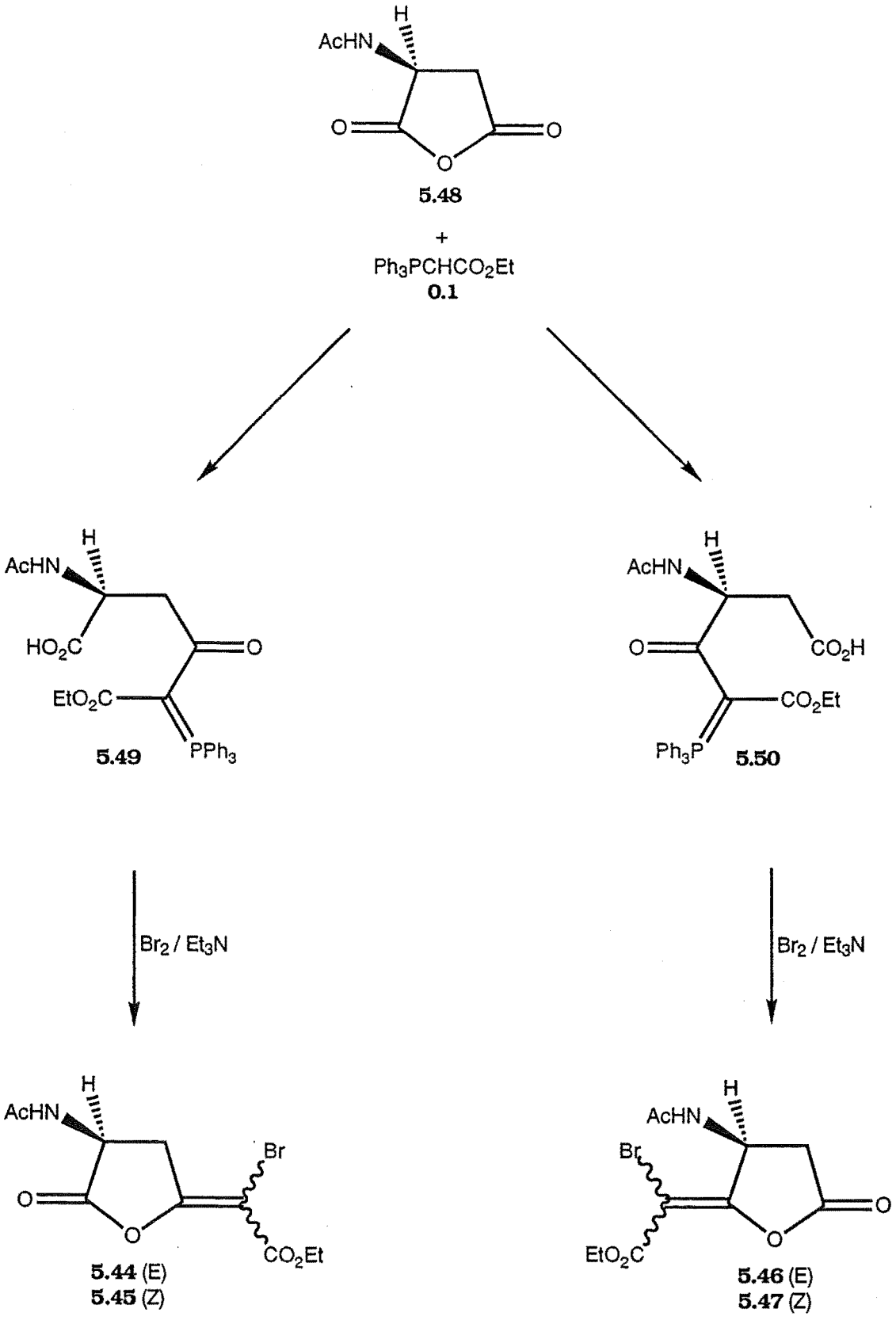

one equivalent of triethylamine and one equivalent of bromine. Immediate decolourisation of the bromine was observed. The stirred solution was allowed to warm to room temperature after 30 minutes. Attempts to purify the bromo enol lactone products by radial chromatography were unsuccessful. The ^{1}H NMR spectrum of the crude product mixture did suggest that bromo enol lactones had formed. In particular, a group of quartets at 4.1-4.28ppm and triplets at 1.15-1.3ppm, characteristic of bromo enol lactones were evident.

The methyl enol lactones **5.53** and **5.54** were synthesised to aid in structure assignment, Scheme 5.8. Reaction of N-acetyl aspartic anhydride **5.48** and methyl ylide **2.53** gave the α- and β-methyl enol lactones **5.53** and **5.54** in a ratio of 64:36, respectively, (53% yield after chromatography).

5.4.1.1:Structure Assignment and MM2 Calculations of Enol Lactones **5.51** and **5.52**, Methyl Enol Lactones **5.53** and **5.54**

The configuration of the methyl enol lactones **5.53** and **5.54** were assigned on the basis of the multiliplicity of the homoallylic coupling between methyl protons and H1, H2, and H3. The regioisomerism is clearly indicated by the multiplicity of the vinyl methyl signal, a triplet (2.0Hz) and a doublet (1.0Hz) for the α and β-enol lactones **5.53** and **5.54**, respectively. Homoallylic coupling is observed in **5.53** by an increased multiplicity of H2 and H3. The H3 chemical shift for the α-*E*-enol lactone **5.51** is identical to that of the similar known[5.1] compound **5.55**, Table 5.7 (again due to deshielding by the ethyl ester in **5.57**). The chemical shift of H2 in **5.51** is very similar to that of H2 in **5.53** and close to H2 of N-acetyl aspartic anhydride **5.48** itself, Table 5.7a. The chemical shift of H3 shows the characteristic downfield shift of 0.5ppm (with respect to N-acetyl

Scheme 5.8: N-Acetyl Aspartic Anhydride Reaction with Ylides 0.1 and 2.53

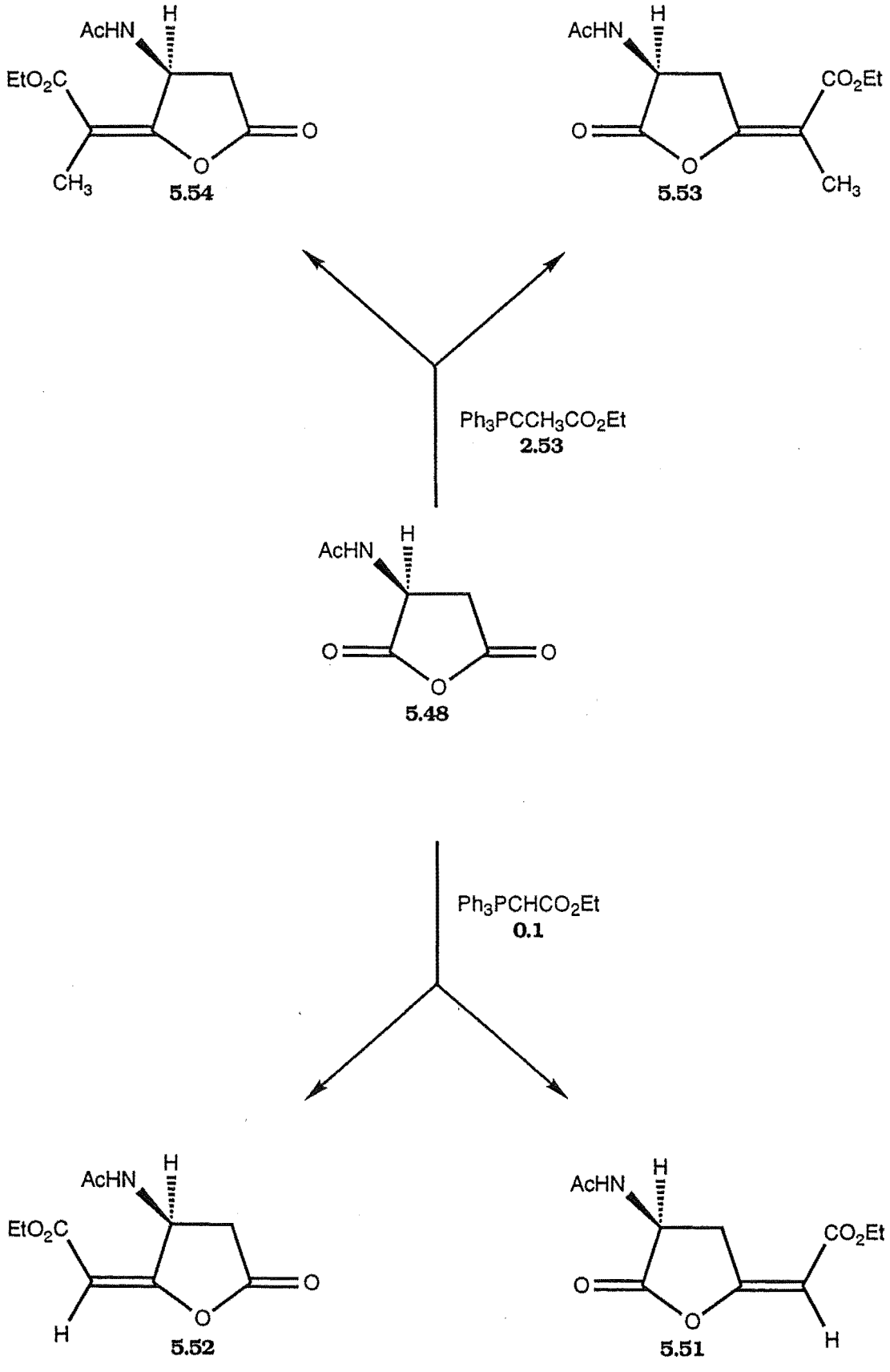

Table 5.7a

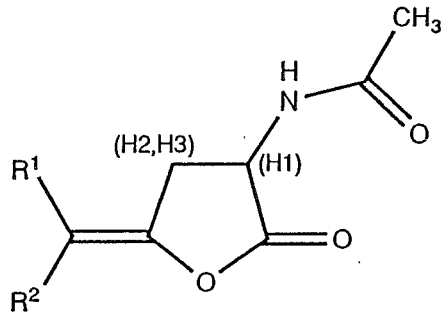

Compound	^{1}H NMR signals (H1)	(H2)	(H3)	Olefinic H	(NH)
5.51: R ^{1}= CO_2Et, R^2 = H	4.80,dd,6.7,10.5	3.22,ddd,2.1,6.7,19.2	3.76,ddd,2.0,10.5,19.3	5.76,t,1.9	no
5.53: R ^{1}= CO_2Et, R^2 = CH_3	4.78,dd,6.9,10.1	3.19,dd,q,2.1,6.7,18.7	3.74,ddq,1.9,10.8,18.9	1.95,t,2.0	7.0,bs
5.55: *R ^{1}= I, R^2 = H	4.78,m	3.15,m		5.90,t,2.0	nr
5.48: Acasp anhydride	5.14,dd,6.4,10.1	2.98,dd,6.4,18.6	3.24,dd,10.1,18.5	-	6.47

*Phenacyl amide, nr = none reported,no = none observed

Table 5.7b

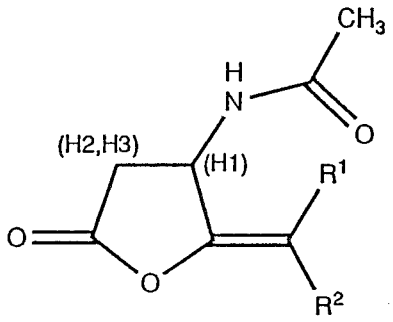

Compound	^{1}H NMR signals (H1)	(H2)	(H3)	Olefinic H	(NH)
5.52: R ^{1}= CO_2Et, R^2 = H	5.62,ddd,1.6,3.1,10.7	2.67,dd,3.2,18.2	3.07dd,10.5,18.4	5.69,d,1.8	no
5.54: R ^{1}= CO_2Et, R^2 = CH_3	4.99,m	2.93,bd,10.2		1.93,d,1.0	6.5,bs

aspartic anhydride and **5.48**) due to the deshielding effect of the ethyl ester when it is *trans* to the lactone oxygen. The chemical shifts of H2 and H3 in the β-enol lactone **5.52** compare quite well with H2 in N-acetyl aspartic anhydride **5.48**. The unresolved ABq for **5.54** is characteristic of β-enol lactones, Table 5.7b. The α and β-enol lactones **5.51** and **5.52** were assigned on the basis of the enol olefinic coupling, a triplet (2.0Hz) for the α-enol lactone **5.51**, and a doublet (1.8Hz) for the β-enol lactone **5.52**. The signals for H1, H2, and H3 are consistent with the methyl enol lactones **5.53** and **5.54**.

Hydrogen bonding is possible between the N-H and the ester carbonyl oxygen in the β–enol lactone **5.52**, Figure 5.19. Similar hydrogen bonding may preferentially stabilise the transition state produced on reaction at the α-carbonyl, Figure 5.19. This hydrogen bonding may also influence the stereochemical preference of the *E*- and *Z*-bromo enol lactones, Figure 5.19.

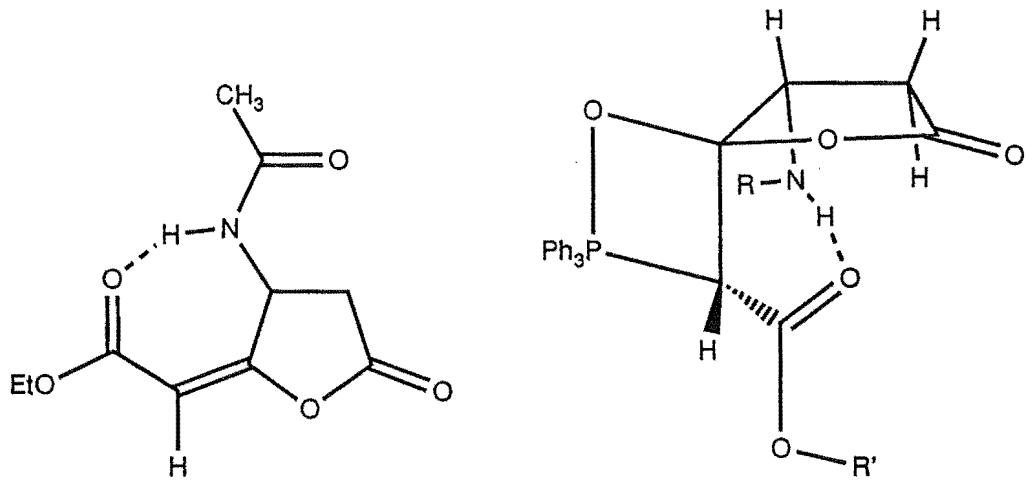

Figure 5.19

Molecular mechanics[2.29] (MM2) calculations were carried out on the isomeric bromo enol lactones **5.46** and **5.47** in order to determine which

is thermodynamically more stable and to examine the possibility of hydrogen bonding between the amide proton and the carbonyl of the ester in the *Z*-bromo enol lactone **5.47**. The *E*- and *Z*-isomers, **5.46** and **5.47**, respectively, were minimised with rotation of the five chain bonds and the ring system. The C7-C8, C8-O10 and N13-C14 bonds required 180° increments as C7, C8 and C14 are sp^2 hybridised carbon atoms, O10-C11 was rotated in 60° increments. The C5-N13 bond required 30° increments as it is a sp^2-sp^3 bond, Figure 5.20.

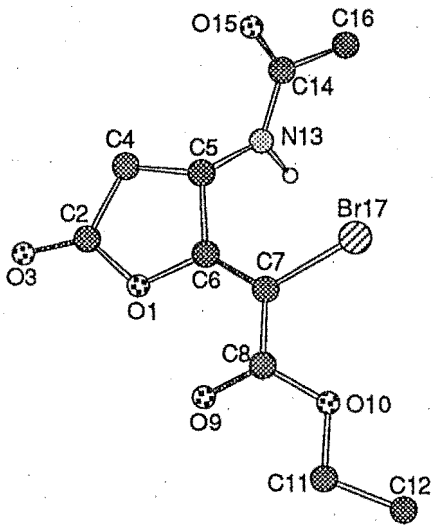

Figure 5.20

The energy minimisation of the *E*-structure produced 78 conformers having energies within 3Kcal/mol of the minimum energy. Application of the Boltzman distribution at 25°C showed that the 10 lowest energy isomers accounted for 45.0% of the population and that the Boltzman average energy was 20.91Kcal/mol. The energy minimisation of the *Z*-structure produced 22 conformers having energies within 3Kcal/mol of the minimum energy. Application of the Boltzman distribution at 25°C in this case revealed that the 8 lowest energy conformers accounted for 95.5% of the population and that the Boltzman average energy was 18.94Kcal/mol, Table

5.8. The four lowest energy conformers for the bromo enol lactones **5.36** and **5.37** are given in Figures 5.21a-b. The smaller number of conformers of the *Z*-structure compared to the *E*-structure is an indication of the limitation of free rotation due to the interaction between the ethyl ester

Figure 5.21a: Four Lowest Energy Conformers of 5.46.

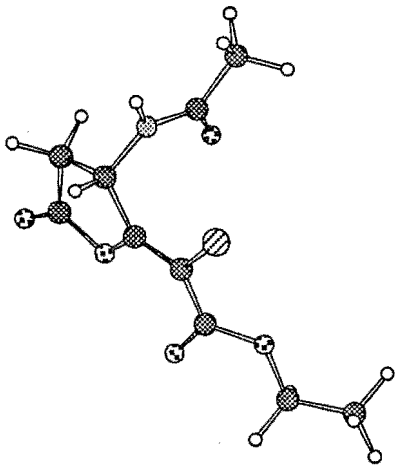

AcAspEBrEL1

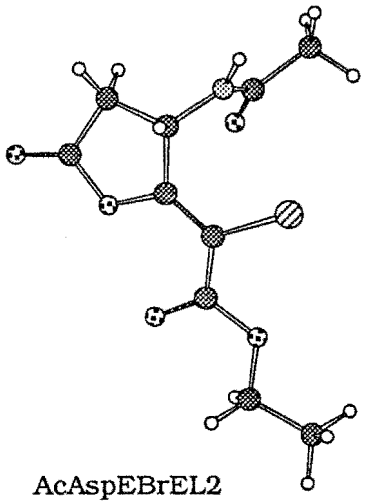

AcAspEBrEL2

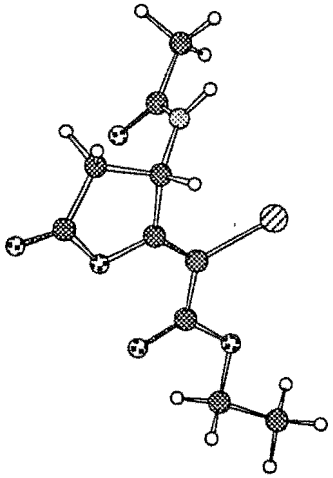

AcAspEBrEL3

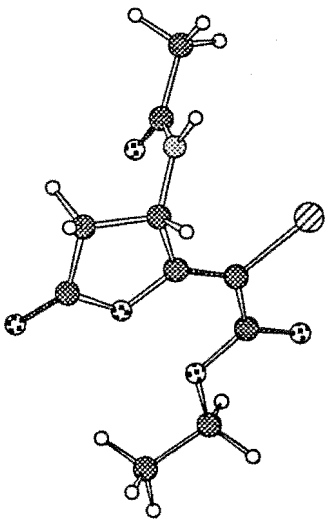

AcAspEBrEL4

Figure 5.21b: Five Lowest Energy Conformers of 5.47.

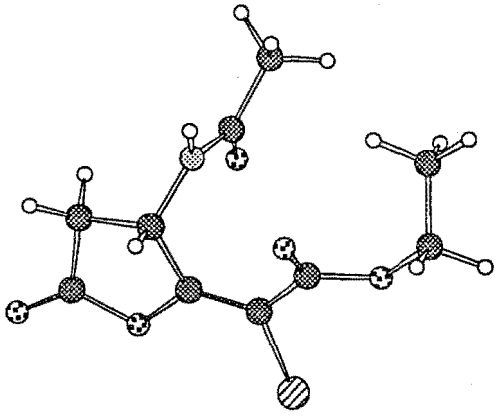

AcAspZBrEL1

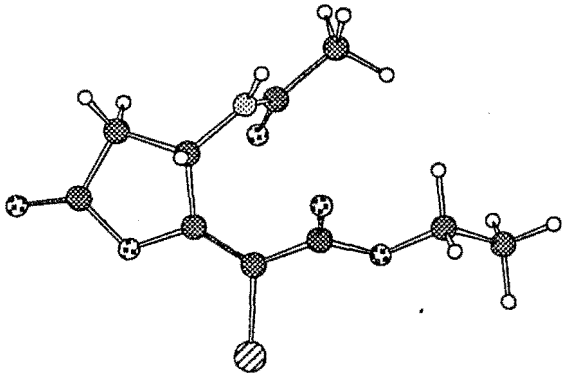

AcAspZBrEL2

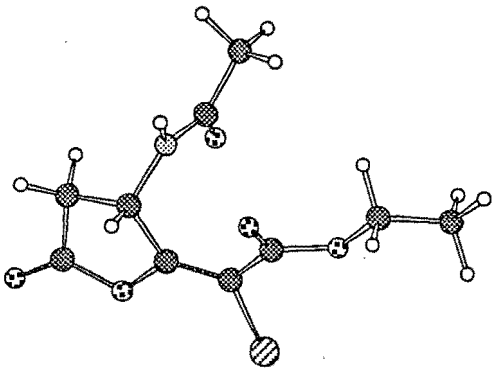

AcAspZBrEL3

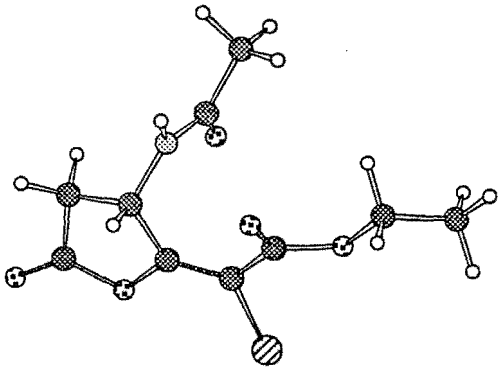

AcAspZBrEL4

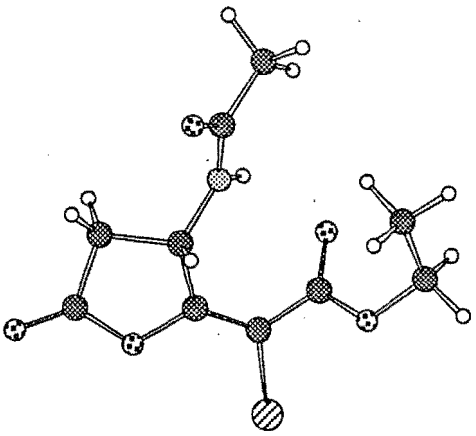

AcAspZBrEL5

Table 5.8: MM2 Energy Minimisations on N-acetyl Aspartic Bromo Enol Lactones 5.36 and 5.37

System	Conformer Population	Energy (Kcal/mol)	Boltzman average Energy (Kcal/mol)	Distance of N13-O9 (Å)
AcAspE-BrEL **5.36**				
	1 = 6.19%	20.389	20.91	
	2 = 5.03%	20.513		
	3 = 4.46%	20.585		
	4 = 4.01%	20.648		
	5 = 3.85%	20.673		
	6 = 3.82%	20.676		
	7 = 3.74%	20.689		
	8 = 3.63%	20.708		
	9 = 3.55%	20.721		
	10 = 3.42%	20.743		
	11 = 3.26%	20.772		
AcAspZ-BrEL **5.37**				
	1 = 29.46%	18.539	18.94	2.670
	2 = 26.56%	18.601		2.705
	3 = 17.47%	18.851		2.650
	4 = 10.99%	19.127		2.626
	5 = 5.12%	19.583		2.570
	6 = 2.65%	19.976		2.534
	7 = 2.07%	20.122		2.577
	8 = 1.21%	20.443		2.587

and the amide moiety. The N13 to O9 separation is well within the limits[1.14] of hydrogen bonding in all the major conformers of **5.37**. However, on close examination of the major conformers, none have the amine proton in the correct orientation for hydrogen bonding. The less thermodynamically stable *E*-isomer **5.51** is produced in the reaction of N-acetyl aspartic anhydride **5.48** and ylide **0.1**. The *Z*-isomer is thermodynamically more stable as was the case in the succinic series (see Chapter 2). This is inspite of the ethyl ester orientation in the *Z*-isomer being opposite in the hydrogen and bromo enol lactones due to a change in substituent priority.

5.4.1.2: Regioselectivity of the Reaction of N-Acetyl Aspartic Anhydride with Ylides **0.1** and **2.53**

The regioselectivity displayed on reaction of N-acetyl aspartic anhydride **5.48** with ylides **0.1** and **2.53** is similar to the corresponding reactions with phenyl succinic anhydride **5.17**. The major attack occurs at the unhindered β-carbonyl (the most hindered pathway across the ring) to give the α-N-acetyl aspartic enol lactone **5.51** and N-acetyl aspartic methyl enol lactone **5.53**. The observations made in the phenyl succinic example, Section 5.3.3, are also relevant to the N-acetyl aspartic example. The disagreement with the Bürgi-Dunitz hypothesis[5.2] represents a further example of monosubstituted succinic anhydrides showing little regioselectivity. The slight regioselectivity of the reactions of N-acetyl aspartic anhydride with the ylides **0.1** and **2.53** ((58:42) and (64:36) respectively) would suggest that the substituent has little effect on the reaction. From the regioselectivity and the results of the MM2 calculations, there is no apparent effect of hydrogen bonding to the substituent contributing to the reaction mechanism.

5.4.2 Cbz-Aspartic Bromo Enol Lactones

The synthesis of N-acetyl aspartic bromo enol lactones via the bromolactonisation reaction of the phosphoranes discussed in the previous section gave problems with regiocontrol and modest yields. A different protecting group was used to determine if the protecting group contributed to these problems. Also, an alternative protecting group was required for the final deprotection of the amine group. A variety of protecting groups are available[5.14]. One of the most widely used for amine protection was the t-butyloxycarbonyl or Boc group[5.15]. When considering

the Boc group as a protecting group it was important to bear in mind the future goals of this reseach.

Future work on the synthesis of bromo enol lactones as mechanism-based inactivators by this research group will attempt to incorporate more substrate recognition features into these molecules. One way to do this is to extend the molecule with peptide chains (Figure 5.22, A, B, or C).

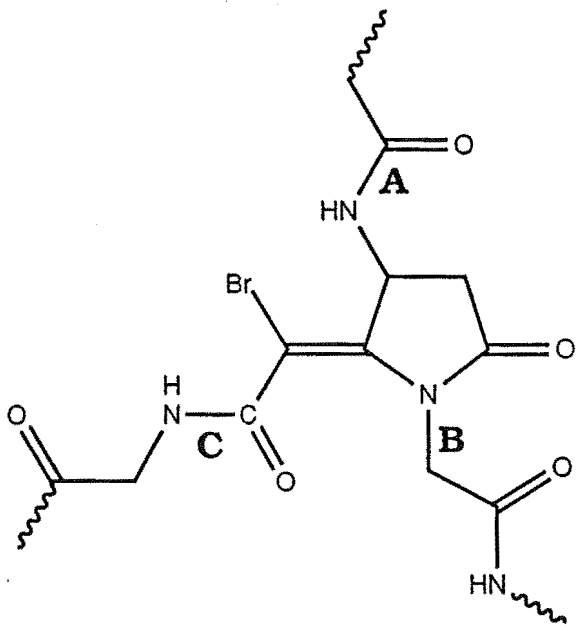

Figure 5.22: Possible Ways of Increasing the Recognition Features of Bromo Enol Lactones. Peptides chain from the amine substituent (A chain); replacement of the lactone oxygen to form a bromo enol lactam and form a peptide chain (B chain); peptide chain from the carbonyl of the ester (C chain).

The extension of a peptide chain from the ester carbonyl (Option C, Figure 5.22) requires the carboxyl group of the ylide to be suitably protected. The protecting group would be removed after the formation of the enol or bromo enol lactone or at the intermediate phosphorane level. This research group has established[5.16] that the t-butyl ester stabilised phosphorane **5.55** reacts similarly to the ethyl ester stabilised phosphorane **2.22** in the formation of enol and halo enol lactones. The t-butyl group is removed under mild acid conditions without the hydrolysis of the enol lactone. The free acid can then be coupled to a peptide chain.

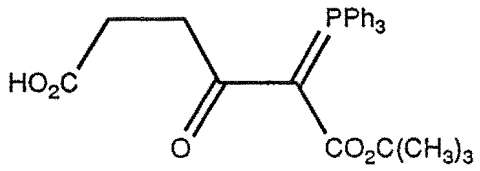

5.55

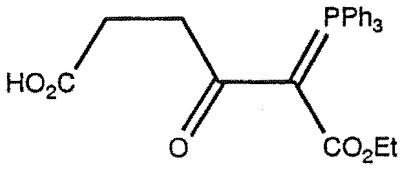

2.22

However, if the amine at position A (Figure 5.22) is protected by a Boc group, the conditions for hydrolysis of the t-butyl ester would also remove the Boc group. The benzyloxycarbonyl[5.17] (Cbz or Z) group is a widely used protecting group. The Cbz group is stable in both mild acid and base and is removed either by catalytic hydrogenation or HBr in acetic acid.

Cbz protected aspartic acid **5.56** is available commercially[5.18] and forms the Cbz-aspartic anhydride **5.57** quantitatively when treated with acetic anhydride at reflux for 4 hours. The reaction of the ylide **0.1** with Cbz-aspartic anhydride was expected to be similar to the reaction with N-acetyl aspartic anhydride. The two phosphoranes **5.58** and **5.59** would enable entry into the synthesis of bromo enol lactones **5.60**, **5.61**, **5.62**, and **5.63**. However, in contrast to the N-acetyl example significant regioselectivity was observed on reaction with ylides **0.1** and **2.53**.

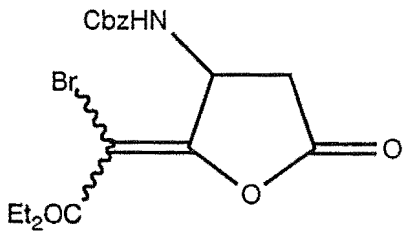

5.60(*E*), 5.61(*Z*)

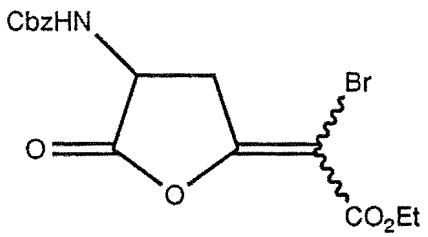

5.62(*E*) , 5.63(*Z*)

The reaction of Cbz-aspartic anhydride **5.57** and ylide **0.1** gave a single phosphorane **5.58** at room temperature in $CDCl_3$, Scheme 5.9. The reaction in $CDCl_3$ was followed by ^1H NMR spectroscopy and it was found

Scheme 5.9: Reaction of N-Cbz-Aspartic Anhydride with Ylide 0.1

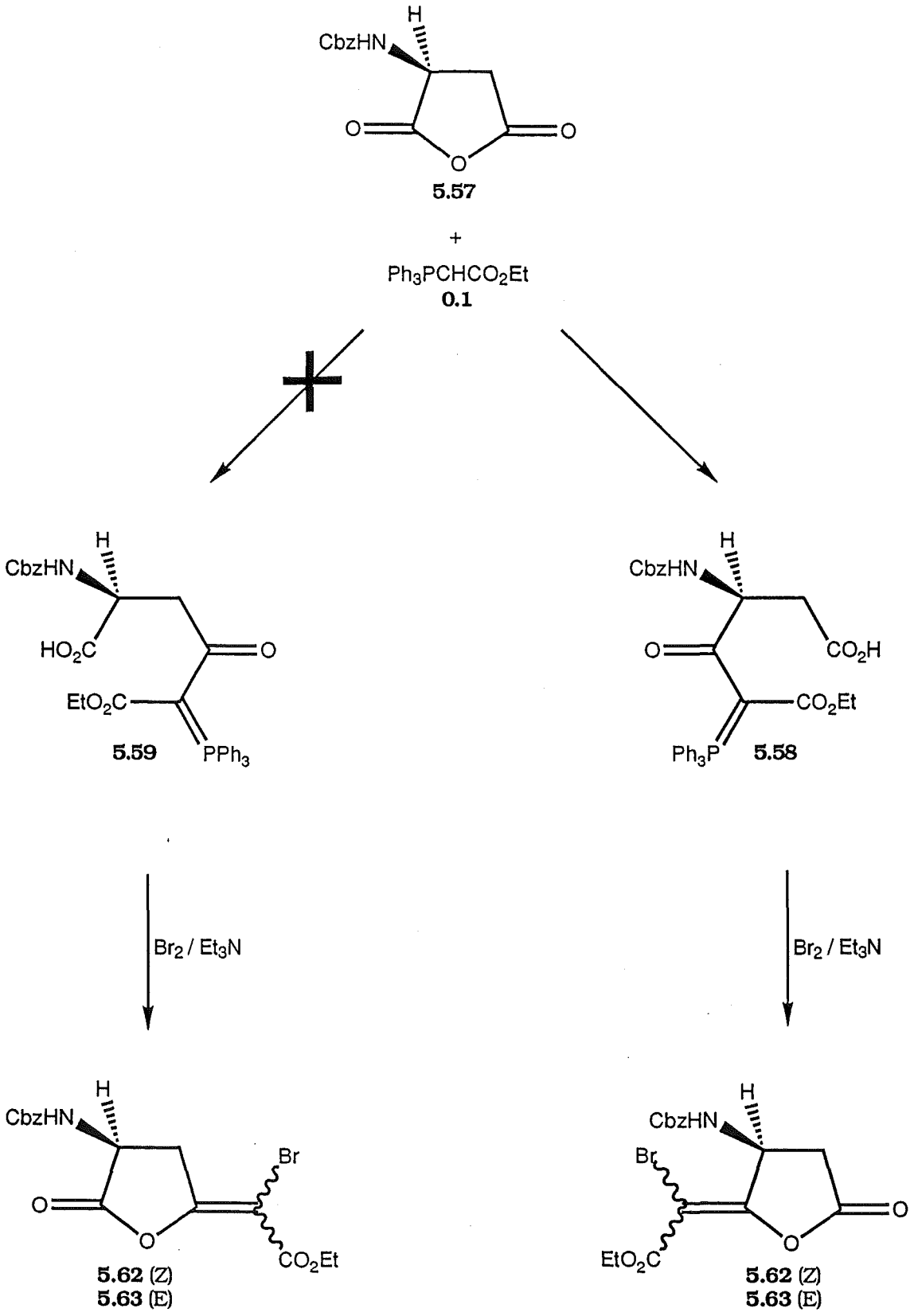

that the level of phosphorane **5.58** increased to a maximum of 66% after 70 minutes. The enol lactone **5.64** also formed at room temperature, 2% after 80 minutes. The phosphorane **5.58**, in $CHCl_3$ at reflux for 24 hours, gave a single enol lactone product **5.64** (79% yield after chromatography), Scheme 5.10.

The Cbz-aspartic methyl enol lactone **5.65** was synthesised to examine the regioselectivity of the reaction and for characterisation purposes, Scheme 5.10. The reaction of Cbz-aspartic anhydride and ylide **2.53** also gave a single methyl enol lactone **5.65** after 24 hours at room temperature in $CDCl_3$. The product methyl enol lactone **5.65** was purified by radial chromatography in a yield of 82%.

The phosphorane **5.58** gave the bromo enol lactones **5.60** and **5.61** under the bromolactonisation conditions. The phosphorane **5.58** was allowed to build up to 66% (by ^1H NMR spectroscopy) from the reaction of Cbz-aspartic anhydride and ylide **0.1**, at room temperature (70 minutes), in $CHCl_3$. The solution was then cooled to -78°C and treated under the now familiar bromolactonisation conditions. The solvent was removed under reduced pressure and the bromo enol lactones **5.60** and **5.61** were purified by radial chromatography in a total yield of 51% (77% based on the acylphosphorane).

5.4.2.1 Structure Assignment of Enol Lactone **5.64** and Methyl Enol Lactone **5.65**

The ^1H NMR spectrum of the methyl enol lactone **5.65** was fully assigned by comparison with previous compounds. The ^1H NMR chemical shifts and coupling patterns for H1, H2, and H3 resonances are almost identical to **5.54** (Table 5.7b). The *E*-stereoisomer is assumed as there are no examples of the methyl ylide **2.53** reacting with an anhydride to give a

Scheme 5.10: CBz-Aspartic Anhydride Reaction with Ylides 0.1 and 2.53

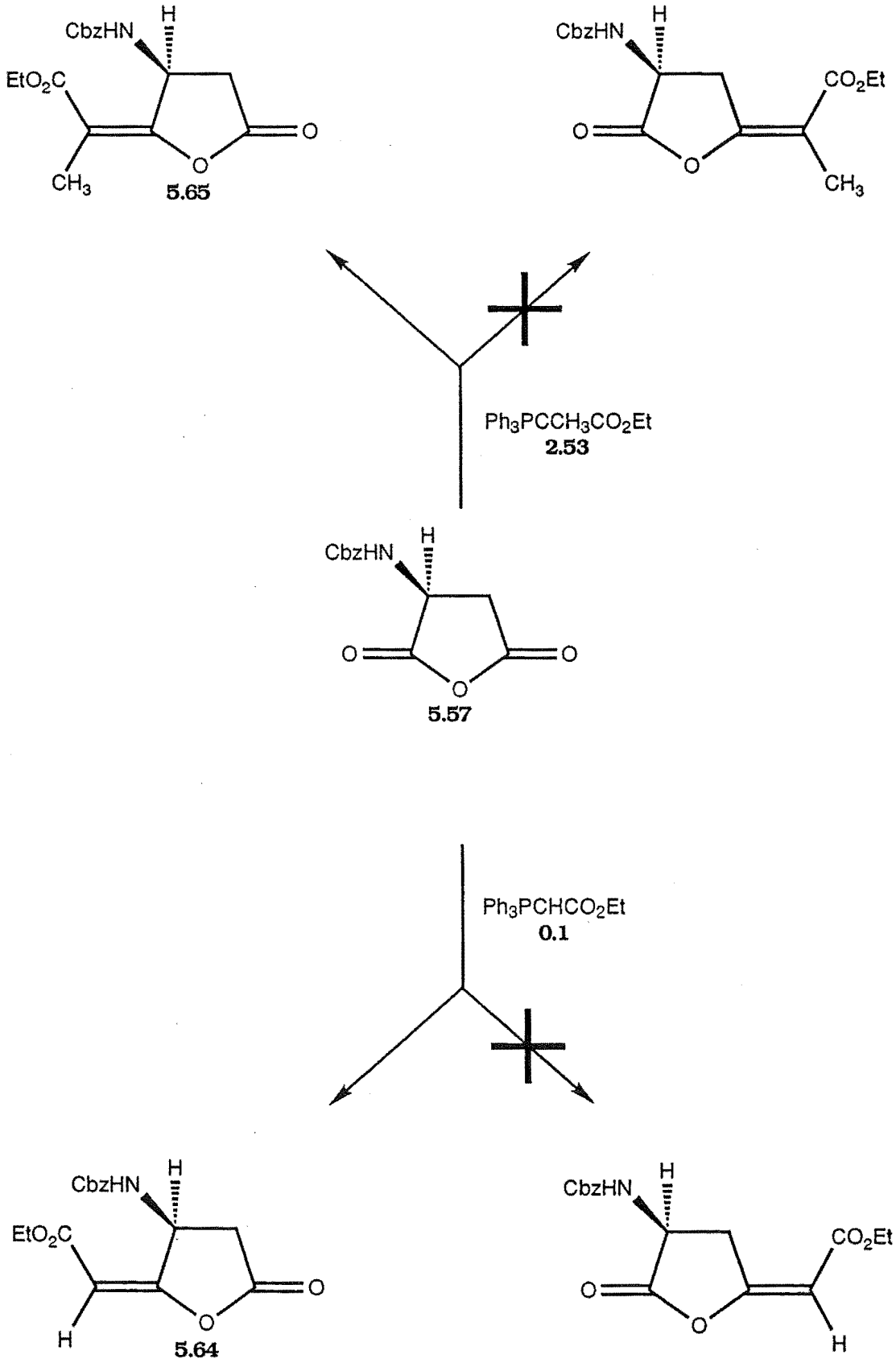

Table 5.9a

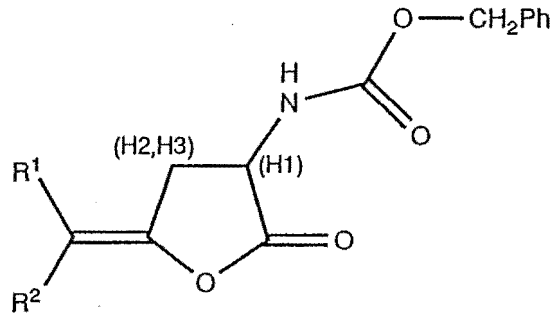

	^{1}H NMR signals					
Compound	(H1)	(H2)	(H3)	Olefinic H	(NH)	(CH_2Ph)
5.62 $R^1 = CO_2Et$, R^2 = Br	4.43,m	3.27,dd,8.7,18.5	3.86,10.4,18.5	-	5.73,bd,6.5	5.12,s
5.63 R^1 = Br, $R^2 = CO_2Et$	4.43,m	3.08,dd,8.2,18.8	3.48,dd,10.6,18.8	-	5.73,bd,6.5	5.12,s
5.69 $R^1 = CO_2Et$, R^2 = H	4.36,bq,7.5	3.25,dd,7.1,18.1	3.88,dd,10.1,18.5	5.63,bs	5.73,bs	5.12,s

Table 5.9b

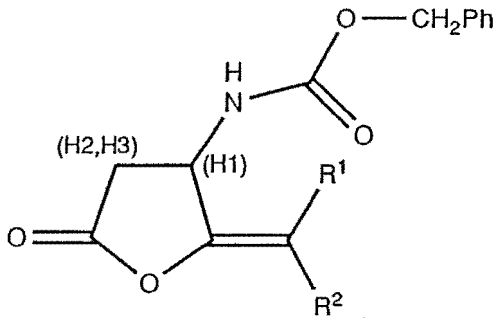

Compound	^{1}H NMR signals (H1)	(H2)	(H3)	Olefinic H	(NH)	(C**H**$_2$Ph)
5.61 R ^{1}= Br, R^2 = CO_2Et	5.01dd,6.2,12.8	3.07,bd,6.6		-	6.05,bs	5.09 abq, 7.2,19.6
5.62 R ^{1}= CO_2Et, R^2 = Br	5.15, m	3.07,bd,6.6		-	6.05,bs	5.09 abq, 7.2,19.6
5.64 R ^{1}= CO_2Et, R^2 = H	4.97,ddd,1.5,6.0,17.62	2.96,bd,11.6		5.74,s	6.05,bs	5.09,abq,8.1,20.3
5.65 R ^{1}= CO_2Et, R^2 = CH_3	5.05,m	2.96,bd,10.2		1.93,s	5.91,bs	5.10,abq,8.1,26.9

Z-methyl enol lactone. Also the ^1H NMR chemical shifts are consistent with related compounds **5.51**, **5.52**, and **5.53** (Table 5.7a,b). The α-*E*-enol lactone **5.64** was assigned on the basis of the similarity of the chemical shifts of the vicinal protons H1, H2, and, H3 resonance signals to those of the methyl enol lactone **5.65** and **5.54**. The phosphorane structure **5.58** was assigned on the basis of the resonance signal at 0.68ppm (CH_3 of the ethyl ester) which decreased as the resonance for the CH_3 of the ethyl ester of the enol lactone (1.24ppm) increased.

5.4.2.2 Regioselectivity of the Reaction of N-Cbz Aspartic Anhydride with Ylides **0.1** and **2.53**

The major reaction at the most hindered carbonyl in this case is consistent with the Bürgi-Dunitz hypothesis[5.2] in that the ylide attacks across the anhydride ring. The four factors postulated in the metal hydride *ab initio* studies (see 5.1: Introduction) are also consistent with the observed regioselectivity. The α-carbonyl is intrinsically more reactive than the β-cabonyl as the amine is electron withdrawing and hence increases the electrophilicity of the α-carbonyl. The steric influence of the substituent benzyl urethane protecting group (Cbz) would be expected to be greater than the N-acetyl group and this would contribute to the greater regiocontrol. The benzyl ester is free to rotate and block the approach of the ylide **0.1** if the Cbz group is in the quasiequatorial position, Figure 5.2. An antiperiplanar effect[5.7] would only contribute to the regiocontrol if the Cbz group was in the quasiaxial position, Figure 5.2. A quasiaxial position for the Cbz group would block the approach of the ylide nucleophile on that face. However, attack of the nucleophile on the β-carbonyl via the opposite face would not be sterically hindered. The chelation effect (see 5.1: Introduction) may also occur if the lone pair of electrons on the

nitrogen of the amine is associated with stabilisation of the positive charge on the phosphorus of the ylide. The regioselectivity and *Z*-stereochemical preference may be a result of the chelation effect and possibly hydrogen bonding. Further stabilisation of the transition states by intramolecular hydrogen bonding may enhance the regioselectivity. The proton on the urethane may hydrogen bond to the carbonyl of the ethyl ester of the betaine or oxaphosphetane, Figure 5.4. This is only possible with attack at the α-carbonyl as the large separation of the N-H and the ester carbonyl produced by attack at the β-carbonyl would not allow hydrogen bonding.

The bromolactonisation reaction proceeds well on the Cbz-aspartic anhydride in contrast to the N-acetyl aspartic system. This is mainly due to the increased acylphosphorane build-up and the successful separation of the bromo enol lactones. The acylphosphorane formation and subsequent reactivity is crucial to the bromolactonisation reaction. The difference in reactivity must be due to the protecting group. The electron withdrawing nature of the nitrogen of the acetyl amide must be less than that of the urethane nitrogen. The electrons of the amide nitrogen would be involved in the amide delocalisation to a greater extent than in the urethane. The oxygen and the nitrogen of the urethane both participate in delocalisation such that the nitrogen has more amine character. The urethane therefore increases the intrinsic reactivity of the α-carbonyl relative to the amide. As in electrophilic substitution of aryl compounds, an amine substituent is weakly activating and the amide substituent is deactivating.

The higher intrinsic reactivity of the Cbz protected aspartic anhydride relative to N-acetyl aspartic anhydride increases the rate of formation of the intermediate phosphorane **5.58**. The intermediate phosphorane **5.58** itself has a higher reactivity than the N-acetyl aspartic anhydride derived phosphoranes **5.49** and **5.50**. This is evidenced by the ease of cyclisation of the phosphoranes **5.64**, **5.49**, and **5.50** at room temperature (**5.49** and **5.50** do not cyclise to N-acetyl aspartic enol

lactones, whereas **5.64** cyclises to form Cbz-aspartic enol lactone, 2% after 80 minutes).

The bromo enol lactones that best mimic an amino acid would have the amine in the α-position (Figure 5.23). The bromo enol lactones **5.60** and **5.61**, produced in the bromolactonisation reaction of the phosphorane **5.58**, have the amine moiety in the hindered β-position. An alternative synthesis was developed in order to synthesise the bromo enol lactones **5.62** and **5.63** with the amine moiety in the α-position.

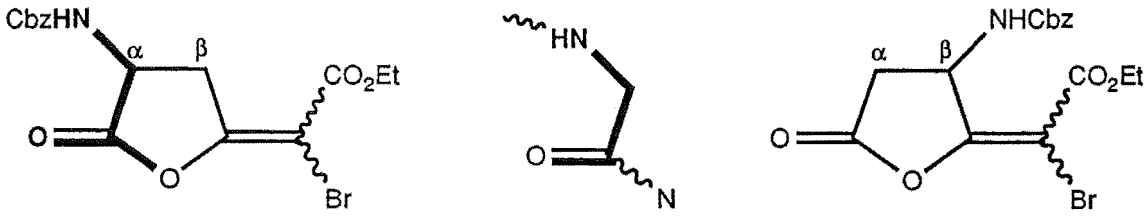

α-Cbz-aspartic bromo enol lactones **5.60** and **5.61**

Natural amino acid

β-Cbz-aspartic bromo enol lactones **5.62** and **5.63**

Figure 5.23

5.4.3 β-Cbz-Aspartic Bromo Enol Lactones

The intrinsic reactivity of the carbonyl groups in Cbz-aspartic anhydride was required to be reversed in order to produce the desired β-phosphorane **5.59**. The α-carboxyl group must therefore be protected, Scheme 5.11. The protecting group must be stable to the conditions for the conversion of the side chain β-carboxylic acid into the acylphosphorane. The protecting group must also be easily removed while stable to the subsequent phosphorane preparation conditions. Equally important, the deprotection of the α–carboxylic acid protecting group must be orthogonal to the deprotection of the amine. The previously investigated (see Chapter 2) acid chloride synthesis of acylphosphorane

Scheme 5.11: Syntheses of α- and β-Cbz-Aspartic Bromo Enol Lactones 5.62, 5.63, 5.60, and 5.61

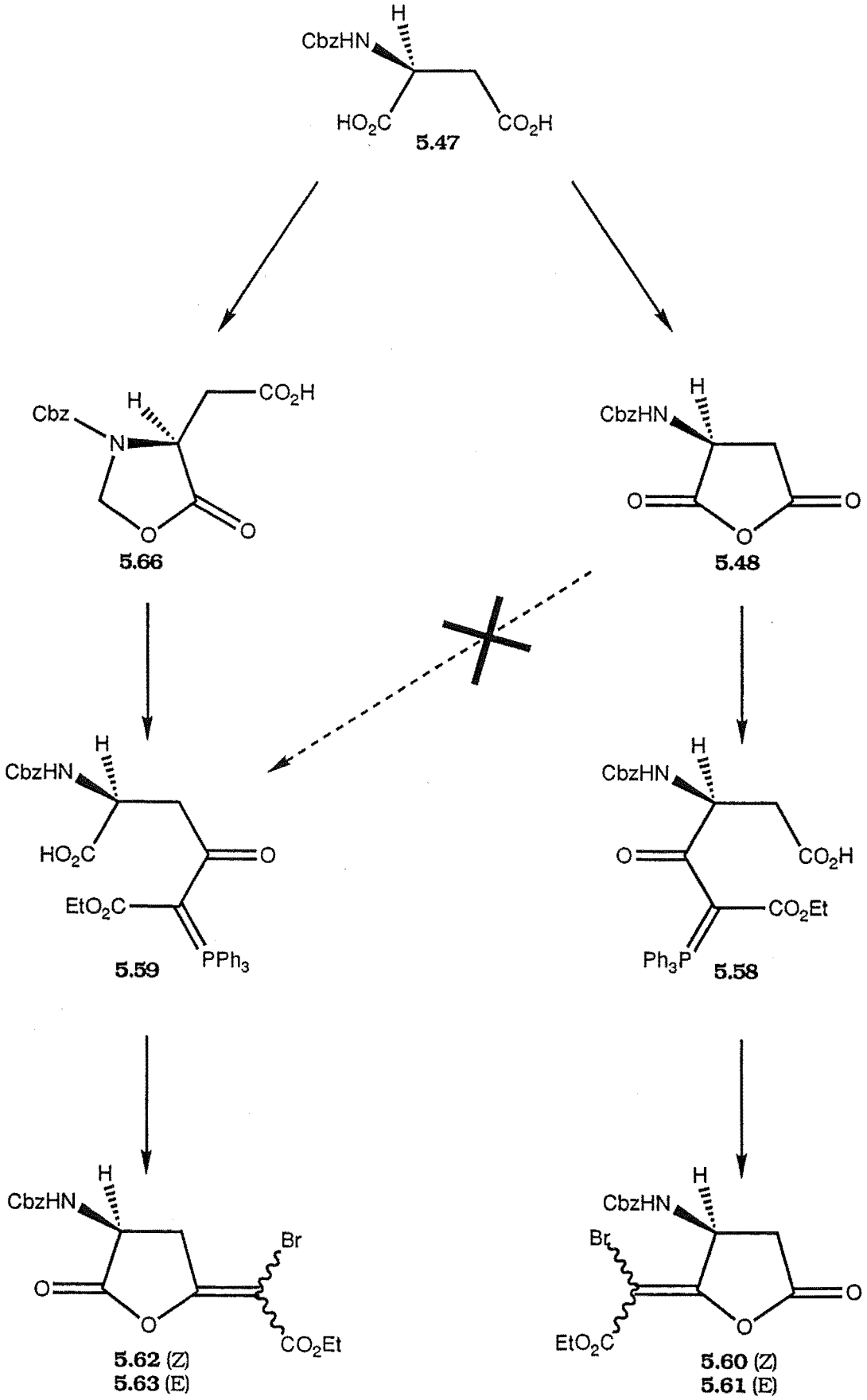

can be used to convert the β-carboxylic acid into the required acylphosphorane. The Cbz protecting group is stable under the reaction conditions of the acid chloride formation, and can be removed by catalytic hydrogenation without effecting the enol lactone moiety. An oxazolidine[5.19] was chosen as the protecting group for the α–carboxylic acid as it also has the advantage of doubly protecting the amine. The α–carboxylic acid can be reformed by mild base catalysed hydrolysis of the oxazolidine. The disadvantage of using an oxazolidine is that the ethyl ester of the phosphorane moiety might also be hydrolysed, so selective hydrolysis conditions were developed. The Cbz group is stable under hydrolysis conditions.

L-aspartic acid **5.47**, paraformaldehyde (2 equiv) and paratoluenesulphonic acid (catalytic amount) were refluxed in benzene for one hour in a Dean Stark apparatus to give the oxazolidine[5.19] **5.66**, Scheme 5.12. Ethyl acetate was added and the solution was washed with K_2CO_3 and water. The organic solution was dried with magnesium sulphate and evaporated under reduced pressure, to give the oxazolidine **5.66**. The β-carboxylic acid of the oxazolidine **5.66** was then converted to the acid chloride **5.67** by reaction with oxalyl chloride (10 equiv) and DMF (catalytic amount) in dry benzene. The acid chloride **5.67** was dissolved in CH_2Cl_2 at 0°C and two equivalents of ylide **0.1** were added with stirring under a N_2 atmosphere. The solution was allowed to warm to room temperature after 30 minutes and then stirred for a further hour. Isolation gave a mixture of the phosphorane **5.68** and protonated ylide **2.50d** which was purified by radial chromatography to give the oxazolidine phosphorane **5.68** in a total yield yield of 76% from L-aspartic acid.

Initial attempts at selective hydrolysis of the oxazolidine and isolation of the free acid were unsuccessful. However, mild hydrolysis conditions were found[5.20] that selectively hydrolysed the oxazolidine **5.68** to give the free acid **5.59** quantitatively. The product oxazolidine

Scheme 5.12: Oxazolidine Synthesis for Formation of Enol Lactone 5.69 and β-Bromo Enol Lactones 5.62 and 5.63

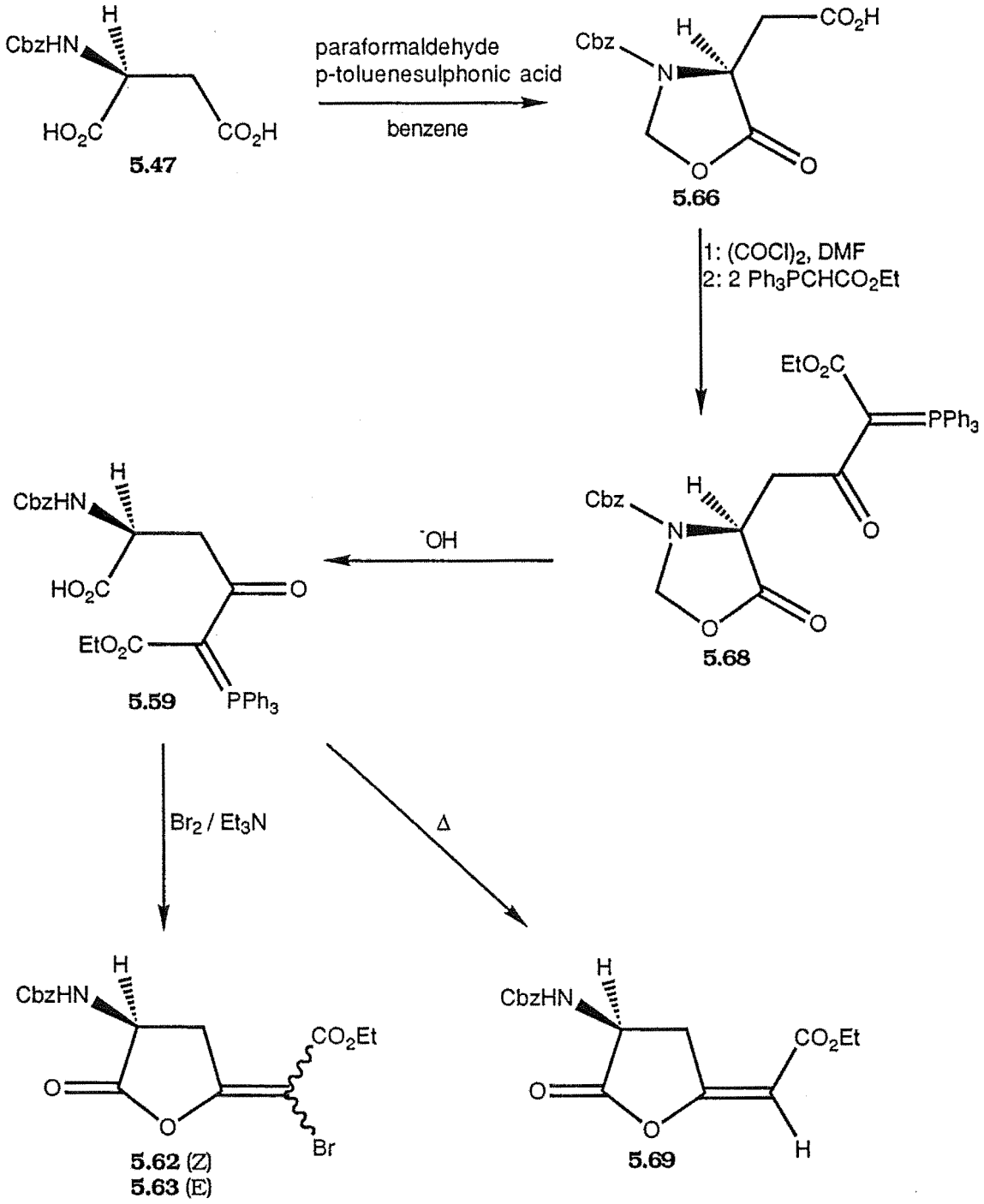

phosphorane **5.68** was dissolved in methanol and 1N NaOH (10 equiv) was added, and the solution was stirred at room temperature for 4 hours. The solution was neutralised carefully with 1N HCl and the solvent was

removed under reduced pressure. The free acid phosphorane **5.59** was quantitatively extracted from the residue with ethyl acetate.

The free acid phosphorane **5.59** was stable at room temperature and the *E*-enol lactone **5.69** was only formed after refluxing **5.59** in $CHCl_3$ for 36 hours. The enol lactone was purified by radial chromatography in a yield of 78%.

The *E*- and *Z*-bromo enol lactones **5.62** and **5.63** were also formed from **5.59** in a ratio of 34:66 respectively under the bromolactonisation conditions. To a stirred solution of the free acid phosphorane **5.59**, in CH_2Cl_2, under N_2, at -78°C, was added one equivalent of triethylamine, followed by one equivalent of bromine. The solution was allowed to warm to room temperature after 30 minutes and stirred for a further hour. The solvent was removed and the bromo enol lactones were purified by radial chromatography in a total yield of 82%.

5.4.3.1 Structure Assignment of β-Bromo Enol Lactone **5.62** and **5.63** .

The ^1H NMR spectrum of the Cbz-L-aspartic β-bromo enol lactones **5.62** and **5.63** were assigned by comparison with the ^1H NMR spectra of Cbz-L-aspartic β-enol lactone **5.69**. The ^1H NMR spectrum of the major bromo enol lactone **5.63** was almost identical to the ^1H NMR spectrum of the enol lactone **5.69**, as shown in Table 5.9b. The minor *E*-bromo enol lactone isomer **5.62** was assigned on the basis of the chemical shifts of the geminal protons H2, and H3.

5.4.4: Preliminary Testing of Bromo Enol Lactones

The aim of this research project was to investigate and develop a new bromolactonisation reaction to include aromatic and amine substituents. This objective has been achieved. Although the synthesis of potential mechanism-based inactivators was not specifically undertaken, some preliminary testing of the bromo enol lactones **2.33**, **2.34**, **3.13**, **3.14**, **4.25** and **4.26** for biological activity and inactivation of chymotrypsin was carried out.

The bromo enol lactones **2.33**, **2.34**, **3.13**, **3.14**, **4.25** and **4.26** were tested for antiviral, antitumour, and antimicrobial activity. The bromo enol lactones **2.33**, **2.34**, **3.13**, and **3.14**, showed slight cytotoxicity, while **4.25** and **4.26** showed a high degree of cytotoxicity and antimicrobial activity.

The inactivation of chymotrypsin was tested by a colorimetric-based assay, preformed according to the method of Kellam[5.21]. The percent (%) inactivation for a 10 fold excess of bromo enol lactone to chymotrypsin was measured relative to a blank (containing substrate only) for a fixed time interval. The bromo enol lactones **2.33**, **2.34**, **3.13**, **3.14**, **4.25**, and **4.26** showed no inhibition of chymotrypsin. A key recognition feature of substrates of chymotrypsin is an aromatic group so it is not surprising that the bromo enol lactones **2.33**, **2.34**, **3.13**, and **3.14** were not recognised as substrates. The aromatic bromo enol lactones **4.25** and **4.26** were also not recognised as substrates which can be rationalised by the position of the aromatic ring. The aromatic ring is the primary recognition feature of a peptide and orientates the scissile bond in the active site. The bromo enol lactones **4.25** and **4.26** lack a CH_2 link to the aromatic ring in the carbon connectivity when compared to the natural substrate, Figure 5.8. The bromo enol lactones **2.82** and **2.83** have been shown[2.40] to be inactivators of chymotrypsin and contain two aromatic rings, one of which is in the same position as in the natural substrate, Figure 5.24. Therefore, it is

likely that the aromatic ring must be at least two carbons from the lactone ester to be recognised as a substrate of chymotrypsin.

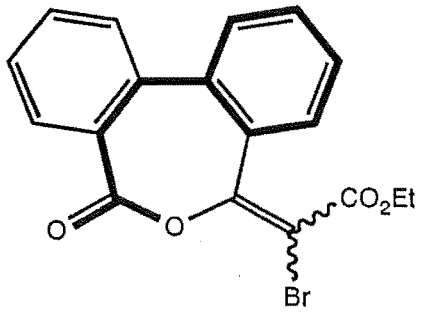

2.82, 2.83

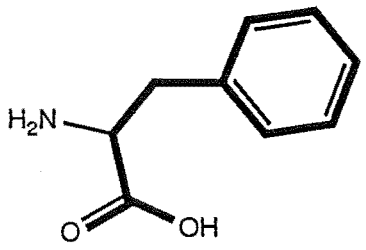

Phenylalanine

Figure 2.24

The bromo enol lactone **2.33** was treated under hydrolysis conditions ($NaOH/CD_3OD$) designed to mimic enzyme catalysed hydrolysis (Scheme 0.6). **2.33** hydrolysed rapidly under these conditions to form the ring opened methoxy ester **5.70**, analogous to the acylenzyme intermediate (Scheme 0.7). The hydrolysis of **2.33** was slower under acidic conditions ($pTsOH/CD_3OD$), and was monitored by ^1H NMR spectroscopy. The glutaric bromo enol lactones **3.13** and **3.14** underwent a similar hydrolysis reaction, and the formed the methoxy ester product, similar to known compounds[5.16].

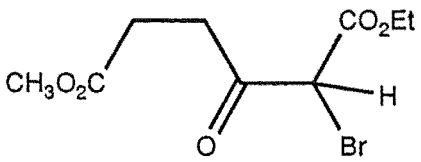

5.70

5.4.5: Future work.

The disadvantage of previous syntheses of halo enol lactones that represent sophisticated amino acid analogues, for example **5.40,** is that they lack stereocontrol. The bromolactonisation reaction reported here is more versatile as it allows the retention of chiral integrity of the starting material. The oxazolidine synthesis may be extended in two ways. The first, is to use an aspartic acid derivative that has an aromatic substituent in the β-position, shown in a general Scheme 5.13. The proposed synthesis is unique in that no synthesis of five membered bromo enol lactones have been reported that have the amine substituent in the α-position and an aromatic substituent in the β-position, Figure 5.25:A. The reported[5.1] syntheses have the amine and aromatic substituents in the α-position, Figure 5.25:B.

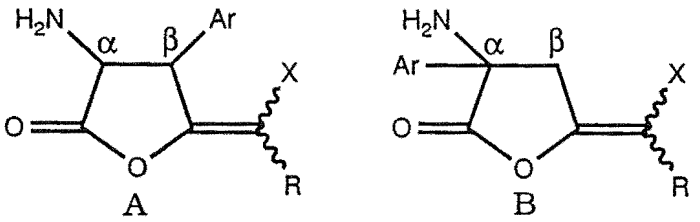

Figure 5.25: A: amine substituent in the α-position and the aromatic substituent in the β-position, B: both substituents in the α-position

Also, the oxazolidine synthesis has the advantage that the exact chirality of the starting material is retained. Thus, not only the natural chirality of the α-phenylalanine is retained, but the chirality at the β-carbon is also retained. The position of the aromatic substituent is crucial in orienting the molecule in the active site of the enzyme. The oxazolidine-bromolactonisation synthesis has the advantage that in theory both diastereoisomers **5.71** and **5.72** (Figure 5.26) can be produced from the respective diasteriomeric starting materials.

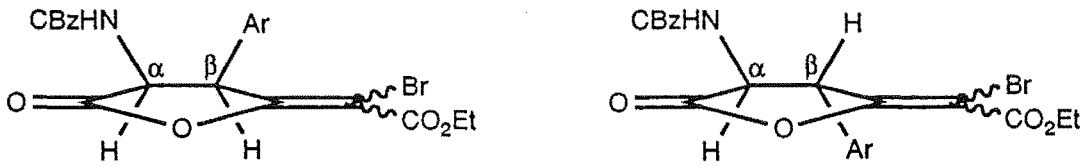

5.71 5.72

Figure 5.26

Scheme 5.13: General Scheme for Oxazolidine Synthesis for α-Amino- and β-Aromatic-Bromo Enol Lactones

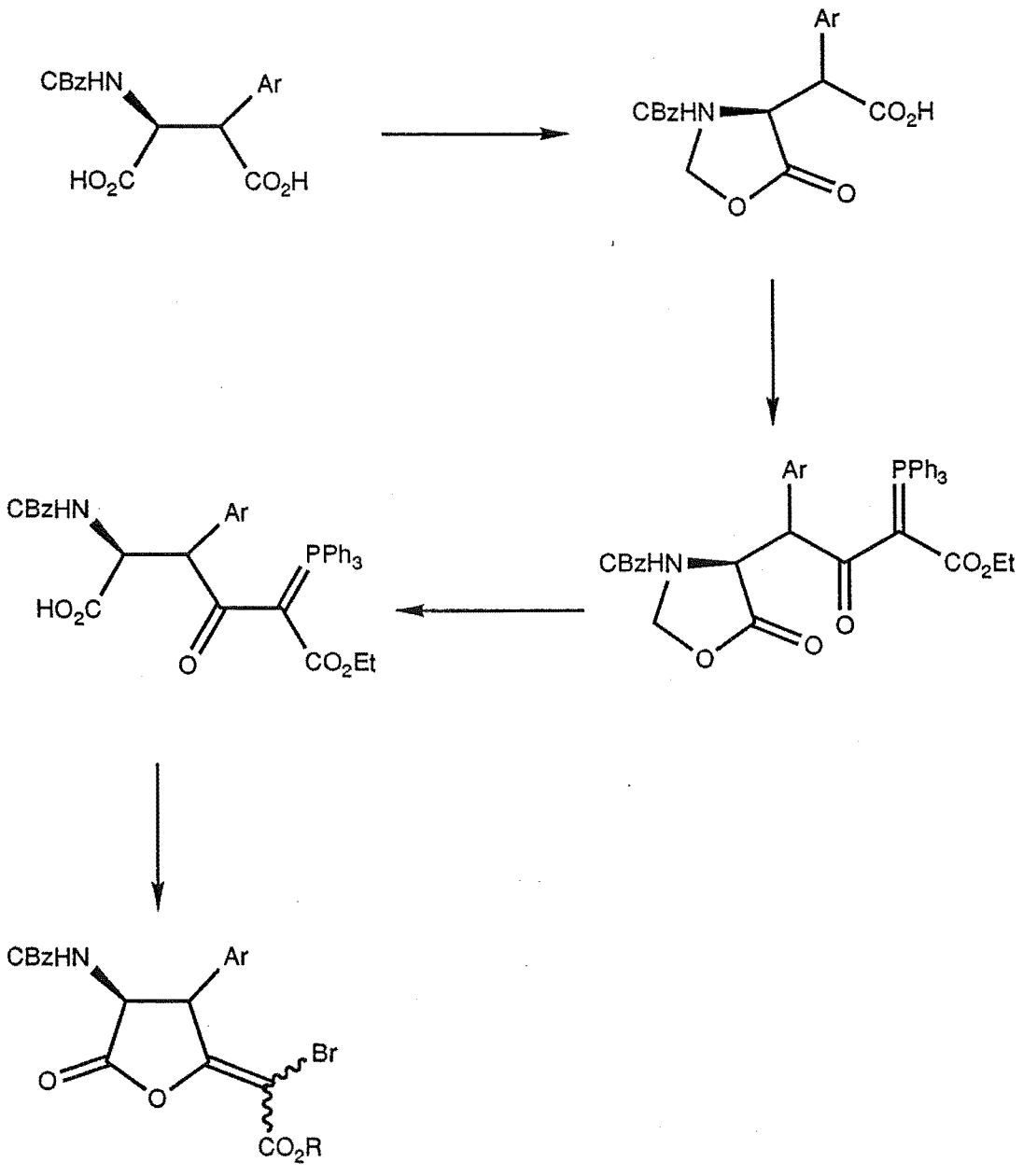

Starting with β-phenyl Cbz-aspatic acid, (Scheme 5.13) the bromolactonisation reaction would yield the bromo enol lactones **5.73** and **5.74**, Figure 2.27. The bromo enol lactones **5.73** and **5.74** totally incorporate the natural substrate L-phenylalanine and the latent reactive bromo enol moiety.

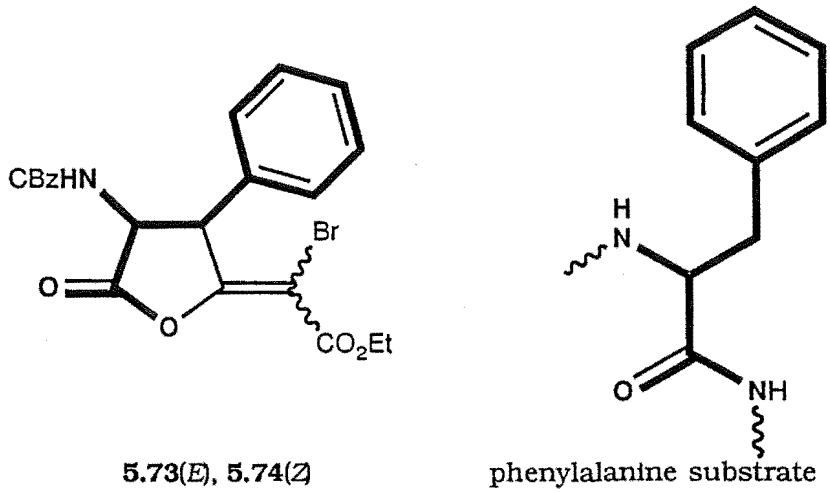

5.73(*E*), **5.74**(*Z*) phenylalanine substrate

Figure 5.27

Preliminary investigations into the synthesis of β-phenyl-Cbz-aspatic bromo enol lactones **5.73** and **5.74** were carried out, but due to lack of time were not completed. The synthesis of RS,SR and RR,SS β-phenyl Cbz-aspatic acid was performed as reported in the literature[5.22], Scheme 5.14. A trial reaction using the RS,SR diastereoisomer as starting material appeared to give the corresponding oxazolidine. However, this work was not continued.

As the oxazolidine-bromolactonisation retains the chiral integrity of starting material, the racemic RS,SR or RR,SS β-phenyl Cbz-aspatic acids would produce RS,SR or RR,SS β-phenyl Cbz-aspatic bromo enol lactones respectively. Literature[5.1] syntheses of halo enol lactones also give racemic products. However, the chiral centre is created in these syntheses

Scheme 5.14: Synthesis of α-Amino and β-Phenyl Starting Material for the Oxazolidine Synthesis

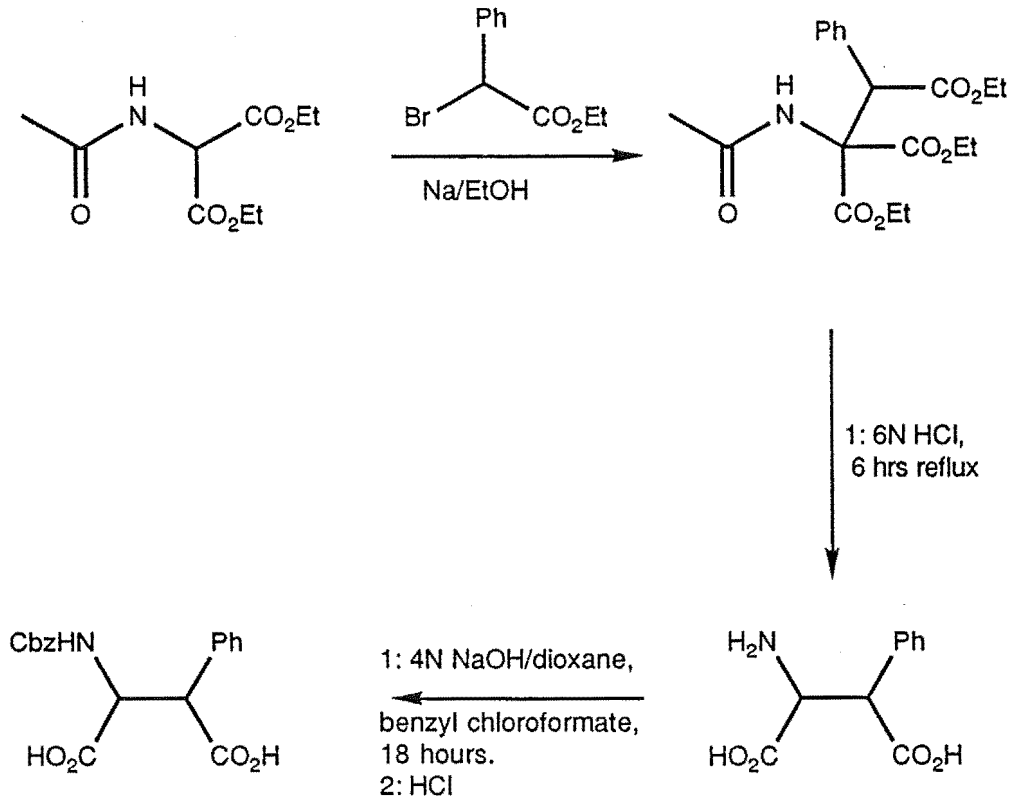

RR,SS insoluble in cold diethyl ether
RS,SR soluble in cold diethyl ether

Scheme 5.15:

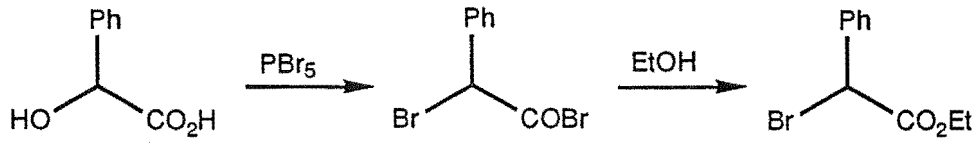

nonstereospecifically to give racemic products. The oxazolidine-bromolactonisation synthesis would yield an optically active bromo enol lactone if a pure enantiomeric starting material was used. Thus the

enantiomeric versatility of the synthesis relies on the synthesis of enantiomeric starting material. The aromatic substituent can be modified by starting with a suitable aromatic α–hydroxy acid, Scheme 5.15.

A second method to extend the oxazolidine-bromolactonisation synthesis is to start with the substrate amino acid, phenylalanine, tryptophan, or tyrosine. This is currently undergoing investigation by this research group. The amine is protected by a phenacyl group and the carboxylic acid is protected by a chiral oxazolidine. The protected amino acid is stereoselectively alkylated with a α-halo acetate, and the free acid is revealed after hydrolysis of the ester. The synthesis is then continued as in Scheme 5.16. Acid chloride formation is followed by reaction with an ylide to form the acylphosphorane. The carboxylic acid is then deprotected followed by bromolactonisation to yield bromo enol lactones of the type **5.75**, Scheme 5.16. This synthesis yields bromo enol lactones that have the amine and aromatic substituents in the α-position, Figure 5.24:B. The stereochemistry is reversed in the alkylation step, yielding the D-bromo enol lactone if the L-amino acid is used and vice versa. The advantage of this synthesis is that it is stereospecific and the pure enantiomers can be produced separately.

The oxazolidine-bromolactonisation synthesis may be extended to include modification of the substituent on the double bond (R in Figure 5.17) of the halo enol lactone. Modification of the R group of the halo enol lactone is important with respect to secondary binding specificity, see Introduction, as the R group is a recognition feature. Modification of the R group is also important to the mechanism of inactivation as the R group may orient the reactive α-halo ketone of the acylenzyme complex. The nucleophilic residues of the active site will be unable to attack the α-halo ketone if it is oriented incorrectly, and thus, the halo enol lactone will not be a mechanism-based inactivator.

Scheme 5.16: Proposed Synthesis of Bromo Enol Lactones of the Type 5.75. (*Successfully completed the synthesis of the free acid to date.)

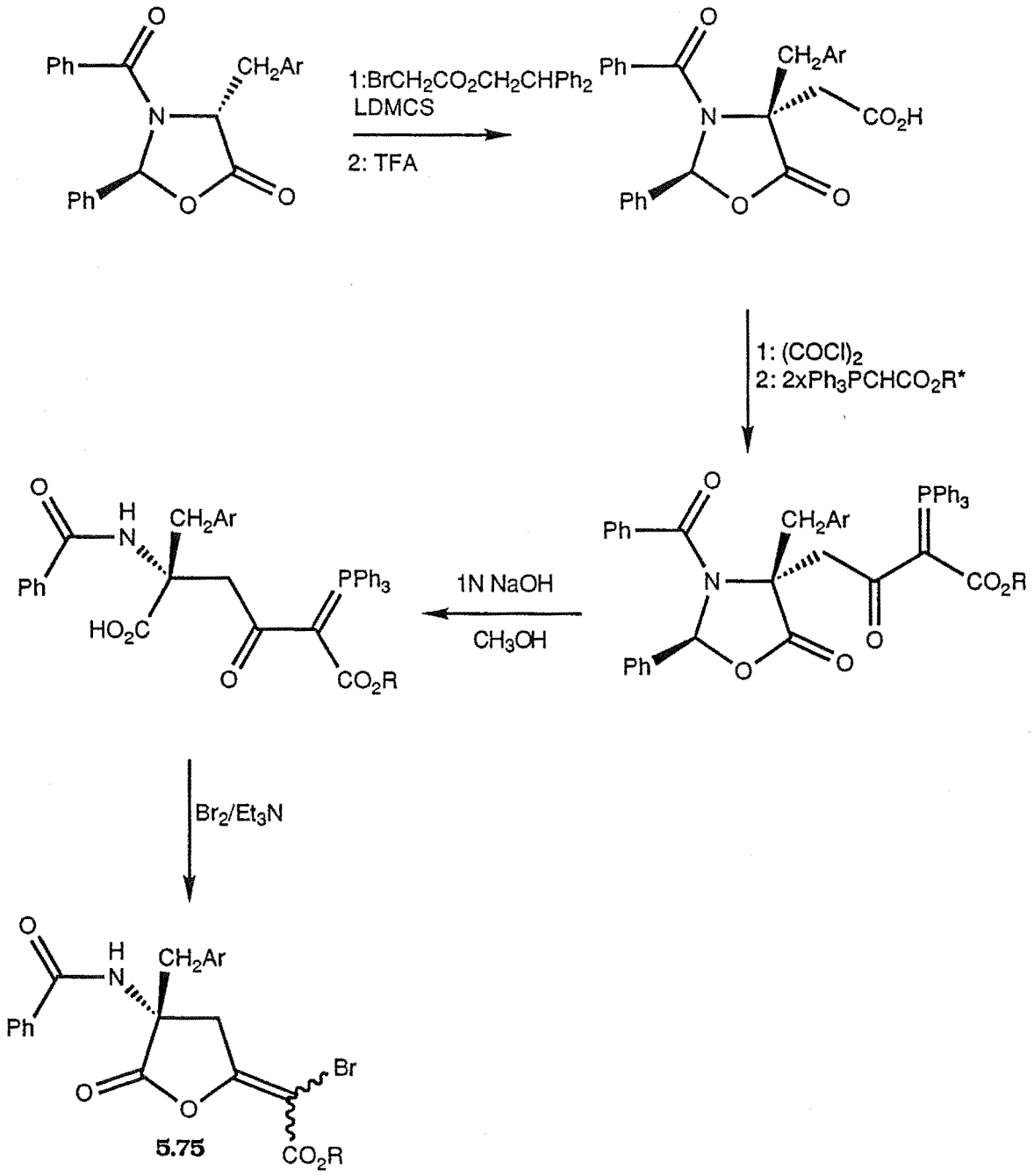

Scheme 5.17: Extension of the Oxazolidine-Bromolactonisation Synthesis to Include Different R Substitution

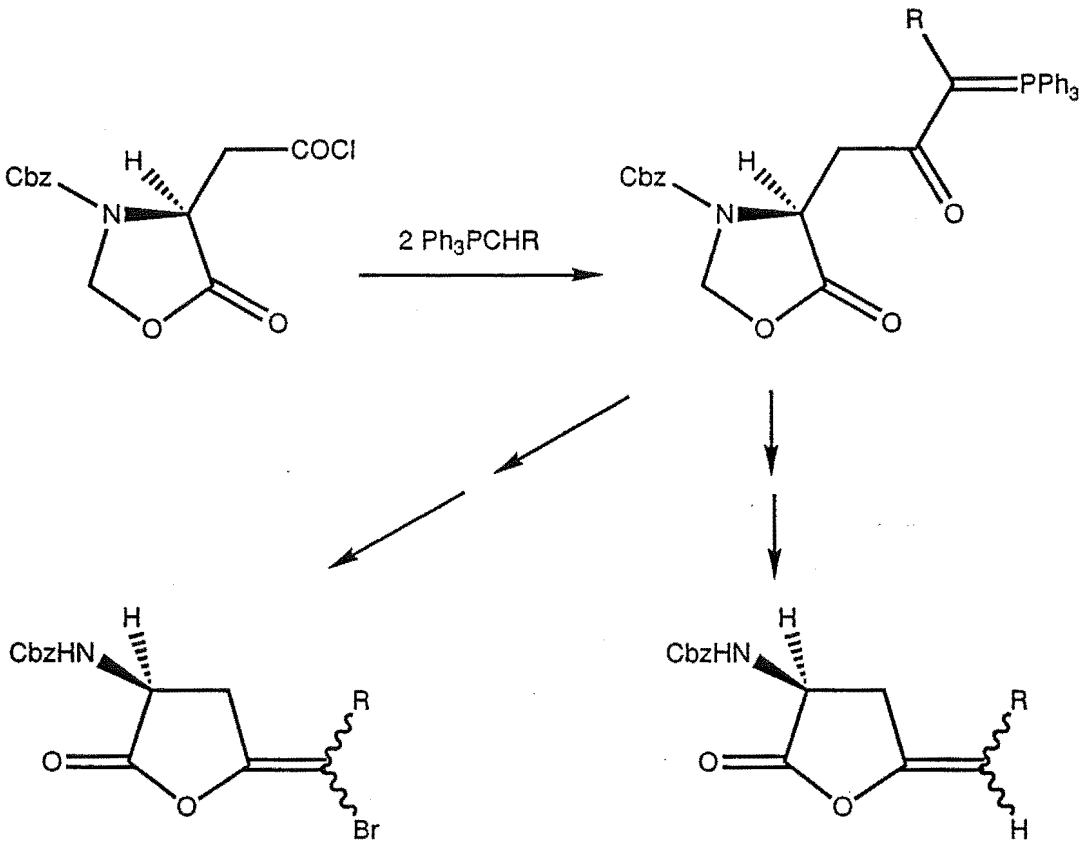

5.5: Summary

The extensions to include amine and aromatic substituents in the bromolactonisation reaction have been achieved. The phenyl glutaric and phenyl succinic bromo enol lactones **5.9**, **5.10**, **5.20**, **5.21**, **5.22**, and **5.23** have been synthesised. Cbz-protected aspartic α- and β-bromo enol lactones have also been synthesised.

Experimental

General

Melting points were obtained using a Reichert Hot Stage Microscope or an Electrothermal Melting Point Apparatus and are uncorrected.

Nuclear Magnetic Resonance (NMR) spectra were obtained on a Varian XL 300 Spectrometer operating at 300 MHz for ^{1}H NMR, 75.5 MHz for ^{13}C NMR and 121.5 MHz for ^{31}P NMR. All spectra were obtained in deuterated chloroform, unless otherwise stated. ^{1}H NMR used a trimethylsilane internal standard, and ^{31}P NMR used an external phosphoric acid reference. NMR is reported as ppm (multiplicity, coupling constants in Hz, assignment).

Infrared (IR) spectra were obtained as nujol plates using a Pye Unicam SP3-300 and Perkin Elmer 1600 FTIR Spectrophotometers using the polystyrene 1603 cm^{-1} absorption as a reference.

Infrared spectra of the keto acid phosphoranes were recorded on a BIO RAD FTS 40 spectrophotometer. Raman spectra were recorded using a Spectra-physics 171 argon-ion laser (excitation at 488.0 nm) and SPEX 1403 double monochromator.

Mass spectra were obtained on a Kratos MS80RFA magnetic sector double focusing mass spectrometer.

Semi-preparative HPLC was carried out on a Varian Model 5000 Liquid Chromatograph using a Roedyne 7125 injector and a Varian UV-50 Ultraviolet Detector operating at 230 nm, with an output to a Hewlet Packard 3390 A Integrator. An Alltech Cyano Semi-preparative Column (25 cm x 10 mm i.d.) was used.

Preparative Chromatography was carried out using a Chromatotron (Harrison Research Inc.), a centrifugally accelerated radial thin layer chromatograph, using glass plates coated with silica gel (P.F. 254 60) of 1 mm, 2 mm or 4 mm thickness. Visualisation of non-coloured compounds was achieved using an ultraviolet lamp.

All chemicals were reagent grade unless otherwise stated. All solvents and anhydrides were purified and dried as outlined in 'Purification of Laboratory Chemicals'[E1]. All anhydrides were synthesised by using acetic anhydride at reflux, unless otherwise stated. N-trifluoroacetyl aspartic anhydride was synthesised using trifluoroacetic anhydride. N-Acetyl aspartic anhydride[5.12] was synthesised using a literature method. Oxalyl chloride was freshly distiled prior to use. The hydrogen[E2], methyl[E3], and bromo[E4] ylides were synthesised and purified by literature methods.

Experimental

Chapter 1

Crystal data for 1-ethoxycarbonyl-5-carboxy-2-oxopentan-1-ylidenetriphenylphosphorane[2.24] ***1.8****(akd).*

$C_{27}H_{27}O_5P$. colourless, crystalised from ethyl acetate, crystal dimensions 0.4 x 0.4 x 0.4 mm. M = 462.49, monoclinic, space group $C_{2/c}$, a = 17.541(10), b = 9.045(5), c = 29.711(20) Å, β = 95.03(5), U = 4666.6 $Å^3$, Z = 8, D_C = 1.32 g cm^{-1}, F(000) = 1952, μ = 1.48cm^{-1}. Using 1.6° ω-scans at scan rate of 7.32° min^{-1}, 4597 unique reflections were collected in the range of $4 < 2\theta < 45°$ and 3133 of these having $I > 3\sigma(I)$ were used in the structural analysis.

Data were recorded at 148 K on a Nicolet R3m four circle diffractometer using Mo - Kα radiation. Cell parameters were determined by least squares refinement of 25 accurately centred reflections in the range of $5 < 2\theta < 35°$. Crystal stability was monitored by recording 3 check reflections (1. 0 0 0, 2. 0 4 0, 3. 0 0 14) every 100 reflections and no significant variations were observed. Data were corrected for Lorentz-polarisation effects but not for absorption.

Direct methods revealed the position of the non-hydrogen atoms and the structure was refined by blocked cascade least-squares techniques. Hydrogen atoms were inserted at calculated positions using a riding model with thermal parameters equal to 1.2 U of their carrier atoms, H5 was located from a difference Fourier map and inserted at that position All non-hydrogen atoms were refined anisotropically (302 parameters). The refinement converged with R = 0.065 and R_w = 0.065. The final difference fourier map showed no significant features. All programs used in the data collection and structure solution are contained in the SHELXTL (Version 4.1) package.[E5]

TABLE 1. Atomic Coordinates ($x10^4$) and Isotropic Thermal Parameters ($Å^2x10^3$) for 1.8(akd).

Atom	x	y	z	U
P	1365(1)	2085	2263(1)	23(1)*
O(1)	1393(1)	-2220(2)	2657(1)	37(1)*
O(5)	-460(1)	-602(2)	416(1)	37(1)*
O(3)	830(1)	805(2)	980(1)	39(1)*
O(4)	-92(1)	-2703(2)	222(1)	36(1)*
O(2)	1483(1)	-182(2)	3376(1)	32(1)*
C(1)	1386(1)	-889(3)	2699(2)	26(1)*
C(2)	1265(1)	178(3)	2091(1)	23(1)*
C(3)	1001(1)	-202(3)	1405(2)	27(1)*
C(4)	886(1)	-1784(3)	1190(2)	28(1)*
C(5)	482(1)	-2329(3)	1599(2)	30(1)*
C(6)	54(1)	-1424(3)	1417(2)	27(1)*
C(7)	-167(1)	-1660(3)	622(2)	26(1)*
C(8)	1617(1)	-1073(3)	4038(2)	43(1)*
C(9)	1718(1)	-23(4)	4690(2)	56(1)*
C(11)	942(1)	2942(3)	2785(1)	21(1)*
C(12)	645(1)	2067(3)	3155(2)	26(1)*
C(13)	342(1)	2722(3)	3612(2)	31(1)*
C(14)	338(1)	4236(3)	3701(2)	30(1)*
C(15)	632(1)	5102(3)	3327(2)	31(1)*
C(16)	932(1)	4481(3)	2864(2)	27(1)*
C(21)	1907(1)	2311(3)	2804(2)	26(1)*
C(22)	1978(1)	3415(3)	3349(2)	33(1)*
C(23)	2400(1)	3600(4)	3736(2)	42(1)*
C(24)	2754(1)	2698(4)	3580(2)	45(1)*
C(25)	2689(1)	1609(4)	3041(2)	47(1)*
C(26)	2267(1)	1399(3)	2658(2)	38(1)*
C(31)	1408(1)	3155(3)	1405(1)	28(1)*
C(32)	1025(1)	3853(3)	1052(2)	36(1)*
C(33)	1058(1)	4714(3)	411(2)	53(1)*
C(34)	1464(2)	4881(4)	114(2)	66(2)*
C(35)	1842(2)	4200(5)	450(2)	69(2)*
C(36)	1821(1)	3330(4)	1104(2)	44(1)*

*Equivalent isotropic U defined as one third of the trace of the orthogonalised U_{ij} tensor

Table 2. Bond lengths (Å) for 1.8(akd).

P-C(2)	1.768(2)	P-C(11)	1.790(3)
P-C(21)	1.805(3)	P-C(31)	1.801(3)
O(1)-C(1)	1.205(3)	O(5)-H(5)	1.037(35)
O(5)-C(7)	1.320(3)	O(3)-C(3)	1.253(3)
O(4)-C(7)	1.205(3)	O(2)-C(1)	1.354(3)
O(2)-C(8)	1.439(3)	C(1)-C(2)	1.456(3)
C(2)-C(3)	1.416(3)	C(3)-C(4)	1.508(4)
C(4)-H(4A)	0.960(1)	C(4)-H(4B)	0.960(1)
C(4)-C(5)	1.532(4)	C(5)-H(5A)	0.960(1)
C(5)-H(5B)	0.960(1)	C(5)-C(6)	1.519(4)
C(6)-H(6A)	0.960(1)	C(6)-H(6B)	0.960(1)
C(6)-C(7)	1.499(4)	C(8)-H(8A)	0.960(1)
C(8)-H(8B)	0.960(1)	C(8)-C(9)	1.494(4)
C(9)-H(9A)	0.960(1)	C(9)-H(9B)	0.960(1)
C(9)-H(9C)	0.960(1)	C(11)-C(12)	1.385(4)
C(11)-C(16)	1.397(4)	C(12)-H(12)	0.960(1)
C(12)-H(13)	1.386(4)	C(13)-H(13)	0.960(1)
C(13)-C(14)	1.376(4)	C(14)-H(14)	0.960(1)
C(14)-C(15)	1.377(4)	C(15)-H(15)	0.960(1)
C(15)-C(16)	1.374(4)	C(16)-H(16)	0.960(1)
C(21)-C(22)	1.382(4)	C(21)-C(26)	1.388(4)
C(22)-H(22)	0.960(1)	C(22)-C(23)	1.378(4)
C(23)-H(23)	0.960(1)	C(23)-C(24)	1.376(4)
C(24)-H(24)	0.960(1)	C(24)-C(25)	1.365(5)
C(25)-H(25)	0.960(1)	C(25)-C(26)	1.380(4)
C(26)-H(26)	0.960(1)	C(31)-C(32)	1.394(4)
C(31)-C(36)	1.383(4)	C(32)-H(32)	0.960(1)
C(32)-C(33)	1.375(4)	C(33)-H(33)	0.960(1)
C(33)-C(34)	1.361(6)	C(34)-H(34)	0.960(1)
C(34)-C(35)	1.367(6)	C(35)-H(35)	0.960(1)
C(35)-C(36)	1.394(5)	C(36)-H(36)	0.960(1)

Table 3. Bond angles (°) for 1.8(akd).

C(2)-P-C(11)	113.1(1)	C(2)-P-C(21)	109.1(1)
C(11)-P-C(21)	108.4(1)	C(2)-P-C(31)	113.8(1)
C(11)-P-C(31)	107.4(1)	C(21)-P-C(31)	104.6(1)
H(5)-O(5)-C(7)	113.0(20)	C(1)-O(2)-C(8)	117.6(2)
O(1)-C(1)-O(2)	121.4(2)	O(1)-C(1)-C(2)	128.3(2)
O(2)-C(1)-C(2)	110.3(2)	P-C(2)-C(1)	119.5(2)
P-C(2)-C(3)	116.9(2)	C(1)-C(2)-C(3)	122.8(2)
O(3)-C(3)-C(2)	119.5(2)	O(3)-C(3)-C(4)	117.9(2)
C(2)-C(3)-C(4)	122.5(2)	C(3)-C(4)-H(4A)	109.1(1)
C(3)-C(4)-H(4B)	109.1(1)	H(4A)-C(4)-H(4B)	109.5(1)
C(3)-C(4)-C(5)	110.8(2)	H(4A)-C(4)-C(5)	109.1(1)
H(4B)-C(4)-C(5)	109.2(1)	C(4)-C(5)-H(5A)	108.3(1)
C(4)-C(5)-H(5B)	108.4(1)	H(5A)-C(5)-H(5B)	109.5(1)

Table 3.(cont.) Bond angles (°) for 1.8(akd).

C(4)-C(5)-C(6)	113.8(2)	H(5A)-C(5)-C(6)	108.4(1)
H(53)-C(5)-C(6)	108.4(1)	C(5)-C(6)-H(6A)	108.4(1)
C(5)-C(6)-H(6B)	108.3(1)	H(6A)-C(6)-H(6B)	109.5(1)
C(5)-C(6)-C(7)	114.0(2)	H(6A)-C(6)-C(7)	108.3(1)
H(6B)-C(6)-C(7)	108.3(2)	O(5)-C(7)-O(4)	123.8(2)
O(5)-C(7)-C(6)	112.0(2)	O(4)-C(7)-C(6)	124.2(2)
O(2)-C(8)-H(8A)	110.1(1)	O(2)-C(8)-H(8B)	110.4(1)
H(8A)-C(8)-H(8B)	109.5(1)	O(2)-C(8)-C(9)	106.5(2)
H(8A)-C(8)-C(9)	110.0(2)	H(8B)-C(8)-C(9)	110.3(2)
C(8)-C(9)-H(9A)	109.7(2)	C(8)-C(9)-H(9B)	109.5(2)
H(9A)-C(9)-H(9B)	109.5(1)	C(8)-C(9)-H(9C)	109.3(2)
H(9A)-C(9)-H(9C)	109.5(1)	H(9B)-C(9)-H(9C)	109.5(1)
P-C(11)-C(12)	119.7(2)	P-C(11)-C(16)	120.1(2)
C(12)-C(11)-C(16)	120.1(2)	C(11)-C(12)-H(12)	120.1(2)
C(11)-C(12)-C(13)	119.8(3)	H(12)-C(12)-C(13)	120.1(2)
C(12)-C(13)-H(13)	120.0(2)	C(12)-C(13)-C(14)	120.0(3)
H(13)-C(13)-C(14)	120.0(2)	C(13)-C(14)-H(14)	120.0(2)
C(13)-C(14)-C(15)	119.9(3)	H(14)-C(14)-C(15)	120.0(2)
C(14)-C(15)-H(15)	119.4(2)	C(14)-C(15)-C(16)	121.2(3)
H(15)-C(15)-C(16)	119.4(2)	C(11)-C(16)-C(15)	119.0(3)
C(11)-C(16)-H(16)	120.5(2)	C(15)-C(16)-H(16)	120.5(2)
P-C(21)-C(22)	121.2(2)	P-C(21)-C(26)	120.0(2)
C(22)-C(21)-C(26)	118.7(2)	C(21)-C(22)-H(22)	119.8(2)
C(21)-C(22)-C(23)	120.2(3)	H(22)-C(22)-C(23)	120.0(2)
C(22)-C(23)-H(23)	119.8(2)	C(22)-C(23)-C(24)	120.4(3)
H(23)-C(23)-C(24)	119.8(2)	C(23)-C(24)-H(24)	120.0(2)
C(23)-C(24)-C(25)	119.9(3)	H(24)-C(24)-C(25)	120.2(2)
C(24)-C(25)-H(25)	119.7(2)	C(24)-C(25)-C(26)	120.2(3)
H(25)-C(25)-C(26)	120.1(2)	C(21)-C(26)-C(25)	120.5(3)
C(21)-C(26)-H(26)	119.7(2)	C(25)-C(26)-H(26)	119.8(2)
P-C(31)-C(32)	119.8(2)	P-C(31)-C(36)	120.6(2)
C(32)-C(31)-C(36)	119.5(2)	C(31)-C(32)-H(32)	119.8(2)
C(31)-C(32)-C(33)	120.3(3)	H(32)-C(32)-C(33)	119.9(2)
C(32)-C(33)-H(33)	120.0(2)	C(32)-C(33)-C(34)	120.1(3)
H(33)-C(33)-C(34)	119.8(2)	C(33)-C(34)-H(34)	119.8(2)
C(33)-C(34)-C(35)	120.4(3)	H(34)-C(34)-C(35)	119.8(2)
C(34)-C(35)-H(35)	119.7(2)	C(34)-C(35)-C(36)	120.8(4)
H(35)-C(35)-C(36)	119.6(2)	C(31)-C(36)-C(35)	118.9(3)
C(31)-C(36)-H(36)	120.4(2)	C(35)-C(36)-H(36)	120.7(2)

TABLE 4. Anisotropic Thermal Parameters ($Å^2x10^3$) for 1.8(akd).

Atom	U_{11}	U_{22}	U_{33}	U_{23}	U_{13}	U_{12}
P	26(1)	18(1)	24(1)	-1(1)	4(1)	-3(1)
O(1)	45(1)1	8(1)	47(1)	3(1)	-3(1)	-1(1)
O(5)	39(1)	33(1)	37(1)	-3(1)	-3(1)	6(1)
O(3)	48(1)	24(1)	41(1)	6(1)	-11(1)	-9(1)
O(4)	49(1)	27(1)	32(1)	-5(1)	5(1)	-2(1)
O(2)	47(1)	22(1)	27(1)	5(1)	1(1)	-4(1)
C(1)	24(1)	21(1)	33(1)	3(1)	4(1)	-3(1)
C(2)	28(1)	15(1)	28(1)	-0(1)	5(1)	-0(1)
C(3)	26(1)	23(1)	33(1)	-2(1)	8(1)	-4(1)
C(4)	29(1)	22(1)	33(1)	-5(1)	4(1)	-3(1)
C(5)	34(1)	22(1)	34(1)	-0(1)	3(1)	-5(1)
C(6)	32(1)	25(1)	27(1)	-1(1)	8(1)	-5(1)
C(7)	27(1)	22(1)	29(1)	2(1)	6(1)	-7(1)
C(8)	48(2)	43(2)	37(2)	13(1)	-6(1)	-4(1)
C(9)	67(2)	62(2)	37(2)	9(2)	-8(2)	-16(2)
C(11)	23(1)	18(1)	21(1)	-2(1)	0(1)	-0(1)
C(12)	32(1)	16(1)	31(1)	-2(1)	5(1)	-1(1)
C(13)	31(1)	27(2)	36(2)	1(1)	10(1)	-2(1)
C(14)	33(2)	28(1)	30(1)	-3(1)	4(1)	7(1)
C(15)	41(2)	18(1)	33(2)	-2(1)	3(1)	6(1)
C(16)	33(1)	19(1)	28(1)	4(1)	3(1)	0(1)
C(21)	25(1)	21(1)	31(1)	1(1)	5(1)	-5(1)
C(22)	31(1)	37(2)	32(1)	-7(1)	4(1)	-2(1)
C(23)	36(2)	53(2)	37(2)	-10(2)	-1(1)	-7(1)
C(24)	28(1)	49(2)	57(2)	5(2)	-4(1)	-6(1)
C(25)	29(2)	38(2)	73(2)	1(2)	8(2)	3(1)
C(26)	32(1)	26(2)	55(2)	-4(1)	6(1)	-2(1)
C(31)	45(2)	17(1)	23(1)	-2(1)	6(1)	-11(1)
C(32)	59(2)	24(1)	26(1)	2(1)	0(1)	-6(1)
C(33)	96(3)	29(2)	31(2)	4(1)	-3(2)	-12(2)
C(34)	118(4)	55(2)	24(2)	8(2)	2(2)	-36(3)
C(35)	88(3)	84(3)	38(2)	-0(2)	26(2)	-43(2)
C(36)	53(2)	50(2)	32(2)	-4(1)	12(1)	-21(2)

The anisotropic temperature factor exponent takes the form:
$-2\pi^2(h^2a^{*2}U_{11} + k^2b^{*2}U_{22} + ...+ 2hka^*b^*U_{12})$

TABLE 5. Hydrogen Coordinates ($x10^4$) and Temperature Factors ($Å^2x10^3$) for 1.8(akd).

Atom	x	y	z	U
H(5)	-603(12)	-714(40)	-144(20)	76(11)
H(4A)	813	-184	3645	33
H(4B)	1144	-2402	1332	33
H(5A)	562	-2287	2142	35
H(5B)	420	-3337	1448	35
H(6A)	130	-394	1474	34
H(6B)	-159	-1687	1777	34
H(8A)	1375	-1726	4146	51
H(8B)	1881	-1646	3954	51
H(9A)	1751	-563	5164	63
H(9B)	1475	676	4703	63
H(9C)	1994	496	4622	63
H(12)	648	1010	3094	33
H(13)	1352	118	3867	39
H(14)	1324	688	4024	38
H(15)	626	6158	3390	37
H(16)	1131	5096	2599	33
H(22)	1734	4057	3455	38
H(23)	2446	4361	4118	51
H(24)	3048	2839	3849	55
H(25)	2937	984	2931	52
H(26)	2222	621	2286	44
H(32)	738	3732	1258	42
H(33)	794	5197	171	61
H(34)	1484	5478	-335	72
H(35)	2127	4328	236	72
H(36)	2087	2855	1340	52

Crystal data for 1-ethoxycarbonyl-5-carboxy-2-oxopent-1-ylidenetriphenylphosphorane[2.24] ***1.8****(akc).*

$C_{27}H_{27}O_5P$. colourless, crystalised from ethyl acetate, crystal dimensions 0.44 x 0.22 x .056 mm. M = 462.49, monoclinic, space group $P2_{1/n}$, a = 9.563(5), b = 19.576(10), c = 13.207(9) Å, β = 109.15(4), U = 2335.7 $Å^3$, Z = 4, D_C = 1.32 g cm^{-1}, F(000) = 976, μ = 1.48 cm^{-1}. Using 1.2° ω-scans at scan rate of 4.88° min^{-1}, 5375 unique reflections were collected in the range of $4 < 2\theta < 45°$ and 3788 of these having $I > 3\sigma(I)$ were used in the structural analysis.

Data were recorded at 148 K on a Nicolet R3m four circle diffractometer using Mo - Kα radiation. Cell parameters were determined by least squares refinement of 25 accurately centred reflections in the range of $5 < 2\theta < 35°$. Crystal stability was monitored by recording 3 check reflections (1. 0 0 0, 2. 0 8 0, 3. 4 0 0) every 100 reflections and no significant variations were observed. Data were corrected for Lorentz-polarisation effects but not for absorption.

Direct methods revealed the position of the non-hydrogen atoms and the structure was refined by blocked cascade least-squares techniques. Hydrogen atoms were inserted at calculated positions using a riding model with thermal parameters equal to 1.2 U of their carrier atoms, H5 was located from a difference Fourier map and inserted at that position All non-hydrogen atoms were refined anisotropically (303 parameters). The refinement converged with, R = 0.047 and R_W = 0.050. The final difference fourier map showed no significant features. All programs used in the data collection and structure solution are contained in the SHELXTL (Version 4.1) package.[E5]

TABLE 1. Atomic Coordinates ($x10^4$) and Isotropic Thermal Parameters ($Å^2x10^3$) for 1.8(akc).

Atom	x	y	z	U
P(1)	1318(1)	9555(1)	2563(1)	16(1)*
O(1)	3526(4)	9606(2)	5647(2)	52(1)*
O(2)	2512(3)	10466(1)	4539(2)	32(1)*
O(3)	658(3)	8336(1)	3325(2)	28(1)*
O(4)	1969(3)	8271(1)	7548(2)	43(1)*
O(5)	3840(3)	7626(1)	8434(2)	35(1)*
C(11)	2162(3)	9011(2)	1823(2)	18(1)*
C(12)	3141(4)	8490(2)	2324(3)	23(1)*
C(13)	3861(4)	8116(2)	1754(3)	30(1)*
C(14)	3594(4)	8247(2)	685(3)	28(1)*
C(15)	2628(4)	8766(2)	176(3)	26(1)*
C(16)	1929(4)	9150(2)	748(2)	23(1)*
C(21)	-676(3)	9539(2)	1997(2)	19(1)*
C(22)	-1443(4)	9256(2)	1015(2)	22(1)*
C(23)	-2986(4)	9300(2)	630(3)	28(1)*
C(24)	-3737(4)	9623(2)	1215(3)	31(1)*
C(25)	-2978(4)	9914(2)	2192(3)	32(1)*
C(26)	-1451(4)	9868(2)	2585(3)	27(1)*
C(31)	1893(3)	10398(2)	2309(2)	18(1)*
C(32)	3393(3)	10507(2)	2465(3)	22(1)*
C(33)	3885(4)	11142(2)	2265(3)	28(1)*
C(34)	2891(4)	11672(2)	1903(3)	30(1)*
C(35)	1396(4)	11567(2)	1741(3)	28(1)*
C(36)	898(4)	10936(2)	1957(3)	23(1)*
C(1)	2731(4)	9800(2)	4777(3)	28(1)*
C(2)	1889(4)	9348(2)	3926(2)	21(1)*
C(3)	1375(4)	8698(2)	4106(3)	30(1)*
C(4)	1532(5)	8409(2)	5198(3)	46(2)*
C(5)	2837(6)	7965(3)	5588(3)	57(2)*
C(6)	2876(4)	7474(2)	6531(3)	34(1)*
C(7)	2845(4)	7828(2)	7531(3)	26(1)*
C(8)	3458(5)	10932(2)	5312(3)	48(2)*
C(9)	3065(6)	11628(2)	4920(4)	53(2)*

*Equivalent isotropic U defined as one third of the trace of the orthogonalised U_{ij} tensor

Table 2. Bond lengths (Å) for 1.8(akc).

P(1)-C(11)	1.805(4)	P(1)-C(21)	1.806(3)
P(1)-C(31)	1.805(3)	P(1)-C(2)	1.749(3)
O(1)-C(1)	1.213(4)	O(2)-C(1)	1.341(4)
O(2)-C(8)	1.445(4)	O(3)-C(3)	1.254(4)
O(4)-C(7)	1.210(5)	O(5)-H(5)	0.855(51)
O(5)-C(7)	1.318(4)	C(11)-C(12)	1.395(4)
C(11)-C(16)	1.390(4)	C(12)-H(12)	0.960(1)
C(12)-C(13)	1.386(6)	C(13)-H(13)	0.960(1)
C(13)-C(14)	1.374(5)	C(14)-H(14)	0.960(1)
C(14)-C(15)	1.390(5)	C(15)-H(15)	0.960(1)
C(15)-C(16)	1.383(5)	C(16)-H(16)	0.960(1)
C(21)-C(22)	1.380(4)	C(21)-C(26)	1.394(5)
C(22)-H(22)	0.960(1)	C(22)-C(23)	1.396(5)
C(23)-H(23)	0.960(1)	C(23)-C(24)	1.370(6)
C(24)-H(24)	0.960(1)	C(24)-C(25)	1.379(5)
C(25)-H(25)	0.960(1)	C(25)-C(26)	1.383(5)
C(26)-H(26)	0.960(1)	C(31)-C(32)	1.397(5)
C(31)-C(36)	1.392(4)	C(32)-H(32)	0.960(1)
C(32)-C(33)	1.386(5)	C(33)-H(33)	0.960(1)
C(33)-C(34)	1.382(5)	C(34)-H(34)	0.960(1)
C(34)-C(35)	1.390(5)	C(35)-H(35)	0.960(1)
C(35)-C(36)	1.386(5)	C(36)-H(36)	0.960(1)
C(1)-C(2)	1.450(4)	C(2)-C(3)	1.411(5)
C(3)-C(4)	1.510(5)	C(4)-H(4A)	0.960(1)
C(4)-H(4B)	0.960(1)	C(4)-C(5)	1.468(7)
C(5)-H(5A)	0.960(1)	C(5)-H(5B)	0.960(1)
C(5)-C(6)	1.564(6)	C(6)-H(6A)	0.960(1)
C(6)-H(6B)	0.960(1)	C(6)-C(7)	1.501(5)
C(8)-H(8A)	0.960(1)	C(8)-H(8B)	0.960(1)
C(8)-C(9)	1.461(6)	C(9)-H(9A)	0.960(1)
C(9)-H(9B)	0.960(1)	C(9)-H(9C)	0.960(1)

Table 3. Bond angles (°) for 1.8(akc).

C(11)-P(1)-C(21)	111.4(1)	C(11)-P(1)-C(31)	102.8(2)
C(21)-P(1)-C(31)	106.5(1)	C(11)-P(1)-C(2)	112.1(1)
C(21)-P(1)-C(2)	110.6(2)	C(31)-P(1)-C(2)	113.1(1)
C(1)-O(2)-C(8)	115.8(2)	H(5)-O(5)-C(7)	113.7(30)
P(1)-C(11)-C(12)	121.6(2)	P(1)-C(11)-C(16)	119.1(2)
C(12)-C(11)-C(16)	119.1(3)	C(11)-C(12)-H(12)	119.8(2)
C(11)-C(12)-C(13)	120.3(3)	H(12)-C(12)-C(13)	119.9(2)
C(12)-C(13)-H(13)	120.0(2)	C(12)-C(13)-C(14)	120.1(3)
H(13)-C(13)-C(14)	120.0(2)	C(13)-C(14)-H(14)	119.9(2)
C(13)-C(14)-C(15)	120.3(4)	H(14)-C(14)-C(15)	119.8(2)
C(14)-C(15)-C(15)	120.2(2)	C(14)-C(15)-C(16)	119.8(3)
H(15)-C(15)-C(16)	120.1(2)	C(11)-C(16)-C(15)	120.5(3)

Table 3.(cont.) Bond angles (°) for 1.8(akc).

C(11)-C(16)-H(16)	119.8(2)	C(15)-C(16)-H(16)	119.8(2)
P(1)-C(21)-C(22)	124.0(3)	P(1)-C(21)-C(26)	116.3(2)
C(22)-C(21)-C(26)	119.6(3)	C(21)-C(22)-H(22)	120.3(2)
C(21)-C(22)-C(23)	119.3(3)	H(22)-C(22)-C(23)	120.4(2)
C(22)-C(23)-H(23)	119.6(2)	C(22)-C(23)-C(24)	120.7(3)
H(23)-C(23)-C(24)	119.7(2)	C(23)-C(24)-H(24)	119.9(2)
C(23)-C(24)-C(25)	120.4(3)	H(24)-C(24)-C(25)	119.7(2)
C(24)-C(25)-H(25)	120.4(2)	C(24)-C(25)-C(26)	119.4(4)
H(25)-C(25)-C(26)	120.2(2)	C(21)-C(26)-C(25)	120.7(3)
C(21)-C(26)-H(26)	119.6(2)	C(25)-C(26)-H(26)	119.7(2)
P(1)-C(31)-C(32)	118.2(2)	P(1)-C(31)-C(36)	122.5(2)
C(32)-C(31)-C(36)	119.3(3)	C(31)-C(32)-H(32)	119.9(2)
C(31)-C(32)-C(33)	120.4(3)	H(32)-C(32)-C(33)	119.8(2)
C(32)-C(33)-H(33)	120.1(2)	C(32)-C(33)-C(34)	120.1(3)
H(33)-C(33)-C(34)	119.8(2)	C(33)-C(34)-H(34)	120.1(2)
C(33)-C(34)-C(35)	119.9(3)	H(34)-C(34)-C(35)	120.0(2)
C(34)-C(35)-H(35)	119.7(2)	C(34)-C(35)-C(36)	120.4(3)
H(35)-C(35)-C(36)	119.9(2)	C(31)-C(36)-C(35)	120.0(3)
C(31)-C(36)-H(36)	120.0(2)	C(35)-C(36)-H(36)	120.0(2)
O(1)-C(1)-O(2)	121.9(3)	O(1)-C(1)-C(2)	124.0(3)
O(2)-C(1)-C(2)	114.1(3)	P(1)-C(2)-C(1)	124.2(3)
P(1)-C(2)-C(3)	112.0(2)	C(1)-C(2)-C(3)	123.7(3)
O(3)-C(3)-C(2)	119.8(3)	O(3)-C(3)-C(4)	115.4(3)
C(2)-C(3)-C(4)	124.6(3)	C(3)-C(4)-H(4A)	109.2(2)
C(3)-C(4)-H(4B)	108.9(2)	H(4A)-C(4)-H(4B)	109.5(1)
C(3)-C(4)-C(5)	111.3(4)	H(4A)-C(4)-C(5)	108.5(3)
H(4B)-C(4)-C(5)	109.5(2)	C(4)-C(5)-H(5A)	108.3(2)
C(4)-C(5)-H(5B)	107.4(3)	H(5A)-C(5)-H(5B)	109.5(1)
C(4)-C(5)-C(6)	116.0(5)	H(5A)-C(5)-C(6)	108.0(2)
H(5B)-C(5)-C(6)	107.5(2)	C(5)-C(6)-H(6A)	108.7(3)
C(5)-C(6)-H(6B)	107.6(2)	H(6A)-C(6)-H(6B)	109.5(1)
C(5)-C(6)-C(7)	114.5(3)	H(6A)-C(6)-C(7)	108.2(2)
H(6B)-C(6)-C(7)	108.2(2)	O(4)-C(7)-O(5)	119.8(3)
O(4)-C(7)-C(6)	124.0(3)	O(5)-C(7)-C(6)	116.2(3)
O(2)-C(8)-H(8A)	109.9(2)	O(2)-C(8)-H(8B)	109.9(2)
H(8A)-C(8)-H(8B)	109.5(1)	O(2)-C(8)-C(9)	108.0(3)
H(8A)-C(8)-C(9)	109.8(3)	H(8B)-C(8)-C(9)	109.7(3)
C(8)-C(9)-H(9A)	109.6(2)	C(8)-C(9)-H(9B)	109.3(3)
H(9A)-C(9)-H(9B)	109.5(1)	C(8)-C(9)-H(9C)	109.5(3)
H(9A)-C(9)-H(9C)	109.5(1)	H(9B)-C(9)-H(9C)	109.5(1)

TABLE 4. Anisotropic Thermal Parameters ($Å^2x10^3$) for 1.8(akc).

Atom	U_{11}	U_{22}	U_{33}	U_{23}	U_{13}	U_{12}
P(1)	15(1)	18(1)	13(1)	-0(1)	4(1)	1(1)
O(1)	69(2)	47(2)	21(1)	-8(1)	-11(1)	11(2)
O(2)	47(1)	22(1)	22(1)	-6(1)	6(1)	-3(1)
O(3)	40(1)	23(1)	27(1)	-2(1)	18(1)	-3(1)
O(4)	53(2)	47(2)	27(1)	3(1)	11(1)	25(1)
O(5)	38(1)	44(2)	20(1)	2(1)	8(1)	20(1)
C(11)	18(1)	20(2)	19(1)	-4(1)	8(1)	-2(1)
C(12)	28(2)	24(2)	21(2)	4(1)	11(1)	2(1)
C(13)	35(2)	27(2)	33(2)	4(1)	17(2)	10(2)
C(14)	31(2)	27(2)	32(2)	-9(1)	18(2)	-2(1)
C(15)	28(2)	35(2)	19(2)	-4(1)	12(1)	-2(1)
C(16)	23(2)	27(2)	17(1)	1(1)	6(1)	1(1)
C(21)	17(1)	19(1)	20(1)	3(1)	6(1)	-2(1)
C(22)	24(2)	22(2)	20(1)	1(1)	6(1)	-1(1)
C(23)	23(2)	33(2)	21(2)	4(1)	-2(1)	-4(1)
C(24)	16(1)	37(2)	36(2)	10(2)	6(1)	1(1)
C(25)	21(2)	40(2)	36(2)	3(2)	12(1)	5(2)
C(26)	21(2)	37(2)	25(2)	-3(1)	9(1)	3(1)
C(31)	21(1)	19(1)	14(1)	-1(1)	4(1)	1(1)
C(32)	23(2)	18(2)	25(2)	0(1)	7(1)	3(1)
C(33)	26(2)	28(2)	30(2)	-2(1)	9(1)	-5(1)
C(34)	42(2)	20(2)	27(2)	-1(1)	11(2)	-6(2)
C(35)	29(2)	22(2)	27(2)	2(1)	3(1)	4(1)
C(36)	22(2)	23(2)	22(2)	-2(1)	3(1)	2(1)
C(1)	34(2)	31(2)	17(1)	-2(1)	5(1)	6(2)
C(2)	24(2)	23(2)	15(1)	2(1)	5(1)	4(1)
C(3)	47(2)	26(2)	19(2)	1(1)	16(2)	5(2)
C(4)	79(3)	32(2)	28(2)	3(2)	18(2)	5(2)
C(5)	79(3)	64(3)	25(2)	-6(2)	13(2)	24(3)
C(6)	50(2)	27(2)	19(2)	-0(1)	3(2)	14(2)
C(7)	30(2)	26(2)	20(2)	3(1)	7(1)	3(1)
C(8)	64(3)	35(2)	35(2)	-16(2)	3(2)	-12(2)
C(9)	70(3)	35(2)	48(3)	-11(2)	11(2)	-7(2)

The anisotropic temperature factor exponent takes the form:
$-2\pi^2(h^2a^{*2}U_{11} + k^2b^{*2}U_{22} + ...+ 2hka^*b^*U_{12})$

TABLE 5. Hydrogen Coordinates ($x10^4$) and Temperature Factors ($Å^2x10^3$) for 1.8(akc).

Atom	x	y	z	U
H(5)	4363(52)	7289(24)	8357(38)	65(15)
H(12)	3319	8393	3068	28
H(13)	4546	7763	2106	35
H(14)	4077	7980	288	35
H(15)	2445	8858	-571	31
H(16)	1279	9516	400	27
H(22)	-921	9029	603	27
H(23)	-3525	9102	-52	32
H(24)	-4798	9648	944	37
H(25)	-3503	10149	2596	38
H(26)	-919	10061	3271	33
H(32)	4087	10140	2714	27
H(33)	4918	11216	2376	34
H(34)	3232	12112	1764	35
H(35)	705	11933	1476	33
H(36)	-131	10870	1865	28
H(4A)	669	8143	5152	57
H(4B)	1619	8779	5692	57
H(5A)	2895	7692	4999	69
H(5B)	3691	8256	5833	69
H(6A)	3760	7203	6706	43
H(6B)	2025	7182	6287	43
H(8A)	3314	10876	5993	59
H(8B)	4476	10845	5389	59
H(9A)	3683	11947	5420	64
H(9B)	2047	11712	4846	64
H(9C)	3204	11680	4237	64

Crystal data for 1-ethoxycarbonyl-5-carboxy-4,4-dimethyl-2-oxopentan-1-ylidenetriphenylphosphorane[2.24] ***1.9****(aki).*

$C_{29}H_{31}O_5P$. colourless, crystalised from ethyl acetate, crystal dimensions 0.5 x 0.4 x 0.3 mm. M = 490.5, triclinic, space group $P\bar{1}$, a = 11.678(7), b = 15.505(9), c = 15.845(9) Å, α = 66.80(5), β = 87.59(5), γ = 78.57(5)°, V= 2582(3) $Å^3$, Z = 4, D_C = 1.26 g cm^{-3}, F(000) = 1040. Using 1.4° ω-scans at scan rate of 4.88° min^{-1}, 9058 unique reflections were collected in the range of $4 < 2\theta < 50°$ and 5305 of these having $I > 3\sigma(I)$ were used in the structural analysis.

Data were recorded at 148 K on a Nicolet R3m four circle diffractometer using Mo - Kα radiation. Cell parameters were determined by least squares refinement of 25 accurately centred reflections in the range of $5 < 2\theta < 35°$. Crystal stability was monitored by recording 3 check reflections (1. 0 0 6, 2. 0 9 0, 3. 3 0 0) every 100 reflections and no significant variations were observed. Data were corrected for Lorentz-polarisation effects but not for absorption.

Direct methods revealed the position of the non-hydrogen atoms and the structure was refined by blocked cascade least-squares techniques. Hydrogen atoms were inserted at calculated positions using a riding model with thermal parameters equal to 1.2 U of their carrier atoms, H5 was located from a difference Fourier map and inserted at that position All non-hydrogen atoms, excluding the phenyl carbons, were refined anisotropically (566 parameters). The refinement converged with R = 0.070 and R_w = 0.053. The final difference fourier map showed no significant features. All programs used in the data collection and structure solution are contained in the SHELXTL (Version 4.1) package.[E5]

TABLE 1. Atomic Coordinates ($x10^4$) and Isotropic Thermal Parameters ($Å^2x10^3$) for 1.9(aki).

Atom	x	y	z	U
P	4384(1)	7199(1)	5982(1)	18(1)*
C(1)	3688(4)	6041(3)	7733(3)	29(2)*
C(2)	4638(4)	6279(3)	7093(3)	20(2)*
C(3)	5774(4)	5722(3)	7269(3)	20(2)*
C(4)	6168(4)	4866(3)	8158(3)	22(2)*
C(5)	7021(4)	4993(3)	8799(3)	20(2)*
C(6)	8121(4)	5331(3)	8317(3)	27(2)*
C(7)	8853(4)	4671(4)	7904(4)	32(3)*
C(8)	1626(4)	6176(5)	7838(4)	80(4)*
C(9)	634(5)	6379(5)	7287(5)	136(5)*
C(12)	5347(2)	6864(2)	4469(2)	26(2)*
C(13)	5397	6473	3809	35(3)*
C(14)	4566	5950	3782	37(3)*
C(15)	3684	5817	4416	34(3)*
C(16)	3633	6208	5076	26(2)*
C(11)	4465	6731	5103	20(2)*
C(22)	6117(3)	7951(2)	6460(2)	24(2)*
C(23)	6855	8604	6281	25(2)*
C(24)	6854	9317	5403	24(2)*
C(25)	6114	9377	4704	22(2)*
C(26)	5377	8725	4884	19(2)*
C(21)	5378	8011	5762	17(2)*
C(32)	2774(2)	8373(2)	6552(2)	27(2)*
C(33)	1680	8920	6577	30(2)*
C(34)	780	9050	5961	32(2)*
C(35)	975	8633	5318	31(2)*
C(36)	2068	8086	5293	23(2)*
C(31)	2968	7956	5909	19(2)*
O(1)	3779(3)	5724(3)	8558(2)	46(2)*
O(2)	2664(3)	6187(2)	7272(2)	37(2)*
O(3)	6503(3)	5912(2)	6627(2)	23(1)*
O(4)	9720(3)	4098(3)	8294(3)	50(2)*
O(5)	8488(3)	4775(2)	7081(2)	34(2)*
C(51)	7393(4)	4018(3)	9599(3)	30(2)*
C(52)	6407(4)	5732(3)	9175(3)	28(2)*

*Equivalent isotropic U defined as one third of the trace of the orthogonalised U_{ij} tensor

TABLE 1(cont). Atomic Coordinates (x10^4) and Isotropic Thermal Parameters (Å^{2}x10^3) for 1.9(aki).

Atom	x	y	z	U
P'	11796(1)	1494(1)	8113(1)	18(1)*
C(1')	10217(4)	1572(3)	9532(3)	21(2)*
C(2')	10535(4)	1300(3)	8770(3)	17(2)*
C(3')	9841(4)	888(3)	8386(3)	20(2)*
C(4')	8679(4)	624(3)	8762(3)	19(2)*
C(5')	7591(4)	1334(3)	8180(3)	20(2)*
C(6')	7639(4)	1525(3)	7146(3)	22(2)*
C(7')	7690(4)	647(3)	6944(3)	23(2)*
C(8')	10743(4)	2189(4)	10572(4)	37(3)*
C(9')	11817(5)	2304(5)	10948(4)	70(4)*
C(12')	10485(3)	3067(2)	6759(2)	32(2)*
C(13')	10130	3684	5856	40(3)*
C(14')	10648	3487	5125	42(3)*
C(15')	11520	2674	5296	35(3)*
C(16')	11875	2057	6198	26(2)*
C(11')	11358	2253	6930	21(2)*
C(22')	12561(3)	3078(2)	8149(2)	41(3)*
C(23')	13264	3514	8481	57(3)*
C(24')	14118	2954	9172	62(4)*
C(25')	14268	1959	9531	54(4)*
C(26')	13564	1523	9199	36(3)*
C(21')	12711	2082	8508	24(2)*
C(32')	13834(3)	436(2)	7747(2)	21(2)*
C(33')	14589	-408	7812	25(2)*
C(34')	14282	-1291	8313	30(2)*
C(35')	13219	-1329	8749	26(2)*
C(36')	12464	-485	8685	23(2)*
C(31')	12771	398	8184	18(2)*
O(1')	9278(3)	1560(2)	9893(2)	31(2)*
O(2')	11079(3)	1828(2)	9865(2)	27(2)*
O(3')	10202(3)	682(2)	7700(2)	23(1)*
O(4')	6843(3)	454(2)	6702(2)	31(2)*
O(5')	8729(3)	59(2)	7060(2)	26(2)*
C(51')	7433(4)	2308(3)	8257(3)	33(3)*
C(52')	6535(4)	879(4)	8578(3)	33(3)*

*Equivalent isotropic U defined as one third of the trace of the orthogonalised U_{ij} tensor

Table 2. Bond lengths (Å) for 1.9(aki).

P-C(2)	1.767(4)	P-C(11)	1.798(4)
P-C(21)	1.804(3)	P-C(31)	1.807(3)
C(1)-C(2)	1.473(7)	C(1)-O(1)	1.203(6)
C(1)-O(2)	1.361(6)	C(2)-C(3)	1.404(6)
C(3)-C(4)	1.515(5)	C(3)-O(3)	1.280(5)
C(4)-H(4A)	0.960(1)	C(4)-H(4B)	0.960(1)
C(4)-C(5)	1.544(8)	C(5)-C(6)	1.542(6)
C(5)-C(51)	1.536(5)	C(5)-C(52)	1.535(8)
C(6)-H(6A)	0.960(1)	C(6)-H(6B)	0.960(1)
C(6)-C(7)	1.530(8)	C(7)-O(4)	1.208(6)
C(7)-O(5)	1.327(7)	C(8)-H(8A)	0.960(1)
C(8)-H(8B)	0.960(1)	C(8)-C(9)	1.388(9)
C(8)-O(2)	1.477(6)	C(9)-H(9A)	0.960(1)
C(9)-H(9B)	0.960(1)	C(9)-H(9C)	0.960(1)
C(12)-C(13)	1.395(1)	C(12)-C(11)	1.395(1)
C(12)-H(12)	0.960(1)	C(13)-C(14)	1.395(1)
C(13)-H(13)	0.960(1)	C(14)-C(15)	1.395(1)
C(14)-H(14)	0.960(1)	C(15)-C(16)	1.395(1)
C(15)-H(15)	0.960(1)	C(16)-C(11)	1.395(1)
C(16)-H(16)	0.960(1)	C(22)-C(23)	1.395(1)
C(22)-C(21)	1.395(1)	C(22)-H(22)	0.960(1)
C(23)-C(24)	1.395(1)	C(23)-H(23)	0.960(1)
C(24)-C(25)	1.395(1)	C(24)-H(24)	0.960(1)
C(25)-C(26)	1.395(1)	C(25)-H(25)	0.960(1)
C(26)-C(21)	1.395(1)	C(26)-H(26)	0.960(1)
C(32)-C(33)	1.395(1)	C(32)-C(31)	1.395(1)
C(32)-H(32)	0.960(1)	C(33)-C(34)	1.395(1)
C(33)-H(33)	0.960(1)	C(34)-C(35)	1.395(1)
C(34)-H(34)	0.960(1)	C(35)-C(36)	1.395(1)
C(35)-H(35)	0.960(1)	C(36)-C(31)	1.395(1)
C(36)-H(36)	0.960(1)	O(5)-H(5)	0.932(24)
C(51)-H(51A)	0.960(1)	C(51)-H(51B)	0.960(1)
C(51)-H(51C)	0.960(1)	C(52)-H(52A)	0.960(1)
C(52)-H(52B)	0.960(1)	C(52)-H(53C)	0.960(1)
P'-C(2')	1.773(4)	P'-C(11')	1.808(3)
P'-C(21')	1.805(4)	P'-C(31')	1.814(3)
C(1')-C(2')	1.440(8)	C(1')-O(1')	1.216(6)
C(1')-O(2')	1.347(7)	C(2')-C(3')	1.410(8)
C(3')-C(4')	1.524(6)	C(3')-O(3')	1.282(6)
C(4')-H(4A')	0.960(1)	C(4')-H(4B')	0.960(1)
C(4')-C(5')	1.556(5)	C(5')-C(6')	1.546(7)
C(5')-C(51')	1.537(8)	C(5')-C(52')	1.532(7)
C(6')-H(6A')	0.960(1)	C(6')-H(6B')	0.960(1)
C(6')-C(7')	1.506(8)	C(7')-O(4')	1.207(7)
C(7')-O(5')	1.335(5)	C(8')-H(8A')	0.960(1)
C(8')-H(8B')	0.960(1)	C(8')-C(9')	1.481(9)
C(8')-O(2')	1.446(7)	C(9')-H(9A')	0.960(1)
C(9')-H(9B')	0.960(1)	C(9')-H(9C')	0.960(1)
C(12')-C(13')	1.395(1)	C(12')-C(11')	1.395(1)
C(12')-H(12')	0.960(1)	C(13')-C(14')	1.395(1)
C(13')-H(13')	0.960(1)	C(14')-C(15')	1.395(1)
C(14')-H(14')	0.960(1)	C(15')-C(16')	1.395(1)
C(15')-H(15')	0.960(1)	C(16')-C(11')	1.395(1)
C(16')-H(16')	0.960(1)	C(22')-C(23')	1.395(1)

Table 2.(cont) Bond lengths (Å) for 1.9(aki).

C(22')-C(21')	1.395(1)	C(22')-H(22')	0.960(1)
C(23')-C(24')	1.395(1)	C(23')-H(23')	0.960(1)
C(24')-C(25')	1.395(1)	C(24')-H(24')	0.960(1)
C(25')-C(26')	1.395(1)	C(25')-H(25')	0.960(1)
C(26')-C(21')	1.395(1)	C(26')-H(26')	0.960(1)
C(32')-C(33')	1.395(1)	C(32')-C(31')	1.395(1)
C(32')-H(32')	0.960(1)	C(33')-C(34')	1.395(1)
C(33')-H(33')	0.960(1)	C(34')-C(35')	1.395(1)
C(34')-H(34')	0.960(1)	C(35')-C(36')	1.395(1)
C(35')-H(35')	0.960(1)	C(36')-C(31')	1.395(1)
C(36')-H(36')	0.960(1)	O(5')-H(5')	0.932(51)
C(51')-H(51A)	0.960(1)	C(51')-H(51B)	0.960(1)
C(51')-H(51C)	0.960(1)	C(52')-H(52A)	0.960(1)
C(52')-H(52B)	0.960(1)	C(52')-H(52C)	0.960(1)

Table 3. Bond angles (°) for 1.9(aki).

C(2)-P-C(11)	112.0(2)	C(2)-P-C(21)	111.5(2)
C(11)-P-C(21)	110.3(1)	C(2)-P-C(31)	109.7(2)
C(11)-P-C(31)	109.8(2)	C(21)-P-C(31)	103.2(2)
C(2)-C(1)-O(1)	126.2(5)	C(2)-C(1)-O(2)	111.0(4)
O(1)-C(1)-O(2)	122.7(4)	P-C(2)-C(1)	122.1(3)
P-C(2)-C(3)	114.7(3)	C(1)-C(2)-C(3)	122.8(3)
C(2)-C(3)-C(4)	123.7(4)	C(2)-C(3)-O(3)	118.4(3)
C(4)-C(3)-O(3)	117.8(4)	C(3)-C(4)-H(4A)	107.8(2)
C(3)-C(4)-H(4B)	107.6(3)	H(4A)-C(4)-H(4B)	109.5(1)
C(3)-C(4)-C(5)	116.4(4)	H(4A)-C(4)-C(5)	107.7(2)
H(4B)-C(4)-C(5)	107.6(2)	C(4)-C(5)-C(6)	113.1(4)
C(4)-C(5)-C(51)	107.3(4)	C(6)-C(5)-C(51)	109.0(3)
C(4)-C(5)-C(52)	110.1(4)	C(6)-C(5)-C(52)	107.8(4)
C(51)-C(5)-C(52)	109.5(4)	C(5)-C(6)-H(6A)	108.1(3)
C(5)-C(6)-H(6B)	108.0(2)	H(6A)-C(6)-H(6B)	109.5(1)
C(5)-C(6)-C(7)	115.0(5)	H(6A)-C(6)-C(7)	108.1(3)
H(6B)-C(6)-C(7)	108.0(2)	C(6)-C(7)-O(4)	122.3(5)
C(6)-C(7)-O(5)	115.9(4)	O(4)-C(7)-O(5)	121.8(6)
H(8A)-C(8)-H(8B)	109.5(1)	H(8A)-C(8)-C(9)	109.8(5)
H(8B)-C(8)-C(9)1	09.4(4)	H(8A)-C(8)-O(2)	110.1(4)
H(8B)-C(8)-O(2)	109.2(3)	C(9)-C(8)-O(2)	108.8(5)
C(8)-C(9)-H(9A)	109.4(4)	C(8)-C(9)-H(9B)	109.7(5)
H(9A)-C(9)-H(9B)	109.5(1)	C(8)-C(9)-H(9C)	109.3(4)
H(9A)-C(9)-H(9C)	109.5(1)	H(9B)-C(9)-H(9C)	109.5(1)
C(13)-C(12)-C(11)	120.0(1)	C(13)-C(12)-H(12)	120.0(1)
C(11)-C(12)-H(12)	120.0(1)	C(12)-C(13)-C(14)	120.0(1)
C(12)-C(13)-H(13)	120.0(1)	C(14)-C(13)-H(13)	120.0(1)
C(13)-C(14)-C(15)	120.0(1)	C(13)-C(14)-H(14)	120.0(1)
C(15)-C(14)-H(14)	120.0(1)	C(14)-C(15)-C(16)	120.0(1)
C(14)-C(15)-H(15)	120.0(1)	C(16)-C(15)-H(15)	120.0(1)

Table 3.(cont.) Bond angles (°) for 1.9(aki).

C(15)-C(16)-C(11)	120.0(1)	C(15)-C(16)-H(16)	120.0(1)
C(11)-C(16)-H(16)	120.0(1)	P-C(11)-C(12)	121.5(1)
P-C(11)-C(16)	118.5(1)	C(12)-C(11)-C(16)	120.0(1)
C(23)-C(22)-C(21)	120.0(1)	C(23)-C(22)-H(22)	120.0(1)
C(21)-C(22)-H(22)	120.0(1)	C(22)-C(23)-C(24)	120.0(1)
C(22)-C(23)-H(23)	120.0(1)	C(24)-C(23)-H(23)	120.0(1)
C(23)-C(24)-C(25)	120.0(1)	C(23)-C(24)-H(24)	120.0(1)
C(25)-C(24)-H(24)	120.0(1)	C(24)-C(25)-C(26)	120.0(1)
C(24)-C(25)-H(25)	120.0(1)	C(26)-C(25)-H(25)	120.0(1)
C(25)-C(26)-C(21)	120.0(1)	C(25)-C(26)-H(26)	120.0(1)
C(21)-C(26)-H(26)	120.0(1)	P-C(21)-C(22)	121.0(1)
P-C(21)-C(26)	119.0(1)	C(22)-C(21)-C(26)	120.0(1)
C(33)-C(32)-C(31)	120.0(1)	C(33)-C(32)-H(32)	120.0(1)
C(31)-C(32)-H(32)	120.0(1)	C(32)-C(33)-C(34)	120.0(1)
C(32)-C(33)-H(33)	120.0(1)	C(34)-C(33)-H(33)	120.0(1)
C(33)-C(34)-C(35)	120.0(1)	C(33)-C(34)-H(34)	120.0(1)
C(35)-C(34)-H(34)	120.0(1)	C(34)-C(35)-C(36)	120.0(1)
C(34)-C(35)-H(35)	120.0(1)	C(36)-C(35)-H(35)	120.0(1)
C(35)-C(36)-C(31)	120.0(1)	C(35)-C(36)-H(36)	120.0(1)
C(31)-C(36)-H(36)	120.0(1)	P-C(31)-C(32)	116.4(1)
P-C(31)-C(36)	123.4(1)	C(32)-C(31)-C(36)	120.0(1)
C(1)-O(2)-C(8)	114.0(4)	C(7)-O(5)-H(5)	123.9(26)
C(5)-C(51)-H(51A)	109.6(3)	C(5)-C(51)-H(51B)	109.6(3)
H(51A)-C(51)-H(51B)	109.5(1)	C(5)-C(51)-H(51C)	109.2(2)
H(51A)-C(51)-H(51C)	109.5(1)	H(51B)-C(51)-H(51C)	109.5(1)
C(5)-C(52)-H(52A)	109.4(3)	C(5)-C(52)-H(52B)	109.4(2)
H(52A)-C(52)-H(52B)	109.5(1)	C(5)-C(52)-H(53C)	109.7(3)
H(52A)-C(52)-H(53C)	109.5(1)	H(52B)-C(52)-H(53C)	109.5(1)
C(2')-P'-C(11')	109.4(2)	C(2')-P'-C(21')	112.4(2)
C(11')-P'-C(21')	107.3(2)	C(2')-P'-C(31')	113.6(2)
C(11')-P'-C(31')	110.4(2)	C(21')-P'-C(31')	103.5(2)
C(2')-C(1')-O(1')	125.7(5)	C(2')-C(1')-O(2')	114.5(4)
O(1')-C(1')-O(2')	119.8(5)	P'-C(2')-C(1')	126.4(4)
P'-C(2')-C(3')	108.7(4)	C(1')-C(2')-C(3')	124.8(4)
C(2')-C(3')-C(4')	123.9(5)	C(2')-C(3')-O(3')	119.8(4)
C(4')-C(3')-O(3')	116.2(5)	C(3')-C(4')-H(4A')	108.3(3)
C(3')-C(4')-H(4B')	108.4(3)	H(4A')-C(4')-H(4B')	109.5(1)
C(3')-C(4')-C(5')	113.8(3)	H(4A')-C(4')-C(5')	108.4(3)
H(4B')-C(4')-C(5')	108.4(3)	C(4')-C(5')-C(6')	113.8(4)
C(4')-C(5')-C(51')	111.3(4)	C(6')-C(5')-C(51')	107.3(3)
C(4')-C(5')-C(52')	106.0(3)	C(6')-C(5')-C(52')	109.1(4)
C(51')-C(5')-C(52')	109.2(4)	C(5')-C(6')-H(6A')	108.1(3)
C(5')-C(6')-H(6B')	108.4(2)	H(6A')-C(6')-H(6B')	109.5(1)
C(5')-C(6')-C(7')	114.0(3)	H(6A')-C(6')-C(7')	108.5(2)
H(6B')-C(6')-C(7')	108.2(2)	C(6')-C(7')-O(4')	123.0(4)
C(6')-C(7')-O(5')	117.2(4)	O(4')-C(7')-O(5')	119.8(5)
H(8A')-C(8')-H(8B')	109.5(1)	H(8A')-C(8')-C(9')	109.6(3)
H(8B')-C(8')-C(9')	110.0(3)	H(8A')-C(8')-O(2')	110.0(2)
H(8B')-C(8')-O(2')	109.8(3)	C(9')-C(8')-O(2')	107.9(4)
C(8')-C(9')-H(9A')	109.6(4)	C(8')-C(9')-H(9B')	109.6(3)
H(9A')-C(9')-H(9B')	109.5(1)	C(8')-C(9')-H(9C')	109.2(3)
H(9A')-C(9')-H(9C')	109.5(1)	H(9B')-C(9')-H(9C')	109.5(1)
C(13')-C(12')-C(11')	120.0(1)	C(13')-C(12')-H(12')	120.0(1)
C(11')-C(12')-H(12')	120.0(1)	C(12')-C(13')-C(14')	120.0(1)

Table 3.(cont.) Bond angles (°) for 1.9(aki).

C(12')-C(13')-H(13')	120.0(1)	C(14')-C(13')-H(13')	120.0(1)
C(13')-C(14')-C(15')	120.0(1)	C(13')-C(14')-H(14')	120.0(1)
C(15')-C(14')-H(14')	120.0(1)	C(14')-C(15')-C(16')	120.0(1)
C(14')-C(15')-H(15')	120.0(1)	C(16')-C(15')-H(15')	120.0(1)
C(15')-C(16')-C(11')	120.0(1)	C(15')-C(16')-H(16')	120.0(1)
C(11')-C(16')-H(16')	120.0(1)	P'-C(11')-C(12')	117.9(1)
P'-C(11')-C(16')	122.1(1)	C(12')-C(11')-C(16')	120.0(1)
C(23')-C(22')-C(21')	120.0(1)	C(23')-C(22')-H(22')	120.0(1)
C(21')-C(22')-H(22')	120.0(1)	C(22')-C(23')-C(24')	120.0(1)
C(22')-C(23')-H(23')	120.0(1)	C(24')-C(23')-H(23')	120.0(1)
C(23')-C(24')-C(25')	120.0(1)	C(23')-C(24')-H(24')	120.0(1)
C(25')-C(24')-H(24')	120.0(1)	C(24')-C(25')-C(26')	120.0(1)
C(24')-C(25')-H(25')	120.0(1)	C(26')-C(25')-H(25')	120.0(1)
C(25')-C(26')-C(21')	120.0(1)	C(25')-C(26')-H(26')	120.0(1)
C(21')-C(26')-H(26')	120.0(1)	P'-C(21')-C(22')	121.3(1)
P'-C(21')-C(26')	118.7(1)	C(22')-C(21')-C(26')	120.0(1)
C(33')-C(32')-C(31')	120.0(1)	C(33')-C(32')-H(32')	120.0(1)
C(31')-C(32')-H(32')	120.0(1)	C(32')-C(33')-C(34')	120.0(1)
C(32')-C(33')-H(33')	120.0(1)	C(34')-C(33')-H(33')	120.0(1)
C(33')-C(34')-C(35')	120.0(1)	C(33')-C(34')-H(34')	120.0(1)
C(35')-C(34')-H(34')	120.0(1)	C(34')-C(35')-C(36')	120.0(1)
C(34')-C(35')-H(35')	120.0(1)	C(36')-C(35')-H(35')	120.0(1)
C(35')-C(36')-C(31')	120.0(1)	C(35')-C(36')-H(36')	120.0(1)
C(31')-C(36')-H(36')	120.0(1)	P'-C(31')-C(32')	120.1(1)
P'-C(31')-C(36')	119.9(1)	C(32')-C(31')-C(36')	120.0(1)
C(1')-O(2')-C(8')	115.2(4)	C(7')-O(5')-H(5')	106.1(27)
C(5')-C(51')-H(51A)	109.2(2)	C(5')-C(51')-H(51B)	109.6(2)
H(51A)-C(51')-H(51B)	109.5(1)	C(5')-C(51')-H(51C)	109.6(2)
H(51A)-C(51')-H(51C)	109.5(1)	H(51B)-C(51')-H(51C)	109.5(1)
C(5')-C(52')-H(52A)	109.3(2)	C(5')-C(52')-H(52B)	109.4(3)
H(52A)-C(52')-H(52B)	109.5(1)	C(5')-C(52')-H(52C)	109.7(3)
H(52A)-C(52')-H(52C)	109.5(1)	H(52B)-C(52')-H(52C)	109.5(1)

TABLE 4.(cont.) Anisotropic Thermal Parameters ($Å^2x10^3$) for 1.9(aki).

Atom	U_{11}	U_{22}	U_{33}	U_{23}	U_{13}	U_{12}
P	18(1)	18(1)	18(1)	-8(1)	4(1)	-4(1)
C(1)	24(3)	23(3)	28(3)	-0(3)	4(2)	-1(2)
C(2)	17(3)	21(3)	20(3)	-5(2)	6(2)	-8(2)
C(3)	24(3)	16(3)	23(3)	-10(2)	-1(2)	-6(2)
C(4)	22(3)	20(3)	22(3)	-8(2)	5(2)	-3(2)
C(5)	18(3)	25(3)	18(3)	-9(2)	0(2)	-4(2)
C(6)	23(3)	36(3)	27(3)	-17(3)	2(2)	-10(3)
C(7)	22(3)	41(4)	34(3)	-15(3)	8(3)	-6(3)
C(8)	32(4)	115(6)	61(5)	8(4)	11(4)	-36(4)
C(9)	49(5)	136(8)	138(8)	43(6)	29(5)	-40(5)
C(12)	36(3)	21(3)	22(3)	-12(2)	7(3)	-3(2)
C(13)	46(4)	32(3)	27(3)	-16(3)	9(3)	-3(3)
C(14)	54(4)	29(3)	24(3)	-12(3)	-12(3)	3(3)
C(15)	40(4)	23(3)	41(4)	-16(3)	-13(3)	-4(3)
C(16)	26(3)	19(3)	33(3)	-8(3)	-1(2)	-5(2)
C(11)	25(3)	16(3)	18(3)	-5(2)	-3(2)	-1(2)
C(22)	24(3)	23(3)	27(3)	-12(3)	4(2)	-2(2)
C(23)	27(3)	23(3)	30(3)	-14(3)	-1(2)	-7(2)
C(24)	22(3)	23(3)	30(3)	-15(3)4	(2)	-3(2)
C(25)	23(3)	21(3)	23(3)	-10(2)	11(2)	-2(2)
C(26)	21(3)	15(3)	20(3)	-8(2)	3(2)	1(2)
C(21)	17(3)	18(3)	22(3)	-11(2)	6(2)	-6(2)
C(32)	27(3)	27(3)	25(3)	-10(3)	5(2)	-5(2)
C(33)	34(3)	27(3)	27(3)	-13(3)	7(3)	-0(3)
C(34)	28(3)	25(3)	35(3)	-5(3)	6(3)	-2(2)
C(35)	24(3)	27(3)	30(3)	-2(3)	-1(2)	-1(2)
C(36)	20(3)	25(3)	25(3)	-10(2)	3(2)	-4(2)
C(31)	15(3)	15(3)	22(3)	-1(2)	8(2)	-5(2)
O(1)	30(2)	68(3)	22(2)	-3(2)	9(2)	-4(2)
O(2)	19(2)	44(2)	35(2)	2(2)	1(2)	-11(2)
O(3)	23(2)	22(2)	21(2)	-8(2)	6(2)	-3(2)
O(4)	27(2)	65(3)	49(3)	-24(2)	-5(2)	19(2)
O(5)	28(2)	44(2)	28(2)	-18(2)	2(2)	8(2)
C(51)	34(3)	25(3)	27(3)	-8(3)	2(3)	-1(3)
C(52)	29(3)	29(3)	29(3)	-16(3)	5(3)	-5(3)
P'	16(1)	20(1)	19(1)	-8(1)	4(1)	-7(1)
C(1')	22(3)	21(3)	16(3)	-5(2)	-1(2)	-1(2)
C(2')	14(3)	23(3)	16(3)	-9(2)	8(2)	-4(2)
C(3')	11(3)	17(3)	27(3)	-5(2)	0(2)	-0(2)
C(4')	19(3)	22(3)	24(3)	-13(2)	8(2)	-14(2)
C(5')	16(3)	21(3)	26(3)	-11(2)	3(2)	-5(2)
C(6')	20(3)	20(3)	25(3)	-8(2)	-1(2)	-1(2)
C(7')	28(3)	24(3)	17(3)	-7(2)	8(2)	-8(2)
C(8')	37(4)	57(4)	40(4)	-38(3)	17(3)	-22(3)
C(9')	68(5)	108(6)	83(5)	-79(5)	30(4)	-45(4)
C(12')	36(3)	27(3)	28(3)	-9(3)	14(3)	-4(3)
C(13')	48(4)	24(3)	28(3)	1(3)	7(3)	10(3)
C(14')	48(4)	46(4)	28(3)	-12(3)	8(3)	-9(3)
C(15')	34(4)	41(4)	24(3)	-11(3)	7(3)	-0(3)
C(16')	18(3)	32(3)	28(3)	-13(3)	5(2)	-6(2)
C(11')	21(3)	18(3)	21(3)	-4(2)	5(2)	-7(2)

TABLE 4.(cont.) Anisotropic Thermal Parameters ($Å^2x10^3$) for 1.9(aki).

Atom	U_{11}	U_{22}	U_{33}	U_{23}	U_{13}	U_{12}
C(22')	58(4)	37(4)	42(4)	-23(3)	20(3)	-30(3)
C(23')	82(5)	59(5)	58(5)	-38(4)	39(4)	-51(4)
C(24')	49(4)	104(6)	84(5)	-78(5)	42(4)	-54(4)
C(25')	20(3)	114(6)	61(4)	-68(5)	13(3)	-18(4)
C(26')	23(3)	62(4)	41(4)	-38(3)	7(3)	-10(3)
C(21')	19(3)	39(3)	29(3)	-23(3)	17(2)	-21(2)
C(32')	11(3)	30(3)	22(3)	-10(2)	2(2)	-8(2)
C(33')	14(3)	36(3)	27(3)	-15(3)	3(2)	-3(2)
C(34')	27(3)	30(3)	29(3)	-14(3)	-5(2)	7(3)
C(35')	25(3)	19(3)	32(3)	-7(3)	-2(2)	-6(2)
C(36')	19(3)	25(3)	25(3)	-9(3)	0(2)	-6(2)
C(31')	17(3)	21(3)	17(3)	-10(2)	3(2)	-3(2)
O(1')	24(2)	49(2)	31(2)	-24(2)	15(2)	-19(2)
O(2')	20(2)	45(2)	30(2)	-27(2)	9(2)	-14(2)
O(3')	18(2)	32(2)	24(2)	-17(2)	7(1)	-9(2)
O(4')	24(2)	47(2)	37(2)	-27(2)	4(2)	-18(2)
O(5')	21(2)	27(2)	38(2)	-22(2)	2(2)	-4(2)
C(51')	31(3)	31(3)	45(4)	-24(3)	-3(3)	-1(3)
C(52')	17(3)	48(4)	43(4)	-26(3)	9(3)	-9(3)

The anisotropic temperature factor exponent takes the form:
$-2\pi^2(h^2a^{*2}U_{11} + k^2b^{*2}U_{22} + ...+ 2hka^*b^*U_{12})$

TABLE 5. Hydrogen Coordinates ($x10^4$) and Temperature Factors ($Å^2x10^3$) for 1.9(aki).

Atom	x	y	z	U
H(4A)	5484	4707	8494	50
H(4B)	6547	4343	8001	50
H(6A)	8608	5386	8759	50
H(6B)	7877	5949	7830	50
H(8A)	1575	6646	8099	50
H(8B)	1687	5553	8323	50
H(9A)	-45	6368	7651	50
H(9B)	686	5909	7027	50
H(9C)	574	7002	6803	50
H(12)	5919	7224	4487	80
H(13)	6004	6564	3372	80
H(14)	4601	5681	3327	80
H(15)	3112	5457	4397	80

TABLE 5.(cont.) Hydrogen Coordinates ($x10^4$) and Temperature Factors ($Å^2x10^3$) for 1.9(aki).

Atom	x	y	z	U
H(16)	3026	6116	5512	80
H(22)	6118	7460	7065	80
H(23)	7364	8563	6762	80
H(24)	7361	9766	5279	80
H(25)	6113	9868	4100	80
H(26)	4868	8766	4403	80
H(32)	3393	8283	6976	80
H(33)	1546	9207	7019	80
H(34)	28	9427	5978	80
H(35)	356	8723	4894	80
H(36)	2202	7799	4850	80
H(5)	7825(21)	5211(23)	6761(24)	50
H(51A)	7924	4071	10014	50
H(51B)	7770	3553	9365	50
H(51C)	6713	3820	9919	50
H(52A)	5717	5537	9478	50
H(52B)	6193	6345	8676	50
H(53C)	6925	5776	9604	50
H(4A')	8667	401	8780	50
H(4B')	8626	609	9374	50
H(6A')	8321	1786	6912	50
H(6B')	6952	1984	6836	50
H(8A')	10216	2796	10316	50
H(8B')	10369	1744	11051	50
H(9A')	11618	2542	11421	50
H(9B')	12189	2748	10465	50
H(9C')	12342	1695	11201	50
H(12')	10129	3202	7262	80
H(13')	9530	4243	5739	80
H(14')	10403	3912	4504	80
H(15')	11876	2539	4793	80
H(16')	12476	1498	6316	80
H(22')	11974	3463	7673	80
H(23')	13161	4199	8234	80
H(24')	14602	3255	9401	80
H(25')	14855	1574	10007	80
H(26')	1366	8838	9446	80
H(32')	14045	1043	7403	80
H(33')	15320	-382	7512	80
H(34')	14801	-1872	8358	80
H(35')	13007	-1936	9094	80
H(36')	11733	-511	8985	80
H(5')	9245(32)	315(31)	7283(31)	50
H(51A)	7398	2213	8893	50
H(51B)	6721	2713	7936	50
H(51C)	8082	2605	7993	50
H(52A)	5837	1292	8240	50
H(52B)	6477	791	9212	50
H(52C)	6628	270	8532	50

Experimental

Chapter 2

Ethyl E- and Z-bromo-(5-oxotetrahydrofuran-2-ylidene)acetate ***2.33*** *and* ***2.34.***

MethodA: Triethylamine (68µl, 0.49mM), followed by bromine (25µl,0.49mM), was added to a stirred solution of 1-ethoxycarbonyl-4-carboxy-2-oxobutan-1-ylidenetriphenylphosphorane[2.24] **1.7** (200mg, 0.45mM), in CH_2Cl_2 (10ml), at O°C, under a N_2 atmosphere. The solution was stirred for a further 20 minutes at O°C, and then allowed to warm to room temperature. The solvent was removed under reduced pressure. The crude ethyl *E*- and *Z*-bromo-5-oxotetrahydrofuran-2-ylideneacetates, **2.33** and **2.34**, were inseparable by radial chromatography, but purified, using a 2mm silica gel plate and eluted with CH_2Cl_2, and gave a white solid, containing a mixture of the isomers, in a yield of 86 mg (77%). ^1H NMR spectroscopy revealed the *E*- and *Z*- isomers to be present in a ratio of 7:3, respectively, in the crude mixture. The two isomers were separated by HPLC, using a 10 mm Econosphere CN column, with a UV spectrographic detector at 256 nm, eluting with CH_2Cl_2 and hexane (25:70), with a flow rate of 4ml min^{-1}, and recystalised from benzene.

MethodB: Pyridinium bromide perbromide (35mg, 0.11mM) was added to a stirred solution of 1-ethoxycarbonyl-4-carboxy-2-oxobutan-1-ylidenetriphenylphosphorane[2.24] **1.7** (50mg, 0.11mM), in CH_2Cl_2 (5ml), at O°C, under a N_2 atmosphere. The solution was stirred for a further 20 minutes at O°C, and then allowed to warm to room temperature. The solvent was removed under reduced pressure. ^1H NMR spectroscopy revealed that ethyl *E*- and *Z*-bromo-5-oxotetrahydrofuran-2-ylideneacetates, **2.33** and **2.34**, formed in a ratio of 7:3 and a total yield of 80% in the crude residue.

Ethyl *E*-bromo-(5-oxotetrahydrofuran-2-ylidene)acetate **2.33**.
Recrystalised from benzene as white plates, Mt. pt. 148-9°C. IR υ_{max}, 2985, 2357, 1833, 1713, 1639, 1253, 1095. Mass Spect. $C_8H_9BrO_4$ requires calc. 247.9685, found 247.9683. ^1H NMR δ ($CDCl_3$) 1.358 (t, 7.0, $OCH_2C\mathbf{H_3}$), 2.78 (m, $(\mathbf{H\text{-}3})_2$), 3.103 (m, $(\mathbf{H\text{-}2})_2$), 4.31 (q, 7.0, $OC\mathbf{H_2}CH_3$). ^{13}C NMR δ ($CDCl_3$) 14.1, 26.0, 27.9, 62.3, 93.9, 158.9, 161.1, 173.4.

Ethyl *Z*-bromo-(5-oxotetrahydrofuran-2-ylidene)acetate **2.34**.
Recrystalised from benzene as flat needles, Mt. pt. 154-6°C. IR υ_{max}, 2953, 2360, 1826, 1692, 1638, 1293, 1080. Mass Spect. $C_8H_9BrO_4$

requires calc. 247.9685, found 247.9682. ^{1}H NMR δ ($CDCl_3$) 1.35 (t, 7.0, $OCH_2C\mathbf{H_3}$), 2.85 (m, $(\mathbf{H\text{-}3})_2$), 3.41 (m, $(\mathbf{H\text{-}2})_2$), 4.28 (t, 7.0, $OC\mathbf{H_2}CH_3$). ^{13}C NMR δ ($CDCl_3$) 14.1, 26.9, 29.1, 62.0, 89.6, 162.9, 163.5, 172.2.

Ethyl 2-bromobutan-2,3-dieneoate ***2.49a.***

Triethylamine (33μL, 0.23mM), followed by freshly distiled acetyl chloride (17μL, 0.23mM), was added to a stirred solution of bromo ylide **2.31** (100mg, 0.23mM) in CH_2Cl_2 (5mL), cooled to 0°C. The solution was allowed to warm to room temperature after 30 minutes and the solvent was removed under reduced pressure. Purification by radial chromatography on a 2mm silica gel plate, eluting with CH_2Cl_2 and ethyl acetate (90/10), gave ethyl 2-bromobutan-2,3-dieneoate **2.49a** as a clear oil, in a yield of 88%(40mg). Mass spectral analysis detected the dimer $C_{12}H_{14}Br_2O_4$ requires calc. 379.9260, found 379.9275, and a small signal for the parent ion, $C_6H_7BrO_2$ requires calc. 189.9630, found 189.9628. IR υ_{max}, 2983, 1960, 1720, 1244. ^{1}H NMR δ ($CDCl_3$) 1.31 (t, 7.2, $OCH_2C\mathbf{H_3}$), 4.28 (q, 7.2, $OC\mathbf{H_2}CH_3$), 5.8 (s, $CCC\mathbf{H_2}$). ^{13}C NMR δ ($CDCl_3$) 14.1, 62.9, 84.1, 118.6, 161.7, 211.8. ^{1}H and ^{13}C NMR data for the allenes **2.49a-d** were consistent with similar allenes reported in the literature[2.39].

Ethyl 2-bromopentan-2,3-dieneoate ***2.49b.***

Triethylamine (33μL, 0.23mM), followed by freshly distiled propionyl chloride (23μL, 0.23mM), was added to a stirred solution of bromo ylide **2.31** (100mg, 0.23mM), in CH_2Cl_2 (5mL), cooled to 0°C. Workup as per **2.49a** gave ethyl 2-bromopentan-2,3-dieneoate **2.49b** as a clear oil, 83%(41mg). IR υ_{max}, 2979, 1949, 1725, 1250. ^{1}H NMR δ ($CDCl_3$) 1.24 (t, 7.2, $OCH_2C\mathbf{H_3}$), 1.84 (d, 7.6, $CHC\mathbf{H_3}$), 4.19 (q, 7.2, $OC\mathbf{H_2}CH_3$), 5.63 (q, 7.5, $CC\mathbf{H}CH_3$). ^{13}C NMR δ ($CDCl_3$) 13.1, 14.2, 62.8, 83.3, 96.3, 162.1, 208.6.

Ethyl 2-bromo-4-methylbutan-2,3-dieneoate ***2.49c.***

Triethylamine (33μL, 0.23mM), followed by freshly distiled isobutyryl chloride (25μL, 0.23mM), was added to a stirred solution of bromo ylide **2.31** (100mg, 0.23mM), in CH_2Cl_2 (5mL), cooled to 0°C. Workup as per **2.49a** gave ethyl 2-bromo-4-methylbutan-2,3-dieneoate **2.49c** as a clear oil, 80%(42mg). IR υ_{max}, 2979, 1967, 1740, 1252. ^{1}H NMR δ ($CDCl_3$) 1.27 (t, 7.1, $OCH_2C\mathbf{H_3}$), 1.90 (s, $(C\mathbf{H_3})_2$), 4.24 (q, 7.1, $OC\mathbf{H_2}CH_3$). ^{13}C NMR δ ($CDCl_3$) 14.2, 19.6, 62.6, 81.3, 107.8, 162.4, 205.9.

Ethyl 2-bromohexan-2,3-dieneoate ***2.49d.***

Triethylamine (33μL, 0.23mM), followed by freshly distiled butyryl chloride (25μL, 0.23mM), was added to a stirred solution of bromo ylide **2.31** (100mg, 0.23mM), in CH_2Cl_2 (5mL), cooled to 0°C. Workup as per **2.49a** gave ethyl 2-bromohexan-2,3-dieneoate **2.49d** as a clear oil, 89%(47mg). IR υ_{max}, 2980, 1962, 1728, 1250. ^{1}H NMR δ ($CDCl_3$) 1.11 (t, 7.3, CH_3CH_2CH), 1.30 (t, 7.2, OCH_2CH_3), 2.26 (m, CH_3CH_2CH), 4.26 (q, 7.2, OCH_2CH_3), 5.77 (t, 6.4, CH_3CH_2CH). ^{13}C NMR δ ($CDCl_3$) 12.4, 14.1, 21.2, 62.5, 103.1, 162.0, 217.7.

Ethyl 5-(diphenylmethoxycarbonyl)pent-4-ene-2-yneoate ***2.67.***

A solution of succinic acid monobenzhydrol ester[1.11] (50mg, .18mM) in benzene (5 ml), containing one drop of DMF, was cooled to 0°C. Oxalyl chloride (0.17ml, 1.8mM) was slowly added, and the solution stirred under a nitrogen atmosphere for 2 hours. The solution was evaporated under reduced pressure, and benzene (5mL) was added, and subsequently evaporated. This was repeated to remove final traces of oxalyl chloride. Evaporation under reduced pressure then gave the acid chloride **2.65** as a pale yellow oil. $CHCl_3$ (5mL) was added, and the solution cooled to 0°C. The bromo ylide **2.31** (150mg, 0.36mM) was added to the stirred cooled solution, and after a further 30 minutes the solution was allowed to warm to room temperature. The solvent was removed under reduced pressure, and the resulting residue purified by radial chromatography on a 1mm silica gel chromatotron plate, eluting with CH_2Cl_2, gave ethyl 5-(diphenylmethoxycarbonyl)pent-4-ene-2-yneoate **2.67**, as a pale yellow oil 47%(28mg). Mass Spect. $C_{21}H_{18}BrO_4$ requires calc. 334.1205, found 334.1281. ^{1} H NMR δ ($CDCl_3$) 1.33 (t, 7.0, OCH_2CH_3), 4.27 (q, 7.0, OCH_2CH_3), 6.59, 6.85 (ABq, 16.0, 39.5, CHCHC), 6.88 (s, $CHPh_2$), 7.26-7.37 (m, $CHPh_2$). ^{13}C NMR δ ($CDCl_3$) 13.9, 62.5, 76.5, 122.3, 126.0, 126.3, 127.5, 137.5, 149.1, 155.8, 167.9.

Ethyl 5-methoxycarbonyl-pent-4-ene-2-yneoate ***2.68*** *and Ethyl 5-methoxycarbonylpent-2,3-dienoate* ***2.70.***

Oxalyl chloride (0.18ml, 1.9mM) was slowly added to a solution of succinic acid monomethyl ester[1.11] (25mg, 0.19mM), in benzene (5 ml), containing one drop of DMF, cooled to 0°C, and the solution stirred under a nitrogen atmosphere for 2 hours. The solution was evaporated under reduced pressure, and benzene (5mL) was added, and subsequently evaporated. This was repeated to remove final traces of oxalyl chloride. Evaporation under reduced pressure then gave the acid chloride as a pale

yellow oil. $CHCl_3$ (5mL) was added, and the solution cooled to 0°C. Reaction with bromo ylide **2.31** (162mg, 0.38mM) and workup as per **2.67** gave a crude mixture containing ethyl 5-methoxycarbonyl-pent-4-ene-2-yneoate **2.68** and ethyl 5-methoxycarbonylpent-2,3-dienoate **2.70** in a 50:50 ratio (by ^1H NMR spectroscopy). Purification by radial chromatography on a 1mm silica gel chromatotron plate, eluting with CH_2Cl_2, gave a clear oil which contained a mixture of **2.68** and **2.70**, (14mg), in a 50:50 ratio (by ^1H NMR spectroscopy). The ^1H and ^{13}C NMR signals for **2.68** and **2.70** were assigned by comparison with **2.67** and **2.49b**, respectively.

Ethyl 5-methoxycarbonyl-pent-4-ene-2-yneoate **2.68**. Mass Spect. $C_9H_{10}O_4$ requires calc. 182.0579, found 182.0590. ^1H NMR δ ($CDCl_3$) 1.29 (t, 7.0, $OCH_2C\mathbf{H_3}$), 3.76 (s, $OC\mathbf{H_3}$), 4.25 (q, 7.0, $OC\mathbf{H_2}CH_3$), 6.42, 6.74 (ABq, 16.2, 47.2, C**H**C**H**C). ^{13}C NMR δ ($CDCl_3$) 14.7, 51.9, 63.2, 81.1, 87.9, 121.3, 135.6, 153.8, 165.8.

Ethyl 5-methoxycarbonylpent-2,3-dienoate **2.70**. ^1H NMR δ ($CDCl_3$) 1.25 (t, 7.0, $OCH_2C\mathbf{H_3}$), 3.25 (d, 7.4, $C\mathbf{H_2}CH$), 3.75 (s, $OC\mathbf{H_3}$), 4.21 (q, 7.0, $OC\mathbf{H_2}CH_3$), 5.83 (t, 7.4, $CH_2C\mathbf{H}$).

Bromination of 1-Ethoxycarbonyl-4-methoxycarbonyl-2-oxo-butan-1-ylidenetriphenylphosphorane ***2.71***.

Triethylamine (12μL, 0.08mM), followed by bromine (5μL, 0.08mM) was added to a stirred solution of **2.71**[1,11] (50mg, 0.08mM) in CH_2Cl_2 at 0°C. After 30 minutes the solution was allowed to warm to room temperature and the solvent was removed under reduced pressure. The residue appeared to contain the acetylene **2.67** by ^1H NMR spectroscopy, but this result was unreproducible.

^1H and ^{13}C NMR Study on C- and O-acylation of Ylide **2.53** by Acid Chlorides.

2-Ethoxycarbonyl-3-oxobutan-2-triphenylphosphonium Chloride ***2.54a*** *and 1-Ethoxy-1-methylcarbonyloxyprop-1-ene-2-triphenylphosphonium Chloride* ***2.55a***.

Methyl ylide **2.53** (50mg, 0.14mM) was added to a solution of acetyl chloride (10μL, 0.14mM), in $CDCl_3$ (0.5mL), at 23°C, in a 3mm OD NMR tube. The reaction was monitored by ^1H, ^{13}C and ^{31}P NMR spectroscopy. 1-Ethoxy-1-methylcarbonyloxyprop-1-ene-2-triphenylphosphonium chloride **2.55a** appeared instantly which completely rearranged to 2-

ethoxycarbonyl-3-oxobutan-2-triphenylphosphonium chloride **2.54a** after 1 hour.

2-Ethoxycarbonyl-3-oxobutan-2-triphenylphosphonium Chloride **2.54a** ^{1}H NMR δ ($CDCl_3$) 1.10 (t, 7.1, $OCH_2C\mathbf{H_3}$), 2.20 (d, 17.7, 1-$C\mathbf{H_3}$), 2.66 (s, $COC\mathbf{H_3}$), 4.15 (q, 7.1, $OC\mathbf{H_2}CH_3$), 7.60-8.00 (m, $\mathbf{Ph_3}P$). ^{13}C NMR δ ($CDCl_3$) 13.3, 21.6, 28.7(2), 64.8, 66.3(50.4), 117.7(86.6), 130.4(12.8), 134.6(10.2), 135.3(3.0), 201.3(4.3). ^{31}P δ ($CDCl_3$) 36.3.

1-Ethoxy-1-methylcarbonyloxyprop-1-ene-2-triphenylphosphonium Chloride **2.55a.** ^{1}H NMR δ ($CDCl_3$) 0.53 (t, 7.1, $OCH_2C\mathbf{H_3}$), 1.65 (d, 14.5, 1-$C\mathbf{H_3}$), 2.49 (s, $COC\mathbf{H_3}$), 3.73 (q, 7.1, $OC\mathbf{H_2}CH_3$), 7.40-8.00 (m, $\mathbf{Ph_3}P$). ^{13}C NMR δ ($CDCl_3$) 12.1(7.5), 12.5, 19.8, 65.5, 75.4(93.5), 117.1(91.7), 129.1(12.8), 132.4(10.0), 133.9, 158.6(12.0), 165.0. ^{31}P δ ($CDCl_3$) 24.3.

2-Ethoxycarbonyl-5-methoxycarbonyl-3-oxopentan-2-triphenylphosphonium Chloride ***2.54b*** *and 1-Ethoxy-1-[1-(2-methoxycarbonylethyl)]carbonyloxyprop-1-ene-2-triphenylphosphonium Chloride* ***2.55b.***

Methyl ylide **2.53** (24mg, 0.07mM) was added to a solution of **2.65**, prepared as for **2.67**, (10mg, 0.07mM), in $CDCl_3$ (0.5mL), at 23°C, in a 3mm NMR tube. The reaction was monitored by ^{1}H, ^{13}C and ^{31}P NMR spectroscopy. 1-Ethoxy-1-[1-(2-methoxycarbonylethyl)]carbonyloxyprop-1-ene-2-triphenylphosphonium chloride **2.55b** appeared instantly which completely rearranged to 2-ethoxycarbonyl-5-methoxycarbonyl-3-oxopentan-2-triphenylphosphonium chloride **2.54b** after 6 hours.

2-Ethoxycarbonyl-5-methoxycarbonyl-3-oxopentan-2-triphenylphosphonium Chloride **2.54b.** ^{1}H NMR δ ($CDCl_3$) 1.10 (t,7.2, $OCH_2C\mathbf{H_3}$), 2.20 (d,18.0, 1-$C\mathbf{H_3}$), 2.66 (m, $(H\text{-}3)_2$), 3.25 (m, (H-2)a), 3.47 (m, (H-2)b), 3.64 (s), 4.15 (q, 7.1, $OC\mathbf{H_2}CH_3$), 7.6-8.0 (m, $\mathbf{Ph_3}P$). ^{13}C NMR δ ($CDCl_3$) 12.1, 20.5, 26.3, 34.2(1.5), 50.6, 63.8, 64.8(50.0), 116.5(86.0),129.3(13.2), 132.9(10.8), 134.3, 164.7, 171.0, 201.2(4.2). ^{31}P NMR δ ($CDCl_3$) 34.0.

1-Ethoxy-1-[1-(2-methoxycarbonylethyl)]carbonyloxyprop-1-ene-2-triphenylphosphonium Chloride **2.55b.** ^{1}H NMR δ ($CDCl_3$) 0.54 (t, 7.1, $OCH_2C\mathbf{H_3}$), 1.67 (d, 14.7, 1-$C\mathbf{H_3}$), 2.84 (m, $(H\text{-}3)_2$), 3.11 (m, $(H\text{-}2)_2$), 3.70 (s, $COC\mathbf{H_3}$), 3.79 (q, 7.1, $OC\mathbf{H_2}CH_3$), 7.40-7.90 (m, $\mathbf{Ph_3}P$). ^{31}P NMR δ ($CDCl_3$) 24.3.

2-Ethoxycarbonyl-5-diphenylmethoxycarbonyl-3-oxopentan-2-triphenylphosphonium Chloride **2.54c** *and 1-Ethoxy-1-[1-(2-diphenylmethoxycarbonylethyl)]carbonyloxyprop-1-ene-2-triphenylphosphonium Chloride* **2.55c**.

Methyl ylide **2.53** (16mg, 0.04mM) was added to a solution of monobenzyl succinic acid chloride[1.11], prepared as for **2.68** and **2.70**, (10mg, 0.04mM), in $CDCl_3$ (0.5mL), at 23°C, in a 3mm NMR tube. The reaction was monitored by ^1H and ^{13}C NMR spectroscopy. 1-Ethoxy-1-[1-(2-diphenylmethoxycarbonylethyl)]carbonyloxyprop-1-ene-2-triphenylphosphonium chloride **2.55c** appeared with time and completely rearranged to 2-ethoxycarbonyl-5-diphenylmethoxycarbonyl-3-oxopentan-2-triphenylphosphonium chloride **2.54c** after 10 hours.
2-Ethoxycarbonyl-5-diphenylmethoxycarbonyl-3-oxopentan-2-triphenylphosphonium Chloride **2.54c** ^1H NMR δ ($CDCl_3$) 1.04 (t, 7.1, $OCH_2C\mathbf{H_3}$), 2.11 (d, 16.0, 1-C**H**$_3$), 2.72 (m, (H-3)$_2$), 3.22 (m, (H-2)a), 3.40 (m, (H-2)b), 4.15 (q, 7.1, $OC\mathbf{H_2}CH_3$), 5.06, 5.09 (ABq, 12.6), 7.30 (C**H**Ph$_2$), 7.6-8.0 (m, **Ph**$_3$P, **Ph**$_2$C). ^{13}C NMR δ ($CDCl_3$) 13.2, 21.6, 27.5, 35.2(2.1), 64.9, 66.1(50.0), 66.3, 117.7(85.6), 127.7, 128.0, 128.3, 130.3(13.0), 134.0(10.0), 135.3, 135.4, 165.9, 171.5, 202.1(4.1).
1-Ethoxy-1-[1-(2-diphenylmethoxycarbonylethyl)]carbonyloxyprop-1-ene-2-triphenylphosphonium Chloride **2.55c**. ^1H NMR δ ($CDCl_3$) 0.50 (t,7.1, $OCH_2C\mathbf{H_3}$), 1.62 (d, 14.6, 1-C**H**$_3$), 2.88 (m, (H-3)$_2$), 3.12 (m, (H-2)$_2$), 3.75 (q, 7.1, $OC\mathbf{H_2}CH_3$), 5.13 (s, C**H**$_2$Ph), 7.30 ($CH_2\mathbf{Ph}$), 7.4-8.00 (**Ph**$_3$P, **Ph**$_2$C). ^{13}C NMR δ ($CDCl_3$) 12.5(7.3), 12.9, 27.6, 28.0, 50.6, 66.0, 75.7(93.4), 117.7(91.6), 129.7(12.8), 133.0(10.4), 134.4(2.9), 159.3(12.1), 168.1, 171.9.

*2-Ethoxycarbonyl-3-oxo-3-phenylpropan-2-triphenylphosphonium Chloride***2.54d** *and 1-Ethoxy-1-phenylcarbonyloxyprop-1-ene-2-triphenylphosphonium Chloride* **2.55d**.

Methyl ylide (31.2mg, 0.09mM) was added to a solution of benzyl chloride (10μL, 0.09mM), in $CDCl_3$ (0.5mL), at 23°C, in a 3mm NMR tube. The reaction was monitored by ^1H and ^{13}C NMR spectroscopy. 1-Ethoxy-1-phenylcarbonyloxyprop-1-ene-2-triphenylphosphonium chloride **2.55d** appeared with time and completely rearranged to 2-ethoxycarbonyl-3-oxo-3-phenylpropan-2-triphenylphosphonium chloride **2.54d** after 24 hours.
2-Ethoxycarbonyl-3-oxo-3-phenylpropan-2-triphenylphosphonium Chloride **2.54d**. ^1H NMR δ ($CDCl_3$) 0.98 (t,7.1, $OCH_2C\mathbf{H_3}$), 2.27 (d, 18.3), 3.99 (m, $OC\mathbf{H_2}CH_3$), 7.4-8.0 (m, **Ph**$_3$P, CO**Ph**). ^{13}C NMR δ ($CDCl_3$) 13.1,

22.1, 64.5, 66.8(49.7), 117.4(86.1), 128-137, 129.8(12.7), 133.8(9.6), 134.4(2.9), 166.0, 208.3.

1-Ethoxy-1-phenylcarbonyloxyprop-1-ene-2-triphenylphosphonium Chloride **2.55d.** ^{1}H NMR δ ($CDCl_3$) 0.55 (t, 7.1, $OCH_2C\mathbf{H_3}$), 1.67 (d, 14.3, 1-$C\mathbf{H_3}$), 3.77 (q, 7.1, $OC\mathbf{H_2}CH_3$), 7.40-8.00 (m, $\mathbf{Ph_3}P$, CO**Ph**). ^{13}C NMR δ ($CDCl_3$) 12.7(7.2), 13.0, 66.1, 76.5(93.6), 118.1(91.7), 127-138, 129.9 (13.2), 133.2(10.5), 134.5(3.0), 160.0(12.4), 161.5.

Crystal data for Ethyl Z-bromo-(5-oxotetrahydrofuran-2-ylidene)acetate ***2.34.***

$C_8H_9BrO_4$, colourless, crystalised from benzene, crystal dimensions 0.58 x 0.10 x 0.04 mm. M = 248.0, space group $P2_1$, a = 11.064(4), b = 5.211(2), c = 16.328(9) Å, β = 104.5(3)°, V= *911.0(6)* Å^3, Z = 8, D_C = 1.26 g cm^{-3}, F(000) = 496. Using 1.1° ω-scans at scan rate of 4.50° min^{-1}, 1173 unique reflections were collected in the range of 4 < 2θ < 45° and 851 of these having I > 3σ(I) were used in the structural analysis.

Data were recorded at 148 K on a Nicolet R3m four circle diffractometer using Mo - Kα radiation. Cell parameters were determined by least squares refinement of 25 accurately centred reflections in the range of 5 < 2θ < 35°. Crystal stability was monitored by recording 3 check reflections (1. 6 0 0, 2. 0 4 0, 3. 0 0 6) every 100 reflections and no significant variations were observed. Data were corrected for Lorentz-polarisation effects and absorption.

A patterson map located the bromine atoms, and direct methods revealed the position of the non-hydrogen atoms and the structure was refined by blocked cascade least-squares techniques. Hydrogen atoms were inserted at calculated positions using a riding model with thermal parameters equal to 1.2 U of their carrier atoms. All non-hydrogen atoms were refined anisotropically (119 parameters). The refinement converged with R = 0.039 and R_W = 0.039. The final difference fourier map showed no significant features. All programs used in the data collection and structure solution are contained in the SHELXTL (Version 4.1) package.[E5]

TABLE 1. Atomic Coordinates (x10^4) and Isotropic Thermal Parameters (Å^{2}x10^3) for 2.34.

Atom	x	y	z	U
Br	8325(1)	1337(2)	0282(1)	20(0)
O1	12984(5)	2816(11)	1170(4)	30(2)
O2	10915(4)	3223(9)	0967(3)	19(2)
O3	8268(5)	6995(10)	1986(3)	22(2)
O4	6807(4)	4516(9)	1136(3)	22(2)
C1	12145(7)	3995(15)	1323(4)	20(2)
C2	12140(6)	6332(15)	1864(4)	19(2)
C3	10772(7)	6747(14)	1858(4)	20(3)
C4	10094(7)	4650(13)	1282(4)	15(2)
C5	8881(6)	4056(14)	1054(4)	16(2)
C6	7986(7)	5374(14)	1439(5)	17(3)
C7	5841(7)	5697(16)	1485(5)	31(3)
C8	5332(8)	6173(16)	9819(6)	37(3)

*Equivalent isotropic U defined as one third of the trace of the orthogonalised U_{ij} tensor

Table 2. Bond lengths (Å) for 2.34.

Br-C5	1.894(7)	C1-C2	1.505(11)
O1-C1	1.191(10)	C2-C3	1.527(10)
O2-C1	1.398(8)	C3-C4	1.512(9)
O2-C4	1.370(9)	C4-C5	1.336(10)
O3-C6	1.212(9)	C5-C6	1.469(11)
O4-C6	1.350(8)	C7-C8	1.503(12)
O4-C7	1.467(10)		

Table 3. Bond angles (°) for 2.34.

C1-O2-C4	110.8(5)	C3-C4-C5	130.3(7)
C6-O4-C7	116.7(6)	Br-C5-C6	119.6(5)
O1-C1-C2	131.2(7)	Br-C5-C4	119.6(6)
O2-C1-C2	109.3(6)	C4-C5-C6	120.7(6)
C1-C2-C3	105.1(6)	O3-C6-C5	124.4(7)
C2-C3-C4	103.7(6)	O3-C6-O4	123.2(7)
O2-C4-C5	118.9(6)	O4-C6-C5	112.4(6)
O1-C1-O2	119.2(7)	O4-C7-C8	109.8(7)
O2-C4-C3	110.7(6)		

TABLE 4. Anisotropic Thermal Parameters ($Å^2x10^3$) for 2.34.

Atom	U_{11}	U_{22}	U_{33}	U_{23}	U_{13}	U_{12}
Br	24(1)	18(1)	16(1)	-4(1)	2(1)	-2(1)
O	119(3)	31(3)	43(4)	-9(3)	13(3)	1(3)
O2	17(3)	20(3)	18(3)	-6(2)	3(2)	0(2)
O3	22(3)	24(3)	19(3)	-6(3)	6(2)	0(2)
O4	17(3)	22(3)	25(3)	-5(2)	1(2)	-1(2)
C1	23(5)	17(4)	18(4)	2(4)	5(3)	-1(4)
C2	22(4)	17(4)	19(4)	15(4)	4(3)	-3(4)
C3	25(4)	16(4)	18(4)	-3(3)	4(3)	-4(4)
C4	22(4)	14(4)	9(4)	5(3)	4(3)	2(3)
C5	20(4)	18(4)	9(3)	-8(4)	3(3)	5(4)
C6	22(5)	14(4)	13(4)	4(4)	-0(3)	0(3)
C7	20(5)	36(6)	40(5)	-6(4)	14(4)	-2(4)
C8	23(5)	34(6)	51(6)	-1(5)	2(4)	9(4)

The anisotropic temperature factor exponent takes the form:
$-2\pi^2(h^2a^{*2}U_{11} + k^2b^{*2}U_{22} + ...+ 2hka^*b^*U_{12})$

TABLE 5. Hydrogen Coordinates ($x10^4$) and Temperature Factors ($Å^2x10^3$) for 2.34.

Atom	x	y	z	U
H2A	12633(6)	6038(15)	2430(4)	30(7)
H2B	12462(6)	7793(15)	1629(4)	30(7)
H3A	10492(7)	8411(14)	1638(4)	30(7)
H3B	10649(7)	6572(14)	2417(4)	30(7)
H7A	5176(7)	4490(16)	1485(5)	30(7)
H7B	6196(7)	6173(16)	2064(5)	30(7)
H8A	4702(8)	8046(16)	1214(6)	30(7)
H8B	4973(8)	7571(16)	0404(6)	30(7)
H8C	5996(8)	9253(16)	1007(6)	30(7)

Experimental

Chapter 3

Ethyl E- and Z-bromo-(6-oxotetrahydropyran-2-ylidene)acetate ***3.13*** *and* ***3.14.***

Triethylamine (66µl, 0.47mM), followed by bromine (25µl, 0.47mM), was added to a stirred solution of 1-ethoxycarbonyl-5-carboxy-2-oxopentan-1-ylidenetriphenylphosphorane[2.24] **1.8** (200mg, 0.43mM), in CH_2Cl_2 (10ml), at O°C, under a N_2 atmosphere. The solution was stirred for a further 20 minutes at O°C, and then allowed to warm to room temperature. The solvent was removed under reduced pressure. ^1H NMR spectroscopy revealed the *E-* , *Z-* , and endo isomers to be present in a ratio of 82:10:8, respectively, in the crude mixture. Separation of the E- and Z-isomers by radial chromatography, using a 2mm silica gel plate and eluted with CH_2Cl_2, gave ethyl *E*-bromo-(6-oxotetrahydropyran-2-ylidene)acetate **3.13** , as a clear oil (79mg), and ethyl *Z*-bromo-(6-oxotetrahydropyran-2-ylidene)acetate **3.14** , as a white solid(10mg), combined yield of 85%(89mg). Ethyl bromo-(6-oxo-5,6-dihydro-4H-pyran-2-yl)acetate **3.19** (endo product) was observed in the crude mixture by ^1H NMR spectroscopy, however, it was not isolated by radial chromatography.)

Ethyl *E*-bromo-(6-oxotetrahydropyran-2-ylidene)acetate **3.13**. IR υ_{max}, 2983, 1714, 1302, 1021. Mass Spect. $C_9H_{11}BrO_4$ requires calc. 261.9841, found 261.9845. ^1H NMR δ ($CDCl_3$) 1.34 (t, 7.0, $OCH_2C\mathbf{H_3}$), 1.97 (m, $CH_2C\mathbf{H_2}CH_2$), 2.67 (t, 6.5, $COC\mathbf{H_2}CH_2$), 2.80 (t, 6.5, $C\mathbf{H_2}C$), 4.29 (q, 7.0, $OC\mathbf{H_2}CH_3$). ^{13}C NMR δ ($CDCl_3$) 14.0, 17.3, 27.2, 29.9, 62.3, 98.0, 155.2, 162.1, 165.4.

Ethyl *Z*-bromo-(6-oxotetrahydropyran-2-ylidene)acetate **3.14**. IR υ_{max}, 2983, 1714, 1310, 1020. Mass Spect. $C_9H_{11}{}^{81}BrO_4$ requires calc. 263.9841, found 263.9827. ^1H NMR δ ($CDCl_3$) 1.35 (t, 7.0, $CH_2C\mathbf{H_3}$), 1.95 (m, $CH_2C\mathbf{H_2}CH_2$), 2.71 (t, 6.4, $COC\mathbf{H_2}CH_2$), 3.16 (t, 6.4, $CH_2C\mathbf{H_2}C$), 4.27 (q, 7.0, $C\mathbf{H_2}CH_3$). ^{13}C NMR δ ($CDCl_3$) 13.9, 17.7, 27.6, 30.6, 62.2, 95.0, 161.0, 163.2, 165.5.

Ethyl bromo-(6-oxo-5,6-dihydro-4H-pyran-2-yl)acetate **3.19**. ^1H NMR δ ($CDCl_3$) 1.36 (t, 7.0, $OCH_2C\mathbf{H_3}$), 1.95 (m, $C\mathbf{H_2}CH_2CH$), 2.44 (m, 6.4, $CH_2C\mathbf{H_2}CH$), 4.30 (q, 7.0, $OC\mathbf{H_2}CH_3$), 5.72 (t, 5.0, $CH_2CH_2C\mathbf{H}$), 5.89 (s, C**H**Br).

Ethyl E- and Z-bromo-(4-methyl-6-oxotetrahydropyran-2-ylidene)acetate ***3.15*** *and* ***3.16.***

Triethylamine (29μl, 0.23mM), followed by bromine (11μl, 0.23mM), was added to a stirred solution of 1-ethoxycarbonyl-5-carboxy-4-methyl-2-oxopentan-1-ylidenetriphenylphosphorane[E6] **3.4** (100mg, 0.21mM), in CH_2Cl_2 (10ml), at O°C, under N_2 atmosphere. ^1H NMR spectroscopy revealed the *E-* and *Z-* isomers to be present in a ratio of 85:15, respectively, in the crude mixture. Separation of the E- and Z-isomers by radial chromatography, using a 2mm silica gel plate and eluted with CH_2Cl_2, gave ethyl *E*-bromo-(4-methyl-6-oxotetrahydropyran-2-ylidene)acetate **3.15** (38mg) and ethyl *Z*-bromo-(4-methyl-6-oxotetrahydropyran-2-ylidene)acetate **3.16** (7mg), as clear oils, in a combined yield of 91%(45mg).

Ethyl *E*-bromo-(4-methyl-6-oxotetrahydropyran-2-ylidene)acetate **3.15.** IR υ_{max}, 2960, 1720, 1300. Mass Spect $C_{10}H_{13}BrO_4$ requires calc. 275.9997, found 276.0058. ^1H NMR δ ($CDCl_3$) 1.12 (d, 6.1, CHC**H$_3$**), 1.32 (t, 7.0, OCH_2C**H$_3$**), 2.30 (m, (**H-2**)a), 2.30 (m, (**H-4**)a), 2.30 (m, (**H-3**)), 2.70 (dd, 2.6, 55, (**H-2**)b), 3.05 (dd, 2.6, 15.5, (**H-4**)b), 4.28 (q, 7.0, O**CH$_2$**CH_3). ^{13}C NMR δ ($CDCl_3$) 14.0, 20.5, 24.9, 35.1. 37.6, 62.4, 98.1, 154.5, 162.2, 165.3.

Ethyl *Z*-bromo-(4-methyl-6-oxotetrahydropyran-2-ylidene)acetate **3.16.** IR υ_{max}, 2960, 1720, 1300. ^1H NMR δ ($CDCl_3$) 1.12 (d,6.0, CHC**H$_3$**), 1.35 (t, 7.0, OCH_2C**H$_3$**), 2.17 (m, C**H**CH_3), 2.33 (dd, 10.4, 17.2, (**H-2**)a), 2.53 (dd, 10.4, 17.4, (**H-4**)a), 2.79 (dd, 1.9, 17.2, (**H-2**)a), 3.53 (ddd, 1.9, 4.3, 17.2, (**H-4**)b), 4.27 (t, 7.0, O**CH$_2$**CH_3). ^{13}C NMR δ ($CDCl_3$) 14.1, 20.4, 25.2, 34.3, 38.3, 62.3, 95.2, 160.0, 163.6, 165.4.

Ethyl E- and Z-bromo-(4,4-dimethyl-6-oxotetrahydropyran-2-ylidene) acetate ***3.17*** *and* ***3.18***

Triethylamine (63μl, 0.45mM), followed by bromine (24μl,0.45mM), was added to a stirred solution of ethyl 1-ethoxycarbonyl-5-carboxy-4,4-dimethyl-2-oxopentan-1-ylidenetriphenylphosphorane[2.24] **1.9** (200mg, 0.41mM), in CH_2Cl_2 (10ml), at O°C, under nitrogen atmosphere. The reaction was worked up as for **3.13** and **3.14**. ^1H NMR spectroscopy revealed the *E-* and *Z-* isomers to be present in a ratio of 88:12, respectively, in the crude mixture. Separation by radial chromatography, using a 2mm silica gel plate and eluted with CH_2Cl_2, gave ethyl *E*-bromo-(4,4-dimethyl-6-oxotetrahydropyran-2-ylidene)acetate **3.17** (81mg) and ethyl *Z*-bromo-(4,4-dimethyl-6-oxotetrahydropyran-2-ylidene)acetate **3.18** (10mg), as clear oils, in a combined yield of 86%(91mg).

Ethyl *E*-bromo-(4,4-dimethyl-6-oxotetrahydropyran-2-ylidene)acetate **3.17**. IR υ_{max}, 2962, 2340, 1781, 1720, 1607, 1258, 1039. Mass Spect. $C_{11}H_{15}BrO_4$ requires calc. 290.0154, found 290.0159. ^{1}H NMR δ ($CDCl_3$) 1.12 (s, 6H), 1.34 (t, 7.1, $OCH_2C\mathbf{H_3}$), 2.47 (s, $COC\mathbf{H_2}C$), 2.65 (s, $CC\mathbf{H_2}C$), 4.30 (q, 7.1, $OC\mathbf{H_2}CH_3$). ^{13}C NMR δ ($CDCl_3$) 13.8, 27.6, 29.7, 40.3, 43.1, 61.9, 98.0, 154.1, 161.9, 165.0.

Ethyl *Z*-bromo-(4,4-dimethyl-6-oxotetrahydropyran-2-ylidene)acetate **3.18**. IR υ_{max}, 2961, 2360, 1784, 1704, 1605, 1264, 1060. Mass Spect. $C_{11}H_{15}BrO_4$ requires calc. 290.0154, found 290.0176. ^{1}H NMR δ ($CDCl_3$) 1.10 (s, 6H), 1.36 (t, 7.1, $OCH_2C\mathbf{H_3}$), 2.53 (s, $COC\mathbf{H_2}C$), 3.01 (s, $CC\mathbf{H_2}C$), 4.29 (q, 7.1, $C\mathbf{H_2}CH_3$). ^{13}C NMR δ ($CDCl_3$) 14.1, 27.7 29.7, 39.7, 44.2, 62.3, 95.6, 159.7, 163.6, 166.1.

Formation of 4-(Diphenylmethoxycarbonyl)butanoyl Chloride ***3.20*** *and subsequent reaction with Bromo Ylide* ***2.31***.

Oxalyl chloride (0.20ml, 2.2mM) was slowly added to a solution of glutaric acid monobenzhydrol ester[1.11] (50mg, 0.22mM), in benzene (5 ml), containing one drop of DMF, cooled to 0°C, and the solution stirred under a nitrogen atmosphere for 2 hours. The solution was evaporated under reduced pressure, and benzene (5mL) was added, and subsequently evaporated. This was repeated to remove final traces of oxalyl chloride. Evaporation under reduced pressure then gave the acid chloride **3.20** as a pale yellow oil. $CHCl_3$ (5mL) was added, and the solution cooled to 0°C. Reaction with bromo ylide **2.31** (77mg, 0.22mM) and workup as per **2.67** failed to yield allene **3.21** or acetylene **3.22**.

Experimental

Chapter 4

Ethyl E- and Z-bromo-(3-oxo-1,3-dihydroisobenzofuran-1-ylidene)acetate ***4.25*** *and* ***4.26.***

Method A: Bromo ylide **2.31** (315mg, 0.74mM) was added to a stirred solution of phthalic anhydride (100mg, 0.68mM), in $CHCl_3$, (10mL), at 25°C. The solution was heated to reflux at 60°C for 2 hours, the solution cooled and the solvent removed under reduced pressure. The ^1H NMR spectrum of the crude mixture revealed ethyl E- and Z-bromo-(3-oxo-1,3-dihydroisobenzofuran-1-ylidene)acetate **4.25** and **4.26** to be present in a ratio of 7:13. Radial chromatography, using a 2mm silica gel plate and eluted with a gradient of CH_2Cl_2 in hexane gave partial separation of the isomers. The first fraction gave a white solid that contained a mixture of **4.25** and **4.26** (146mg), the second fraction contained pure **4.26** (22mg), as a white solid, and gave a combined yield of 85%(166mg). **4.26** was recrystalised from ethyl acetate/petroleum ether as striated needles, mt.pt. 214-215°C.

Method B: Ylide **0.1** (233mg, 0.67mM) was added to a stirred solution of phthalic anhydride(100mg, 0.67mM), in $CHCl_3$ (10mL), at 0°C. ^1H NMR spectroscopy revealed after 30 minutes that the keto acid phosphorane **4.17**[2.1] was present in 65% yield. Further time resulted in a decrease in yield due to the formation of enol lactones **4.15** and **4.16**. Triethylamine (62μL, 0.44mM), followed by bromine (23μL, 0.44mM) was then added and the solution was stirred for a further 30 minutes at 0°C. The solvent was removed under reduced pressure. ^1H NMR spectroscopy of the crude product was consistent with **4.25** and **4.26** being present in a ratio of 7:13, respectively. Purification by radial chromatography, on a 2mm silica gel chromatotron plate eluting with CH_2Cl_2, gave a white solid containing a mixture of ethyl *E*- and *Z*-bromo-(3-oxo-1,3-dihydroisobenzofuran-1-ylidene)acetate **4.25** and **4.26**, total yield of 55% (109mg, 85% based on the amount of the intermediate **4.17** generated). Mass Spect. on the mixture of isomers, $C_{12}H_9BrO_4$ requires calc. 295.9685, found 295.9685. IR υ_{max}, (mixture) 3170, 1785, 1741, 1711, 1242, 1032.

Ethyl *E*- bromo-(3-oxo-1,3-dihydroisobenzofuran-1-ylidene)acetate **4.25**
^1H NMR δ ($CDCl_3$) 1.42 (t, 7.1, $OCH_2C\mathbf{H_3}$), 4.42 (q, 7.1, $OC\mathbf{H_2}CH_3$), 7.75 (t,

8.0, **H6**), 7.82 (t, 8.0, **H5**), 8.0 (d, 8.0, **H4**), 8.70 (d, 8.0, **H7**). ^{13}C NMR δ ($CDCl_3$) 14.2, 62.9, 96.3, 126.2, 126.8, 127.0, 132.3, 161.7, 164.8.
Ethyl *Z*-bromo-(3-oxo-1,3-dihydroisobenzofuran-1-ylidene)acetate **4.26** ^1H NMR δ ($CDCl_3$) 1.43 (t, 7.1, $OCH_2C\mathbf{H_3}$), 4.42 (q, 7.1, $OC\mathbf{H_2}CH_3$), 7.67 (t, 8.0, **H6**), 7.78 (t, 8.0, **H5**), 7.95 (d, 8.0, **H4**), 8.58 (d, 8.0, **H7**). ^{13}C NMR δ ($CDCl_3$) 14.1, 63.0, 96.9, 125.9, 126.4, 126.8, 132.0, 135.4, 153.7, 163.1, 164.5.

Ethyl Z-bromo-(4-methyl-3-oxo-1,3-dihydroisobenzofuran-1-ylidene)acetate **4.34**, *and Ethyl E- and Z-bromo-(7-methyl-3-oxo-1,3-dihydroisobenzofuran-1-ylidene)acetate* **4.32** *and* **4.33**

Bromo ylide **2.31** (291mg, 0.68mM) was added to a stirred solution of 3-methylphthalic anhydride (100mg, 0.62mM), in $CHCl_3$ (10ml), at 25°C, and stirring was continued for a further 4 hours. The solvent was removed under reduced pressure. Radial chromatography, using a 2mm silica gel chromatotron plate eluting with CH_2Cl_2 gave one fraction, a white solid, containing **4.32**, **4.33**, and **4.34** , in a ratio of 15:8:3 (by ^1H NMR spectroscopy), in a total yield of 53% (102mg). Separation was achieved by HPLC using a 10 mm Econosphere CN column, with a UV spectrographic detector at 256 nm, eluting with CH_2Cl_2 and hexane (25:70) with a flow rate of 4ml min^{-1}. Mass Spect. on the mixture containing **4.32**, **4.33**, and **4.34**, $C_{13}H_{11}BrO_4$ requires calc. 309.9841, found 309.9852.
IR (mixture) υ_{max}, 3173, 2923, 1715, 1666, 1590, 1300, 1130.
Ethyl *E*-bromo-(7-methyl-3-oxo-1,3-dihydroisobenzofuran-1-ylidene)acetate **4.32**. ^1H NMR δ ($CDCl_3$) 1.38 (t, 7.1, $OCH_2C\mathbf{H_3}$), 2.74 (s, $C\mathbf{H_3}$), 4.38 (q, 7.1, $OC\mathbf{H_2}CH_3$), 7.48 (d, 8.0, **H4**), 7.68 (m, **H5**), 8.49 (d, 8.0, **H6**)
Ethyl *Z*-bromo-(7-methyl-3-oxo-1,3-dihydroisobenzofuran-1-ylidene)acetate **4.33.** ^1H NMR δ ($CDCl_3$) 1.38 (t, 7.1, $OCH_2C\mathbf{H_3}$), 2.72 (s, $C\mathbf{H_3}$), 4.38 (q, 7.1, $OC\mathbf{H_2}CH_3$), 7.43 (d, 8.0, **H4**), 7.62 (m, **H5**), 8.39 (d, 8.0, **H6**).
Ethyl *Z*-bromo-(4-methyl-3-oxo-1,3-dihydroisobenzofuran-1-ylidene)acetate **4.34.** ^1H NMR δ ($CDCl_3$) 1.38 (t, 7.1, $OCH_2C\mathbf{H_3}$), 2.72 (s, $C\mathbf{H_3}$), 4.38 (q, 7.1, $OC\mathbf{H_2}CH_3$), 7.45 (d, 8.0, **H5**), 7.67 (m, **H6**), 8.90 (d, 8.0, **H7**).
^{13}C NMR δ ($CDCl_3$) (mixture) 13.7, 14.0, 14.1, 21.7, 22.0, 62.1, 62.2, 62.5, 110.4, 116.0, 127-130, 154.3, 155.3, 160.2, 162.4, 167.0.

Ethyl E- and Z-bromo-(4-nitro-3-oxo-1,3-dihydroisobenzofuran-1-ylidene)acetate ***4.41*** *and* ***4.42****, and Ethyl E- and Z-bromo-(7-nitro-3-oxo-1,3-dihydroisobenzofuran-1-ylidene)acetate* ***4.43*** *and* ***4.44****.*

Ylide **0.1** (233mg, 0.67mM) was added to a stirred solution of 3-nitrophthalic anhydride (100mg, 0.67mM), in $CHCl_3$ (10ml), at 25°C. After 4 hours stirring, the intermediate phosphoranes **4.35** and **4.36** were present in 67% (determined by ^1H NMR spectroscopy signals for the ethyl ester δ ($CDCl_3$) 0.38 (t, 7.1, $OCH_2C\mathbf{H_3}$), 3.47 (q, 7.1, $OC\mathbf{H_2}CH_3$)). The solvent was removed under reduced pressure. CH_2Cl_2 (10mL) was added and the resulting solution was cooled to 0°C. Triethylamine (63µl, 0.45mM), followed by bromine (24µl, 0.45mM), was added and stirring was continued for a further 30 minutes at 0°C. The solvent was removed, and a yellow residue containing the nitrophthalic bromo enol lactones was obtained. Purification by radial chromatography, using a 2mm silica gel chromatotron plate, eluting with a gradient of CH_2Cl_2 in hexane, removed triphenylphosphine oxide, and gave the nitrophthalic bromo enol lactones as a yellow oil. The nitrophthalic bromo enol lactones could not be separated by HPLC, using a 10 mm Econosphere CN column, with a UV spectrographic detector at 256 nm, and a gradient of CH_2Cl_2 in hexane. Tentative assignment of **4.41** and **4.42** in the ^1H NMR spectrum of the mixture was made by comparison with the previously synthesised phthalic bromo enol lactones.

Mass Spect. on the mixture of isomers, $C_{12}H_8BrNO_4$ requires calc. 340.9535, found 340.9628. IR (mixture) υ_{max}, 3200, 1731, 1537, 1120.

Ethyl *Z*-bromo-(4-nitro-3-oxo-1,3-dihydroisobenzofuran-1-ylidene)acetate **4.41**. ^1H NMR δ ($CDCl_3$) 1.41 (t, 7.1, $OCH_2C\mathbf{H_3}$), 4.39 (q, 7.1, $OC\mathbf{H_2}CH_3$), 8.08 (d, 8.0, **H5**), 7.94 (m, **H6**), 8.93 (d, J 8.0, **H7**)

Ethyl *E*-bromo-(4-nitro-3-oxo-1,3-dihydroisobenzofuran-1-ylidene)acetate **4.42.** ^1H NMR δ ($CDCl_3$) 1.41 (t, 7.1, $OCH_2C\mathbf{H_3}$), 4.39 (q, 7.1, $OC\mathbf{H_2}CH_3$), 8.01 (t, 8.0, **H6**), 8.12 (d, 8.0, **H5**), 9.01 (d, J 8.0, **H7**). ^{13}C NMR δ ($CDCl_3$) (mixture) 12.7, 13.0, 13.1, 62.3, 63.6, 63.7, 115.8, 115.9, 116, 116.3, 127-133, 146.4, 149.3, 155.2, 155.3, 163.4, 163.5, 166.8, 167.0, 167.2, 167.8.

Crystal data for of Z-bromo-(3-oxo-1,3-dihydroisobenzofuran-1-ylidene)acetate ***4.26.***

$C_{12}H_9BrO_4$. colourless, crystalised from ethyl acetate and hexane, crystal dimensions 0.2x 0.2 x 0.7 mm. M = 297, space group $C_{2/n}$, a = 15.752(16), b = 13.052(12), c = 12.378(11) Å, β = 118.68(5)°, V= 2232(4) $Å^3$, Z = 8, D_c = 1.26 g cm^{-3}, F(000) = 1184. Using 1.7° ω-scans at scan rate of 7.32° min^{-1}, 855 unique reflections were collected in the range of $4 < 2\theta < 45°$ and 692 of these having $I > 3\sigma(I)$ were used in the structural analysis.

Data were recorded at 148 K on a Nicolet R3m four circle diffractometer using Mo - Kα radiation. Cell parameters were determined by least squares refinement of 25 accurately centred reflections in the range of $5 < 2\theta < 35°$. Crystal stability was monitored by recording 3 check reflections (1. 1 1 3, 2. -4-2 0, 3. -4 2 0) every 100 reflections and no significant variations were observed. Data were corrected for Lorentz-polarisation effects and absorption.

A patterson map located the bromine atoms, and direct methods revealed the position of the non-hydrogen atoms and the structure was refined by blocked cascade least-squares techniques. Hydrogen atoms were inserted at calculated positions using a riding model with thermal parameters equal to 1.2 U of their carrier atoms. All non-hydrogen atoms were refined anisotropically (115 parameters). The refinement converged with R = 0.079 and R_w = 0.051. The final difference fourier map showed no significant features. All programs used in the data collection and structure solution are contained in the SHELXTL (Version 4.1) package.[E5]

TABLE 1. Atomic Coordinates (x10^4) and Isotropic Thermal Parameters (Å^{2}x10^3) for 4.26.

Atom	x	y	z	U
Br	3536(1)	5947(1)	6440(2)	54(1)*
O(1)	2363(8)	8769(8)	8043(10)	56(7)*
O(2)	3010(8)	7869(9)	7072(10)	49(4)
O(3)	4436(11)	6405(10)	4950(14)	92(11)*
O(4)	4887(11)	8030(10)	5476(13)	77(10)*
C(1)	2803(12)	8799(13)	7480(16)	43(5)
C(2)	3214(13)	9591(13)	7072(16)	49(5)
C(3)	3165(13)	10656(13)	7191(17)	54(6)
C(4)	3535(13)	11266(14)	6637(16)	56(6)
C(5)	3953(12)	10853(16)	5998(15)	52(5)
C(6)	4030(12)	9810(14)	5864(16)	58(6)
C(7)	3655(11)	9204(12)	6437(15)	43(5)
C(8)	3567(15)	8061(14)	6486(19)	61(5)
C(9)	3842(14)	7227(12)	6095(17)	57(11)*
C(10)	4448(14)	7288(14)	5484(16)	48(11)*
C(11)	4965(16)	6424(15)	4130(23)	88(15)*
C(12)	5874(18)	6314(16)	5011(21)	92(16)*

*Equivalent isotropic U defined as one third of the trace of the orthogonalised U_{ij} tensor

Table 2. Bond lengths (Å) for 4.26.

Br-C(9)	1.845(18)	O(1)-C(1)	1.195(29)
O(2)-C(1)	1.412(23)	O(2)-C(8)	1.404(32)
O(3)-C(10)	1.324(24)	O(3)-C(11)	1.593(39)
O(4)-C(10)	1.193(26)	C(1)-C(2)	1.434(29)
C(2)-C(3)	1.403(24)	C(2)-C(7)	1.372(32)
C(3)-H(3)	0.960(1)	C(3)-C(4)	1.352(31)
C(4)-H(4)	0.960(1)	C(4)-C(5)	1.360(32)
C(5)-H(5)	0.960(1)	C(5)-C(6)	1.384(28)
C(6)-H(6)	0.960(1)	C(6)-C(7)	1.371(30)
C(7)-C(8)	1.502(25)	C(8)-C(9)	1.343(30)
C(9)-C(10)	1.477(36)	C(11)-H(11A)	0.960(1)
C(11)-H(11B)	0.960(1)	C(11)-C(12)	1.328(28)
C(11)-H(12A)	1.324(41)	C(12)-H(12A)	0.980(1)
C(12)-H(12B)	0.980(1)	C(12)-H(12C)	0.980(1)

Table 3. Bond angles (°) for 4.26.

C(1)-O(2)-C(8)	109.0(15)	C(10)-O(3)-C(11)	114.7(17)
O(1)-C(1)-O(2)	118.6(16)	O(1)-C(1)-C(2)	135.5(18)
O(2)-C(1)-C(2)	105.9(18)	C(1)-C(2)-C(3)	128.4(22)
C(1)-C(2)-C(7)	112.0(16)	C(3)-C(2)-C(7)	119.5(20)
C(2)-C(3)-H(3)	120.8(14)	C(2)-C(3)-C(4)	118.2(21)
H(3)-C(3)-C(4)	121.0(12)	C(3)-C(4)-H(4)	119.4(12)
C(3)-C(4)-C(5)	120.5(18)	H(4)-C(4)-C(5)	120.1(12)
C(4)-C(5)-H(5)	118.3(12)	C(4)-C(5)-C(6)	123.7(20)
H(5)-C(5)-C(6)	118.0(13)	C(5)-C(6)-H(6)	122.9(13)
C(5)-C(6)-C(7)	114.9(20)	H(6)-C(6)-C(7)	122.0(11)
C(2)-C(7)-C(6)	123.1(16)	C(2)-C(7)-C(8)	105.1(19)
C(6)-C(7)-C(8)	131.7(20)	O(2)-C(8)-C(7)	106.9(18)
O(2)-C(8)-C(9)	115.5(18)	C(7)-C(8)-C(9)	137.5(25)
Br-C(9)-C(8)	119.0(20)	Br-C(9)-C(10)	118.2(13)
C(8)-C(9)-C(10)	122.6(19)	O(3)-C(10)-O(4)	124.9(24)
O(3)-C(10)-C(9)	110.5(18)	O(4)-C(10)-C(9)	124.6(19)
O(3)-C(11)-H(11A)	112.1(9)	O(3)-C(11)-H(11B)	111.6(8)
H(11A)-C(11)-H(11B)	109.5(1)	O(3)-C(11)-C(12)	99.4(22)
H(11A)-C(11)-C(12)	112.1(14)	H(11B)-C(11)-C(12)	112.0(14)
O(3)-C(11)-H(12A)	142.7(20)	H(11A)-C(11)-H(12A)	88.5(13)
H(11B)-C(11)-H(12A)	88.2(13)	C(12)-C(11)-H(12A)	43.4(11)
C(11)-C(12)-H(12A)	68.1(20)	C(11)-C(12)-H(12B)	121.2(13)
H(12A)-C(12)-H(12B)	109.5(1)	C(11)-C(12)-H(12C)1	27.2(13)
H(12A)-C(12)-H(12C)	109.5(1)	H(12B)-C(12)-H(12C)	109.5(1)
C(11)-H(12A)-C(12)	68.5(15)		

TABLE 4. Anisotropic Thermal Parameters ($Å^2x10^3$) for 4.26.

Atom	U_{11}	U_{22}	U_{33}	U_{23}	U_{13}	U_{12}
Br	61(1)	39(1)	73(1)	8(2)	42(1)	-1(2)
O(1)	65(8)	53(9)	80(9)	-8(7)	58(8)	-9(7)
O(3)	153(14)	45(9)	155(14)	-40(9)	136(13)	-35(9)
O(4)	112(13)	38(9)	115(13)	-13(9)	82(11)	-16(9)
C(9)	80(16)	32(12)	71(14)	6(11)	46(13)	-0(12)
C(10)	65(15)	39(13)	62(14)	-1(11)	47(13)	-6(11)
C(11)	83(18)	43(14)	111(22)	-19(14)	26(17)	-15(14)
C(12)	98(24)	58(16)	64(18)	-22(13)	-7(18)	-26(16)

The anisotropic temperature factor exponent takes the form:
$-2\pi^2(h^2a^{*2}U_{11} + k^2b^{*2}U_{22} + ...+ 2hka^*b^*U_{12})$

TABLE 5. Hydrogen Coordinates ($x10^4$) and Temperature Factors ($Å^2x10^3$) for 4.26.

Atom	x	y	z	U
H(3)	2893	10941	7671	75
H(4)	3478	11996	6671	65
H(5)	4207	11309	5614	62
H(6)	4353	9526	5443	70
H(11A)	4865	7060	3695	97
H(11B)	4759	5866	3554	97
H(12A)	5827	6360	4194	202(61)
H(12B)	6131	5640	5369	202(61)
H(12C)	6308	6851	5544	202(61)

Experimental

Chapter 5

Phenyl Glutaric Anhydride Series

Ethyl E- and Z-bromo-(4-phenyl-6-oxotetrahydropyran-2-ylidene)acetate ***5.9*** *and* ***5.10.***

A solution containing 3-phenylglutaric anhydride **5.11** (100mg, 0.53mM) and ylide 0.1 (201mg, 0.58mM) was heated at reflux in $CHCl_3$ for 1 hour. The solvent was removed under reduced pressure, ^1H NMR spectroscopy revealed the keto acid phosphorane **5.12**, to have formed in 90%. CH_2Cl_2 (10mL) was added and the resulting solution was cooled to 0°C. Triethylamine (67µl, 0.48mM), followed by bromine (25µl, 0.48mM), was added to this solution and stirred for a further 30 minutes at 0°C. ^1H NMR spectroscopy revealed the *E-* and *Z-* isomers to be present in a ratio of 86:14, respectively, in the crude mixture. The solvent was removed, and the residue purified and separated by radial chromatography, using a 2mm silica gel plate and eluted with CH_2Cl_2, and gave ethyl *E-* and *Z*-bromo-(4-phenyl-6-oxotetrahydropyran-2-ylidene)acetate **5.9** (100mg) and **5.10** (17mg), as clear oils, combined yield of 72%.

1-ethoxycarbonyl-5-carboxy-2-oxo-4-phenylpentan-1-ylidenetriphenylphosphorane **5.12**. ^1H NMR δ ($CDCl_3$) 0.61 (t, 7.1, $OCH_2C\mathbf{H_3}$), 2.49 (dd, 6.9, 13.9, (**H-3**)$_2$), 3.26 (dd, 8.1, 13.8, (**H-4**)), 3.51 (dd, 5.7, 19.6, (**H-5**)$_2$), 3.62 (m, $OC\mathbf{H_2}CH_3$), 7.17-7.67 (m, $\mathbf{Ph_3}P$, **Ph**). ^{13}C NMR δ ($CDCl_3$) 13.5, 37.0, 392, 43.6, 58.7, 125.8(94), 127.6, 128.1, 128.4, 128.6, 131.7(3), 132.9(10), 144.0, 167.3(14), 175.0, 195.4(3.1).

Ethyl *E*-bromo-(4-phenyl-6-oxotetrahydropyran-2-ylidene)acetate **5.9**. Mass Spect. $C_{15}H_{15}BrO_4$ requires calc. 338.0154, found 338.0156. ^1H NMR δ ($CDCl_3$) 1.36 (t, 7.1, $OCH_2C\mathbf{H_3}$), 2.72 (dd, 12.4, 18.0, (**H-2**)a), 2.76 (dd, 12.0, 17.0, (**H-4**)a), 2.98 (ddd, 2.2, 4.2, 17.0, (**H-2**)b), 3.3 (m, **H-3**), 3.3 (m, (**H-4**)b), 4.32 (q, 7.1, $OC\mathbf{H_2}CH_3$), 7.19-7.42 (m, **Ph**). ^{13}C NMR δ ($CDCl_3$) 14.1, 34.9, 35.2, 36.9, 62.4, 98.3, 126.3, 127.8, 129.2, 140.3, 154.0, 162.1, 165.1.

Ethyl *Z*-bromo-(4-phenyl-6-oxotetrahydropyran-2-ylidene)acetate **5.10**. ^1H NMR δ ($CDCl_3$) 1.33 (t, 7.1, $OCH_2C\mathbf{H_3}$), 2.82 (dd, 11.6, 23.2, (**H-2**)a), 2.9 (dd 11.6, 23.0, (**H-4**)a), 3.28 (m, **H-3**), 3.32 (ddd, 2.2, 4.6, 17.4, (**H-2**)b), 3.89 (ddd, 2.2, 4.2, 17.1, (**H-4**)b), 4.25 (q, 7.1, $OC\mathbf{H_2}CH_3$), 7.20-7.51 (m, **Ph**). ^{13}C NMR δ ($CDCl_3$) 14.1, 34.0, 35.5, 37.6, 62.4, 104.5, 126.4, 127.8, 129.2, 140.2, 159.4, 163.5, 165.3.

Ethyl E-4-phenyl-6-oxotetrahydropyran-2-ylideneacetate ***5.13***.

A solution containing 3-phenylglutaric anhydride **5.11** (100mg, 0.53mM) and ylide **0.1** (201mg, 0.58mM) was heated at reflux in $CHCl_3$ for 24 hours. The solvent was removed under reduced pressure. Purification by radial chromatography, using a 2mm silica gel plate and eluted with CH_2Cl_2, gave ethyl *E*-4-phenyl-6-oxotetrahydropyran-2-ylideneacetate **5.13** as a clear oil (137mg) 86%.

Ethyl *E*-4-phenyl-6-oxotetrahydropyran-2-ylideneacetate **5.13**. Mass Spect. $C_{15}H_{16}O_4$ requires calc. 260.1048, found 260.1060. ^1H NMR δ ($CDCl_3$) 1.31 (t, 7.1, $OCH_2C\mathbf{H_3}$), 2.80 (dd, 12.2, 22.5, (**H-2**)a), 2.89 (ddd, 2.3, 12.4, 20.3, (**H-4**)a), 3.05 (dd, 2.7, 4.1, 22.3, (**H-2**)b), 3.26 (m, **H-3**), 3.98 (ddd, 2.4, 4.0, 20.3, (**H-4**)b), 4.23 (q, 7.1, $O\mathbf{CH_2}CH_3$), 5.71 (d, 2.8, 1H), 7.20-7.51 (m, **Ph**). ^{13}C NMR δ ($CDCl_3$) 13.1, 34.3, 34.5, 37.7, 61.7, 101.5, 126.4, 127.3, 129.2, 140.23, 155.3, 163.4, 165.8.

Phenyl Succinic Anhydride Series

Ethyl E-4-phenyl-5-oxotetrahydrofuran-2-ylideneacetate ***5.31*** *and Ethyl E-3-phenyl-5-oxotetrahydrofuran-2-ylideneacetate* ***5.32***.

A solution containing phenyl succinic anhydride **5.17** (100mg, 0.57mM) and ylide **0.1** (197mg, 0.57mM) was heated at reflux in $CHCl_3$ for 6 hours. The residue obtained on removing the solvent under reduced pressure contained ethyl *E*-4-phenyl-5-oxotetrahydrofuran-2-ylideneacetate **5.31** and ethyl *E*-3-phenyl-5-oxotetrahydrofuran-2-ylideneacetate **5.32**. in a ratio of 62:38 (by ^1H NMR spectroscopy). The *E*-enol lactones **5.31** and **5.32** were purified, by radial chromatography, using a 2mm silica gel chromatotron plate, and eluted with CH_2Cl_2. and gave a white solid containing both isomers, (72mg, 55%). The enol lactones were separated by HPLC using a 10 mm Econosphere CN column, with a UV spectrographic detector at 256 nm, eluting with CH_2Cl_2 and hexane (22:78) with a flow rate of 4ml min^{-1}. Mass Spect. on mixture of isomers, $C_{14}H_{14}O_4$ requires calc. 246.0892, found 246.0899.

Ethyl *E*-4-phenyl-5-oxotetrahydrofuran-2-ylideneacetate **5.31**. ^1H NMR δ ($CDCl_3$) 1.31 (t, 7.1, $OCH_2C\mathbf{H_3}$), 3.49 (ddd, 2.3, 6.3, 16.8, (**H-3**)a), 3.92 (ddd, 2.1, 10.5, 16.8, (**H-3**)b), 4.05 (dd, 6.3, 10.5, **H-4**), 4.30 (q, 7.1, $O\mathbf{CH_2}CH_3$), 5.79 (t, 2.1, $C\mathbf{H}CO_2Et$), 7.25-7.51 (m, **Ph**). ^{13}C NMR δ ($CDCl_3$) 13.9, 40.3, 49.7, 60.1, 97.6, 127.2, 129.0, 129.1, 140.9, 167.4, 173.7, 177.5.

Ethyl *E*-3-phenyl-5-oxotetrahydrofuran-2-ylideneacetate **5.32**. ^1H NMR δ ($CDCl_3$) 1.38 (t, 7.1, $OCH_2C\mathbf{H_3}$), 2.67 (dd, 2.7, 18.4, (**H-4**)a), 3.19 (dd,

10.1, 18.4, (**H-4**)b), 4.34 (q, 7.1, OCH_2CH_3), 5.06 (ddd, 1.8, 2.7, 10.1, **H-3**), 5.81 (d, 1.8, $CHCO_2Et$), 7.25-7.51 (m, **Ph**). ^{13}C NMR δ ($CDCl_3$) 14.1, 34.8, 43.9, 60.0, 127.9, 128.8, 129.3, 165.5, 174.8, 176.0.

*^1H NMR Spectroscopy Study on Solvent Effects of the Reaction of **5.17** with Ylide **0.1**.*

Ylide **0.1** (20mg, 0.6mM) was added to a solution containing phenyl succinic anhydride **5.17** (10mg, 0.06mM), and was heated at reflux in $CDCl_3$ (5mL). An identical reaction using THF at reflux was run simultaneously. The reactions were monitored by ^1H NMR spectroscopy of selected signals **5.31** (5.79ppm, t, 2.1, $CHCO_2Et$), **5.32** (5.81ppm, d, 1.8, $CHCO_2Et$), **5.33** (5.85ppm, ddd, 1.4, 2.7, 9.0, $CHCH_2$), and **5.34** (5.41, td, 1.6, 7.0, $CHCH_2$) over 60 hours. **5.33** and **5.34** were not characterised, but they had almost identical chemical shifts as **5.25** and **5.26**[5,6]. See Table 5.4 for results of NMR study.

*Ethyl E- and Z-bromo-(3-phenyl-5-oxotetrahydrofuran-2-ylidene)acetate **5.20** and **5.21**, and Ethyl E- and Z-bromo-(4-phenyl-5-oxotetrahydrofuran-2-ylidene)acetate **5.22** and **5.23***

The ylide **0.1** (395mg, 1.14mM) was added to a stirred solution of phenyl succinic anhydride(200mg, 1.14mM), in $CHCl_3$ (10mL), at 25°C. After 60 minutes the acylphosphoranes **5.18** and **5.19** had formed in a ratio of 62:38, respectively, and a total maximum of 44% (by ^1H NMR spectroscopy, intermediate signals **5.18** δ ($CDCl_3$) 0.57 (t, 7.0, OCH_2CH_3), 3.68 (q, 7.0, OCH_2CH_3), **5.19** δ ($CDCl_3$) 0.65 (t, 7.0, OCH_2CH_3), 3.50 (q, 7.0, OCH_2CH_3)). Triethylamine (70μL, 0.50mM), followed by bromine (26μL, 0.50mM), was added and the solution was stirred for a further 30 minutes at 0°C. The solvent was removed under reduced pressure. ^1H NMR spectroscopy of the crude mixture revealed **5.20**, **5.21**, **5.22**, and **5.23** in a ratio of 24:12:55:9, respectively. Purification by radial chromatography, on a 2mm silica gel chromatotron plate eluting with CH_2Cl_2, gave a mixture of the four isomers as a pale yellow oil, total yield of 38%(139mg, 86% based on the amount of acylphosphoranes **5.18** and **5.19**). Partial separation of the four isomers by HPLC using a 10 mm Econosphere CN column, with a UV spectrographic detector at 256 nm, eluting with CH_2Cl_2 and hexane (25:70) with a flow rate of 4ml min^{-1}, gave a small amount of pure **5.21** (2mg). Mass Spect. on the mixture of four isomers, $C_{14}H_{13}BrO_4$ requires calc. 324.0000, found 324.0012.
Ethyl E-bromo-(3-phenyl-5-oxotetrahydrofuran-2-ylidene)acetate **5.20**. ^1H NMR δ ($CDCl_3$) 1.35 (t, 7.1, OCH_2CH_3), 3.21 (dd, 6.9, 18.7, (**H-4**)a), 3.63

(dd, 10.3, 18.7, (**H-4**)b), 4.08 (dd, 6.9, 10.2, **H-3**), 4.32 (q, 7.1, OCH_2CH_3), 7.25-7.64 (m, **Ph**).

Ethyl Z-bromo-(3-phenyl-5-oxotetrahydrofuran-2-ylidene)acetate **5.21**. ^1H NMR δ ($CDCl_3$) 1.37 (t, 7.1, OCH_2CH_3), 3.48 (dd, 6.7, 19.1, (**H-4**)a), 3.95 (dd, 10.5, 19.1, (**H-4**)b), 4.15 (dd, 6.7, 11.1, **H-3**), 4.34 (q, 7.1, OCH_2CH_3), 7.25-7.64 (m, **Ph**).

Ethyl E-bromo-(4-phenyl-5-oxotetrahydrofuran-2-ylidene)acetate **5.22**. ^1H NMR δ ($CDCl_3$) 1.31 (t, 7.0, OCH_2CH_3), 2.73 (dd, 3.0, 18.7, (**H-3**)a), 3.26 (dd, 10.1, 18.7, (**H-3**)b), 4.32 (q, 7.0, OCH_2CH_3), 4.54 (dd, 3.0, 10.1, **H-4**), 7.25-7.64 (m, **Ph**).

Ethyl Z-bromo-(4-phenyl-5-oxotetrahydrofuran-2-ylidene)acetate **5.23**. ^1H NMR δ ($CDCl_3$) 1.38 (t, 7.0, CH_2CH_3), 2.75 (dd, 2.3, 18.3, (**H-3**)a), 3.20 (dd, 10.0, 18.5, (**H-3**)b), 4.37 (q, 7.0, OCH_2CH_3), 5.10 (dd, 2.3, 10.1, **H-4**), 7.25-7.64 (m, **Ph**). ^{13}C NMR δ ($CDCl_3$) (mixture) 13.1, 13.2, 13.9, 44-55, 62.1, 62.3, 63.5, 94.0, 95.6, 99.1, 127-134, 161-172.

Ethyl E-2-(4-phenyl-5-oxotetrahydrofuran-2-ylidene)propionate ***5.35*** *and Ethyl E-2-(3-phenyl-5-oxotetrahydrofuran-2-ylidene)propionate* ***5.36***.

A solution containing phenyl succinic anhydride **5.17** (100mg, 0.57mM) and methyl ylide **2.53** (206mg, 0.57mM) was heated in $CHCl_3$ at reflux, for 6 hours. The solvent was removed under reduced pressure and the residue contained ethyl *E*-2-(4-phenyl-5-oxotetrahydrofuran-2-ylidene)propionate **5.35** and ethyl *E*-2-(3-phenyl-5-oxotetrahydrofuran-2-ylidene)propionate **5.36** in a ratio of 74:26 (by ^1H NMR spectroscopy). The *E*-enol lactones **5.35** and **5.36** were purified by radial chromatography, using a 2mm silica gel chromatotron plate and eluted with CH_2Cl_2, gave a white solid containing both isomers, total yield of 68%(101mg). Mass Spect. on the mixture $C_{15}H_{16}O_4$ requires calc. 260.1048, found 260.1053.

Ethyl *E*-2-(4-phenyl-5-oxotetrahydrofuran-2-ylidene)propionate **5.35**. ^1H NMR δ ($CDCl_3$) 1.29 (t, 7.0, OCH_2CH_3), 2.96 (t, 1.5, CH_3), 3.45 (ddq, 1.5, 6.4, 17.1, (**H-3**)a), 3.89 (ddq, 1.5, 10.2, 17.1, (**H-3**)b), 4.05 (dd, 6.4, 10.2, **H-4**), 4.30 (q, 7.0, OCH_2CH_3), 7.25-7.64 (m, **Ph**). ^{13}C NMR δ ($CDCl_3$) 13.2, 25.9, 41.2, 49.3, 60.9, 103.0, 127.9, 128.4, 129.7, 141.2, 165.3, 170.2, 173.1.

Ethyl *E*-2-(3-phenyl-5-oxotetrahydrofuran-2-ylidene)propionate **5.36**. ^1H NMR δ ($CDCl_3$) 1.30 (t, 7.0, OCH_2CH_3), 2.64 (dd, 2.2, 18.2, (**H-4**)a), 2.98 (d, 1.5, CH_3), 3.22 (dd, 10.0, 18.2, (**H-4**)a), 4.31 (q, 7.0, OCH_2CH_3), 5.05 (ddq, 1.5, 2.2, 10.0, **H-3**), 7.25-7.64 (m, **Ph**). ^{13}C NMR δ ($CDCl_3$) 13.4, 28.4, 35.3, 42.1, 60.3, 101.3, 127.6, 127.9, 128.7, 140.1, 167.3, 172.1, 173.4.

Acetyl Protected Aspartic Anhydride Series

Ethyl E-4-acetamido-5-oxotetrahydrofuran-2-ylideneacetate ***5.51*** *and Ethyl E-3-acetamido-5-oxotetrahydrofuran-2-ylideneacetate* ***5.52.***

A solution containing N-acetyl aspartic anhydride **5.17** (100mg, 0.64mM) and ylide **0.1** (221mg, 0.64mM) was heated in $CHCl_3$ at reflux, for 48 hours. The residue obtained on removal of the solvent under reduced pressure contained ethyl *E*-4-acetamido-5-oxotetrahydrofuran-2-ylideneacetate **5.51** and ethyl *E*-3-acetamido-5-oxotetrahydrofuran-2-ylideneacetate **5.52** in a ratio of 58:42 (by ^1H NMR spectroscopy). The *E*-enol lactones **5.51** and **5.52** were purified by radial chromatography, using a 2mm silica gel chromatotron plate and eluted with ethyl acetate:CH_2Cl_2 (15:85), and gave fractions that contained both isomers, combined yield of 68%. Mass Spect. on mixture $C_{10}H_{12}NO_4$ requires calc. 227.0793, found 227.0800.

Ethyl *E*-4-acetamido-5-oxotetrahydrofuran-2-ylideneacetate **5.51**. ^1H NMR δ ($CDCl_3$) 1.36 (t, 7.0, $OCH_2C\mathbf{H_3}$), 2.91 (s, $C\mathbf{H_3}$), 3.22 (ddd, 2.1, 6.7, 19.2, (**H-3**)a), 3.76 (ddd, 2.0, 10.5, 19.3, (**H-3**)b), 4.39 (q, 7.0, $OC\mathbf{H_2}CH_3$), 4.80 (dd, 6.7, 10.5, **H-4**), 5.76 (t, 1.9, $C\mathbf{H}CO_2Et$). ^{13}C NMR δ ($CDCl_3$) 13.1, 23.5, 47.3, 56.1, 61.9, 62.8, 98.8, 158.3, 163.0, 176.7.

Ethyl *E*-3-acetamido-5-oxotetrahydrofuran-2-ylideneacetate **5.52**. ^1H NMR δ ($CDCl_3$) 1.37 (t, 7.0, $OCH_2C\mathbf{H_3}$), 2.67 (dd, 3.2, 18.2, (**H-4**)a), 2.90 (s, $C\mathbf{H_3}$) 3.07 (dd, 10.5, 18.4, (**H-4**)b), 4.38 (q, 7.0, $OC\mathbf{H_2}CH_3$), 5.62 (ddd, 1.6, 3.1, 10.7, **H-3**), 5.69 (d, 1.8, $C\mathbf{H}CO_2Et$) ^{13}C NMR δ ($CDCl_3$) 12.9, 23.6, 47.3, 54.1, 62.0, 104.1, 158.1, 162.5, 172.9, 173.1.

Ethyl E- and Z-bromo-(4-acetamido-5-oxotetrahydrofuran-2-ylidene)acetate ***5.44*** *and* ***5.45*** *and Ethyl E- and Z-bromo-(3-acetamido-5-oxotetrahydrofuran-2-ylidene)acetate* ***5.46*** *and* ***5.47.***

A solution containing N-acetyl aspartic anhydride **5.48** (100mg, 0.64mM) and ylide **0.1** (221mg, 0.64mM) was heated in $CHCl_3$ at reflux, for 90 minutes. The acylphosphoranes **5.49** and **5.50** formed in a ratio of 80:20, respectively, and a total maximum of 80% (by ^1H NMR spectroscopy, intermediate signals **5.49** δ ($CDCl_3$) 0.67 (t, 7.0, $OCH_2C\mathbf{H_3}$), **5.50** δ ($CDCl_3$) 0.63 (t, 7.0, $OCH_2C\mathbf{H_3}$)). The solution was cooled to 0°C, and triethylamine (70μL, 0.50mM), followed by bromine (26μL, 0.50mM), were added. After stirring for a further 30 minutes at 0°C, the solvent was removed under reduced pressure and gave a residue containing a small amount of bromo enol lactone products (15% based on the ^1H NMR spectroscopy resonance integrals for the quartet signals for the bromo enol lactones and of starting material). Radial chromatography on a 2mm silica

gel chromatotron plate using a gradient of ethyl acetate in CH_2Cl_2 failed to isolate the bromo enol lactone products, but gave one fraction as an yellow oil (16mg), that contained characteristic ^1H NMR resonances for the ethyl ester of bromo enol lactones. Mass Spect. on that fraction, $C_{10}H_{12}Br\ NO_4$ requires calc. 304.9899, found 304.9912. ^1H NMR δ ($CDCl_3$) 1.29 (t, 7.0, $OCH_2C\mathbf{H_3}$), 1.33 (t, 7.0, $OCH_2C\mathbf{H_3}$), 1.36 (t, 7.0, $OCH_2C\mathbf{H_3}$), 1.37 (t, 7.0, $OCH_2C\mathbf{H_3}$), 4.27 (q, 7.1, $OC\mathbf{H_2}CH_3$), 4.32 (q, 7.1, $OC\mathbf{H_2}CH_3$), 4.37 (q, 7.1, $OC\mathbf{H_2}CH_3$), 4.39 (q, 7.1, $OC\mathbf{H_2}CH_3$).

Ethyl E-2-(4-acetamido-5-oxotetrahydrofuran-2-ylidene)propionate **5.53** *and Ethyl E-2-(3-acetamido-5-oxotetrahydrofuran-2-ylidene)propionate* **5.54**.

A solution containing N-acetyl aspartic anhydride **5.48** (100mg, 0.64mM) and methyl ylide **2.53** (206mg, 0.64mM) was heated at reflux in $CHCl_3$ for 6 hours. The solvent was removed under reduced pressure and the residue contained **5.53** and **5.54** in a ratio of 64:36 (by ^1H NMR spectroscopy). The *E*-enol lactones **5.53** and **5.54** were purified by radial chromatography, using a 2mm silica gel chromatotron plate and eluted with ethyl acetate:CH_2Cl_2 (15:85), as a clear oil containing both isomers, a combined yield of 53%(77mg). Mass Spect. on mixture of isomers, $C_{11}H_{15}NO_4$ requires calc. 241.0950, found 241.0971.
Ethyl *E*-2-(4-acetamido-5-oxotetrahydrofuran-2-ylidene)propionate **5.53**. ^1H NMR δ ($CDCl_3$) 1.31 (t, 7.0, $OCH_2C\mathbf{H_3}$), 1.95 (t, 2.0, $CC\mathbf{H_3}$), 2.91 (s, $COC\mathbf{H_3}$), 3.19 (ddq, 2.1, 6.7, 18.7, (**H-3**)a), 3.74 (ddq, 1.9, 10.8, 18.9, (**H-3**)b), 4.29 (q, 7.0, $OC\mathbf{H_2}CH_3$), 4.78 (dd, 6.9, 10.1, **H-4**). ^{13}C NMR δ ($CDCl_3$) 13.1, 23.3, 28.1, 46.3, 53.1, 61.1, 105.1, 156.1, 163.5, 169.1, 171.5.
Ethyl *E*-2-(3-acetamido-5-oxotetrahydrofuran-2-ylidene)propionate **5.54**. ^1H NMR δ ($CDCl_3$) 1.37 (t, 7.0, $OCH_2C\mathbf{H_3}$), 1.93 (d, 1.0, $CC\mathbf{H_3}$), 2.90 (s, $COC\mathbf{H_3}$), 2.93 (bd, 10.2, $(\mathbf{H\text{-}4})_2$), 4.29 (q, 7.0, $OC\mathbf{H_2}CH_3$), 4.99 (m, **H-3**), 6.5 (bs, N**H**). ^{13}C NMR δ ($CDCl_3$) 13.9, 23.7, 29.9, 48.9, 55.0, 62.3, 101.4, 156.3, 162.9, 165.6, 177.7.

Cbz Aspartic Anhydride Series

Ethyl E-3-N-benzyloxycarbonylamido-5-oxotetrahydrofuran-2-ylideneacetate **5.64**.

A solution containing N-benzyloxycarbonyl-L-aspartic anhydride **5.57** (50mg, 0.20mM) and ylide **0.1** (70mg, 0.20mM) was heated at reflux in $CHCl_3$ for 24 hours. The solvent was removed under reduced pressure. The crude ethyl *E*-3-N-benzyloxycarbonylamido-5-oxotetrahydrofuran-2-ylideneacetate **5.64** was purified by radial chromatography, using a 2mm

silica gel chromatotron plate and eluted with ethyl acetate:CH_2Cl_2 (15:85), gave a white oil, 79%(51mg). Mass Spect. $C_{16}H_{17}NO_4$ requires calc. 319.1056, found 319.1069.
Ethyl *E*-3-N-benzyloxycarbonylamido-5-oxotetrahydrofuran-2-ylideneacetate **5.64**. ^{1}H NMR δ ($CDCl_3$) 1.31 (t, 7.0, $OCH_2C\mathbf{H_3}$), 2.96 (bd, 11.6, $(\mathbf{H\text{-}4})_2$), 4.29 (q, 7.0, $OC\mathbf{H_2}CH_3$), 4.97 (ddd, 1.5, 6.0, 17.62, **H-3**), 5.09 (ABq, 8.1, 10.3, $OC\mathbf{H_2}Ph$), 5.74 (bs, $C\mathbf{H}CO_2Et$), 6.05 (bs, N**H**) 7.25-7.60 (m, **Ph**). ^{13}C NMR δ ($CDCl_3$) 13.9, 45.7, 50.8, 60.8, 66.3, 98.8, 125-131, 137.0, 156.0, 163.3, 167.7, 171.2.

Ethyl E-2-(3-N-benzyloxycarbonylamido-5-oxotetrahydrofuran-2-ylidene)propionate ***5.65***.

A solution containing N-benzyloxycarbonyl-L-aspartic anhydride **5.57** (50mg, 0.20mM) and ylide **2.53** (73mg, 0.20mM) in $CHCl_3$, at room temperature, was stirred for 24 hours. The solvent was removed under reduced pressure. The crude ethyl *E*-2-(3-N-benzyloxycarbonylamido-5-oxotetrahydrofuran-2-ylidene)propionate **5.65** was purified by radial chromatography, using a 2mm silica gel chromatotron plate and eluted with ethyl acetate:CH_2Cl_2, (15:85), and gave a white oil, 82%(53mg).
Ethyl *E*-2-(3-N-benzyloxycarbonylamido-5-oxotetrahydrofuran-2-ylidene)propionate **5.65**. ^{1}H NMR δ ($CDCl_3$) 1.31 (t, 7.0, $OCH_2C\mathbf{H_3}$), 1.93 (s, $CC\mathbf{H_3}$), 2.96 (bd, 10.2, $(\mathbf{H\text{-}4})_2$), 4.29 (q, 7.0, $OC\mathbf{H_2}CH_3$), 5.05 (m, **H-3**), 5.10 (ABq, 8.1, 12.1, $OC\mathbf{H_2}Ph$), 5.91 (bs, N**H**),7.25-7.60 (m, **Ph**). ^{13}C NMR δ ($CDCl_3$) 13.9, 30.4, 48.8, 50.5, 60.5, 66.4, 107.2, 128.4, 128.6, 129.0, 135.7, 156.1, 161.1, 168.3, 171.6.

Ethyl E- and Z-bromo-(3-N-benzyloxycarbonylamido-5-oxotetrahydrofuran-2-ylidene)acetate ***5.60*** *and* ***5.61***.

Ylide **0.1** (139mg, 0.40mM) was added to a stirred solution of N-benzyloxycarbonyl-L-aspartic anhydride **5.57** (100mg, 0.40mM), in $CHCl_3$ (10mL), at 25°C. After 60 minutes the acylphosphorane **5.58** formed to a maximum of 66% (by ^{1}H NMR spectroscopy intermediate signals **5.58** δ ($CDCl_3$) 0.64 (t, 7.0, $OCH_2C\mathbf{H_3}$)). Triethylamine (38μL, 0.27mM), followed by bromine (14μL, 0.27mM) were added and stirring was continued for a further 30 minutes at 0°C. The solvent was removed under reduced pressure. The residue contained ethyl *E*- and *Z*-bromo-(3-N-benzyloxycarbonylamido-5-oxotetrahydrofuran-2-ylidene)acetate **5.60** and **5.61** in a ratio of 3:5 (by ^{1}H NMR spectroscopy). Purification was by radial chromatography, using a 2mm silica gel chromatotron plate and eluted with ethyl acetate:CH_2Cl_2 (15:85), gave a pale yellow oil that contained

5.60 and **5.61**, 51%(81mg, 77% yield based on the amount of acylphosphorane **5.58**). Mass Spect. on mixture, $C_{16}H_{16}BrNO_4$ requires calc. 397.0161, found 397.0178.

Ethyl *E*-bromo-(3-N-benzyloxycarbonylamido-5-oxotetrahydrofuran-2-ylidene)acetate **5.60**. ^{1}H NMR δ ($CDCl_3$) 1.31 (t, 7.0, $OCH_2C\mathbf{H_3}$), 3.07 (bd, 6.6, **(H-4)**$_2$), 4.29 (q, 7.0, $OC\mathbf{H_2}CH_3$), 5.01 (dd, 6.2, 12.8, **H-3**), 5.09 (ABq, 7.2, 9.8, $OC\mathbf{H_2}Ph$), 6.05 (bs, **NH**), 7.25-7.60 (m, **Ph**).

Ethyl *Z*-bromo-(3-N-benzyloxycarbonylamido-5-oxotetrahydrofuran-2-ylidene)acetate **5.60**. ^{1}H NMR δ ($CDCl_3$) 1.35 (t, 7.0, $OCH_2C\mathbf{H_3}$), 3.09 (bd, 6.6, **(H-4)**$_2$), 4.31 (q, 7.0, $OC\mathbf{H_2}CH_3$), 5.09 (ABq, 7.2, 9.8, $OC\mathbf{H_2}Ph$), 5.15 (m, $C\mathbf{H}CO_2Et$), 6.05 (bs, **NH**), 7.25-7.60 (m, **Ph**). ^{13}C NMR δ ($CDCl_3$) (mixture) 13.9, 14.2, 45.3, 48.9, 50.5, 53.1, 61.9, 62.0, 65.9, 66.1, 94.5, 95.1, 127-130, 135.4, 156.0, 156.6, 161.1, 162.8, 166.7, 168.4 170.9.

Oxazolidinone Aspartic Series

(S)-3-Benzyloxycarbonyl-5-oxo-4-oxazolidineacetic Acid ***5.66***.

A solution containing N-benzyloxycarbonyl-L-aspartic acid[5.18] (200mg, 0.51mM), paraformaldehyde(45mg, 1.2mM), and p-toluenesulphonic acid.H_2O (9mg, 0.04mM) was heated in benzene (30mL), at reflux, for 60 minutes, in a Dean-Stark apparatus. Ethyl acetate (5mL) was added and the solution was washed with 0.3N K_2CO_3 (1mL) and H_2O (2x1mL), and dried with magnesium sulphate. The solvent was removed under reduced pressure and gave (S)-3-Benzyloxycarbonyl-5-oxo-4-oxazolidineacetic acid **5.66** as a white oil, 90%(129mg), and was not purified further, as it was sufficiently pure by ^{1}H and ^{13}C NMR on comparison with the known compound.

(S)-3-Benzyloxycarbonyl-5-oxo-4-oxazolidineacetic acid **5.66**. ^{1}H NMR δ ($CDCl_3$) 3.10 (m, **(H-2)**a), 3.32 (m, **(H-2)**b) 4.29 (dd, 5.8, 5.8, **(H-4)**), 5.19 (s, $C\mathbf{H_2}OPh$) 5.25 (bs, $NC\mathbf{H}_\alpha O$), 5.55 (bs, $NC\mathbf{H}_\beta O$), 7.29-7.37 (m, **Ph**). ^{13}C NMR δ ($CDCl_3$) 34.6, 51.3, 66.5, 78.9, 128.3, 128.6, 135.0, 152.2, 172.4, 175.0, 178.2.

1-ethoxycarbonyl-3-(3-N-benzyloxycarbonyl-5-oxo-4-oxazolidine)-2-oxoprop-1-ylidenetriphenylphosphorane ***5.68***.

To a stirred solution of (S)-3-Benzyloxycarbonyl-5-oxo-4-oxazolidineacetic acid **5.66** (100mg, 0.36mM), in benzene (20mL) under an N_2 atmosphere, at 0°C, was added DMF (1 drop), followed by slow addition of oxalyl chloride (0.32mL, 3.6mM). The solution was allowed to warm to room temperature after 1 hour, and stirred for a further 14 hours.

The solution was evaporated under reduced pressure and benzene (5mL) was added, and subsequently evaporated to remove any remaining oxalyl chloride. Final evaporation under reduced pressure gave the acid chloride **5.67** as a yellow oil. $CHCl_3$ (10mL) was added and the solution was again cooled to 0°C with stirring. The ylide **0.1** (251mg, 0.72mM) was then added, and after a further 30 minutes the solution was allowed to warm to room temperature. The solvent was removed under reduced pressure to yield the crude residue containing 1-ethoxycarbonyl-3-(3-benzyloxycarbonyl-5-oxo-4-oxazolidine)-2-oxopropan-1-ylidenetriphenylphosphorane **5.68** and protonated ylide **2.50d**. as a straw coloured solid. The oxazolidinephosphorane **5.68** was isolated by radial chromatography on a 2mm silica gel chromatotron plate eluting with ethyl acetate/CH_2Cl_2 (30:70) and gave a straw coloured flakey solid, in a yield of 84%(187mg). The oxazolidinephosphorane **5.68** was not recrystalised as it was pure by ^1H NMR spectroscopy.

1-ethoxycarbonyl-3-(3-N-benzyloxycarbonyl-5-oxo-4-oxazolidine)-2-oxopropan-1-ylidenetriphenylphosphorane **5.68**. IR υ_{max}, 3021, 2990, 1724, 1480, 1315. ^1H NMR δ ($CDCl_3$) 0.71 (t, 7.0, $OCH_2C\mathbf{H_3}$), 3.40 (m, **(H-3)**$_2$), 3.78 (q, 7.0, $OC\mathbf{H_2}CH_3$), 4.20 (m, **H-4**), 5.15 (s, $C\mathbf{H_2}OPh$), 5.30 (m, $NC\mathbf{H_2}O$), 7.35-7.7 (m, $\mathbf{Ph_3}P$, **Ph**). ^{13}C NMR δ ($CDCl_3$) 14.1, 37.2, 53.3, 59.7, 66.9, 78.9, 79.8, 128.3, 128.6, 135.0, 152.2, 162.6, 172.4, 175.0, 195.2. ^{31}P NMR δ ($CDCl_3$) 17.9.

1-Ethoxycarbonyl-4-N-benzyloxycarbonylamido-4-carboxy-2-oxobutan-1-ylidenetriphenylphosphorane ***5.59***.

NaOH (1mL, 1N) was added to a stirred solution of 1-(ethoxycarbonyl)-3-(3-N-benzyloxycarbonyl-5-oxo-4-oxazolidine)-2-oxopropan-1-ylidenetriphenylphosphorane **5.68** (150mg, 0.24mM), in methanol (3mL), at room temperature. After 4 hours, the solvent was removed under reduced pressure to yield a white solid residue. The free acid **5.59** was extracted with ethyl acetate (2 x 5mL) and the organic phase dried with magnesium sulphate. The solvent was removed under reduced pressure and gave 1-ethoxycarbonyl-4-benzyloxycarbonylamido-4-carboxy-2-oxobutan-1-ylidenetriphenylphosphorane **5.59** as a cream coloured solid(145mg, quantitative). IR υ_{max}, 3500-2700, 2679, 2360, 1714, 1504, 1440, 1274. ^1H NMR δ ($CDCl_3$) 0.671 (t, 7.0, $OCH_2C\mathbf{H_3}$), 3.10 (ddd, 1.0, 8.4, 15.0, **(H-3)**a), 3.75 (q, 7.0, $OC\mathbf{H_2}CH_3$), 3.68 (m, **(H-3)**b), 4.07(dd, 1.5, 15.0, **H-4**), 5.15 (ABq, 9.2, 9.6, $OC\mathbf{H_2}Ph$), 5.89 (d, 11.0, **NH**), 7.25-7.7 (m, $\mathbf{Ph_3}P$, **Ph**). ^{13}C NMR δ ($CDCl_3$) 13.5, 42.3, 50.5, 59.4, 76.7,

125.1, 127.9, 128.4, 128.8, 131.9, 132.3, 133.1, 133.3, 142.6, 155.4, 166.8, 173.1, 194.2. ^{31}P NMR δ ($CDCl_3$) 17.5.

Ethyl E-4-N-benzyloxycarbonylamido-5-oxotetrahydrofuran-2-ylideneacetate ***5.69.***

A solution of 1-ethoxycarbonyl-4-N-benzyloxycarbonylamido-4-carboxy-2-oxobutan-1-ylidenetriphenylphosphorane **5.59** (30mg, 0.05mM) was heated in $CHCl_3$ at reflux for 36 hours. The solvent was removed under reduced pressure and residue chromatographed by radial chromatography using a 1mm silica gel chromatotron plate and gave ethyl *E*-4-N-benzyloxycarbonylamido-5-oxotetrahydrofuran-2-ylideneacetate **5.69**, as a clear oil, 78% (12mg).

Ethyl *E*-4-N-benzyloxycarbonylamido-5-oxotetrahydrofuran-2-ylideneacetate **5.69**. ^{1}H NMR δ ($CDCl_3$) 1.34 (t, 7.0, $OCH_2C\mathbf{H_3}$), 3.25 (dd, 7.1, 18.1, (**H-3**)a), 3.88 (dd, 10.1, 18.5, (**H-3**)b), 4.32 (q, 7.1, $OC\mathbf{H_2}CH_3$) 4.36 (bq, 7.5, **H-4**), 5.12 (s, $OC\mathbf{H_2}Ph$), 5.63 (bs, $C\mathbf{H}CO_2Et$), 5.73 (bs, N**H**), 7.30-7.38 (m, **Ph**). ^{13}C NMR δ ($CDCl_3$) 13.8, 44.1, 53.1, 61.1, 65.9, 100,1, 128.4, 128.9, 135.1, 155.2, 167.1, 175.6.

Ethyl E- and Z-bromo-(4-N-benzyloxycarbonylamido-5-oxotetrahydrofuran-2-ylidene)acetate ***5.62*** *and* ***5.63.***

Triethylamine (21μl, 0.15mM) followed by bromine (8μl, 0.15mM) were added to a stirred solution of ethyl 1-ethoxycarbonyl-4-N-benzyloxycarbonylamido-4-carboxy-2-oxobutan-1-ylidenetriphenyl phosphorane **5.59** (90mg, 0.15mM), in CH_2Cl_2 (10ml), at O°C under N_2 atmosphere. The solution was stirred for a further 20 minutes at O°C, and then allowed to warm to room temperature. The solvent was removed under reduced pressure, and the residue containing ethyl *E*- and *Z*-bromo-(4-N-benzyloxycarbonylamido-5-oxotetrahydrofuran-2-ylidene)acetate **5.62** and **5.63** in a ratio of 34:66 (by ^{1}H NMR spectroscopy) was purified by radial chromatography using a 2mm silica gel plate and eluted with ethyl acetate/CH_2Cl_2 (15:85), and gave a clear oil that contained both isomers, total yield of 86 mg (77%). Mass Spect. on mixture $C_{16}H_{16}BrNO_4$ requires calc. 397.0161, found 397.0178

Ethyl *E*-bromo-(4-N-benzyloxycarbonylamido-5-oxotetrahydrofuran-2-ylidene)acetate **5.62**. ^{1}H NMR δ ($CDCl_3$) 1.38 (t, 7.0, $OCH_2C\mathbf{H_3}$), 3.27 (dd, 8.7, 18.5, (**H-3**)a), 3.86 (10.4, 18.5, (**H-3**)b), 4.38 (q, 7.1, $OC\mathbf{H_2}CH_3$) 4.43 (bq, 7.5, **H-4**), 5.12 (s, $OC\mathbf{H_2}Ph$), 5.73 (bd, 6.5, N**H**), 7.30-7.38 (m, **Ph**).

Ethyl *Z*-bromo-(4-N-benzyloxycarbonylamido-5-oxotetrahydrofuran-2-ylidene)acetate **5.63**. ^{1}H NMR δ ($CDCl_3$) 1.38 (t, 7.0, $OCH_2C\mathbf{H_3}$), 3.08 (dd,

8.2, 18.8, (**H-3**)a), 3.48 (dd, 10.6, 18.8, (**H-3**)b), 4.38 (q, 7.1, OCH_2CH_3) 4.43 (bq, 7.5, **H-4**), 5.12 (s, OCH_2Ph), 5.73 (bd, 6.5, **NH**), 7.30-7.38 (m, **Ph**). ^{13}C NMR δ ($CDCl_3$) (mixture) 13.5, 14.0, 45.8, 47.1, 50.1, 51.1, 62.5, 62.8, 66.5, 67.2, 94.0, 96.3, 127-129, 135.2, 135.6, 152.9, 154.0, 155.3, 157.9, 162.3, 163.5, 170.2, 172.1.

Biological and Preliminary Hydrolysis Testing of Bromo Enol Lactones

Antimicrobial Assay

Bacteria or fungi at a known concentration are mixed with Mueller Hinton or Potato dextrose agar and poured into petri dishes so that after incubation a 'lawn' of bacteria/fungi will grow over the dish. Samples are pipetted onto 6 millimetre diameter filter paper disks and their solvents evaporated. These are then placed onto the seeded agar dishes (with appropriate solvent and positive controls) and incubated. If the samples show any activity against the bacteria / fungi (i.e. are antimicrobial) there will be zones of radius of inhibition outside the disk. The six organisms that are currently tested against are: *Escherichia coli. Bacillus subtilis. Pseudomonas aeruginosa. Candida albicans. Trichophyton mentagrophytes. and Cladosporium resinae.*

2.33 and **2.34**, B. subtilis SM4, E. coli HM3, C. alb SM2, **3.13** and **3.14**, B. subtilis SM2, E. coli GR1, **4.25** and **4.26**, B. subtilis SM2, C. alb $GR3^{E7}$.

Antiviral Assay

Samples are pipetted onto 6 millimetre diameter filter paper disks and their solvents evaporated. These are then placed directly onto BSC-1 cells (African Green Monkey kidney), infected with either Herpes simplex type 1 virus (ATCC VR 733) or Polio virus type 1(Pfiser vaccine strain), then incubated. Assays are examined after 24 hours, using an inverted microscope, for the size of antiviral and or cytotoxic zones, and the type of cytotoxicity.

2.33 and **2.34**, C4,T1, **3.13** and **3.14**, C2, T7, **4.25** and **4.26**, C5, $T8^{E7}$.

P388 Antitumor Assay

Samples are pipetted onto a well containing P388 cells (2×10^5). 5µl sample aliquots of P388 are placed in duplicate wells for solvent, positive (Mitomycin C), and cell controls. Assays are incubated at 36°C, 5% CO_2, for 72 hours and the number of live cells are read by a Coulter Counter to obtain % inhibition.

2.33 and **2.34**, none detected, **3.13** and **3.14**, none detected, **4.25** and **4.26**, 71%, 2^{+E7}.

α-Chymotrypsin Assay

To the wells of a microtitre plate was added 100 µl of aqueous test solution or 50 µl of acetonitrile extract with 50 µl of water, 50 µl of 0.4 M Tris-HCl buffer, pH 7.6 and 50 µl of α-chymotrypsin (9 Units cm^{-3} in 50 mM Tris-HCl buffer, pH 7.6). The plate was then preincubated at 37°C for 30 minutes and then 100 µl of substrate, N-succinyl phenylalanine 4-nitroanilide (1 mg cm^{-3} in 50 mM Tris-HCl buffer, pH 7.6) added. The O.D. of the plate was then read at 410 nm and incubated for 60 minutes at 37°C and then read again.
2.33 and **2.34**, none detected, **3.13** and **3.14**, none detected, **4.25** and **4.26**, none detected.

*Preliminary ^1H NMR Spectroscopic Hydrolysis Study on **2.33**, **3.13**, and **3.14**.*

NaOH (2mg, 0.05mM) was added to **2.33** (5mg, 0.02mM), in CD_3OD (0.5mL), in a 3mm NMR tube, at 23°C, and the hydrolysis was monitored by ^1H NMR spectroscopy. Ethyl 2-bromo-5-methoxycarbonyl-3-oxo-pentanoate **2.70** appeared rapidly. p-Toluenesulphonic acid (4mg, 0.02mM) was added to **2.33** (5mg, 0.02mM), in CD_3OD (0.5mL), in a 3mm NMR tube, at 23°C, and the hydrolysis was monitored by ^1H NMR spectroscopy. The hydrolysis product **2.70** appeared slowly. The analogous acid hydrolysis reaction with **3.13** and **3.14**, on silica gel soaked with methanol, formed ethyl 2-bromo-6-methoxycarbonyl-3-oxo-hexanoate.
Ethyl 2-bromo-5-methoxycarbonyl-3-oxo-pentanoate **2.70**. ^1H NMR δ ($CDCl_3$) 1.35 (t, 7.1, $OCH_2C\mathbf{H_3}$), 2.54 (t, 7.2, $C\mathbf{H_2}CO_2$), 3.05 (bt, 7.2, $C\mathbf{H_2}COC$), 4.07 (q, 7.1, $OC\mathbf{H_2}CH_3$).
Ethyl 2-bromo-6-methoxycarbonyl-3-oxo-hexanoate. ^1H NMR δ ($CDCl_3$) 1.32 (t, 7.1, $OCH_2C\mathbf{H_3}$), 1.96 (m, $CH_2C\mathbf{H_2}CH_2$), 2.37 (t, 7.0, $C\mathbf{H_2}CO_2$), 2.86 (bt, 7.0, $C\mathbf{H_2}COC$), 3.68 (s, $OC\mathbf{H_3}$), 4.27 (q, 7.1, $OC\mathbf{H_2}CH_3$), 4.78 (s, C**H**Br).

References

0.1 Straudinger, H., Meyer, J., *Helv. Chim. Acta.*, 1919, **2**, 619.

0.2 Michaelis, A., Kohler, E., *Chem. Ber.*, 1899, **32**, 1566.

0.3 Johnson, A. J., 'Ylid Chemistry', 1966, Academic Press, New York.

0.4 Wittig, G., Geissler, G., *Liebigs Ann. Chem.*, 1953, **44**, 580.

0.5 Murphy, P. J., Brennan, J., *Chem. Soc. Rev.*, 1988, **17**, 1, and references cited therein.

0.6 Maryonoff, B. E., Reitz, A. B., *Chem. Rev.*, 1989, **89**, 830, and references cited therein.

0.7 Boutagy, J., Thomas, R., *Chem. Rev.*, 1974, **74**, 87.

0.8 Maercker, A., *Organic React*, 1966, **14**, 270.

0.9 'Phosphorus 31 NMR in stereochemical analysis', Verkede, J. G., Quin L. D., Ed. 1987, VCH Publishers Inc., Florida.

0.10 (a) Bestmann, H. J., *Angew. Chem. Int. Ed. Engl.*, 1965, **4**, 583., (b) Bestmann, H. J., *ibid*, 1965, **4**, 645., (c) Bestmann, H. J., *ibid*, 1965, **4**, 830.

0.11 Massy-Westropp, R. A., Price, M. F., *Aust. J. Chem.*, 1980, **33**, 333.

0.12 Pattenden, G., *Fortschr. Chem. Org. Naturst.*, 1978, **35**, 133, and references cited therein.

0.13 Rando, R. R., *Science*, 1974, **185**, 320.

0.14 Daniels, S. B., Cooney, E., Sofia, M. J., Chakravarty, P. K., Sofia, M. J., Katzenellenbogen, J. A., *J. Biol. Chem.*, 1983, **258**(24), 15046, and references cited therein.

0.15 Kraft, G. A., Katzenellenbogen, J. A., *J. Am. Chem. Soc.*, 1981, **103**, 5459.

0.16 Silverman, R. B., 'Mechanism-based enzyme inactivation: Chemistry and Enzymology', Vol I, 1988, CRC Press, Florida, and references cited therein.

0.17 (a) Lienhard, C. E., *Science*, 1973, **180**, 149., (b) Rich, R. D. J., *Med. Chem.*, 1985, **28**, 149., (c) Imperiali, B. B., Abeles, R. H., *Biochemistry*, 1986, **25**, 3760.

0.18 Jencks, W. P., 'Cold Spring Harbor Symposia on Quantitative Biology', 1987, **LII**, 65.

0.19 Lerner, R. A., Tramontano, A., *Scientific American*, 1988, **258**(3), 58.

0.20 Baek, D. J., Reed, P. E., Daniels, S. B., Katzenellenbogen, J.A., *Biochemistry*, 1990, **29**, 4305.

0.21 Baker, B. R., 'Design of active site directed irreversible enzyme inhibitors', 1967John Wiley and Sons, New York.

0.22 (a) Walsh, C., *Tetrahedron*, 1982, **38**(7), 871., (b) Abeles, R.H., Maycock, A.L., *Acc. Chem. Res.*, 1976, **9**(9), 313., (c) Rando, R., *Acc. Chem. Res.*, 1975, **8**(9), 281.

0.23 Wood, W. A., Gunsalus, T. C., *J. Biol. Chem.*, 1949, **181**, 171.

0.24 Endo, K., Helmkamp, G. M., Bloch, K. J., *J. Biol. Chem.*, 1970, **245**, 2293.

0.25 Copp, L. J., Drants, A., Spencer, R. W., *Biochemistry*, 1987, **26**, 169.

0.26 Dugas, H., 'Bioorganic Chemistry', 2nd Ed. 1989, Springer-Verlag, New York Inc.

0.27 Fersh, A., 'Enzyme structure and mechanism.', 2nd Ed., 1985, W. H. Freeman & Co., USA

0.28 Rawn, D. J., 'Biochemistry Internation Ed', 1989, Neil Patterson, North Carolina.

1.1 Etter, M. C., *Acc. Chem. Res.*, 1990, **23**(4), 120, and references cited therein.

1.2 Sadekov, I. D., Minkin, V.I., Lutskii A. E., *Russian Chemical Reviews*, 1970, **39**, 179.

1.3 Leninger, A. L., 'Principles of Biochemistry', 1982, Worth Publishers Inc., New York.

1.4 Joesten, M. D., Schaad, L. J., 'Hydrogen Bonding', 1974, Marcel Dekker, New York.

1.5 Vanderhoff, P. A., Lalancette, R. A., Thompson, H. W., *J. Org. Chem.*, 1990, **55**, 1696, and references cited therein.

1.6 Abell, A. D., Morris, K. B., McKee, V., *Aust. J. Chem.*, 1990, **43**, 765.

1.7 Tsuboi, S., Fukumoto, H., Wada, H., Takeda, A., Fukuyama, K., *Bull. Chem. Soc. Jpn.*, 1987, **60**, 689.

1.8 Iman, M., Bouyssou, P., Chenault, J., *Synthesis*, 1990, 631.

1.9 (a) Lang, R. W., Hansen, H. J., *Helv. Chim. Acta*, 1980, **63**, 438., (b) Aitken, A. R., Atherton, J. I., *J. Chem. Soc. Chem. Commun.*, 1985, 1140.

1.10 Abell, A. D., Clark, B. M., Robinson, W. T., *Aust. J. Chem.*, 1988, **41**, 1243, and references cited therein.

1.11 Morris, K. B., MSc Thesis, University of Canterbury, 1990.

1.12 Abell, A. D., Clark, B. M., Robinson, W. T., *Aust. J. Chem.*, 1989, **42**, 2225.

1.13 Leiserowitz, L., *Acta Crystallogr., Sect. B.*, 1976, **32**, 775.

1.14 Greenwood, N. N., Earnshaw, A., 'Chemistry of the Elements,' 1984, p.65, Pergamon Press.

1.15 Eliel, E. L., Allinger, N. L., Angyal, S. J., 'Conformational Analysis', 1965, p.41, Wiley, New York.

1.16 Vanderhoff, P. A., Thompson, H. W., Lalancette, R. A., *Acta Crystallogr., Sect. C*, 1986, **C42**, 1766.

1.17 Thenappan, A., Burton, D. J., *J. Org. Chem.*, 1991, **56**, 273.

1.18 Snyder, J. P., Bestman, H. J., *Tetrahedron Letts.*, 1970, **38**, 3317.

1.19 Kayser, M. H., Hooper, D. L., *Can. J. Chem.*, 1990, **12**, 2123, and references cited therein.

1.20 Cameron, A. F., Duncauson, F. D., Freer, A. A., Armstrong, V. W., Ramage, R., *J. Chem. Soc., Perkin Trans 2*, 1975, 1030.

1.21 Thompson, H. W., Vanderhoff, P. A., Lalancette, R. A., *Acta Crystallogr., Sect. C*, 1991, **C47**, 1443.

1.22 'Raman Spectroscopy', Szymansky, H. A., Ed., 1967, Plenum Press, New York.

1.23 Williams, D. H., Fleming, I., 'Spectroscopic Methods in Organic Chemistry,' 2nd ed, 1973, p.58, MacGraw-Hill, UK.

2.1 Abell, A. D., Massy-Westropp, R. A., *Aust. J. Chem.*, 1982, **35**, 2077.

2.2 Massy-Westropp, R. A., Reynolds, G. D., Spotswood, T. M., *Tetrahedron Letts.*, 1966, **18**, 1939.

2.3 Gallo, G. G., Goronelli, G., Vigevani, A., Lancini, G. C., *Tetrahedron*, 1969, **25**, 5677.

2.4 Lardelli, G., Dijkstra, G., Harles P. D., Bolidingl, J., *Rec. Trav. Chim.*, Pays-Bay 1966, **85**, 43.

2.5 (a) Tam, T. F., Spencer, R. W., Thomas, E. M., Copp, L. J., Krantz, A., *J. Am. Chem. Soc.*, 1984, **106**, 6849., (b) Spencer, R. W., Tam, T. F., Thomas, E., Robinson, V. J., Krantz, A., *J. Am. Chem. Soc.*, 1986, **108**, 5589.

2.6 (a) Kazlauskas, R., Murphy, P. T., Quinn, R. J., Wells, R. J., *Tetrahedron Letts.*, 1977, **1**, 37., (b) Pettus, J. A. Jr., Wing, R. H., Sims, J. J.,*Tetrahedron Letts.*, 1977, **1**, 41.

2.7 (a) Groutas, W. C., Stanga, M. A., Brubaker, M.J., *J. Am. Chem. Soc.*, 1989, **111**, 1931., (b) Groutas, W. C., Brubaker, M. J., Stanga, M. A., Castrisos, J. C., Crowley, J. P., Schatz, E.J., *J. Med. Chem.*, 1989, **32**, 1607.

2.8 Chan, D. H. T., Marder, T. B., Milstein, D., Taylor, N. J., *J. Am. Chem. Soc.*, 1987, **109**, 6385.

2.9 Doi, J. T., Luehr, G. W., Carmen, D. D., Leppsmeyer, B. C., *J. Org. Chem.*, 1989, **54**, 2764.

2.10 Ochiai, M., Takaoka, Y., Masaki, Y., Inenaga, M., Nagao, Y., *Tetrahedron Letts.*, 1989, **30**(48), 6701.

2.11 Wells D. R., *Aust. J. Chem.*, 1963, **16**, 165.

2.12 Flitsch, W., Schindler, S. R., *Synthesis*, 1975, 685.

2.13 Gosney, I., Rowley, A. G., 'Organophosprus Reagents in Organic Synthesis', Cadogan, J. I. G., Ed., 1979, Academic Press, New York.

2.14 Olah, G. A., Krishnamurthy, V. V., *J. Am. Chem. Soc.*, 1982, **104**, 3987.

2.15 (a) Wittig, G., Schöllkopf, U., *Chem. Ber.*, 1954, **87**, 1318., (b) Wittig, G., Haag, W., *Chem. Ber.*, 1955, **88**, 1654.

2.16 (a) Vedejs, E., Meier, G. P., Snoble, K. A. J., *J. Am. Chem. Soc.*, 1981, **103**, 2823., (b) Vedejs, E., Fleck, T., Hara, S., *J. Org. Chem.*, 1987, **52**, 4639., (c) Vedejs, E., Marth, C.F., *J. Am. Chem. Soc.*, 1989, 111, 1519.

2.17 Reitz, A. B., Nortey, S. O., Jordon, A. D., Mutter, M. S., Maryanoff, R. E., *J. Org. Chem.*, 1986, **51**, 3302.

2.18 Birum, G. H., Matthews, C. N., *J. Chem. Soc. Chem. Commun.*, 1967, 137.

2.19 Rameirez. F., Smith, C. P., Pilot, J. F., *J. Am. Chem. Soc.*, 1968, **90**, 6726.

2.20 (a) Bestman, H. J., *Pure and Applied Chem.*, 1979, **51**, 51, *ibid*, 1980, 52, 771., (b) Bestman, H. J., Vorstrowsky, O., *Top. Curr. Chem.*, 1983, **109**, 85.

2.21 Mislow, K., *Acc. Chem. Res.*, 1970, **3**(10), 321.

2.22 Vedejs, E. Snoble, K. A. J., *J. Am. Chem. Soc.*, 1973, **95**, 5778.

2.23 Ingham, C. F., Massy-Westropp, R. A., Reynolds, G. D., Thorpe, W. D., *Aust. J. Chem.*, 1975, **28**, 2499.

2.24 (a) Doyle, I. R., Massy-Westropp, R. A., *Aust. J. Chem.*, 1982, **35**, 1903., (b) Abell, A. D., Doyle, I. R., Massy-Westropp, R. A., *Aust. J. Chem.*, 1982, **35**, 2277.

2.25 Chopard, P. A., Searle, R. J. G., Dewitt, F. H., *J. Org. Chem.*, 1965, **30**, 1015.

2.26 Abell, A. D., Heinicke, G. W., Massy-Westropp, R. A., *Synthesis*, 1985, 764.

2.27 Hamper, B. C. *J. Org. Chem.*, 1988, **53**, 5558, and references cited therein.

2.28 (a) Schlosser, M., Christman, K. F., *Synthesis*, 1969, 38., (b) Schlosser, M., Christman, K. F., Piskala, A., Coffinet, D., *Synthesis*, 1971, 29., (c) Schlosser, M., *Top. Stereochem.*, 1970, **5**, 1., (d) Corey, E. J., Shulman, J. I., Yamamoto, H., *Tetrahedron Letts.*,

1970, **6**, 447., (e) Corey, E. J, Ulrich, P., Venkateswarla, A., *Tetrahedron Letts.*, 1977, **37**, 3231., (f) Maryanoff, B. E., Reitz, A. B., Duhl-Emswiler, B. A., *J. Am. Chem. Soc.*, 1985, **107**, 217., (g) Grieco, P. A., Takigawa, T., Vedananda, T. R., *J. Org. Chem.*, 1985, **50**, 3111.

2.29 Allinger, N.L., Burkert. U., 'Molecular Mechanics' (ACS Monograph 177) Am. Chem. Soc. Washington D.C. 1982. Calculations performed using Model Version 2.98.

2.30 (a) Tendil, J., Verny, M., Vessiére, R., *Bull. Soc. Chim. France*, 1972, **10**, 4028.

2.31 (a) Verny, M., Vessiére, R., *Bull. Soc. Chim. France*, 1967, **6**, 2210., (b) Osborne, N. F., *J. Chem. Soc. Perkin Trans I*, 1982, 1429.

2.32 (a) Kohl-Mines, E., Hansen, H. J., *Helv. Chim. Acta*, 1985, **68**, 2244, and references cited therein., (b) Cooke, M. P. Jr., Burman, D. L. *J. Org. Chem.*, 1982, **47**, 4955., (c) Bestman, H. J., Hartung, H., *Angew Chem. Int. Edit. Engl.*, 1963, **2**(4), 214., (d) Bestmann, H. J., Graf, G., Hartung, H., Kolewa, S.,Vilsmaier, E., *Chem. Ber.*, 1970, **103**, 2794., (e) Lang, R. W., Hansen, H. J., *Helv. Chim. Acta.*, 1979, **62**(151), 1458.

2.33 Patai S., 'The Chemistry of ketenes, allenes, and related compounds', 1980, J. Wiley, New York.

2.34 (a) Gray, G. A., *J. Am. Chem. Soc.*, 1973, **95**, 7736., (b) Weigert, F.J. Roberts, J. D., *Inorg. Chem.*,1973, **12**, 313. (c) Albright, T. A., Freeman, W. J., Schweizer, E. E., *J. Am. Chem. Soc.*,1975, **7**, 940.

2.35 Crouse, D. M., Wehman, A. T., Schweizer, E. E., *J. Chem. Soc., Chem. Commun.*, 1968, 866.

2.36 Ramirez, F., Dershowitz, S., *J. Org. Chem.*, 1957, **22**, 41.

2.37 Bestmann, H. J., Kumar, K., Schaper, W., *Angew. Chem. Int. Ed. Engl.*, 1983, **22**, 167.

2.38 Gough, S. T. D., Tripett, S., *J. Chem. Soc.*, 1962, 2333.

2.39 McCulloch, A., W., McInnes, A., G., *Can. J. Chem.*, 1974, **52**, 3569, and references cited therein.

2.40 Hoult, D. A., MSc Thesis, University of Canterbury, 1991.

3.1 Fischer, G., *Natural Product Review*, 1988, 465.

3.2 (a) Daniels, S. B., Katzenellenbogen, J. A., *Biochemistry*, 1986, **25**, 1436, and references cited therein., (b) Sofia, M. J., Katzenellenbogen, J. A., *J. Med. Chem.*, 1986, **29**, 230.

3.3 (a) Naruto, S., Motoc, I., Marshall, G.R., *Eur. J. Med. Chem.*, 1985, **20**(6), 533., (b) Naruto, S., Motoc, I., Marshall, G.R., Daniels, S.B.,

Sofia, M.J., Katzenellenbogen, J.A., *J. Am. Chem. Soc.*, 1986, **107**, 5262.

3.4 Nozaki, H., Yamaguti, Z., Okada, T., Noyoni, R., Kawanich, M., *Tetrahedron*, 1967, **23**, 3993.

4.1 Knight, D. W., Patternden, G., *J. Chem. Soc. Perkins Trans 1*, 1975, **635**, 641.

4.2 Hemmi, K., Harper, J. W., Powers, J. C., *Biochemistry*, 1985, **24**, 1841.

4.3 Rigaudy, J., Derible, P., *Bull. Soc. Chim. France.*, 1965, 3047.

4.4 (a) Howe, R., *J. Org. Chem.*, 1973, **38**, 4164., (b) Kunzek, H., Rühlmann, K., *J. Organometallic Chem.*, 1972, **42**, 391.

4.5 Allahdad, A., Knight, D. W., *J. Chem. Soc. Perkins Trans 1.*, 1982, 1855.

5.1 (a) Daniels, S. B., Cooney, E., Sofia, M. J., Chakravarty, P. K., Sofia, M. J., Katzenellenbogen, J. A., *J. Org. Chem.*, 1985, **50**, 2331., (b) Chakravarty, P. K., Kraft, G. A., Katzenellenbogen, J. A., *J. Biol. Chem.*, 1982, **257**(2), 610., (c) Sofia, M. J., Chakravarty, P. K., Katzenellenbogen, J. A., *J. Org. Chem.*, 1983, **48**, 3318.

5.2 (a) Bürgi, H. B., Dunitz, J. D., Shefter, E. J., *J. Am. Chem. Soc.*, 1973, **95**, 5065., (b) Bürgi, H. B., Dunitz, J. D., Lehn, J. M., Wipff, P., *Tetrahedron*, 1974, **30**, 1563., (c) Bürgi, H. B., Lehn J.M., Wipff P., *J. Am. Chem. Soc.*, 1974, **96**, 1956.

5.3 (a) Wijnberg, J. B., Speckamp, W. N., Shoemaker, H. E., *Tetrahedron Letts.*, 1974, **46**, 4073., (b) Wijnberg, J. B., Speckamp, W. N., *Tetrahedron Letts.*, 1975, **46**, 4035., (c) Wijnberg, J.B., *Tetrahedron*, 1978, **34**, 179., (d) Rosenfield, R., Dunitz, J. D., *Helv. Chim. Acta*, 1978, **61**(202), 2176.

5.4 Brendhougen, K., Fikke, K., Seip, H. M., *Acta. Chem. Scand.*,1973, **27**, 1101.

5.5 (a) Kayser, M. H., Eisenstein, O., *Can. J. Chem.*, 1981, **59**, 2457. (b) Kayser, M. H., Morand, P., *Tetrahedron Letts.*, 1979, 8, 695., (c) Kayser, M. H., Morand, P., *Can. J. Chem.*, 1978, **56**, 1523., (d) Kayser, M. H., Wiff, G., *Can. J. Chem.*, 1982, **60**, 1192.

5.6 Kayser, M. H., Breau L., *Can. J. Chem.*, 1989, **67**, 1401.

5.7 Kayser, M. H., Morand, P., *J. Org. Chem.*, 1979, **44**,1338.

5.8 (a) Koer, F.J., Altona, C., *Recueil, Journal of the Royal Nederlands Chem. Soc.*, 1974, 93(5)., (b) Koer, F.J., Altona, C., *Recueil, Journal of the Royal Nederlands Chem. Soc.*, 1975, **94**(6).

5.9 Standard Varian Pulse Sequences.

5.10 Newsoroff, G. P., Sternhell, S., *Aust. J. Chem.*, 1972, **25**, 1669.

5.11 Weygand, F., Klinke, P., Eigen, I., *Chem. Ber.*, 1956, **89**, 1897.

5.12 Kovacs, J., Kovacs, H. N., Ballina, R., *J. Am. Chem Soc.*, 1967, **85**, 1839.

5.13 Easton, C. J., Tan, E. W., Hay, M. P., *J. Chem. Soc. Chem. Commun.*, 1989, 385.

5.14 (a) Bodanszky, M., 'Principles of Peptide Synthesis', 1984, Springer-Verlag, New York., (b) Bodanszky, M., Bodanszky, A., ' Practice of Peptide Synthesis', 1984, Springer-Verlag, New York., (c) Meienhofer, J., 'Chemistry and Biochemistry of the Amino Acids', Barrett, G. C., Ed., 1985, Chapman and Hall, New York.

5.15 Nagasawa, T., Kuroiwa, K., Narita, K., Isowa. Y., *Bull. Chem. Soc. Jap.*, 1973, **46**, 1269.

5.16 Abell, A. D., Taylor, J. M., unpublished results.

5.17 Carpino, L. A., *Acc. Chem. Res.*, 1973, **6**(6), 191.

5.18 Sigma Chemical Company Ltd.

5.19 Scholtz, J. M., Bartlett, P. A., *Synthesis*, 1989, 542.

5.20 Itoh, M., *Chem. Pharm. Bull.*, 1969, **17**(8), 1679.

5.21 Kellam, S. J., Ph.D. Thesis, C.N.A.A. London, 1989.

5.22 (a) Bochenska, M., Biernat, J. F., *Roczniki Chemii Ann. Soc. Chim. Polonorum*, 1974, **48**, 445., (b) Bochenska, M., Janiak T., Biernat, J. F., *Roczniki Chemii Ann. Soc. Chim. Polonorum*, 1976, **50**, 243.

E1 Perrin, D., D., Armarego, W., L., F., Perrin, D., R., 'Purification of laboratory chemicals', 2nd ed., 1982, Pergamon Press, New York.

E2 Casey, M., Leonard, J., Lugo, B., Procter, G., 'Advanced practical organic chemistry', 1990, p233. Blackie, Chapman and Hall, New York.

E3 Isler, O., Gutmann, H., Motaovn, M., Rüegg, R., Ryser, G., Zeller, P., *Helv. Chim. Acta.*, 1957, **57**, 1247.

E4 Denny, D., B., Ross, S., T., *J. Org. Chem.*, 1962, **27**, 998.

E5 Sheldrick, G., M., SHELXTL User manual and Package, Revision 4, 1984, Nicolt XRD Corporation, Madison, Wisconson.

E6 Kindly gifted by R. A. Massy-Westropp.

E7 In house assays, Marine Chemistry Group, Chem. Dept., University of Canterbury.